universität wien

DISSERTATION / DOCTORAL THESIS

Titel der Dissertation / Title of the Doctoral Thesis

„Parallel and adaptive processes during ecotype formation in *Heliosperma pusillum*“

verfasst von / submitted by

Aglaia Szukala, MSc

angestrebter akademischer Grad / in partial fulfilment of the requirements for the degree of

Doctor of Philosophy (PhD)

Wien, 2022 / Vienna, 2022

Studienkennzahl lt. Studienblatt / degree programme code as it appears on the student record sheet:	UA 794 685 437
Dissertationsgebiet lt. Studienblatt / field of study as it appears on the student record sheet:	Biologie
Betreut von / Supervisor:	Assoz. Prof. Dipl.-Ing. Dr. Ovidiu Paun

Acknowledgements

I would like to express my deepest thanks to Ovidiu Paun for the opportunity to investigate intriguing research questions and work on a wonderful plant system. He helped me to improve my analytical skills and scientific thinking, allowing me to explore the matter independently, but also providing constructive feedback. Among others, thank you for truly caring about my scientific path, for giving me the chance to present our work at many international conferences and meetings, and go to Germany and Switzerland for a research stay abroad.

I would also like to thank my two co-supervisors, Magnus Nordborg and Joachim Hermisson, for the insightful comments and support during my work. My gratitude also goes to the other faculty members of the doctoral school of population genetics that have provided regular and constructive feedback. The advisory board meeting of the doctoral school was always one of the most instructive experiences of the year. I wish to extend my thanks to the advisory board committee: Andrew Clark, Nick Barton, Virginie Courtier-Orgogozo, and John Parsch.

I wish to thank Peter Schönswetter, Božo Frajman, Clara Bertel, and Emiliano Trucchi for setting the basis of this work, supporting me in different ways and giving important feedback on the study system.

Special thanks goes to Thibault Leroy for his precious feedback on my manuscripts and enlightening seminars and chats about demographic modeling, mutation rates and other evolutionary topics. I wish to thank also Jaqueline Hess for being a supportive mentor during the initial phase of this work, as well as Daniele Filiault for the insightful feedback and nice chats.

Acknowledgements

I had a very good time during my research stay in Alex Widmer and Daniel Schubert labs. I would like to thank both of them for the opportunity to join their research and be, even if only for a short time, a part of their teams. In this context, I wish to thank very much Simone Fior and Hirzi Luqman for their important input to my work in Zürich, as well as Claire Jourdain, Léa Faivre, Teresa Kowar, Melissa Romich, and Ruth Lintermann for their help and support during my stay in Berlin.

I am also very greatful to Nicolas Bierne and Sophie Karrenberg, who kindly agreed to review this work, and Sam Yeaman for the helpful insights, corrections, and constructive suggestions.

Laboratory work is heavy and demanding, nevertheless technicians often get only limited recognition. I would like to recognize the invaluable assistance of Daniela Paun, Marie Huber, Juliane Baar, and Carles Ferré Ortega in the lab. Also, thanks to Daniela Pirkebner, Marianne Magauer, Martina Imhiavan, and Daniel Schlorhaufer for their work on plants cultivation and crossings in Innsbruck.

It would have been hard to enjoy the doctoral studies as much as I did without having around good friends and fellows. Very heartful thanks go to my colleagues and friends Mimmi Eriksson, Christina Hedderich, Gil Yardeni, Huiying Shang, Clara Groot Crego, Thomas Wolfe, Sonja Lečić, Marie Brandrud, Luiz Cauz, Marta Pelizzola, Lauri Törmä, Wei-Yun Lai, Sheng-Kai Hsu, Florian Schwarz, Sabine Felkel, Sophie Lokatis, and Liliana Pinek. Also to my artisitc friends Lisa Alice & Co., Ricarda & Julian, Helena & Steffen, Martin, Gabriele, Sarinzi, Camilla, Maria, Alice, and Giovanna, thanks for being incredibly good friends and nourishing my creative side.

On a more personal level, I wish to thank my beloved ones: my incredibly supportive husband Roman and my daughter Nerea, who are the main drivers of my energy and happiness. I was asked many times the lovely question *"mamma, have you finished writing the big book?"*. Well, here it is: "the big book".

Abstract

Independent instances of divergence with similar phenotypic outcomes provide natural evolutionary replicates to investigate the adaptation to new ecological niches. The plant *Heliosperma pusillum* forms montane and alpine ecotypes that maintain different phenotypes when grown under the same conditions for multiple generations and show a home-site fitness advantage in reciprocal transplantations. Noteworthy, previous work suggested that the montane ecotype diverged from the alpine multiple times independently in different geographic areas. This doctoral work seeks to improve our knowledge of the evolutionary history of the *H. pusillum* ecotypes and exploit this system to dig into the repeatability of (epi-)genetic mechanisms behind phenotypic divergence, adaptation, and possibly speciation in natural evolutionary replicates. We sought to find molecular patterns that affect repeated ecotype divergence in the short-term and, potentially, lead to stable differentiation on the evolutionary scale.

In the first chapter, we compare alternative demographic scenarios using the site frequency spectrum as summary statistics and perform differential expression analyses of plants grown in a common garden. Our results confirm the independent instances of divergence with only rare gene flow between ecotype pairs. We find that the hairy montane ecotype adapted to dry and poor light conditions by altering the expression of genes involved in trichome formation, response to drought, differing light availability, and biotic stressors. Despite the similarity of functions affected across the different divergence events, we detect little parallelism of genes differentially expressed between ecotypes across origins, indicating that changes in different genes and pathway components led to similar outcomes independently. Polygenic adaptation thus produces non-parallel genetic

divergence, providing alternative substrates to reproducible outcomes in repeated ecotype formation.

The second chapter aims to disentangle plastic from constitutive gene expression divergence shaping ecotype adaptation by means of analyses of plants grown in reciprocal transplantations. Interestingly, we observe that the derived montane ecotype bears significantly higher plasticity of gene expression then the alpine. Genes that change expression plastically are involved in ecologically relevant functions that are partly shared with genes that differ constitutively in their expression between ecotypes. We conclude that enhanced expression plasticity likely evolved in response to drier and warmer environments in this plant system, suggesting that a gain in plasticity can confer a fitness advantage in novel challenging environments.

Finally, the third chapter explores one of the possible mechanisms behind transcriptional and post-transcriptional divergence and plasticity, by means of analyses of small RNAs activity in common garden and reciprocal transplantations settings. Our results show that small RNAs play a pivotal role in regulating differential defense responses to multiple (a-)biotic stressors. Between 12 and 27% of all differentially targeted genomic regions (DTRs) include coding regions, depending on the growing environment and the ecotype pair analyzed, while a major proportion of DTRs are intergenic. We recover enhanced differences in small RNAs targeting genomic regions among ecotype pairs, suggesting that evolutionary replicates can evolve in largely different directions with regard to small RNAs activity. Also, concordant patterns of plasticity recovered in DTRs and gene expression suggest that small RNAs are a driving force behind previously observed differences in gene expression plasticity between ecotypes.

Altogether, this doctoral work provides critical insights into the repeatability of functional differentiation in parallelly evolved ecotype pairs. We show that phenotypic convergence often has a redundant basis, evolving via different gene expression and regulatory changes, and involves the repeated evolution of increased gene expression plasticity mediated by stable (epi-)genetic regulatory mechanisms.

Kurzfassung

Unabhängige Ereignisse von Divergenz, die zu ähnlichen phänotypischen Ergebnissen führen, bieten evolutionäre Replikate, um die Anpassung an neue ökologische Nischen zu untersuchen. Die Pflanze *Heliosperma pusillum* bildet montane und alpine Ökotypen aus, die ihre unterschiedlichen Phänotypen beibehalten, wenn sie über mehrere Generationen hinweg in Kultur unter einheitlichen Bedingungen in einem "Common Garden" angebaut werden, und die bei reziproken Transplantationen einen Fitnessvorteil in ihrem jeweiligen Heimatstandort beweisen. Frühere Arbeiten deuten darauf hin, dass sich der montane Ökotyp in verschiedenen geografischen Gebieten mehrfach unabhängig vom alpinen Ökotyp entwickelt hat. Diese Doktorarbeit soll unser Wissen über die Evolutionsgeschichte der *H. pusillum*-Ökotypen verbessern und dieses System nutzen, um die Wiederholbarkeit der (epi)genetische Mechanismen hinter der phänotypischen Divergenz, der Anpassung und möglicherweise der Artbildung zu untersuchen. Unser Ziel war es molekulare Muster zu finden, die sich kurzfristig auf die wiederholte Divergenz von Ökotypen auswirken und möglicherweise zu einer stabilen evolutionären Divergenz führen.

Im ersten Kapitel vergleichen wir alternative demografische Szenarien unter Verwendung des "site frequency spectrum" als summarische Statistik und führen Analysen der differentiellen Expression von Pflanzen durch, die in einem Common Garden angebaut wurden. Unsere Ergebnisse bestätigen die Unabhängigkeit der Divergenzereignisse mit nur seltenem Genfluss zwischen Ökotypenpaaren. Wir stellen fest, dass sich der behaarte montane Ökotyp mittels einer Veränderung der Genexpression an trockene und lichtarme Bedingungen angepasst hat, insbesondere jener Gene, die an der Trichombildung sowie an der Reaktion auf Trockenheit, unterschiedliche Lichtverfügbarkeit und biotische Stress-

faktoren beteiligt sind. Trotz der Ähnlichkeit der Funktionen, die über die verschiedenen Divergenzereignisse hinweg betroffen sind, stellen wir nur wenig Parallelität bei den Genen fest, die zwischen den Ökotypen unterschiedlich exprimiert werden. Dieses Ergebnis deutet darauf hin, dass Veränderungen verschiedener Gene und Komponenten der Signalwege unabhängig voneinander zu ähnlichen Ergebnissen führen. Polygene Anpassung führt also zu nicht-paralleler genetischer Divergenz und bietet alternative Wege für reproduzierbare Ergebnisse bei der wiederholten Bildung von Ökotypen.

Das zweite Kapitel zielt darauf ab, die plastische von der konstitutiven Genexpressionsdivergenz zu trennen, und zwar durch Analysen von Pflanzen, die in reziproken Transplantationen gewachsen sind. Interessanterweise stellen wir fest, dass der abgeleitete montane Ökotyp eine deutlich höhere Plastizität der Genexpression aufweist als der alpine Ökotyp. Gene, die sich in der Expression plastisch verhalten, sind an ökologisch relevanten Funktionen beteiligt, die sie teilweise mit Genen teilen, die sich konstitutiv in ihrer Expression zwischen Ökotypen unterscheiden. Wir kommen zu dem Schluss, dass sich die erhöhte Expressionsplastizität in dem montanen Ökotyp wahrscheinlich als Reaktion auf trockenere und wärmere Umgebungen entwickelt hat, was im wiederum nahelegt, dass ein Gewinn an Plastizität in neuen, Stress-reichen Umgebungen zu einem Fitnessvorteil führen kann.

Im dritten Kapitel wird schließlich mittels Analysen der Aktivität von kleinen RNAs in Common Garden sowie bei reziproken Transplantationen einer der möglichen Mechanismen hinter transkriptioneller und posttranskriptioneller Divergenz und Plastizität untersucht. Unsere Ergebnisse zeigen, dass kleine RNAs eine zentrale Rolle bei der Regulierung unterschiedlicher Abwehrreaktionen gegen mehrere (a)biotische Stressoren spielen. Zwischen 12 und 27% aller differentiell angezielten genomischen Regionen (DTRs) umfassen kodierende Regionen, abhängig von der Wachstumsumgebung und dem analysierten Ökotypenpaar, während ein größerer Teil der DTRs intergenisch ist. Wir entdecken verstärkte Unterschiede bei den DTRs als bei der differential Genexpression, was ein Hinweis dafür ist, dass sich evolutionäre Replikate in Bezug auf die Aktivität kleiner RNAs in weitgehend unterschiedliche Richtungen sich entwickelt haben. Außerdem deuten

übereinstimmende Muster der Plastizität in DTRs und Genexpression darauf hin, dass kleine RNAs eine treibende Kraft hinter den zuvor beobachteten Unterschieden in der Plastizität der Genexpression zwischen Ökotypen sind.

Insgesamt bietet diese Doktorarbeit wichtige Einblicke in die Wiederholbarkeit der funktionellen Divergenz bei der parallelen Evolution von Ökotypen. Wir zeigen, dass die phänotypische Konvergenz oft eine redundante Grundlage hat, die sich aus verschiedenen Genexpressions- und regulatorischen Veränderungen ergibt, und dass sie, mittels stabilen (epi)genetische Regulationsmechanismen, zur wiederholten Evolution einer erhöhten Plastizität der Genexpression führt.

Contents

Introduction

Living organisms respond to changes in the surrounding (a-)biotic environment through short-term and long-term ecological and evolutionary responses. The molecular mechanisms behind evolution have been a long-lasting object of study, where the major focus has been given to the accumulation of genetic divergence through mutations (i.e. single-nucleotide polymorphisms, indels, and structural variation) and its maintenance dynamics through selective and neutral long-term processes (e.g. Felsenstein, 1976; Kimura, 1983; Lynch et al., 2016). Nevertheless, the primary sphere in which change is induced is the present interaction between organisms and environment. This is modulated by different mechanisms that can fluctuate and be reversible, but are translated into and affect the evolutionary divergence in the long-term. Today, the fast change induced by the action of humans on the natural environment requires us to improve our understanding of the integration of short- and long-term processes.

Short-term phenotypic changes can be achieved by means of plasticity (Schlichting & Pigliucci, 1998), which is the reversible, non-genetic adjustment of the mean phenotype of a population in response to a change in the surrounding environment. By contrast, evolutionary changes result in heritable phenotypic divergence and a fitness advantage of adapted populations underlied by genetic differentiation (Kawecki & Ebert, 2004; Savolainen et al., 2013). At the interface between these two processes, epigenetic modifications of gene expression can arise as a response to environmental stimuli and stressors causing short-term, non-heritable phenotypic acclimation (Y. Ding et al., 2012; Friedrich et al., 2019; Quint et al., 2016), but were also shown to be sometimes inherited across generations affecting phenotypic variation on a longer time scale (Eriksson et al., 2020;

Holeski et al., 2012; Jablonka & Raz, 2009; Paun et al., 2010). Notably, the rate of epimutations was shown to be higher than that of genetic mutations (Tal et al., 2010). Lastly, a large mutation accumulation experiment in *Arabidopsis thaliana* (Monroe et al., 2022) recently suggested that epigenome-associated mutation bias could contribute to short-term environmental effects on how the genome mutates.

Heritable phenotypic divergence may be adaptive if the underlying (epi-)genetic differentiation was driven by natural selection (Darwin, 1859), but non-adaptive evolutionary change can result from mutation, drift and demography (Kimura, 1968; Wrigth, 1931). Similarly, short-term plastic responses may be adaptive if they shift the phenotype toward a new optimum, but can also result from adjustments to e.g. stress conditions that do not increase the mean fitness of a population or are even maladaptive. Understanding the genomic processes underlying evolution, including the linkage between short-term responses and heritable (epi-)genetic divergence, and the contribution of adaptive vs non-adaptive changes, is a major goal in evolutionary biology and ecology.

This doctoral work aims to enlarge our knowledge about the molecular processes behind population divergence and adaptation by means of transcriptomic analyses of altitudinal ecotypes in the plant species *Heliosperma pusillum* (Waldst. and Kit.) Rchb. (Caryophyllaceae). Conspecific populations that are referred to as ecotypes (Lowry, 2012; Turesson, 2010) are mostly interfertile, despite being characterized by stable ecological and phenotypic differentiation, possibly as a result of local adaptation. Fragmentation of the distribution range and further barriers to gene-flow can enhance differentiation via drift and accumulation of mutations, possibly until the ecotypes are not capable of further interbreeding. A main advantage of our system of choice is that ecotype divergence was suggested to have occurred multiple times in independent instances of evolution (Trucchi et al., 2017). As I will further explain, these replicates of the evolutionary process (*parallel evolution*) represent a powerful avenue to study the relative contribution of neutral and adaptive processes in shaping divergence. Also, ecotypes represent an initial stage in the process of speciation, which we consider particularly sensible to capture information about both short- and long-term mechanisms. Disentangling the complex contribution of

neutral and adaptive, short- and long-term processes to ecotype formation in *H. pusillum* is therefore the primary object of this work.

In the following pages, I will first introduce the concept of *parallel evolution* and its importance for the discovery of the evolutionary mechanisms behind adaptation and divergence. Second, I will introduce *polygenic adaptation* and its implications for the action of natural selection on genomic variation and phenotype evolution. How complex traits adapt to new selection pressures is indeed a topic of debate. Third, I will describe the study system *H. pusillum* in order to clarify why it was chosen to answer our research questions. Fourth, I will introduce the methodological approach used. Last, I will give a concise outline of the specific aims of this work, as well as a description of the content of all chapters.

Parallel evolution: a powerful means to study adaptation to changing environments

One aspect of great interest in evolution is to which degree the evolutionary process is deterministic. A non-random and constrained evolution implies that we might be able to predict, at least to a certain degree, the probability and mode of evolution of populations and species in response to environmental change. Discovering the deterministic component of adaptation and disentangling it from its arbitrary part is therefore essential. One way to detect key directional processes is to investigate cases of repeated evolution, meaning that a similar phenotype evolved multiple times in independent evolutionary lineages concurrently with an ecological condition in which it is adaptive. There is general agreement that any outcome appearing again and again in independent instances of evolution is the product of natural selection (Stern, 2013). Repeated evolution therefore allows to disentangle directional from random evolutionary processes.

More specific terms exist to define repeated evolution depending on the genetic processes underlying the recurrent phenotypic convergence and the phylogenetic distance between evolutionary lineages. The term *parallel evolution* has mostly been used to describe the

repeated evolution from standing genetic variation, often reported among more closely related lineages. Some examples of parallel evolution via standing variation include the adaptation to freshwater in sticklebacks through the loss of the lateral plates (Jones et al., 2012), the adaptation to myxoma virus in rabbits (Alves et al., 2019), stick insects adaptation to host plant species (Soria-Carrasco et al., 2014), the replicated series of introductions in invasive marine mussels (Fraïsse et al., 2016; Popovic et al., 2021; Simon et al., 2020), and humans adaptation to high altitudes (Foll et al., 2014). On the other hand, *convergent evolution* mostly describes repeated evolution among distantly related lineages by *de novo* independent mutations (Bull et al., 1997; Dobler et al., 2012; Witt & Huerta-Sánchez, 2019). This dichotomy of terms implies that the genetic mechanisms driving the evolution of similar phenotypes can be shared (*parallelism*, usually at the *intra*specific level) or different (*convergence*, usually at the *inter*specific level).

Here, I wish to drive the attention to two aspects that are relevant for this work (extensive reviews can be found in e.g. Arendt & Reznick 2008; Bolnick et al. 2018; Elmer & Meyer 2011; Schluter & Nagel 1995; Stern 2013). First, multiple studies showed that the phylogenetic distance between lineages is not necessarily associated with the degree of sharedness of the underlying molecular processes (Cooper et al., 2003; Derome et al., 2006; Hoekstra & Nachman, 2003; Wichman et al., 1999). For instance, we find that the same mutation in the *mcr1* gene drives coat or skin color polymorphism across distant taxa (e.g. reptiles, Rosenblum et al. 2004, birds, Theron et al. 2001, and mammals, Ritland et al. 2001), but the same phenotype is not driven by this genetic locus within-species (Manceau et al., 2010; Rosenblum et al., 2010). Second, several authors (Arendt & Reznick, 2008; Bolnick et al., 2018; Oke et al., 2017) noticed that parallel phenotypic evolution is mostly driven by a continuum of non-parallel to fully-parallel processes and therefore proposed to abandon the distinction between these terms.

Indeed, multiple properties of a study system can influence parallelism, including variation in the strength of gene flow, selection and drift, the effective population size (N_e), the demographic history, the extent of habitat differentiation, and the genetic architecture of adaptive traits (MacPherson & Nuismer, 2017; Yeaman et al., 2018).

Figure 1 offers a simplistic representation and summary of the different processes that can influence the probability of parallel evolution. When selection, gene flow, and demographic parameters happen in combination with a relatively simple architecture of the adaptive traits, highly parallel evolutionary outcomes are expected (Fig. 1a). Note that this scenario strongly resembles laboratory experiments, even though a polygenic architecture of the adaptive traits can shift the observed evolutionary patterns closer to scenario (b) of Fig. 1 even under artificially identical laboratory conditions (see e.g. Barghi et al. 2019 and the next paragraph). Natural populations are more often affected by processes such as in Fig. 1b. In this case, several variables can lead to less parallel evolutionary trajectories, such as, pronounced variation in the strength of selection due to e.g. local adaptation, and varying N_e, and variation in gene flow (i.e. both between ancestral and derived populations, as well as among derived populations). Additionally, intrinsic properties of the evolving system, such as a polygenic trait architecture and the different propensities for phenotypic plasticity, can lead to low parallelism, even when phenotypic convergence of certain traits is observed across evolutionary replicates. Given all these aspects, in the current work the term parallel evolution refers to the repeated evolution of similar phenotypes in independent evolutionary lineages, without referring to specific shared or non-shared molecular mechanisms.

Polygenic adaptation and the repeatability of evolution

A pivotal question concerning the process of adaptation is how many (epi-)genetic variants do contribute to an adaptive trait or, more broadly, a fitness advantage. This question is relevant also for the study of parallel evolution, given that the amount of variants contributing to adaptation can affect repeatability at the molecular level. Since the advent of genomics (Perbal, 2015), whole genome scans via e.g. genome-wide-association-studies (GWAs) have become a powerful means to detect adaptive variants. Despite several advances in this direction, one major issue encountered was that only a minor portion of trait heritability and variation could be explained (Manolio et al., 2009). Indeed, most

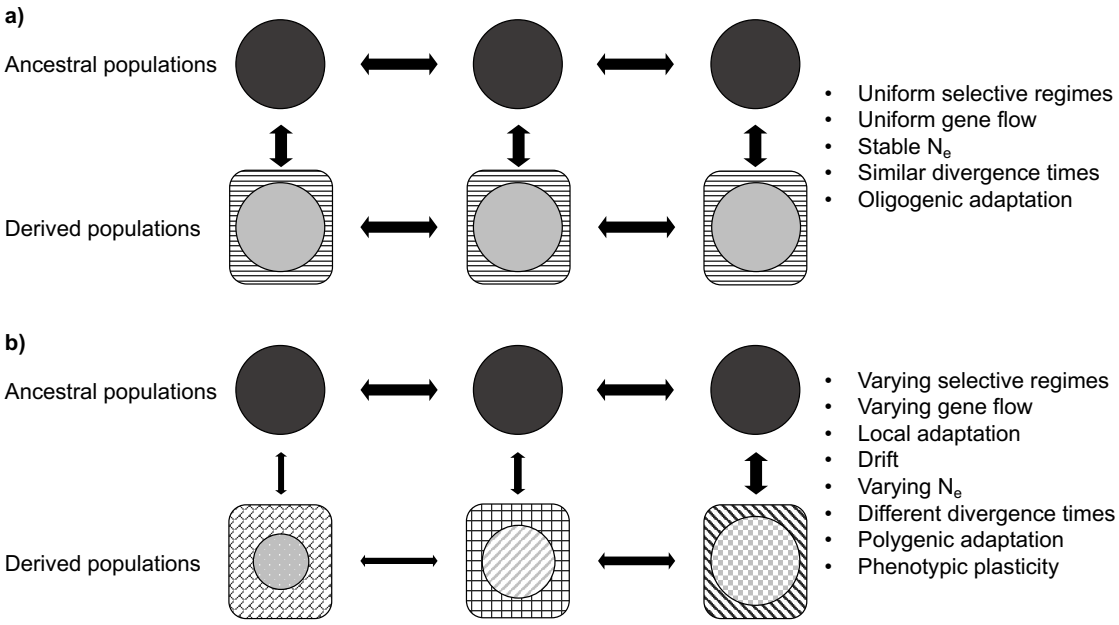

Fig. 1. Multiple processes can influence parallel evolution leading to highly parallel (a) or less parallel (b) evolutionary routes. Black and gray circles represent ancestral and derived populations, respectively, featuring independent divergence events. Note that the gray color in all derived populations represents a putative convergent phenotype. The squares around the circles represent the novel environment. In both circles and squares the weft symbolizes the repeatability of the evolutionary process, with respect to geno- and phenotypic outcomes (circles), and environmental and demographic conditions (squares). **(a)** Highly similar selection, gene flow, and demographic parameters, as well as an oligogenic architecture of adaptive traits lead to highly parallel evolutionary replicates. **(b)** A combination of extrinsic (selection and demography) and intrinsic (genetic architecture and plasticity) factors can drive less parallel evolutionary outcomes despite phenotypic convergence of some traits.

variation in quantitative phenotypic traits results from a large number of small-effect loci that are not easily detectable even with large sample sizes (e.g. Purcell et al., 2014).

Adaptive traits governed by very large numbers of variants are said to bear a polygenic genetic architecture (where genetic architecture can be defined as the sum of all loci contributing to a trait, their effect sizes, genomic position and their interaction, i.e. patterns of linkage, epistasis, and pleiotropy). Disentangling the relative effects of drift and natural selection on quantitative trait divergence has been the object of several studies (Leinonen et al., 2013; Luo et al., 2014). A feature of polygenic traits is genetic

redundancy, i.e. different combinations of alleles can produce the optimal phenotype (Goldstein & Holsinger, 1992). Moreover, redundant genetic loci likely contribute only transiently to the phenotype (Yeaman, 2015), meaning that the adaptive architecture (Barghi et al., 2020; Pritchard et al., 2010) of a trait is likely to vary strongly over time. It is still unclear how redundancy can impact the repeatability of molecular patterns underlying parallel evolution. Nevertheless, a growing number of studies speaks for a fundamental role of polygenic traits architecture and redundancy affecting parallelism both in natural (Bourret et al., 2014; Hämälä et al., 2020; Hancock et al., 2010; Lim et al., 2019; X. F. Ma et al., 2010; Rougeux et al., 2019), as well as artificial (Barghi et al., 2019; Cooper et al., 2003; Nguyen Ba et al., 2019) evolutionary replicates.

Heliosperma pusillum: an emerging study system for parallel ecological divergence

This work investigates parallel and adaptive processes in the plant species *H. pusillum*. Ecotype formation within this species has been previously proposed to be a case of parallel evolution featuring recurrent divergence of montane and alpine ecotypes in at least five geographic localities in the south-eastern Alps (Trucchi et al., 2017). The ecotypes have been shown to bear a fitness advantage in their respective ecological niches by means of reciprocal transplantation experiments (Bertel et al., 2018), demonstrating that their divergence is adaptive. Notably, no evidence of reproductive isolation was found between the ecotypes (Bertel, Hülber, et al., 2016), and their conspecificity was confirmed using isolation-by-distance analyses based on restriction site-associated data (RAD-seq) (Trucchi et al., 2017). Therefore, despite the clear ecological and morphological divergence which remains stable over a few generations in a common garden (author's own observation), the ecotypes represent a case of incipient ecological speciation with no intrinsic barriers to gene-flow.

H. pusillum is a diploid plant ($2n = 24$) with a relatively small genome (1C = 1.32 pg, Temsch et al. 2010), hence well-suited for genomic and transcriptomic analyses.

Lastly, despite being a non-model system, *H. pusillum* has been the object of several past investigations (Bertel, Buchner, et al., 2016; Bertel, Hülber, et al., 2016; Bertel et al., 2018, 2017; Flatscher et al., 2012; Frajman et al., 2009; Frajman & Oxelman, 2007; Trucchi et al., 2017, 2016), demonstrating its ecological and evolutionary relevance, but also opening a number of intriguing research questions. The following paragraphs will describe *H. pusillum* in a more comprehensive way than in the single chapters and outline the major advances from previous works.

Brief systematic and biogeographic localization of *H. pusillum*

Heliosperma (Rchb.) Rchb. is a small genus of caespitose perennial herbs within the tribe Sileneae (Caryophyllaceae) that split from its sister clade *Silene* L. around 14 Myr ago (Frajman et al., 2009). A crest of long papillae on the seeds represents the unique characteristic of *Heliosperma* and gives the name to the genus (i.e. *helios* = sun and *sperma* = seed). Its distribution stretches from the Spanish Cordillera Cantabrica in the West, over the Alps and Apennines to the Carpathians in the East. The taxonomic characterization of the three main species within the genus – i.e. *H. macranthum*, *H. alpestre* and *H. pusillum* – is of complex resolution, since these three lineages result from a complex history of homoploid hybridization with closely related lineages (Frajman et al., 2009). Indeed, several species were described within *Heliosperma*. While *H. alpestre* and *H. macranthum* are morphologically well distinct from all other taxa, *H. pusillum* s.l. is more variable. In this species, two groups of lineages can be distinguished based on the elevation at which they occur: a low elevation and a high elevation one. The high elevation group includes more broadly distributed taxa that mostly grow above the timberline and are morphologically more uniform, mostly glabrous or sparsely hairy (Fig. 2b,e). This high elevation group also includes *H. pusillum* s.s (Fig. 2a-e). The low elevation group includes narrow endemics of the south-eastern Alps and the Balkan Peninsula, growing in canyons or under cliff overhangs and typically characterized by a dense indumentum (Fig. 2f,i), despite a higher level of morphological variation is present in this group (e.g. with regard to flower color).

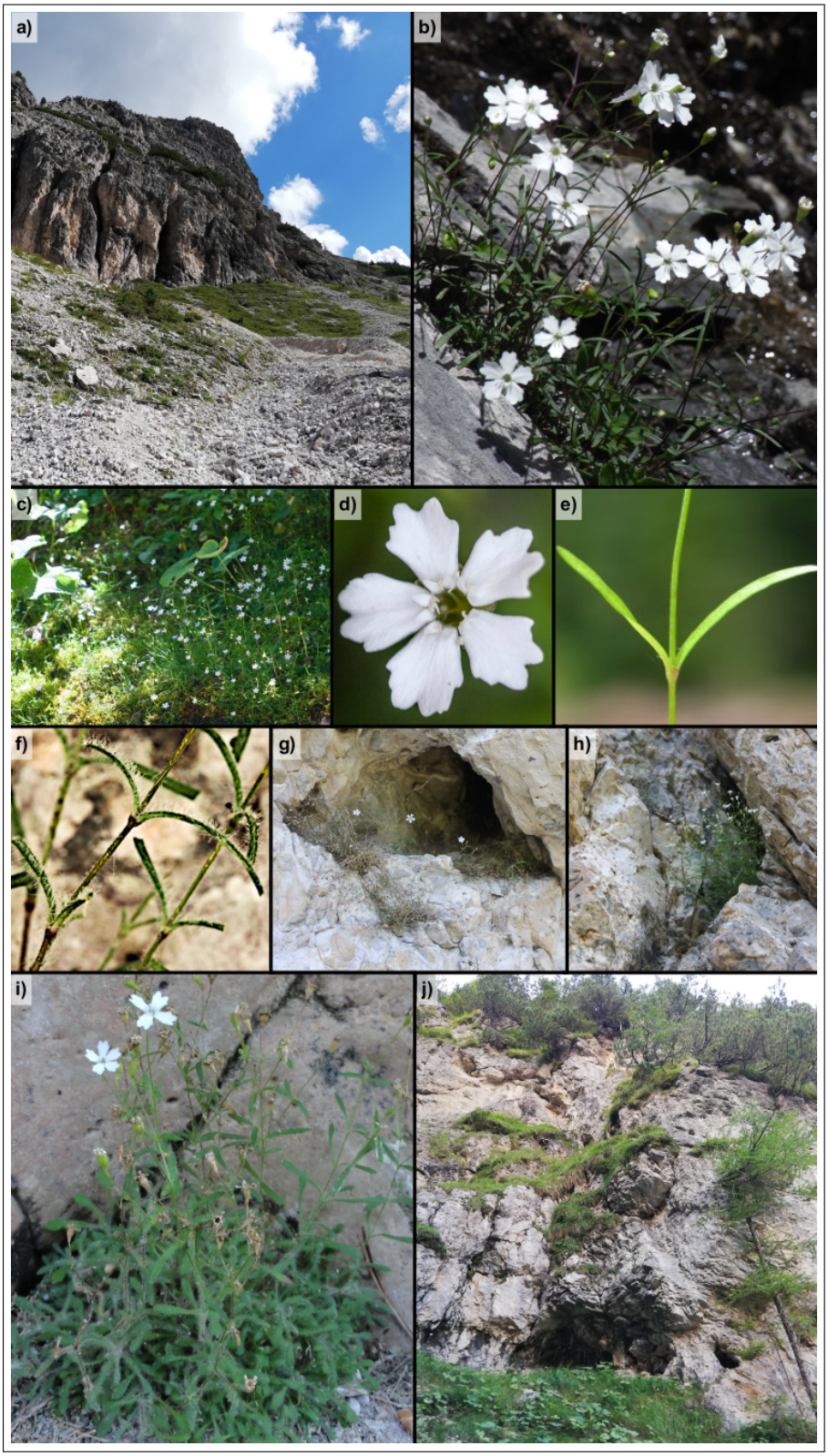
a)
b)
c)
d)
e)
f)
g)
h)
i)
j)

Fig. 2. Overview of ecotype differentiation in *H. pusillum*: alpine ecotype (a-e), montane ecotype (f-j). (a,c) Alpine rocky scree and grassland in Pragser Dolomiten (Italy). **(b,d,e)** Alpine ecotype with flower **(d)**, and glabrous leaves and stalk **(e)**. **(f,i)** Montane ecotype with pubescent leaves and stalk **(i)**. **(g,h,j)** Montane environment characterized by rock overhangs. (Photographs: A. Szukala **(a,c,g,h,j)**, M. Sonnleitner **(b,i)**, and M. Eriksson **(d,e,f)**).

One of these low elevation taxa is the montane ecotype of *H. pusillum* s.s. previously described at the species rank as *H. veselskyi* occurring in the south-eastern Alps (Fig. 2f-j). *H. pusillum* s.s. is mainly represented by the widespread alpine ecotype (Fig. 2a-e) occurring on open and moist screes (Fig. 2 a,c) across the mountain chains of central Europe, between 1,400 and 2,300 m, usually above the timberline. The montane ecotype (Fig. 2f-j) has a significantly disjoint distribution in the south-eastern Alps, with less than ten known, small populations (ca. 40-100 individuals) occurring in the montane belt (i.e. 500-1,300 m, always below the timberline) below overhanging rocks (Fig. 2g,h,j).

Ecological and morphological ecotype divergence

The environmental differentiation between alpine and montane populations features several climate parameters. Average temperatures are significantly higher at the montane sites, while higher temperature amplitude resulting from lower daily minimum and higher daily maximum were recorded in the alpine sites (Bertel, Buchner, et al., 2016). Also, significant differences in moisture (dry mountain vs. wet alpine habitats), humus content (higher in mountain vs. lower in alpine), and availability of light (shaded mountain vs. open alpine) have been recorded (Bertel et al., 2018). Further, a biotic divergence between the two habitat types has been evidenced in the phyllosphere of the plants using metagenomic approaches (Trucchi et al., 2017), whereas significantly distinct herbivore pressures are hypothesized between the niches.

Potentially as a result of the last aspect, the alpine type is mostly glabrous (Fig. 2b,e), while the montane is covered by a dense indumentum with multicellular glands releasing

sticky secretions (Fig. 2f,i, Bertel et al. 2018, 2017). It is still unclear and a debated topic if this striking differentiation in hair coverage between ecotypes results from an adaptive response to herbivory (Fig. 3), and/or drought, or represents a successful strategy to reduce seeds dispersal in the montane niche, where individuals are strictly confined to small spots below and on rocks. Further anatomical differences include the growth habit (smaller alpine vs larger montane), flower size (larger alpine vs smaller montane), leaf and cuticle thickness (thicker in alpine and thinner in montane) and stomatal density (higher in alpine vs lower in montane). Different photosynthetic rates and osmotic cellular adjustments were recorded for the two ecotypes in a common garden under uniform light, and watering conditions, respectively (Bertel, Buchner, et al., 2016). Interestingly, Bertel, Buchner, et al. (2016) also found a restricted reaction norm relative to light conditions in the alpine ecotype, suggesting the possibility of reduced plasticity in this ecotype compared to the montane one. Overall, montane populations showed higher morphological and physiological variability then alpine ones, despite equally uniform environmental conditions being measured across localities at both altitudes (Bertel et al., 2018). This observation might be in line with the history of parallel divergence of ecotype pairs across the range of co-occurrence, and suggests that parallelly evolved montane populations underwent slightly different adaptive histories.

Methodological approach: transcriptomics of plants grown in different experimental conditions

This work mainly relies on a reduced representation high-throughput sequencing technique, namely RNA sequencing (RNA-seq), widely used to track down the quantity and sequence information of transcripts in a biological sample (Griffith et al., 2015; Ozsolak & Milos, 2011). RNA-seq has several advantages compared to other technologies used to identify transcripts (e.g. microarray technology; Cieślik & Chinnaiyan 2018). For instance, it does not rely on pre-defined sequence information for transcript discovery and the amount of transcripts sequenced cannot reach saturation (i.e. as due to the scanner in microarray).

Ideally, the full amount of transcripts present in a certain cell, tissue or organism at a certain time point can be discovered and quantified using RNA-seq (Griffith et al., 2015). Also, compared to other reduced representation sequencing approaches such as restriction site associated DNA markers (RAD) and exon capture, RNA-seq has the important advantage of allowing single nucleotide polymorphism (SNPs) and indels discovery, as well as the quantification of a basic phenotype, namely gene expression, and its modifications driven by the environment.

Given these characteristics, RNA-seq appears functional to investigate distinct aspects of ecotype evolution, including demographic history, genetic variation under selection, phenotypic (i.e. expression) plasticity, and the activity of expression regulatory elements (small RNAs) affecting observed differences. In this work, we performed whole transcriptome analyses of plants grown in a common garden set-up, as well as in reciprocal transplantations at the natural growing sites, and using multiple parallelly evolved pairs of ecotypes as evolutionary replicates. Using this approach, we aimed to estimate repeatability of expression evolution across evolutionary replicates, and disentangle plastic from constitutive expression differentiation between ecotypes. The transcriptomic analyses rely on a reference genome of *H. pusillum* that was assembled and annotated within this doctoral work.

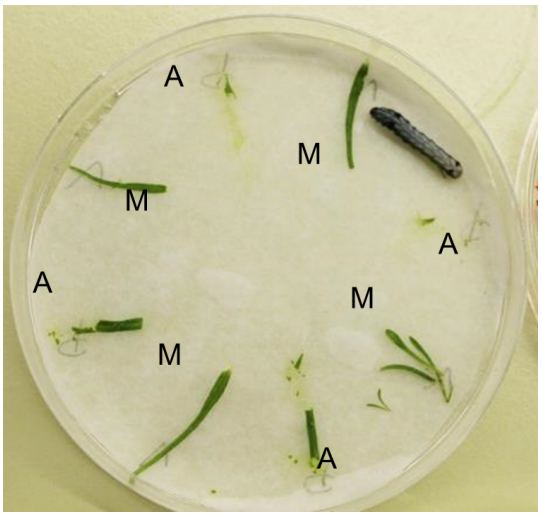

Fig. 3 Preliminary results from herbivory assays, showing that caterpillars prefer non-trichomy leaves of the alpine (A) ecotype against the montane (M) ecotype (Szukala et al., unpublished).

It is a good practice to keep in mind also the limitations connected to our method of choice. In contrast to e.g. proteomics, RNA-seq does not give information about what is effectively transcribed into proteins (i.e. post-transcriptional level). This work

partly captures the post-transcriptional level of gene expression by analyzing the targeting activity of genes by small RNAs (third chapter). For instance, if a gene is found to be differentially expressed between two conditions and is at the same time consistently differentially targeted by small RNAs, there are two lines of evidence for the differential usage of this gene in the compared groups. Still, since we miss a direct inference of metabolite levels in our analyses, we recognise that there is a certain degree of uncertainty regarding the biological interpretation of our results.

Another disadvantage concerns biological replication (Hicks et al., 2018). RNA-seq is designed for low levels of replication that are compensated via deep sequencing. Still, low numbers of biological replicates negatively affect the statistical power for variants discovery in selection scans and demographic analyses. For the latter type of analyses, it is also not ideal to deal with sites under selection (e.g. frequent purifying selection on third codon positions in protein coding regions), as well as linked loci that are affected by hitchhiking (Smith & Haigh, 1974) or background selection (Charlesworth et al., 1993). Due to these evolutionary forces, site frequency spectra can show an excess of rare variants (Nordborg et al., 1996) affecting the resulting parameters retrieved via demographic models.

Aims of the work and chapters outline

This doctoral thesis aims to advance our understanding of the molecular processes driving parallel ecotype divergence in *H. pusillum*. More specifically, we aimed to assess the degree of repeatability of the evolutionary patterns across evolutionary replicates (i.e. different ecotype pairs), in order to drive broader conclusions about parallelism in nature. The three chapters presented in this thesis deal with different drivers of divergence, but similarly aim to detect repetitive patterns among ecotype pairs. While the first chapter is focused on assessing repeatability of the evolutionary footprints of adaptation, the second, and, even more, the third chapters investigate processes that shape short-term responses but are translated into evolutionary change.

The first chapter begins by investigating the demographic history and population

genetics of four ecotype pairs, and it then goes on to assess parallelism at the level of gene expression, functional divergence, and selection outliers. Gene expression divergence is assessed by means of different methods, namely differential expression analysis (Robinson et al., 2010) and redundancy analysis (Forester et al., 2018). This double approach aims to detect both very strong expression differentiation in each pair (differential expression), as well as softer shifts in expression across pairs associated with the variable ecotype across populations (redundancy analysis). Our findings point to a low amount of shared gene expression and single nucleotide polymorphism differentiation across pairs, but recover a surprising similarity of biological functions enriched in non-shared diverged loci. In sum, this chapter uncovers highly redundant molecular patterns of ecotype differentiation, since limited parallelism at the genetic level matches pronounced parallelism at the functional one.

The second chapter aims to disentangle the roles of expression plasticity vs constitutive expression divergence shaping ecotype formation. By means of reciprocal transplantations at the natural growing sites, reaction norms of expression are depicted showing enhanced expression plasticity in the derived, montane ecotype of two ecotype pairs. Further, analyses of private genetic variation suggest that enhanced plasticity in the montane ecotype represents a derived state. Thus, our results point to an important role of plasticity shaping initial phases of ecological divergence, and possibly driving adaptive responses.

Lastly, the third chapter investigates the role of small RNAs (smRNAs) shaping transcriptional and post-transcriptional divergence and plasticity. Differential targeting by smRNAs of different genomic regions, and in particular genes, appears to vary strongly among ecotype pairs, whereas we recover again similar functions enriched in networks. Our results further suggest that smRNAs are a driving force behind previously observed differences in expression plasticity but also shape different degrees of constitutive ecotype differentiation.

1. Polygenic routes lead to parallel altitudinal adaptation

Authors: **Szukala A**, Lovegroove-Walsh J, Luqman H, Fior S, Wolfe T, Frajman B, Schoenswetter P & Paun O.

Reference: **Szukala A**, Lovegrove-Walsh J, Luqman H, Fior S, Wolfe T, Frajman B, Schönswetter P, Paun O. 2022. Polygenic routes lead to parallel altitudinal adaptation in *Heliosperma pusillum* (Caryophyllaceae). *Molecular Ecology* (in print).

Status: accepted for publication in *Molecular Ecology*.

Own contribution: performed parts of the wet lab work; performed bioinformatics analyses including structural and functional genome annotation, differential expression and redundancy analysis, demographic modelling, estimations of genetic diversity and structure, detection of selection outliers, and GO terms enrichment; derived the analytical results, and prepared result visualizations; wrote the first draft of the manuscript; revised the manuscript.

1.1. Abstract

Understanding how organisms adapt to the environment is a major goal of modern biology. Parallel evolution - the independent evolution of similar phenotypes in different populations - provides a powerful framework to investigate the evolutionary potential of populations, the constraints of evolution, its repeatability and therefore its predictability. Here, we quantified the degree of gene expression and functional parallelism across replicated ecotype formation in *Heliosperma pusillum* (Caryophyllaceae), and gained insights into the architecture of adaptive traits. Population structure analyses and demographic modelling support a previously formulated hypothesis of parallel polytopic divergence of montane and alpine ecotypes. We detect a large proportion of differentially expressed genes (DEGs) underlying divergence within each replicate ecotype pair, with a strikingly low amount of shared DEGs across pairs. Functional enrichment of DEGs reveals that the traits affected by significant expression divergence are largely consistent across ecotype pairs, in strong contrast to the non-shared genetic basis. The remarkable redundancy of differential gene expression indicates a polygenic architecture for the diverged adaptive traits. We conclude that polygenic traits appear key to opening multiple routes for adaptation, widening the adaptive potential of organisms.

Keywords: Altitudinal adaptation, *Heliosperma pusillum*, Polygenic architecture, Parallel divergence, RNA-seq, Demography, Ecotypes.

1.2. Introduction

Independent instances of adaptation with similar phenotypic outcomes are powerful avenues for exploring the mechanisms and timescale of adaptation and divergence (Agrawal, 2017; Arendt & Reznick, 2008; Buckley et al., 2019; Knotek et al., 2020; Turner et al., 2010). A broad range of parallel to non-parallel genetic solutions can be causal to phenotypic similarity. Thus, evolutionary replicates converging to a similar phenotypic optimum offer insight into the constraints on evolution and help disentangle the nonrandom or more "predictable" actions of natural selection from confounding stochastic effects such as drift and demography (Lee & Coop, 2019). In particular, repeated formation of conspecific ecotypes (Nosil et al., 2017, 2009) are pivotal to enhancing our understanding of the processes leading to adaptation in response to a changing environment.

A number of studies have shown that parallelism at the genotype level can be driven by either standing genetic variation, possibly shared across lineages through pre- or post-divergence gene flow (Alves et al., 2019; Colosimo et al., 2005; Cooper et al., 2003; Jones et al., 2012; Louis et al., 2021; Soria-Carrasco et al., 2014; Thompson et al., 2019; Van Belleghem et al., 2018), or, more rarely, by recurrent de novo mutations with large phenotypic effects (Chan et al., 2010; Hoekstra et al., 2006; Projecto-Garcia et al., 2013; Tan et al., 2020; Zhen et al., 2012). These sources of adaptive variation produce phenotypic similarities via the same genetic locus, regardless of whether it was acquired independently or present in the ancestral gene pool (Stern, 2013).

On the other hand, there is compelling evidence of phenotypic convergence resulting from non-parallel signatures of adaptation (Elmer et al., 2014; Rellstab et al., 2020; Yeaman et al., 2016), even among closely related populations (Fischer et al., 2021; Steiner et al., 2009; Wilkens & Strecker, 2003) and replicated laboratory evolution (Barghi et al., 2019). A typical example is the convergent evolution of a lighter coat pigmentation in beach mouse populations of the Gulf of Mexico and the Atlantic Coasts driven by different mutations (Steiner et al., 2009).

Such cases suggest that evolutionary replicates can follow diverse non-parallel genetic

routes and relatively few molecular constraints exist in the evolution of adaptive traits (Arendt & Reznick, 2008; Losos, 2011). The degree of parallelism during adaptation to similar selective pressures across taxa reveals that genomic signatures of adaptation are often redundant (Fischer et al., 2021; Mandic et al., 2018; Wilkens & Strecker, 2003). The evolution of phenotypic similarity can involve highly heterogeneous routes depending on variation in gene flow, strength of selection, effective population size, demographic history, and extent of habitat differentiation, leading to different degrees of parallelism (MacPherson & Nuismer, 2017; Yeaman et al., 2018). This complex range of processes including non-parallel to parallel trajectories have also been described using the more comprehensive term continuum of (non)parallel evolution (Bolnick et al., 2018; Stuart et al., 2017).

Recently, a quantitative genetics view of the process of adaptation has gained attention among evolutionary biologists (Barghi et al., 2020), complementing existing models on adaptation via selective sweeps. Accordingly, selection can act on different combinations of loci, each of small effect, leading to shifts in the trait mean through changes in multiple loci within the same molecular pathway (Hermisson & Pennings, 2017; Höllinger et al., 2019). Thus, key features of polygenic adaptation are that different combinations of adaptive alleles can contribute to the selected phenotype (Barghi et al., 2020) and that the genetic basis of adaptive traits is fluid, due to the limited and potentially short-lived contribution of individual genetic loci to the phenotype (Yeaman, 2015). This genetic redundancy (Goldstein & Holsinger, 1992; Láruson et al., 2020; Nowak et al., 1997) can lead to non-parallel genomic changes in populations evolving under the same selective pressure. Footprints of selection acting on polygenic traits have been detected in a wide range of study systems, such as in fish (Therkildsen et al., 2019) and in cacao plants (Hämälä et al., 2020), potentially fostering convergent adaptive responses and phenotypes during independent divergence events (Hämälä et al., 2020; Lim et al., 2019; Rougeux et al., 2019).

A current major challenge is predicting adaptive responses of populations and species to environmental change. Despite several advances, it is still unclear which adaptive

signatures are expected to be consistent across evolutionary replicates, especially when selection acts on complex traits. Important aspects to investigate are the architecture of adaptive traits (simple/monogenic, oligogenic or polygenic) and the repeatability of genetic responses in independent instances of adaptation (Yeaman et al., 2018). A polygenic architecture may facilitate alternative pathways leading to the same phenotypic innovation, diminishing the probability of parallel evolution at the genotype level, but likely enhancing the adaptive potential of populations at the phenotypic level (Boyle et al., 2017). To date, we observe a steady increase of plant studies addressing (non-)parallel evolution both at the genotype and phenotypic level (e.g. Bohutínská et al., 2021; Cai et al., 2019; James, Arenas-Castro, et al., 2021; James, Wilkinson, et al., 2021; Konečná et al., 2019; Rellstab et al., 2020; Roda et al., 2013; Tan et al., 2020; Trucchi et al., 2017; Yeaman et al., 2016). Still more attention should be given to specifically assessing parallelism in light of the idea of genetic redundancy that have been emphasized over the past few years.

Altitudinal ecotypes of *Heliosperma pusillum* s.l. (Waldst. & Kit.) Rchb. (Caryophyllaceae) offer a system to study this process. In the Alps, this species includes an alpine ecotype (1,400–2,300 m above sea level) widely distributed across the mountain ranges of southern and central Europe, and a montane ecotype (500–1,300 m) endemic to the south-eastern Alps (Fig. 1a). The latter was previously described from scattered localities as *H. veselskyi* Janka, but the two ecotypes are highly interfertile (Bertel, Hülber, et al., 2016) and isolation-by-distance analyses confirmed their conspecificity (Trucchi et al., 2017). While the alpine ecotype has a relatively continuous distribution in moist screes above the timberline, the montane ecotype forms small populations (typically $<$ 100 individuals) below overhanging rocks.

Previous work (Bertel, Buchner, et al., 2016; Bertel et al., 2018) reported substantial abiotic differences between the habitats preferred by the two ecotypes. For example, differences in average temperature (montane: warm vs. alpine: cold), temperature amplitude, the degree of humidity (montane: dry vs. alpine: humid) and light availability (montane: shade vs. alpine: full sunlight) were found between the two altitudinal sites.

Moreover, metagenomics (Trucchi et al., 2017) showed evidence of distinct microbial communities in the respective phyllospheres. The two ecotypes also differ significantly in their physiological response to light and humidity conditions in a common garden (Bertel, Buchner, et al., 2016). Finally, the montane ecotype is covered by a dense glandular indumentum, which is absent in the alpine populations (Bertel et al., 2017; Frajman & Oxelman, 2007).

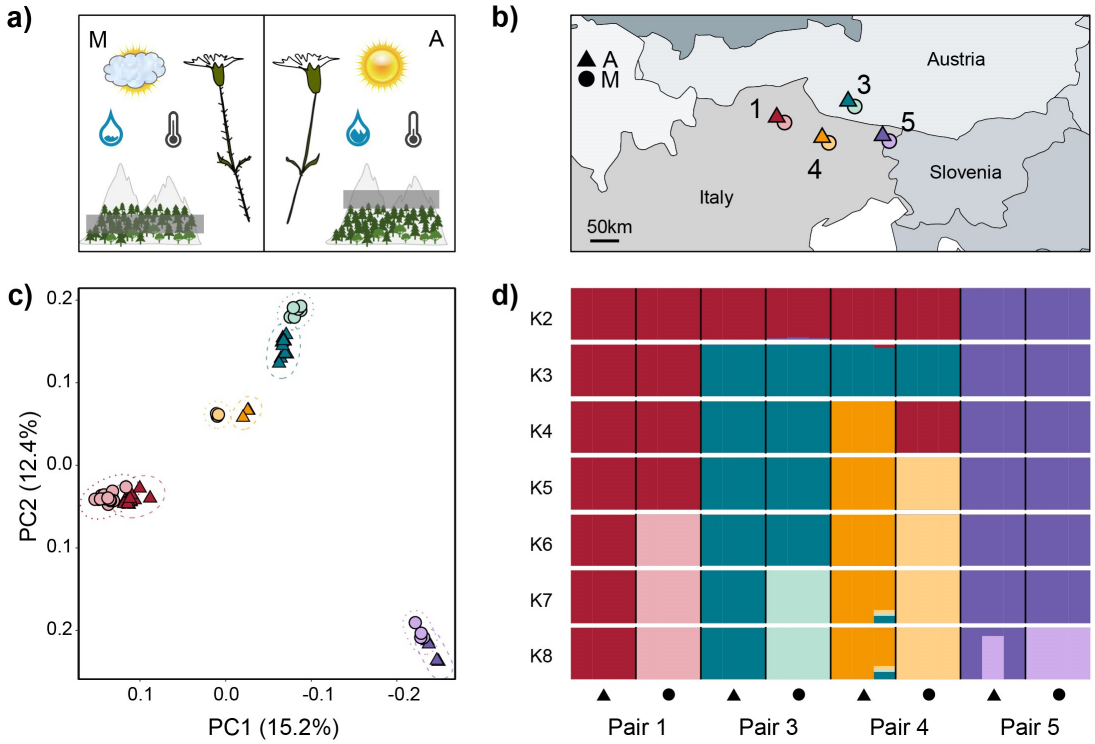

Figure 1. Study system, sampling setup, and genetic variation among four montane (M, circles) - alpine (A, triangles) ecotype pairs of *Heliosperma pusillum*. Color coding of populations is consistent across panels. The numbering of the ecotype pairs is consistent with previous work (Bertel et al., 2018). **(a)** Graphic description of the main ecological and morphological differences between the ecotypes. **(b)** Geographic map showing the location of the analyzed populations in the southeastern Alps. **(c)** Clustering of individuals along the first two vectors of a principal component analysis. **(d)** Bar plot showing the assignment of individuals to the clusters identified by NgsAdmix for K = 2 through 8.

Both ecotypes show higher fitness at their native sites in reciprocal transplantation experiments (Bertel et al., 2018), confirming an adaptive component to their divergence.

Common garden experiments across multiple generations further rejected the hypothesis of a solely plastic response shaping the phenotypic divergence observed (Bertel et al., 2017). Most importantly, population structure analyses based on genome-wide SNPs derived from restriction site-associated DNA (RAD-seq) markers (Trucchi et al., 2017) supported a scenario of five parallel divergence events across the six investigated ecotype pairs. Hereafter, we use the term "ecotype pairs" to indicate single instances of divergence between alpine and montane ecotypes across their range of co-occurrence.

The combination of ecological, morphological, and demographic features outlined above renders *H. pusillum* a well-suited system to investigate the mechanisms driving local recurrent altitudinal adaptation in the Alps. Here, we quantify the magnitude of gene expression and functional parallelism across ecotype pairs, by means of RNA-seq analyses of plants grown in a common garden. We also investigate the independent evolution of ecotype pairs more in depth than previously. More specifically, this study asks (1) how shared are gene expression differences between ecotypes among evolutionary replicates or, in other words, is the adaptation to elevation driven by expression changes in specific genes or in different genes affecting similar traits; (2) how shared is the functional divergence encoded by differentially expressed genes (DEGs) among evolutionary replicates; and (3) do we find consistent signatures of selection on coding sequence variation across evolutionary replicates?

1.3. Materials and Methods

1.3.1. Reference genome assembly and annotation

We assembled de novo a draft genome using short and long read technologies for an alpine individual of *H. pusillum* that descended from population 1, from a selfed line over three generations. DNA for long reads was extracted from etiolated tissue after keeping the plant for one week under no light conditions. DNA was extracted from leaves using a CTAB protocol adapted from Cota-Sánchez et al. (2006). Illumina libraries were prepared with IlluminaTruSeq DNA PCR-free kits (Illumina) and sequenced as 150 bp paired-end

reads on Illumina HiSeq X Ten by Macrogen Inc. (Korea). PacBio library preparation and sequencing of four SMRT cells on a Sequel I instrument was done at the sequencing facility of the Vienna BioCenter Core Facilities.

MaSuRCA v.3.2.5 (Zimin et al., 2013) was used to perform a hybrid assembly using 192.3 Gb (ca 148) Illumina paired-end reads and 14.9 Gb (ca 11.5) PacBio single-molecule long reads. The assembled genome was structurally annotated ab initio using Augustus (Stanke et al., 2006) and GeneMark-ET (Lomsadze et al., 2014), as implemented in BRAKER1 v.2.1.0 (Hoff et al., 2016) with the options *–softmasking=1 –filterOutShort*. Mapped RNA-seq data from three different samples was used to improve *de novo* gene finding.

A transcriptome was assembled using Trinity v.2.4.0 (Haas et al., 2013) to be used in MAKER−P v.2.31.10 (Campbell et al., 2014) annotation as expressed sequence tag (EST). We used as additional evidence the transcriptome of the closely related *Silene vulgaris* (Sloan et al., 2012). The annotation was further improved during the MAKER−P analyses by supplying gene models identified using BRAKER1, and by masking a custom repeat library generated using RepeatModeler v.1.0.11 (`http://www.repeatmasker.org/RepeatModeler/`). Gene models identified by both BRAKER1 and MAKER−P were functionally annotated using Blast2GO (Götz et al., 2008). BUSCO v.2.0 (Simão et al., 2015) was used for quality assessment of the assembled genome and annotated gene models using as reference the embryophyta_odb10 dataset.

1.3.2. Sampling, RNA library preparation and sequencing

Our main aim was to test the repeatability of the molecular patterns and functions that distinguish the alpine from the montane ecotype in different ecotype pairs. To achieve this goal, we performed DE analyses on 24 plants grown in common garden settings at the Botanical Garden of the University of Innsbruck, Austria. Wild seeds were collected from four alpine/montane ecotype pairs in the south-eastern Alps (Fig. 1b, Table S1). The numbering of localities is consistent with that used in Bertel et al. (2018) and the acronyms corresponding to Trucchi et al. (2017) are added in Table S1. All seeds were set

to germination on the same day and the seedlings were grown in uniform conditions. One week before RNA fixation, the plants were brought to a climate chamber (Percival PGC6L set to 16 h 25 °C three lamps/8 h 15 °C no lamps). Then, fresh stalk-leaf material, sampled at a similar developmental stage for all individuals, was fixed in RNAlater in the same morning and kept at -80 °C until extraction. Total RNA was extracted from ca 90 mg leaves using the mirVana miRNA Isolation Kit (Ambion) following the manufacturer's instructions. Residual DNA has been digested with the RNase-Free DNase Set (Qiagen); the abundant ribosomal RNA was depleted by using the Ribo-Zero rRNA Removal Kit (Illumina). RNA was then quantified with a NanoDrop2000 spectrophotometer (Thermo Scientific), and quality assessed using a 2100 Bioanalyzer (Agilent). Strand-specific libraries were prepared with the NEBNext Ultra Directional RNA Library Prep Kit for Illumina (New England Biolabs). Indexed, individual RNA-seq libraries were sequenced with single-end reads (100 bp) on 11 lanes of Illumina HiSeq 2500 at the NGS Facility at the Vienna BioCenter Core Facilities (VBCF; `https://www.viennabiocenter.org/`). Two samples (A1a and A4b) were sequenced with paired-end reads (150 bp) with the initial aim of assembling reference transcriptomes.

To identify genetic variants under selection we extended the sampling by including 41 additional transcriptomes of individuals from ecotype pairs 1 and 3 (Fig. 1b) grown in a transplantation experiment (Chapter 2 of this thesis; Table S1). The procedure used to prepare the RNA-seq libraries was the same as described above, except that the indexed, individual libraries have been sequenced with single-end reads (100 bp) on Illumina NovaSeq S1 on 2 lanes at the Vienna BioCenter Core Facilities.

1.3.3. Genetic diversity and structure

RNA-seq data was demultiplexed using BamIndexDecoder v.1.03 (`http://wtsi-npg.github.io/illumina2bam/#BamIndexDecoder`) and raw sequencing reads were cleaned to remove adaptors and quality filtered using trimmomatic v.0.36 (Bolger et al., 2014). Individual reads were aligned to the reference genome using STAR v.2.6.0c (Dobin et al., 2013). Mapped files were sorted according to the mapping position and duplicates

were marked and removed using Picard v.2.9.2 (`https://broadinstitute.github.io/picard/`). The individual bam files were further processed using GATK v.3.7.0 function IndelRealigner to locally improve read alignments around indels. Subsequently, we used a pipeline implemented in ANGSD v.0.931 (Korneliussen et al., 2014) to estimate genotype likelihoods. The latter might be more reliable than genotype calling for low coverage segments, in particular when handling data with strongly varying sequencing depth among regions and individuals such as RNA-seq. Briefly, ANGSD was run to compute posterior probabilities for the three possible genotypes at each variant locus (considering only bi-allelic SNPs), taking into account the observed allelic state in each read, the sequencing depth and the Phred-scaled quality scores. ANGSD was run with the options *-GL 2 -doMajorMinor 1 -doMaf 1 -SNP_pval 2e-6 -minMapQ 20 -minQ 20 -minInd 12 -minMaf 0.045 -doGlf 2*. A significant portion of RNA-seq data includes protein coding regions expected to be under selection. To investigate genetic structure and demography the dataset was further filtered to keep genetic variants at four-fold degenerate (FFD) sites using the Bioconductor package VariantAnnotation in R (Obenchain et al., 2014).

A covariance matrix computed from the genotype likelihoods of FFD variants at unlinked positions (i.e., one per 10 Kb windows) was used for principal component analysis using PCAngsd v.0.99 (Meisner & Albrechtsen, 2018). To test for admixture, we run NgsAdmix (Skotte et al., 2013) on genotype likelihoods at FFD unlinked sites. The number of clusters tested for the admixture analysis ranged from K = 1 to K = 9. The seed for initializing the EM algorithm was set to values ranging from 10 to 50 to test for convergence. Finally, the K best explaining the variance observed in the data was evaluated using the Evanno method (Evanno et al., 2005) in CLUMPAK (`http://clumpak.tau.ac.il/bestK.html`). Result plotting was performed using R v.3.5.2.

For each population we estimated the average global Watterson's theta (θw) and average pairwise nucleotide diversity (π). Estimates were based on the maximum likelihood of the folded SFS calculated with realSFS in ANGSD using *-minQ 20* and *-minMapQ 30*. We computed the estimates implementing a sliding window approach with windows of 50 Kb and a step of size 10 Kb and divided each window estimate by the number of

variant and invariant sites covered by data in that window. To test for departures from mutation/drift equilibrium we computed Tajima's D (Tajima 1989) based on the estimates of π and θw. We estimated between-population differentiation as F_{st} for all pairs of populations at high and low elevation respectively, as well as for pairs of ecotypes across localities. F_{st} statistics were carried out in ANGSD using the folded joint site frequency spectra (jSFS) for all population pairs as summary statistics. Given that no suitable outgroup sequence was available, the ancestral state was unknown. As a consequence, we observed a deviation from the expected SFS for some populations (i.e. a high frequency of sites with fixed alternate alleles) when polarizing toward the major allele throughout the alpine populations. Therefore, we produced site allele frequency likelihoods using ANGSD settings *-dosaf 1 -GL 2 -minQ 20 -P 8 -skipTriallelic 1 -doMajorMinor 1 -anc reference.genome.fasta*, limiting the analysis to the set of FFD sites using the *-sites* option. Finally, we used the *-fold* option to fold the spectra when using realSFS (for further analyses in ANGSD), and using a custom R script to fold the spectra into fastsimcoal2 format (for coalescent simulations in fastsimcoal2).

1.3.4. Testing alternative demographic scenarios

We performed coalescent simulations to differentiate between two different possible explanations behind the patterns of genetic structure observed. One possible scenario implies multiple, polytopic divergence events between the ecotypes, whether or not gene flow was involved. Another possibility is that the two ecotypes diverged only once, whereas subsequent gene flow between ecotypes in each pair could have homogenized their genetic background. Therefore, we tested two contrasting topologies for each combination of two ecotype pairs (Fig. 2): one model assuming a single origin (1-origin) of each ecotype, and one assuming independent between-ecotype divergence across geographic localities (2-origins). Additionally, for each topology two scenarios were evaluated: one in absence of migration between populations (strict isolation, SI) and one with continuous migration between demes (isolation with migration, IM). In line with the results from the population structure analyses our expectation was to find higher migration rates between ecotypes

within each ecotype pair (solid lines in Fig. 2).

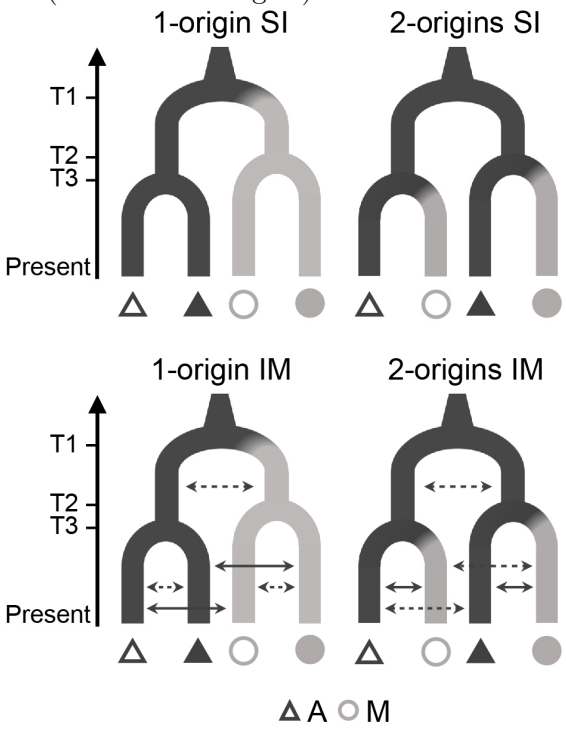

Figure 2. Alternative topologies tested using Fastsimcoal2 for all combinations of two ecotype pairs. Strict isolation (SI, upper panels) and isolation with migration (IM, lower panels) were modeled. Solid arrows in the IM models indicate higher migration rates expected between ecotypes at each locality according to population structure results. Divergence times T2 and T3 were allowed to vary (i.e., T2 > T3 but also T3 > T2 were modeled), whereas T1 was always the oldest event. Triangles and circles represent populations of the alpine (A) and the montane (M) ecotype, respectively. Filled and empty symbols represent different ecotype pairs.

We evaluated which demographic scenario (1-origin vs 2-origins) explains our data using fastSimcoal2 v.2.6.0.3 (Excoffier et al., 2013). We tested four populations at a time, i.e. with two ecotype pairs in each simulation, using for each analysis the jSFS for all six combinations of populations as summary statistics. For all models we let the algorithm estimate the effective population size (N), the mutation rate (μ) and the time of each split (T1, T2 and T3, Fig. 2). Although N, μ and the time of split between ecotypes in each pair have been previously estimated by Trucchi et al. (2017), we started with broad search ranges for the parameters to not constrain a priori the model. The final priors of the simulations were set for a mutation rate between 1e-8 and 1e-10, the effective

population size between 50 and 50,000 (alpine populations) and 50 and 5,000 (montane populations), and for the time of each split between 1,000 and 100,000 generations ago. We forced T1 to predate T2 and T3, and performed separate simulations setting T2 > T3 and T3 > T2, respectively. For the models including gene flow, migration rate (m) between any pair of demes was initially set to a range between 10e-10 and two.

The generation time in *H. pusillum* was reported to be 1 year (Flatscher et al., 2012; Trucchi et al., 2017). While most populations in the montane zone flower during the first year after germination, this is not the case in the alpine environment, where plants usually start to flower in the second year after germination. Therefore, 1 year is most likely an underestimation of the intergeneration interval, which is more realistically around 3 years. While this parameter does not affect the overall results in terms of topology, it should be considered carefully in terms of divergence times between ecotypes that were previously hypothesized to be post-glacial (Flatscher et al., 2012; Trucchi et al., 2017).

FastSimcoal2 was run excluding monomorphic sites (*-0* option). We performed 200,000 simulations and ran up to 50 optimizations (ECM) cycles to estimate the parameters. To find the global optimum of the best combination of parameter estimates, we performed 60 replicates of each simulation run. The MaxEstLhood is the maximum estimated likelihood across all replicate runs, while the MaxObsLhood is the maximum possible value for the likelihood if there was a perfect fit of the expected to the observed site frequency spectrum. We report the difference between these two estimates (ΔL) for each model and ΔAIC scores (i.e., the difference between the AIC for the best possible model and the tested model) to compare models with different numbers of parameters. Finally, the parameter estimations of the best run were used to simulate the expected jSFS and test the goodness of fit of the topology plus parameter estimates to the observed data.

1.3.5. Differential gene expression analysis

Only unique read alignments were considered to produce a table of counts using FeatureCounts v.1.6.3 (Liao et al., 2014) with the option *-t gene* to count reads mapping to gene features. DE analyses were performed using the Bioconductor package EdgeR v.3.24.3

(Robinson et al., 2010). The count matrix was filtered, keeping only genes with mean counts per million (cpm) higher than 1. Data normalization to account for library depth and RNA composition was performed using the weighted trimmed mean of M-values (TMM) method. The estimateDisp() function of edgeR was used to estimate the trended dispersion coefficients across all expressed tags by supplying a design matrix with ecotype pair and ecotype information for each sample. We implemented a generalized linear model (glm) to find gene expression differences between low and high elevation ecotypes by taking into account the effects of the covariates ecotype and ecotype pair on gene expression. A likelihood ratio test (lrt) was used to test for DE genes between ecotypes in each pair. The level of significance was adjusted using Benjamini-Hochberg correction of p-values to account for multiple testing (threshold of FDR < 0.05). The statistical significance of the overlaps between lists of DEGs was tested using a hypergeometric test implemented in the Bioconductor package SuperExactTest (M. Wang et al., 2015) and the number of genes retained after trimming low counts as background. Finally, to compare the repeatability of gene usage in DEGs to the neutral expectation and to the repeatability of selection outliers detected (see below), we computed the Jaccard index for any two ecotype pairs and the C-hypergeometric score metric that was specifically developed with the scope of comparing repeatability of the evolutionary process across multiple lineages (Yeaman et al., 2018).

1.3.6. Functional interpretation of DEGs

We performed separate gene ontology (GO) enrichment analyses for the lists of DEGs of each ecotype pair and gave special attention to functions that were shared among lists of DEG. We also performed similar GO terms enrichments after excluding any DEGs shared between at least two ecotype pairs. This additional analysis was performed to clarify if sets of fully non-shared DEGs would result in similar enriched functions. Fisher test statistics implemented in the Bioconductor package topGO v.2.34.0 (`https://bioconductor.org/packages/release/bioc/html/topGO.html`) were run with the algorithm "weight01" to test for over-representation of specific functions conditioned on neighbouring terms.

Multiple testing correction of p-values (FDR correction) was applied and significance was assessed below a threshold of 0.05. DEGs were also explicitly searched for protein coding genes and transcription factors underlying the formation of trichomes and visually checked using R.

1.3.7. Detection of multilocus gene expression variation

To detect gene expression changes underlying adaptive traits with a strongly polygenic basis we performed a conditioned (partial) redundancy analysis (cRDA) of the gene expression data using the R package vegan v.2.5-6 (Oksanen et al., 2019). The cRDA approach is well suited to identify groups of genes showing expression changes that covary with the "ecotype" variable while controlling for population structure (Bourret et al., 2014; Forester et al., 2018). As a table of response variables in the cRDA we used the cpm matrix after filtering using a mean cpm higher than 1 as in the DE analysis. First, the cRDA includes a multiple regression step of gene expression on the explanatory variable "ecotype". In our case, the RDA was conditioned to remove the effects of the geographic ecotype pair using the formula "$\sim$ ecotype + Condition(pair)". In the second step, a principal component analysis (PCA) of the fitted values from the multiple regression is performed to produce canonical axes, based on which an ordination in the space of the explanatory variable is performed. The first axis of the cRDA therefore shows the variance explained by the constrained variable "ecotype", while the second axis is the first component of the PCA nested into the RDA, representing the main axis of unconstrained variance. The significance of the cRDA was tested with ANOVA and 1,000 permutations. Each gene was assigned a cRDA score that is a measure of the degree of association between the expression level of a gene and the variable "ecotype". Outliers were defined as genes with scores above the significance thresholds of $\pm$ 2 and, respectively, $\pm$ 2.6 standard deviations from the mean score of the constrained axis, corresponding to p-value thresholds of 0.05 and 0.01, respectively.

1.3.8. SNPs calling and detection of selection outliers

To detect outlier genetic variants potentially under divergent selection during ecotype adaptation to different elevations, we computed per locus F_{st} based on the sfs of the genotype likelihoods computed in ANGSD. Selection outliers analyses were carried out on ecotype pairs 1 and 3, for which we had a minimum of 10 individuals in each population analyzed. To account for low coverage values in DEGs, a site would be retained if a minimum low coverage of four would be found in at least seven individuals. Consequently, ANGSD was run with the options *-dosaf 1 -GL 2 -minQ 20 -MinMapQ30 -skipTriallelic 1 -doMajorMinor 1 -doCounts 1 -setMinDepthInd 4 -minInd 7 -setMaxDepthInd 150*. We then computed the sfs using the *-fold 1* option and ran the ANGSD script realSFS with the option *-whichFst 1* to compute the Bathia et al. (2013) F_{st} estimator by gene following the procedure described at `https://github.com/ANGSD/angsd/issues/239`. We then defined as F_{st} outliers those loci falling in the top 5% of the F_{st} distribution. To understand if DEGs carry stronger signatures of selection than other genes, we compared the F_{st} distribution of 1,000 randomly selected genes to the F_{st} distribution of DEGs and tested the difference in mean using a permutation test. Finally, we computed the Jaccard index and C-hypergeometric score (Yeaman et al., 2018) to compare repeatability in selection outliers to the repeatability in usage of DEGs.

1.4. Results

1.4.1. Reference genome assembly and annotation

Our hybrid *de novo* genome assembly recovered a total length of 1.21 Gb of scaffolds corresponding to 93% of the estimated genome size (1C = 1.3 pg; Temsch et al. 2010). The draft *H. pusillum* genome v.1.0 was split into 75,439 scaffolds with an N50 size of 41,616 bp. RepeatModeler identified 1,021 repeat families making up roughly 71% of the recovered genome. This high proportion of repetitive elements aligns well with observations in other plant genomes. Structural annotations identified 25,661 protein-coding genes with an average length of 4,570 bp (Fig. S2a and b). All protein-coding genes were found

on 8,632 scaffolds that belong to the longest tail of the contig length distribution (Fig. S2c). Nevertheless, we also observed in our assembly comparatively long contigs that do not contain any gene models (Fig. S2c). Of the total set of genes, 17,009 could be functionally annotated (Götz et al., 2008; Haas et al., 2013). When running BUSCO on the annotated mRNA, a total of 82.4% of the set of single-copy conserved BUSCO genes were found. A BUSCO search on the part of the genome remaining after hard masking genes, could still identify 9.6% conserved BUSCO orthologs within 'non-genic' regions. This Whole Genome Shotgun project has been deposited at DDBJ/ENA/GenBank under the accession JAIUZE000000000.

1.4.2. Genetic diversity and structure

Two alpine individuals of pair 3 (A3b and A3c, Table S1) were found to be highly introgressed with genes from the alpine population of pair 4 (Fig. S1a), and have been discarded from subsequent genetic analyses, retaining a total of 63 individuals for further analyses based on SNPs. This dataset was also used to test the hypothesis of parallel ecotype divergence in *H. pusillum* suggested by Trucchi et al. (2017).

Within-population allelic diversity (average pairwise nucleotide diversity, π, and Watterson's theta, θw), Tajima's D, as well as F_{st}, are reported in Table S2. Average π showed similar values across alpine and montane populations, ranging from π_{A4} = 0,0016 $\pm$ 0.0012 to π_{A1} = 0.0032 $\pm$ 0.0016 in the alpine ecotype, and from π_{M4} = 0.0016 $\pm$ 0.0012 to π_{M1} = 0.0026 $\pm$ 0.0015 in the montane. Watterson's theta ranged from θw_{A4} = 0.0015 $\pm$ 0.0012 to θw_{A1}= 0.0033 $\pm$ 0.0016 and from θw_{M4} = 0.0016 $\pm$ 0.0011 to θw_{M1} = 0.0027 $\pm$ 0.014 in the alpine and montane ecotype, respectively. We did not observe a clear alpine versus montane distinction of within-population allelic diversity. Global Tajima's D estimates were always close to 0 (Table S2, Fig. S3), suggesting that these populations are within neutral-equilibrium expectations, and that both alpine and montane populations were not affected by major changes in population size in the recent past.

To explore F_{st} and population structure we filtered a dataset of 7,107 putatively neutral

variants at unlinked FFD sites from 63 individuals representing the four ecotype pairs (Fig. 1b, Table S1). Averaged pairwise F_{st} tended to be slightly higher between montane than between alpine populations (weighted F_{st} = 0.28-0.56 for alpine, and weighted F_{st} = 0.39-0.52 for montane; Table S2). Between-ecotypes F_{st} was lower than F_{st} between pairs, except in the case of pair 4 (weighted F_{st} = 0.48), consistent with overall high expression differentiation between ecotypes in this pair as described below.

We further investigated the population structure with principal component analyses (PCA) and an admixture plot, both based on genotype likelihoods computed in ANGSD. In the PCA (Fig. 1c) the analyzed populations cluster by geography, in line with previous results (Trucchi et al. 2017). The first component (15.2% of explained variance, Fig. 1c) shows a clear east-west separation of the ecotype pairs. The second component (12.4% of explained variance, Fig. 1c) places ecotype pair 5 closer to pair 1 and most distant from pair 3 showing a north-south separation.

We performed two rounds of population structure inference to test the effects of uneven sample size on the inferred clusters. We compared the results inferred using the set of 63 accessions to those inferred when randomly subsampling all populations to three individuals (i.e., the minimum number of individuals per population in our dataset). With uneven sampling, we observed that the individuals from populations with reduced sampling size (i.e., ecotype pair 4) tended to be assigned to populations of higher sampling density (Fig. S1b), an otherwise known problem affecting population structure analyses (Meirmans, 2019; Puechmaille, 2016). Consistent with the clustering observed in the PCA, pair 5 was first separated from the other pairs (K = 2, Fig. 1d). The best three Ks were 2, 3 and 7, in this order, confirming an enhanced separation of pair 5 from the rest, while the two ecotypes in this pair are the least diverged (K = 7, Fig. 1d), consistent with a lower degree of expression differentiation in this pair (Fig. 3).

1.4.3. Demographic model selection, parallelism and gene flow

Delta Akaike information criteria (ΔAIC) for each demographic model tested in fastSimcoal2 are summarized in Table S3a and c. In the absence of gene flow (SI models),

our simulations consistently showed that the 2-origins topologies are preferred over the 1-origin hypotheses. However, IM models (i.e., allowing gene flow) always achieved a higher likelihood than SI models (Table S3a). The 2-origins IM scenario again achieved a better likelihood in five out of six ecotype pairs comparisons. The 1-origin IM model was preferred for pairs 3-4. For each parameter we took as a final estimate the 95% confidence intervals CI of the ten best model estimates. The CI of the times of divergence and effective population size (Ne) from the best model estimates are reported in Table S3b. We computed migration rate estimates for each model including both directions of migration for all combinations of ecotype populations from two pairs (Table S3d). We found migration rates to be very low across all comparisons and scenarios tested (upper limit of the CI always below 0.015); generally they were estimated to be lower between different ecotype pairs than between ecotypes in each pair (Table S3d).

1.4.4. Patterns of differential gene expression between ecotypes

We analyzed gene expression in a common garden to identify genes with divergent expression between ecotypes, as these are hypothesized to underlie phenotypic differentiation and adaptation to different altitudinal niches. After trimming genes with low expression across samples we retained a dataset of 16,389 genes on which we performed DE analyses.

A major proportion of DEGs were found to be unique to each pair (colored area of the bars in Fig. 3a and b). This pattern was particularly enhanced in pair 5, in which ca 85% of DEGs were not shared with other pairs, while ca 70%, 65% and 80% of DEGs were unique to pairs 1, 3 and 4, respectively (Fig. 3, Fig. S4). Although the overlap of DEGs was significantly higher than chance expectations ($p < 0.01$) for several comparisons, our analyses recovered an overall low number of shared DEGs. In contrast to expectations, we found across all ecotype pairs that only two and zero genes were consistently over- and under-expressed in the montane compared to the alpine ecotype, respectively. Consistently, Jaccard similarity indexes computed for any two ecotype pairs were very low, lying between 0.005 and 0.09 (Table S4). Given the null expectation that any gene in our trimmed dataset could contribute to ecotype divergence (i.e., background

set including 16,389 genes), C-hypergeometric scores across all pairs were equal to 8.46 and 9.16 for genes under- and overexpressed in the montane ecotype compared to the alpine.

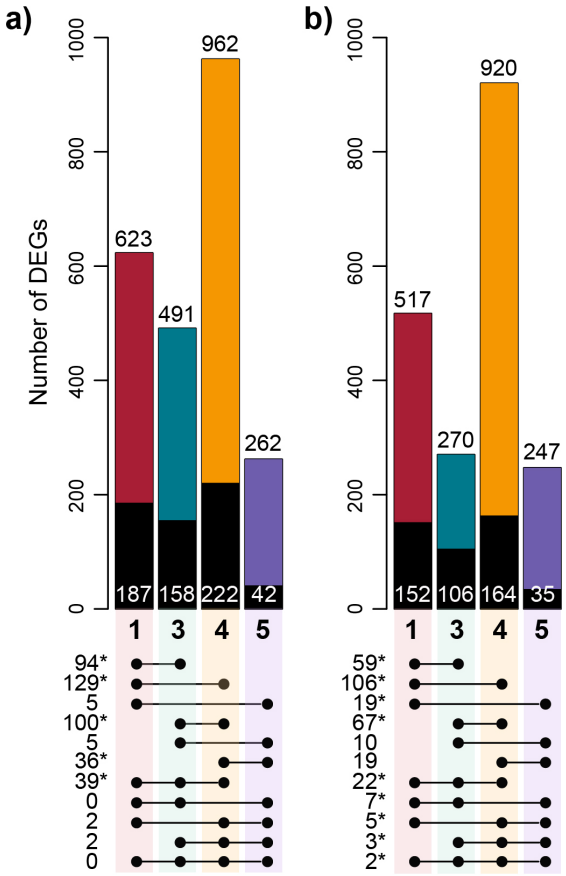

Figure 3. Differentially expressed genes (DEGs) at each ecotype pair show low overlap across different pairs. Colors represent the ecotype pair as in Fig. 1. Histograms show the number of DEGs (FDR < 0.05) underexpressed **(a)** and overexpressed **(b)** in the montane ecotype compared to the alpine in each pair. Colored and black areas of the bars show the amount of DEGs unique to each ecotype pair and, respectively, shared with at least one other pair. Numbers reported on top of the bars show the total amount of DEGs between ecotypes per pair and category. Numbers on the black areas show the amount of DEGs shared with at least one other pair. Linked dots below bars show the amount of shared DEGs between two, three or four pairs. Stars indicate that the overlap is significantly higher than chance expectations (hypergeometric test, $p < 0.01$).

The number of DEGs varied relatively widely across ecotype pairs. DEGs were almost four times higher in pair 4 (highest degree of expression differentiation) compared to

pair 5 (lowest degree of expression differentiation), while the difference in DEGs was less pronounced between pairs 1 and 3. This result is consistent with the PCA of normalized read counts (Fig. S5a) and the multidimensional scaling plot of gene expression (Fig. S5b). The relative degree of expression differentiation between ecotypes at different geographic localities is also consistent with their degree of genetic differentiation (F_{st}, Table S2). The second component of the PCA of gene expression (13.8% of variance explained, Fig. S5a), as well as the second dimension of logFC of the multidimensional scaling analysis (Fig. S5b), tend to separate the two ecotypes. Interestingly, gene expression appears more uniform across the montane accessions compared to the alpine ones, even if the overall expression divergence between different populations was not significantly different between ecotypes (Wilcoxon signed rank test $p = 0.56$; Fig. S6 and Table S5).

1.4.5. Parallel multilocus gene expression variation

We performed a cRDA of gene expression to elucidate if a different analytical framework would provide more power to detect common genes with opposite expression patterns between ecotypes across all evolutionary replicates. Redundancy analysis is thought to be a good approach to detect changes between conditions (in our case, ecotypes), even when such differences are subtle and possibly masked by other factors (Forester et al., 2018).

We found that 1.8% of total expression variation was explained by divergence between montane and alpine ecotypes across all ecotype pairs (Fig. 4), consistent with the low overlap of DEGs across evolutionary replicates. Also consistent with the low number of shared DEGs, the ANOVA test of the full model was not significant ($F = 1.39$, $p = 0.18$), confirming that most expression differences between ecotypes in our dataset do not follow consistent routes across ecotype pairs. We further searched for cRDA outliers to identify genes with consistent, albeit subtle, changes in expression across ecotypes. The transcript score was transformed into a z-score with a distribution ranging from -3.55 to 3.43 (Fig. S7). We identified 115 genes at a significance level $p < 0.01$ (2.6 SD), and 739 at a significance $p < 0.05$ (2 SD) with an outlier expression between the two ecotypes that was consistent across all pairs. Overlaps with DEGs identified in edgeR are reported

in Fig. S8.

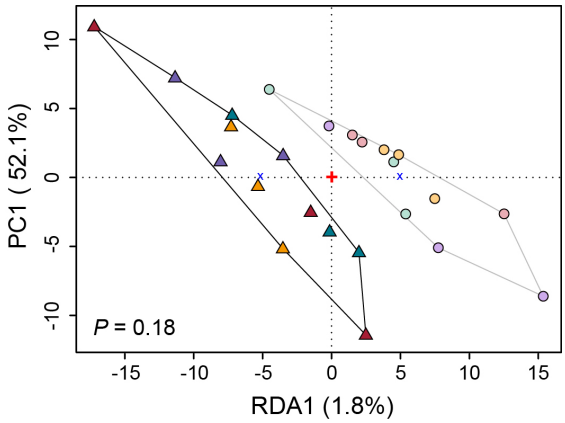

Figure 4. Expression divergence between accessions of the alpine and the montane ecotypes captured with conditioned redundancy analysis (cRDA). Colors represent the populations as in Fig. 1. Triangles and circles represent alpine (A) and montane (M) individuals, respectively, whereas the black and grey lines delimited clusters correspond to the alpine and the montane ecotypes, respectively. The ANOVA test of the full model was not significant ($p = 0.18$), confirming that most expression differences between ecotypes in our dataset do not follow consistent routes across ecotype pairs.

1.4.6. Ecological and biological significance of DEGs

In stark contrast to the low overlap at the level of individual genes affected by DE, we observed evidence of convergence in the enriched biological functions across DEG lists of each ecotype pair. To allow easier interpretation, we exemplify in Fig. 5 a subset of the significantly enriched GO terms that can be easily related to the ecological and morphological ecotype divergence. Enrichments among all DEGs (Fig. 5a, Table S6a), but also after excluding shared DEGs (Fig. 5b, Table S6b) are reported. We observed that GO terms enriched (adjusted $p < 0.05$) in genes that were differentially expressed without exclusion of shared DEGs included trichome development, light and cold response, drought response including regulation of stomatal activity, responses to biotic stress and plant growth (Fig. 5a, Table S6a). These enrichments appeared to be largely consistent

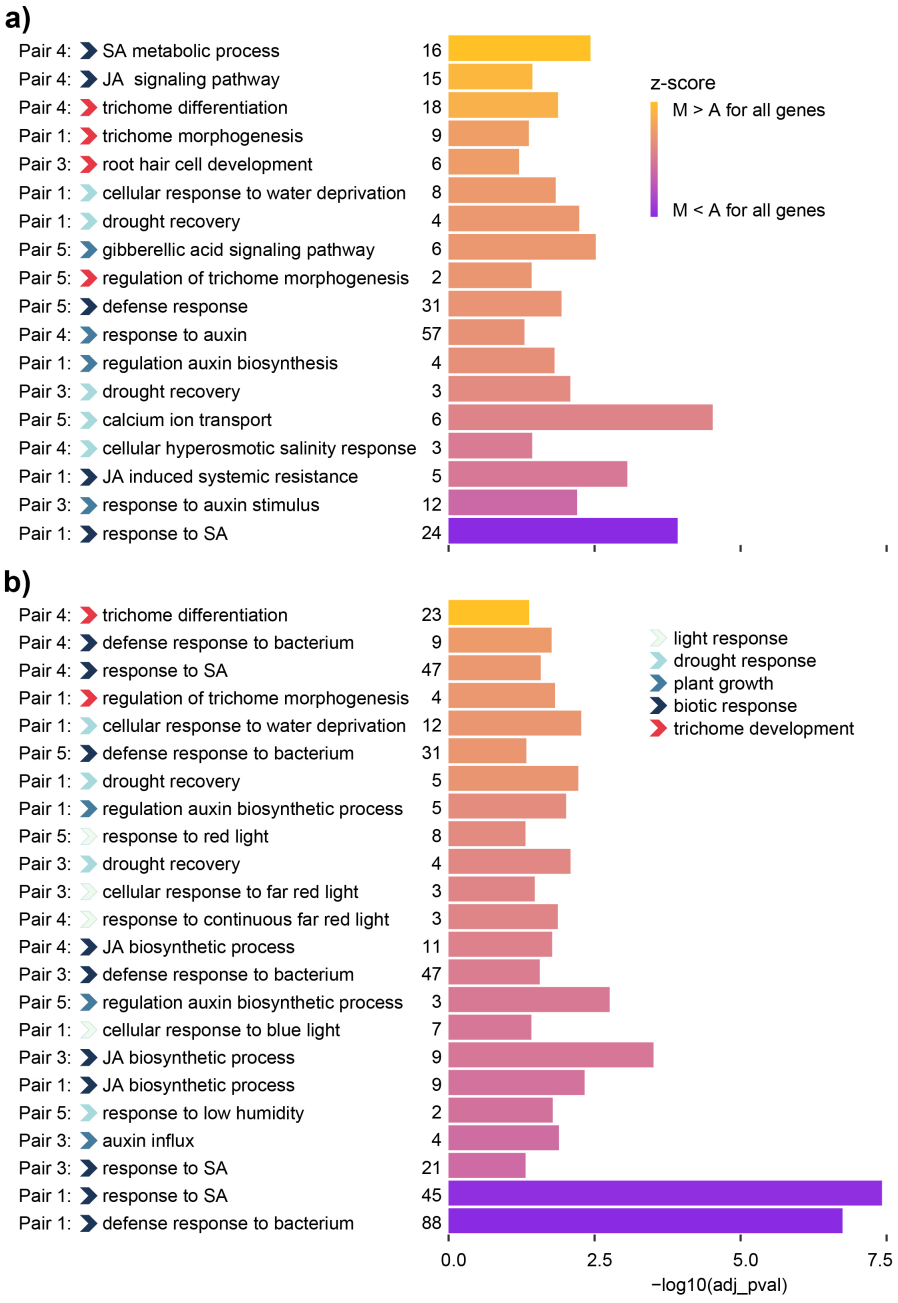

Figure 5. Functional enrichment of differentially expressed genes (DEGs), showing that across ecotype pairs similar biological processes appear linked to adaptation to the different elevations. GO terms enrichment including all DEGs (a) and excluding shared DEGs (b). The ecotype pair in which a certain term is found to be enriched is specified on the left side of the plots. The broad category to which the GO terms pertain is indicated with colored arrows, according to the legend. The size of the bars shows the adjusted significance of the enriched GO terms (Fisher's test). Numbers left of the bars show the number of DEGs underlying the corresponding GO term. The z-score (color scale of the bars) was computed based on the log fold-change of gene expression, whereas positive and negative values show over- and underexpression in the montane ecotype respectively. ABA, abscisic acid; JA, jasmonic acid; UV, ultraviolet radiation.

among the different ecotype pairs, even after excluding the shared DEGs (Fig. 5b, Table S6b). The z-score indicated that the GO terms related to trichome development were represented by genes that tended to be overexpressed in the montane ecotype (Fig. 5a and b), while the overall degree of over- and underexpression of genes underlying other convergent GO terms across pairs varied depending on the specific function of the genes affecting the respective molecular pathway. We also analyzed enriched biological processes in cRDA gene outliers (Table S7), since these genes possibly underlie biologically and ecologically relevant adaptive traits. Consistent with the DE results, cRDA outlier genes were significantly enriched for defense responses, including jasmonic and salicylic acid related pathways, as well as response to light, cold, ozone and water deprivation.

In the GO enrichment analysis of the cRDA outliers we did not find significantly enriched GO terms related to trichome development. Consistently, the genes underlying this trait identified in DE analyses were not shared by different ecotype pairs. We observed that some genes known to be involved in trichome formation in *A.thaliana* and found to be expressed in our transcriptomes were significantly differentially expressed in some of the ecotype pairs but not in others, or showed consistent changes in expression between ecotypes even if not significant after FDR correction (examples shown in Fig. 6). For instance, the gene IBR3, a Indole-3-butyric acid response gene, known to promote hair elongation (Strader et al., 2010; Velasquez et al., 2016) was always overexpressed in the montane ecotype as compared to the alpine (Fig. 6). This same gene was also significantly differentially expressed in three out of four ecotype pairs in previous DEG analyses before correction of p-values for multiple testing (Fig. 6).

1.4.7. (Non-)Shared adaptive outlier loci

To identify possible candidate genes under divergent selection in independent divergence events, we searched for coding genomic regions with pronounced allelic divergence between ecotypes in pairs 1 and 3. We excluded ecotype pairs 4 and 5 from this analysis because of the low number of individuals available from these populations.

Two sets of 3,300 and 2,811 genes were retained in pair 1 and 3, respectively, for F_{st}

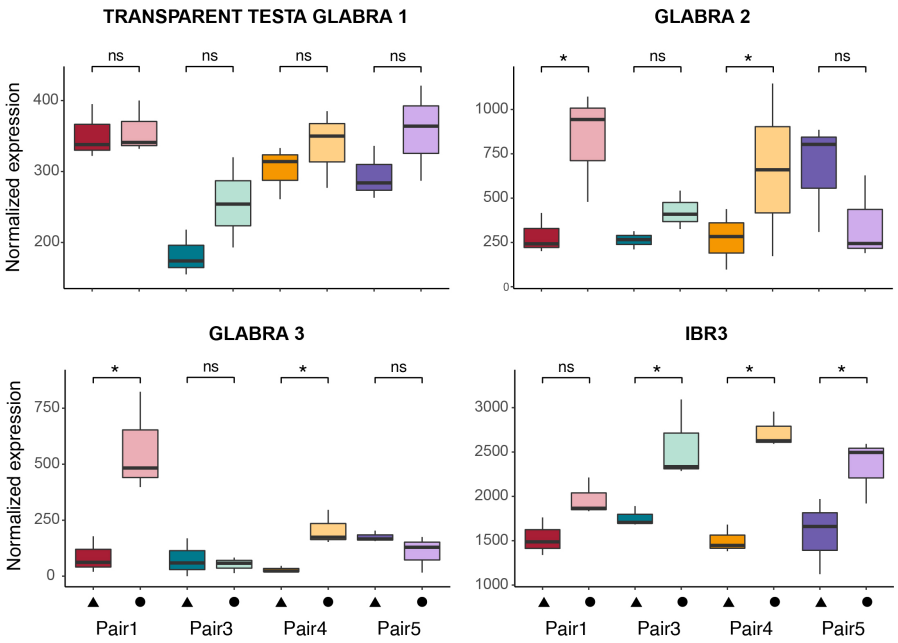

Figure 6. Examples of expression of genes known to be related to trichome formation and elongation in plants. Colors represent the populations as in Fig. 1. Triangles and circles represent populations of the alpine (A) and the montane (M) ecotype, respectively. Stars indicate significant differential expression ($p < 0.05$) before false discovery rate (FDR) correction. Non-significant differences are marked with ns.

analyses with 2,766 genes shared by both pairs. We found that the F_{st} distribution of DEGs in each pair did not significantly differ from the F_{st} distribution of 1,000 randomly selected genes (Fig. S9, permutation test $p = 0.4$ in both pair 1 and 3), suggesting that the identified DEGs were not positioned in regions under stronger selection than other protein coding regions. We detected 165 and 141 F_{st} outlier genes in pair 1 and 3, respectively. Eighteen genes containing outlier SNPs were shared by both pairs, a number significantly higher than expected by chance ($p = 0.001$). The lower Jaccard index recovered in selection outliers (Jaccard index = 0.0003) compared to DEGs of these ecotype pairs (Jaccard index equal to 0.092 and 0.081 for genes under- or overexpressed in the montane compared to the alpine of the pairs 1 and 3, Table S4) indicates that the similarity of selection outliers is even less pronounced than the similarity of DEGs. We recovered a C-hypergeometric score equal to 4.2, which confirms that the shared F_{st} outlier genes are less distant from the null expectation than the overlap of DEGs. Functional

annotations of the 18 shared genes containing outlier SNPs are reported in Table S8. Among those candidate genes, we found genes involved in defense response (At1g53570, At3g18100), ion channel and transport activity (At5g57940, At3g25520, At1g34220), and regulation of transcription and translation (At3g18100, At3g25520, At1g18540). Ten and seven F_{st} outlier genes were also differentially expressed in pair 1 and 3, respectively, but not shared by both pairs.

1.5. Discussion

Parallel evolution has long been recognised as a powerful process to study adaptation, overcoming intrinsic limitations of studies on natural populations that often miss replication (Elmer & Meyer, 2011). In this work, we aimed to investigate the genetic basis of adaptation to different elevations in the plant *Heliosperma pusillum*. We asked in particular to what extent different ecotype pairs show signatures of parallel evolution in this system.

Our genetic structure analyses and coalescence-based demographic modelling were in line with a scenario of parallel, polytopic ecotype divergence, as suggested previously by a marked dissimilarity of the genomic landscape of differentiation between ecotype pairs revealed by RAD-seq data (Trucchi et al., 2017). In our demographic investigations, parallel divergence always obtained greater support under a strict isolation model. Still, models including low amounts of gene flow were shown to be more likely. Additionally, in one comparison (i.e., including ecotype pairs 3 and 4) the single origin IM scenario aligned more closely with the data than the two origins IM. This result is consistent with greater co-ancestry observed for these two pairs with respect to other comparisons (Fig. 1c and d). Nevertheless, the estimates of migration rates between different ecotype pairs were overall extremely low (i.e., always lower than 1.2e-03), indicating that each ecotype pair diverged in isolation from other pairs, even when it is not straightforward to distinguish between the different models (i.e. 1-origin vs 2-origins) in the case of pairs 3 and 4.

Our results from selection scans showed that only few diverged genes, likely under

selection during adaptation to different elevations, were shared between the two ecotype pairs analyzed (i.e., pair 1 and 3), while over 87% of putatively adaptive loci were unique to each pair. This high degree of unique outliers, consistent with RADseq results from a previous investigation (Trucchi et al., 2017), supports a scenario of mainly independent evolutionary history of different ecotype pairs. However, we cannot exclude the possibility that a few shared loci, likely from standing genetic variation, might have played a role in shaping the ecotype divergence of different evolutionary replicates in our system.

Global Tajima's D estimates were close to 0, suggesting that the recent past of all these populations was not affected by major bottlenecks or population expansions. Consistently, within-population diversity was similar across montane and alpine ecotypes, likely reflecting ancestral variation before altitudinal divergence. Due to the low number of individuals available for ecotype pairs 4 (three individuals per ecotype) and 5 (four individuals per ecotype), these estimates should be considered with caution. However, previous work using an RNA-seq-derived dataset of synonymous variants similar to ours (Fraïsse et al., 2018) showed that model selection based on the joint site frequency spectrum is robust to the numbers of individuals and loci. Nevertheless, future analyses should aim for enlarged sampling sizes.

We further asked how consistent across divergence events are the molecular processes underlying ecotype formation. We screened the expression profiles of four ecotype pairs grown in a common garden to shed light on the genetic architecture of the adaptive traits involved in parallel adaptation to divergent elevations, as well as to warmer/dry vs. colder/humid conditions. We found strikingly few DEGs shared across all four ecotype pairs, with most DEGs unique to one ecotype pair, suggesting that convergent phenotypes do not consistently rely on changes in expression of specific genes. Interestingly, montane populations were shown to be morphologically more diverged among each other than alpine populations, despite the similarity of ecological conditions across localities in both the montane and alpine niche (Bertel et al., 2018). Therefore, both morphological disparity, as well as different DEGs implicated in differentiation across lineages might reflect differing functional strategies to adapt to the montane/alpine environment.

1. Polygenic routes lead to parallel altitudinal adaptation

The low sharedness of DEGs was most strongly driven by ecotype pair 5, which we also showed to bear a lower degree of shared ancestry with the other pairs in the genetic structure analyses (Fig. 1c-d). Given that ecotype pair 5 is the most eastern in terms of geographic distribution, it can be hypothesized that this pair represents a more distinct lineage, as break zones in the distribution of genetic diversity and distribution of biota have been identified to the West of this area of the Alps (Thiel-Egenter et al., 2011). This pair was shown also to be the earliest diverging among the four lineages included here (Trucchi et al., 2017), and this locality lies closest to the margin of the last glacial maximum (LGM) ice sheet. Following the retreat of the ice sheet, it is likely that this area could have been colonized first, whereas the ancestors of other ecotype pairs likely needed more time to migrate northwards prior to the onset of divergence. An alternative explanation might involve two different LGM refugia for pair 5 and the other three pairs. Our sampling was not appropriate to further test hypotheses of biogeographic nature. Even so, our results suggest that parallel evolution is analyzed at different levels of coancestry in our dataset. This implies that parallel signatures of ecotype evolution can decrease significantly, even within a relatively small geographic range. This view is in line with previous findings of unexpectedly heterogeneous differentiation between freshwater and marine sticklebacks across the globe, including more distant lineages (Fang et al., 2020).

Despite the low parallelism in gene activity, we identified across the ecotype pairs a high reproducibility of the biological processes related to ecological (i.e., different water and light availability, temperature and biotic stress) and morphological (i.e. glandular trichomes absence/presence) divergence at the two elevations. Functional enrichment of responses to biotic stress are consistent with the biotic divergence between the two habitat types, featuring distinct microbiomes (Trucchi et al., 2017) and accompanying vegetation (Bertel et al., 2018). The dichotomy of convergence in enriched GO terms, but a low amount of shared DEGs, indicates that different redundant genes likely concur to shape similar phenotypic differentiation, as expected under polygenic adaptation (Barghi et al., 2020). Shared genes containing selection outliers were involved in partly similar

biological processes as those affected by DEGs, albeit noting that they may not be directly the targets of selection. Nevertheless, we found that shared selection outliers include regulatory elements of transcription, such as the MYB4R1 (gene At3g18100) transcription factor, and it is therefore possible that such *trans* regulatory elements under divergent selection cause at least part of the expression divergence observed. A largely *trans* control of expression divergence is consistent with our results that show that DEGs (together with their *cis* regulatory regions) do not generally reside within regions of high differentiation (i.e., F_{st}) between the ecotypes.

The presence (montane ecotype) or absence (alpine ecotype) of multicellular glandular hairs on the plants represents a striking morphological difference in our system. Trichome formation has been studied extensively in Brassicaceae, especially in *Arabidopsis*, where this trait is controlled by a relatively simple regulatory pathway shared across the family (Chopra et al., 2019; Hilscher et al., 2009; Hülskamp, 2004; Hülskamp et al., 1994; Marina & Martin, 2009; Tominaga-Wada et al., 2011). Still, a certain degree of genetic redundancy has been shown to underlie trichome formation in *Arabidopsis* (Khosla et al., 2014). Studies on other plant lineages, such as cotton (Machado et al., 2009), snapdragons (Tan et al., 2020), *Artemisia* (Shi et al., 2018) and tomato (Chang et al., 2018), highlighted that the genetic basis of multicellular glandular trichomes formation does not always involve the same loci as in *Arabidopsis*. Trichome formation outside of the Brassicaceae family likely involves convergent changes in different genetic components (Serna & Martin, 2006; Tan et al., 2020) and has been reported to be initiated even as an epigenetic response to herbivory in *Mimulus guttatus* (Scoville et al., 2011).

We expected to find evidence of specific genes controlling trichome development in our transcriptome dataset. Indeed, we did observe a change in regulation of particular genes underlying trichome formation and elongation pathways across ecotype pairs. Interestingly, these genes were not-shared by different ecotype pairs, which was unexpected given the relatively simple genetic architecture of this trait in *A. thaliana*. Also, key genes known to underlie hair initiation in *A. thaliana*, or elongation and malformation in other plant species, were differentially expressed in some ecotype pairs, but not in all of them.

Analyses of replicated evolution in laboratory experiments on bacteria (Cooper et al., 2003; Fong et al., 2005), yeast (Nguyen Ba et al., 2019) and *Drosophila* (Barghi et al., 2019) have provided insights about adaptation, showing that redundant trajectories can lead to the same phenotypic optimum, when selection acts on polygenic traits. In line with other studies on diverse organisms including whitefish (Rougeux et al., 2019), hummingbirds (Lim et al., 2019), snails (Ravinet et al., 2016) and frogs (Y. B. Sun et al., 2018), our results suggest that convergent phenotypes can be achieved via changes in different genes affecting the same molecular pathway and, ultimately, adaptive traits, and that this polygenic basis might facilitate repeated adaptation to different elevations via alternative routes. Consistently, a polygenic architecture of adaptive differentiation was uncovered also in *Silene* (Gramlich et al., 2021), a close relative of *Heliosperma*.

In conclusion, this study adds evidence to recent findings showing that polygenic traits and genetic redundancy open multiple threads for adaptation, providing the substrate for reproducible outcomes in convergent divergence events. Future studies using transcriptomics as well as genomic approaches should focus on genotype-by-environment interactions, e.g., in reciprocal transplantation experiments, to further deepen our understanding of the process of adaptation in *H. pusillum*.

1.6. Acknowledgements

This work was financially supported by the Austrian Science Fund (FWF) through the doctoral programme (DK) grant W1225-B20 to a faculty team, including O.P., and through grant Y661-B16 to O.P. We thank Nicholas Barton, Andrew Clark, Virginie Courtier-Orgogozo, Joachim Hermisson, Thibault Leroy, Magnus Nordborg, John Parsch, Christian Schlötterer, Emiliano Trucchi, Daniele Filiault, Alex Widmer, Kay Hodgins, Sam Yeaman and two anonymous reviewers for insightful comments and feedback. We thank Juliane Baar, Marie Huber, Carles Ferré Ortega and Daniela Paun for their support during laboratory work and data acquisition, Marianne Magauer and Daniela Pirkebner for producing the selfed line, as well as Martina Imhiavan and Daniel Schlorhaufer from

the Botanical Garden of the University of Innsbruck for the cultivation of the plants. Computational resources were provided by the Vienna Scientific Cluster (VSC) and the Life Science Compute Cluster (LiSC) of the University of Vienna. A permit to conduct the presented research activities was granted by the Parco Naturale Dolomiti Friulane (no. 1943); for the Austrian federal state Tirol no such permit was necessary.

1.7. Authors contributions

OP designed the study concept; **AS**, **OP**, and **JL-W** performed laboratory work; **PS** and **BF** supported seeds sampling and cultivation of the plants; **OP** assembled the genome draft; **AS** performed all other bioinformatic analyses, including genome structural and functional annotation, differential expression and redundancy analysis, demographic modelling, estimations of genetic diversity and structure, detection of selection outliers, and GO terms enrichment; **AS** derived the analytical results, and prepared the first figure drafts that were than improved together with **OP**; **OP**, **SF**, **HL**, and **TW** provided feed-back on the analyses; **AS** wrote the first draft of the manuscript; **OP** and **AS** revised the manuscript with contributions from all other authors.

1.8. Data accessibility

All raw read data was uploaded to NCBI and can be found under Bioproject ID PRJNA760819. The new Heliosperma pusillum genome assembly v1.0 is available from GenBank (BioProject ID PRJNA739571, accession number JAIUZE000000000). Scripts used to perform the analyses can be found under this gitHub repository `https://github.com/aglaszuk/Polygenic_Adaptation_Heliosperma/`.

Supporting information - Chapter 1

Figure S1. (a) NgsAdmix results (K = 3 and 4) for ecotype populations in locality 3 and 4 showing that individuals A3b and A3c (marked on the figure) are highly introgressed from population A4. **(b)** NgsAdmix results (K = 2 through 8) for the ecotype pairs using the dataset including 63 accessions, i.e. without random downsampling of each population to the same number of individuals (compare to Fig. 1d in the main text). The colors represent different gene pools.

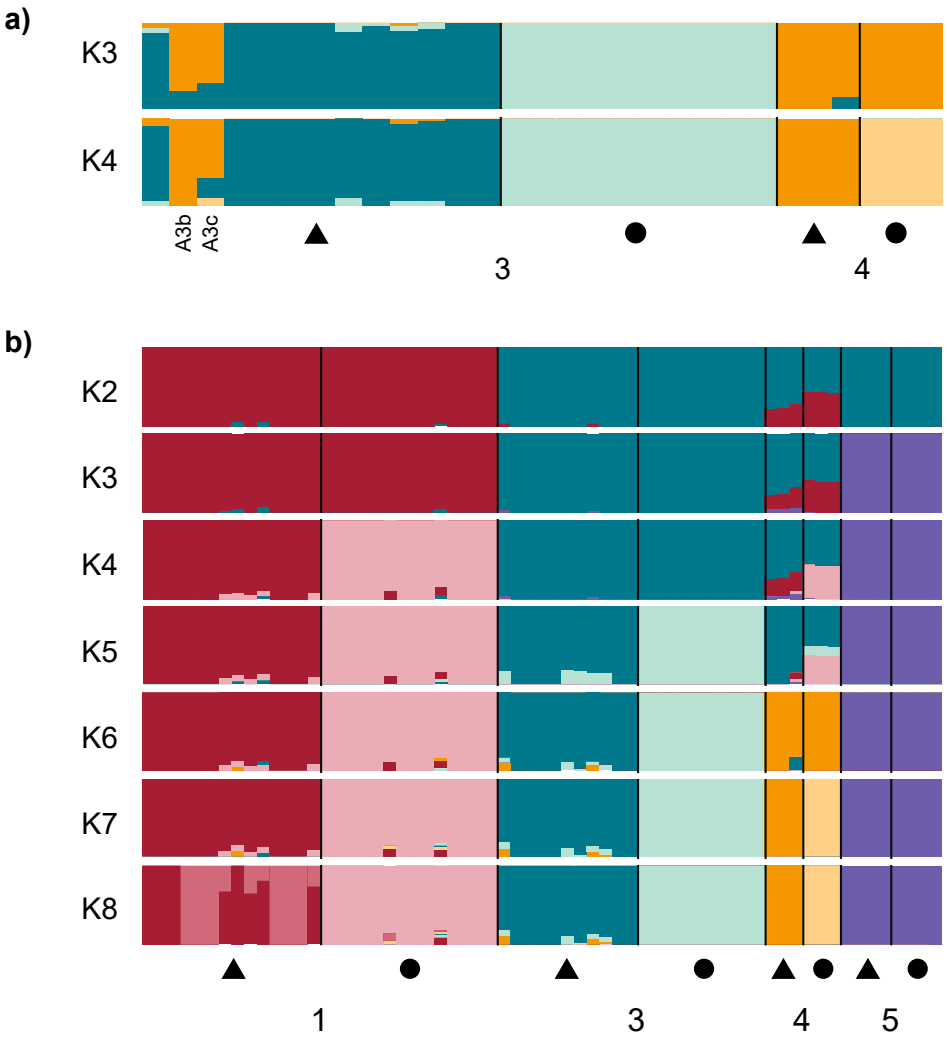

Figure S2. (a) Gene length distribution of the *Heliosperma* genome assembly. **(b)** Distribution of the amount of exons per gene. **(c)** Contig length distribution. Highlighted in darker grey color is the proportion of contigs containing genes.

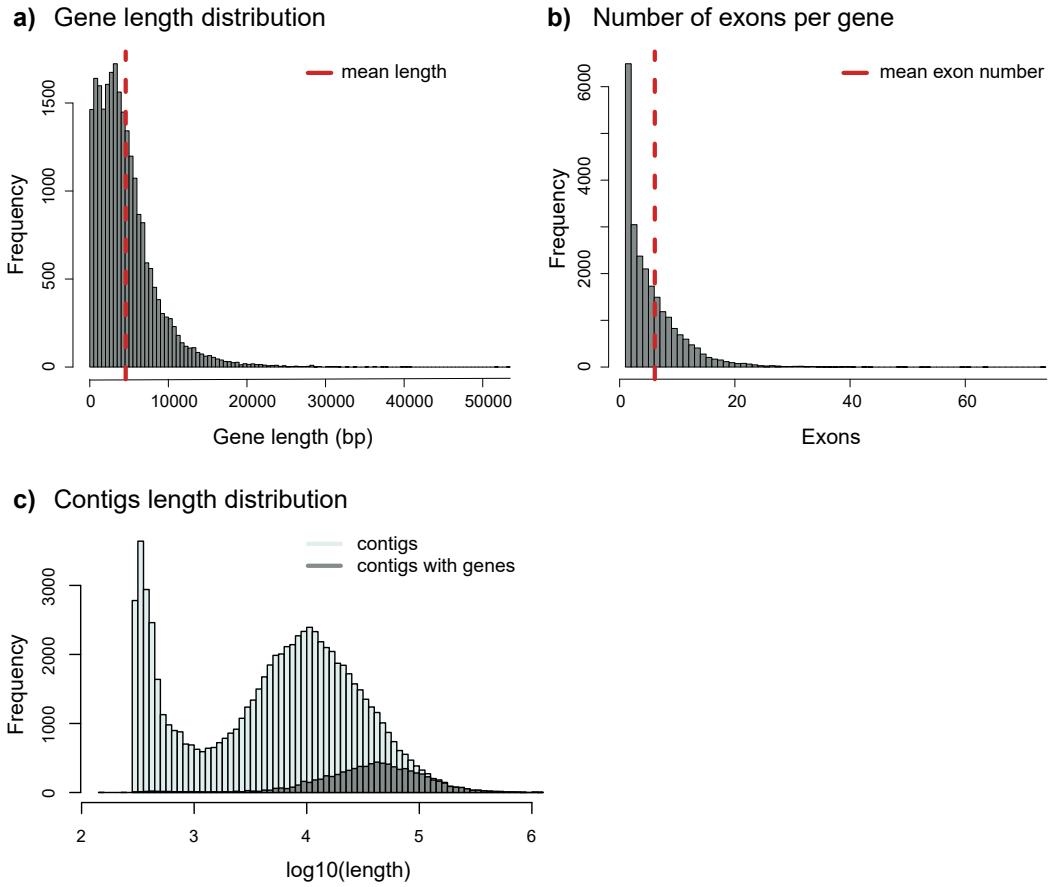

Figure S3. Population-wise distribution of Tajima's D estimates computed per window of size 50Kb with a step of 10Kb. Colors represent the populations as in Fig. 1 in the main text. A - alpine populations; M - montane populations.

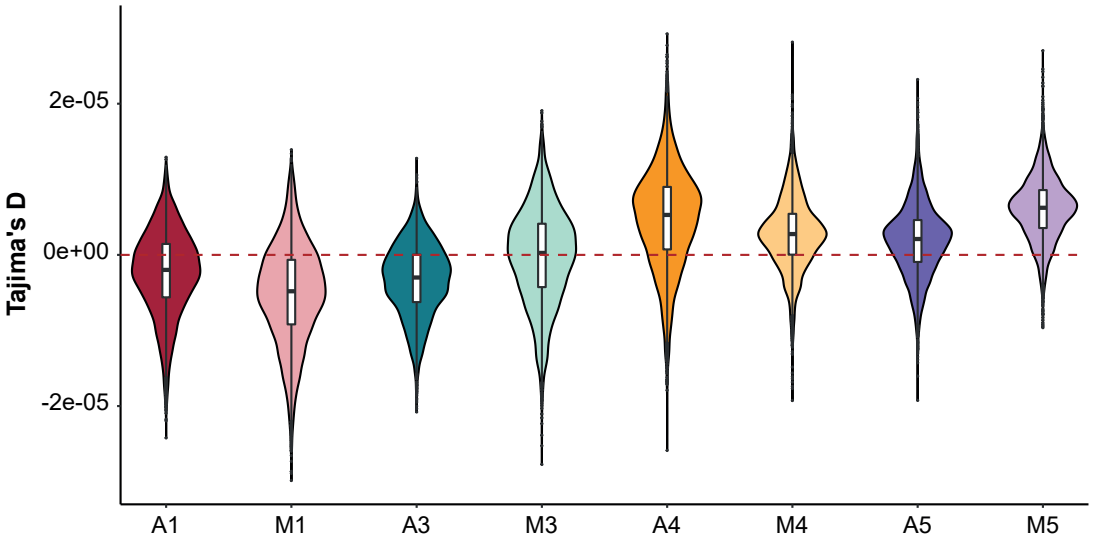

Figure S4. Scatterplots of differentially expressed genes between ecotypes, showing ecotype pairs comparisons and the amount of shared DEG (red dots).

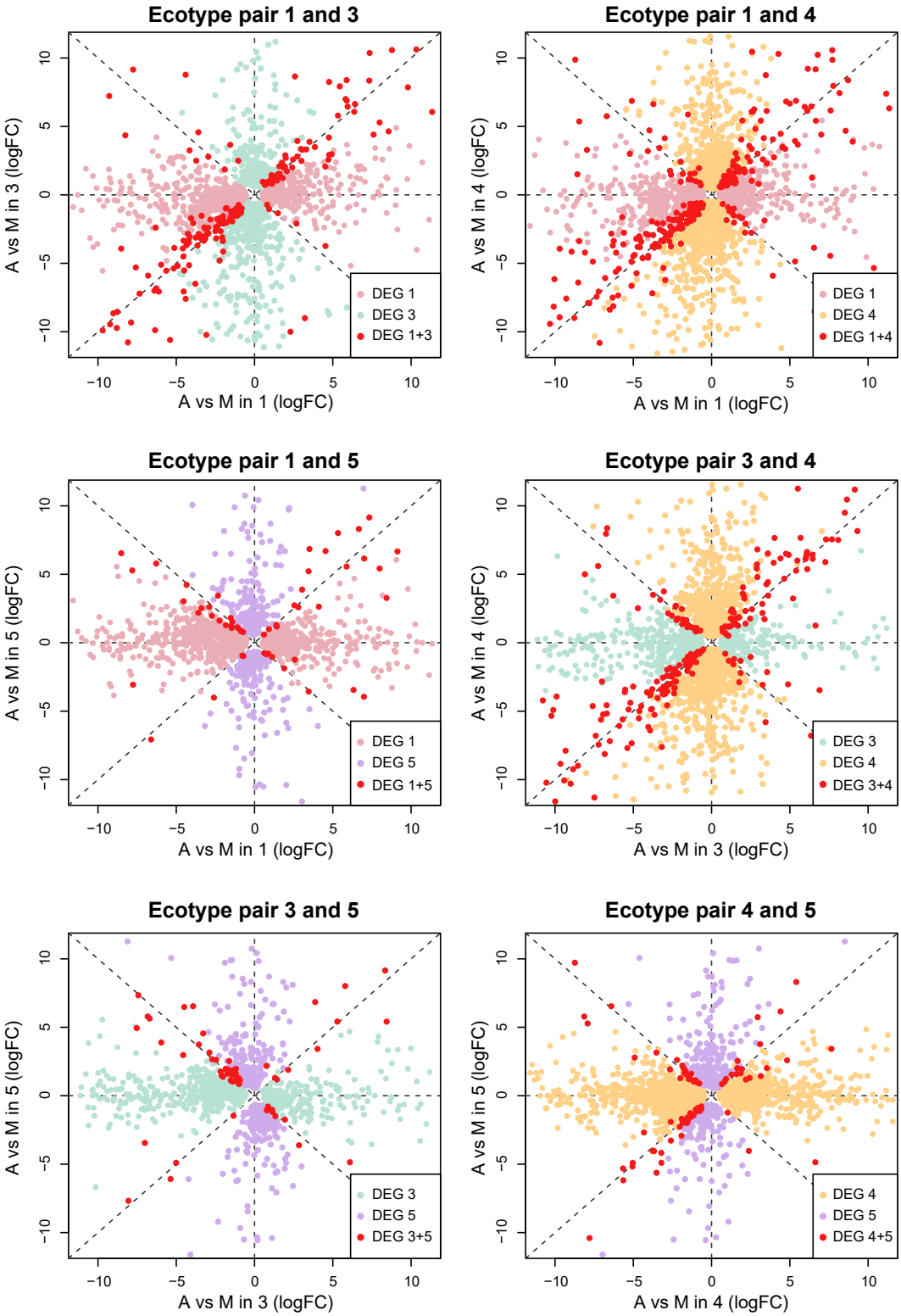

Figure S5. (a) PCA (dimensions 1 to 3) based on normalized gene expression counts. **(b)** Multidimensional scaling plots (dimensions 1 to 3) of logFC of gene expression counts after normalization. Colors represent populations as in Fig.1b. Circles represent montane individuals; triangles show alpine accessions.

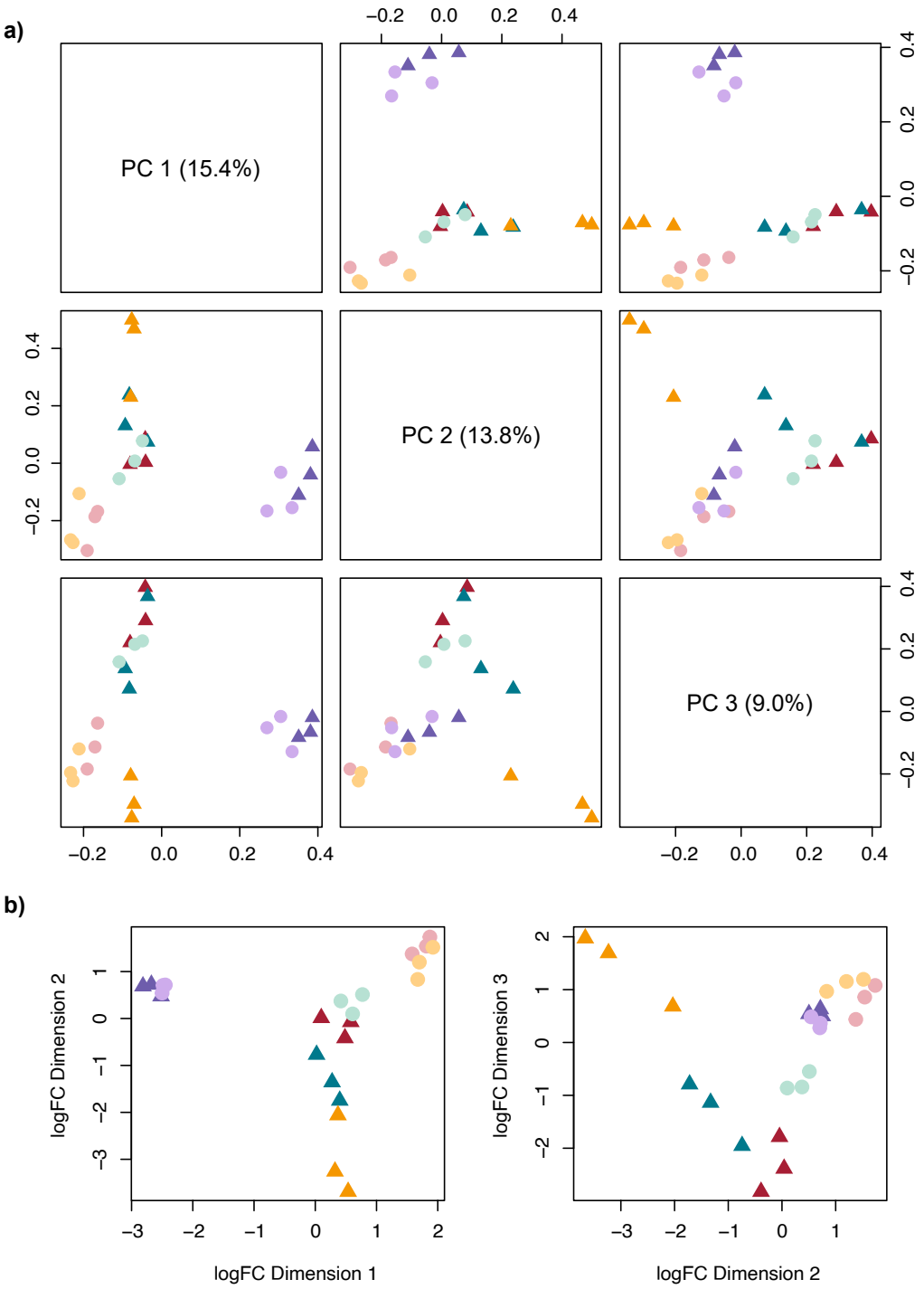

Figure S6. Boxplots showing the degree of gene expression divergence between populations of the alpine and montane ecotype, respectively. The difference between the means was statistically tested using Wilcoxon signed rank test and found to be not significant (p = 0.56).

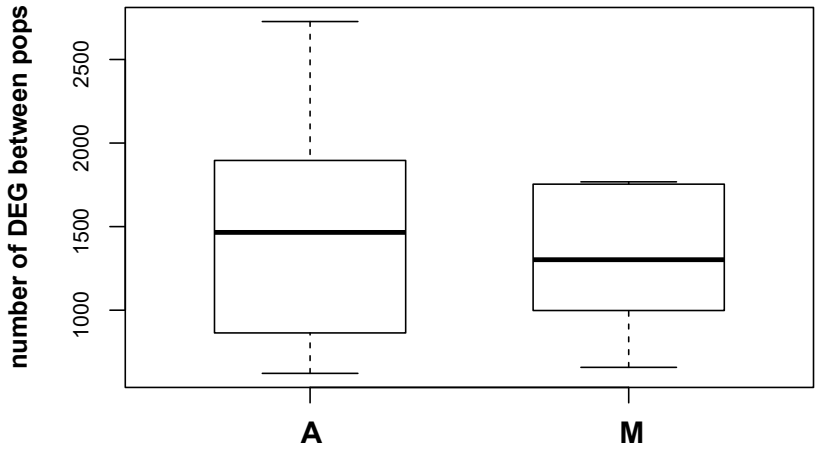

Figure S7. Z-score distribution obtained from the cRDA transcripts scores. Dashed and full red lines correspond to significance thresholds of p-value of 0.05 and 0.01, respectively.

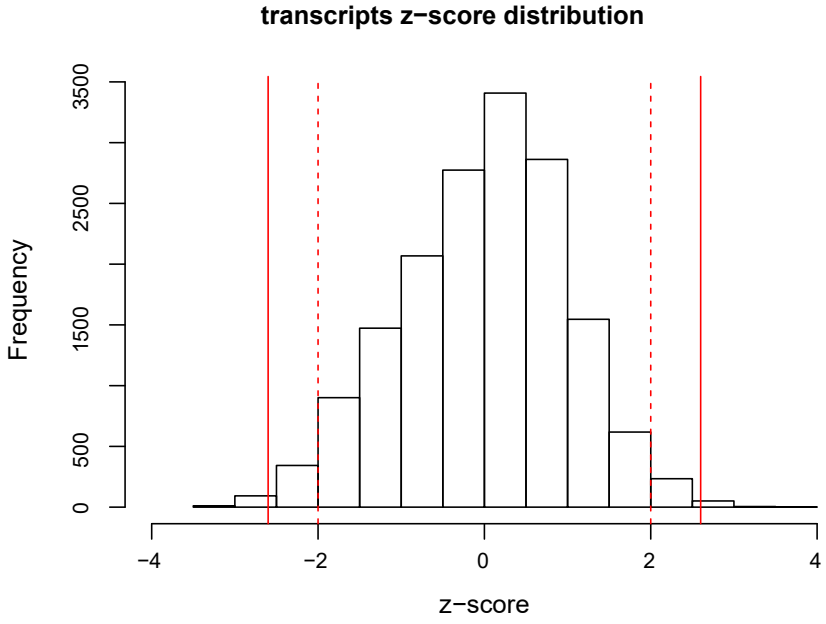

Figure S8. Venn diagrams showing overlaps between lists of DEGs and 739 cRDA outliers. Genes underexpressed (a) and overexpressed (b) in the montane ecotype compared to the alpine at each pair and in the cRDA analysis.

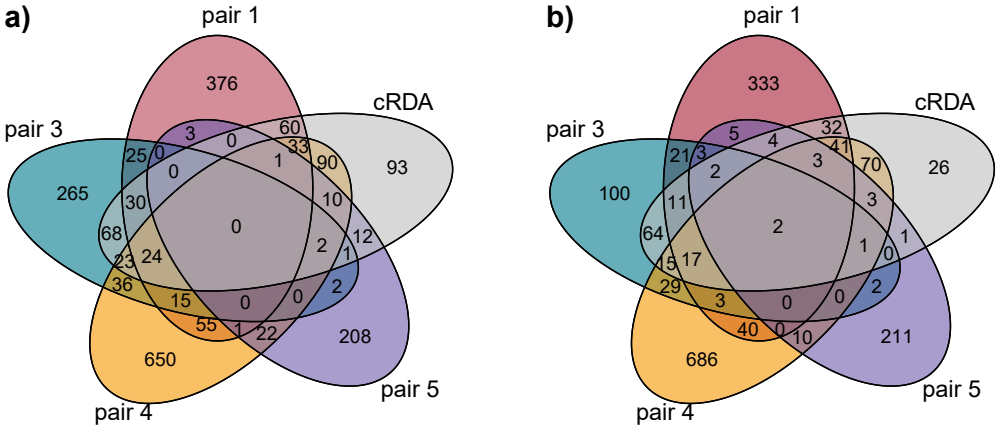

Figure S9. Distribution of F_{ST} in 1,000 randomly selected genes (white bars) compared to DEGs (black bars) in ecotype pair 1 (**a**) and 3 (**b**). Dotted lines show the mean F_{ST} values.

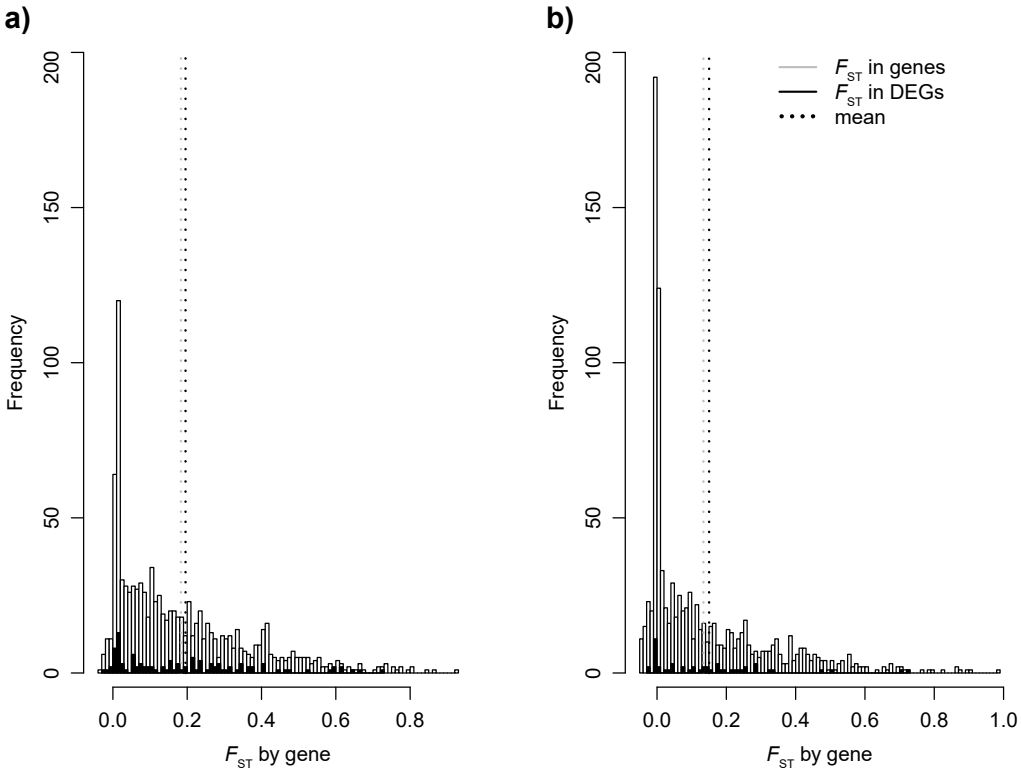

Table S1. Details regarding the accessions included in the present study. Stars in the column Sample ID refer to samples used in the differential expression analyses.

Sample ID	Ecotype	Ecotype Pair	Locality (original population)	Longitude	Latitude	Altitude (m)	Acronyms
A1A∗	Alpine	1	Italy: Trentino-Alto Adige: Dolomiti di Gardena /Grödner Dolomiten	11.768 E	46.601 N	2290	PVA
A1B	Alpine	1	Italy: Trentino-Alto Adige: Dolomiti di Gardena /Grödner Dolomiten	11.768 E	46.601 N	2290	PVA
A1C∗	Alpine	1	Italy: Trentino-Alto Adige: Dolomiti di Gardena /Grödner Dolomiten	11.768 E	46.601 N	2290	PVA
A1D∗	Alpine	1	Italy: Trentino-Alto Adige: Dolomiti di Gardena /Grödner Dolomiten	11.768 E	46.601 N	2290	PVA
A1DA	Alpine	1	Italy: Trentino-Alto Adige: Dolomiti di Gardena /Grödner Dolomiten	11.768 E	46.601 N	2290	PVA
A1DB	Alpine	1	Italy: Trentino-Alto Adige: Dolomiti di Gardena /Grödner Dolomiten	11.768 E	46.601 N	2290	PVA
A1DD	Alpine	1	Italy: Trentino-Alto Adige: Dolomiti di Gardena /Grödner Dolomiten	11.768 E	46.601 N	2290	PVA
A1DE	Alpine	1	Italy: Trentino-Alto Adige: Dolomiti di Gardena /Grödner Dolomiten	11.768 E	46.601 N	2290	PVA
A1DF	Alpine	1	Italy: Trentino-Alto Adige: Dolomiti di Gardena /Grödner Dolomiten	11.768 E	46.601 N	2290	PVA
A1UA	Alpine	1	Italy: Trentino-Alto Adige: Dolomiti di Gardena /Grödner Dolomiten	11.768 E	46.601 N	2290	PVA
A1UB	Alpine	1	Italy: Trentino-Alto Adige: Dolomiti di Gardena /Grödner Dolomiten	11.768 E	46.601 N	2290	PVA
A1UC	Alpine	1	Italy: Trentino-Alto Adige: Dolomiti di Gardena /Grödner Dolomiten	11.768 E	46.601 N	2290	PVA
A1UD	Alpine	1	Italy: Trentino-Alto Adige: Dolomiti di Gardena /Grödner Dolomiten	11.768 E	46.601 N	2290	PVA
A1UE	Alpine	1	Italy: Trentino-Alto Adige: Dolomiti di Gardena /Grödner Dolomiten	11.768 E	46.601 N	2290	PVA
M1A∗	Montane	1	Italy: Trentino-Alto Adige: Dolomiti di Gardena /Grödner Dolomiten	11.77 E	46.564 N	1690	VVA

Table S1. ...continued.

M1B∗	Montane	1	Italy: Trentino-Alto Adige: Dolomiti di Gardena /Grödner Dolomiten	11.77 E	46.564 N	1690	VVA
M1C	Montane	1	Italy: Trentino-Alto Adige: Dolomiti di Gardena /Grödner Dolomiten	11.77 E	46.564 N	1690	VVA
M1D∗	Montane	1	Italy: Trentino-Alto Adige: Dolomiti di Gardena /Grödner Dolomiten	11.77 E	46.564 N	1690	VVA
M1DA	Montane	1	Italy: Trentino-Alto Adige: Dolomiti di Gardena /Grödner Dolomiten	11.77 E	46.564 N	1690	VVA
M1DC	Montane	1	Italy: Trentino-Alto Adige: Dolomiti di Gardena /Grödner Dolomiten	11.77 E	46.564 N	1690	VVA
M1DD	Montane	1	Italy: Trentino-Alto Adige: Dolomiti di Gardena /Grödner Dolomiten	11.77 E	46.564 N	1690	VVA
M1DF	Montane	1	Italy: Trentino-Alto Adige: Dolomiti di Gardena /Grödner Dolomiten	11.77 E	46.564 N	1690	VVA
M1DJ	Montane	1	Italy: Trentino-Alto Adige: Dolomiti di Gardena /Grödner Dolomiten	11.77 E	46.564 N	1690	VVA
M1UA	Montane	1	Italy: Trentino-Alto Adige: Dolomiti di Gardena /Grödner Dolomiten	11.77 E	46.564 N	1690	VVA
M1UB	Montane	1	Italy: Trentino-Alto Adige: Dolomiti di Gardena /Grödner Dolomiten	11.77 E	46.564 N	1690	VVA
M1UC	Montane	1	Italy: Trentino-Alto Adige: Dolomiti di Gardena /Grödner Dolomiten	11.77 E	46.564 N	1690	VVA
M1UD	Montane	1	Italy: Trentino-Alto Adige: Dolomiti di Gardena /Grödner Dolomiten	11.77 E	46.564 N	1690	VVA
M1UE	Montane	1	Italy: Trentino-Alto Adige: Dolomiti di Gardena /Grödner Dolomiten	11.77 E	46.564 N	1690	VVA
A3A∗	Alpine	3	Austria: Kärnten: Lienzer Dolomiten	12.877 E	46.762 N	2055	PHO
A3B∗	Alpine	3	Austria: Kärnten: Lienzer Dolomiten	12.877 E	46.762 N	2055	PHO
A3C∗	Alpine	3	Austria: Kärnten: Lienzer Dolomiten	12.877 E	46.762 N	2055	PHO
A3DC	Alpine	3	Austria: Kärnten: Lienzer Dolomiten	12.877 E	46.762 N	2055	PHO
A3DD	Alpine	3	Austria: Kärnten: Lienzer Dolomiten	12.877 E	46.762 N	2055	PHO

Table S1. ...continued.

A3DE	Alpine	3	Austria: Kärnten: Lienzer Dolomiten	12.877 E	46.762 N	2055	PHO
A3DF	Alpine	3	Austria: Kärnten: Lienzer Dolomiten	12.877 E	46.762 N	2055	PHO
A3DA	Alpine	3	Austria: Kärnten: Lienzer Dolomiten	12.877 E	46.762 N	2055	PHO
A3UA	Alpine	3	Austria: Kärnten: Lienzer Dolomiten	12.877 E	46.762 N	2055	PHO
A3UC	Alpine	3	Austria: Kärnten: Lienzer Dolomiten	12.877 E	46.762 N	2055	PHO
A3UD	Alpine	3	Austria: Kärnten: Lienzer Dolomiten	12.877 E	46.762 N	2055	PHO
A3UE	Alpine	3	Austria: Kärnten: Lienzer Dolomiten	12.877 E	46.762 N	2055	PHO
A3UF	Alpine	3	Austria: Kärnten: Lienzer Dolomiten	12.877 E	46.762 N	2055	PHO
M3A∗	Montane	3	Austria: Kärnten: Lienzer Dolomiten	12.901 E	46.774 N	790	VHO
M3B∗	Montane	3	Austria: Kärnten: Lienzer Dolomiten	12.901 E	46.774 N	790	VHO
M3C∗	Montane	3	Austria: Kärnten: Lienzer Dolomiten	12.901 E	46.774 N	790	VHO
M3DA	Montane	3	Austria: Kärnten: Lienzer Dolomiten	12.901 E	46.774 N	790	VHO
M3DB	Montane	3	Austria: Kärnten: Lienzer Dolomiten	12.901 E	46.774 N	790	VHO
M3DC	Montane	3	Austria: Kärnten: Lienzer Dolomiten	12.901 E	46.774 N	790	VHO
M3DE	Montane	3	Austria: Kärnten: Lienzer Dolomiten	12.901 E	46.774 N	790	VHO
M3DF	Montane	3	Austria: Kärnten: Lienzer Dolomiten	12.901 E	46.774 N	790	VHO
M3UA	Montane	3	Austria: Kärnten: Lienzer Dolomiten	12.901 E	46.774 N	790	VHO
M3UB	Montane	3	Austria: Kärnten: Lienzer Dolomiten	12.901 E	46.774 N	790	VHO
A4A∗	Alpine	4	Italy: Friuli-Venezia Giulia: Val Cimoliana	12.48 E	46.391 N	1700	PCI
A4B∗	Alpine	4	Italy: Friuli-Venezia Giulia: Val Cimoliana	12.48 E	46.391 N	1700	PCI
A4C∗	Alpine	4	Italy: Friuli-Venezia Giulia: Val Cimoliana	12.48 E	46.391 N	1700	PCI
M4A∗	Montane	4	Italy: Friuli-Venezia Giulia: Val Cimoliana	12.489 E	46.38 N	1180	VCI
M4B∗	Montane	4	Italy: Friuli-Venezia Giulia: Val Cimoliana	12.489 E	46.38 N	1180	VCI
M4C∗	Montane	4	Italy: Friuli-Venezia Giulia: Val Cimoliana	12.489 E	46.38 N	1180	VCI
A5B∗	Alpine	5	Italy: Friuli-Venezia Giulia: Alpi Giulie	13.459 E	46.376 N	1820	PNE

Table S1. ...continued.

A5C∗	Alpine	5	Italy: Friuli-Venezia Giulia: Alpi Giulie	13.459 E	46.376 N	1820	PNE
A5D∗	Alpine	5	Italy: Friuli-Venezia Giulia: Alpi Giulie	13.459 E	46.376 N	1820	PNE
A5E	Alpine	5	Italy: Friuli-Venezia Giulia: Alpi Giulie	13.459 E	46.376 N	1820	PNE
M5A∗	Montane	5	Italy: Friuli-Venezia Giulia: Alpi Giulie	13.459 E	46.388 N	1170	VNE
M5C∗	Montane	5	Italy: Friuli-Venezia Giulia: Alpi Giulie	13.459 E	46.388 N	1170	VNE
M5D	Montane	5	Italy: Friuli-Venezia Giulia: Alpi Giulie	13.459 E	46.388 N	1170	VNE
M5E∗	Montane	5	Italy: Friuli-Venezia Giulia: Alpi Giulie	13.459 E	46.388 N	1170	VNE

Table S2. Measures of within-population genetic diversity (Watterson's theta, θw, and pairwise nucleotide diversity, π) and global Tajima's D, as well as global population genetic differentiation F_{st} (unweighted and weighted values output by ANGSD are reported on the left and right side of the backslash, respectively) of eight populations of *Heliosperma pusillum* investigated here. A, alpine ecotype; M, montane ecotype.

Population	**Mean(θw) (± SD)**	**Mean(π) (± SD)**	**Mean Tajima's D (± SD)**
A1	0,0033 ± 0,0016	0,0032 ± 0,0016	-2,38e-06 ± 5,56e-06
M1	0,0027 ± 0,0014	0,0026 ± 0,0015	-5,14e-06 ± 6,59e-06
A3	0,0027 ± 0,0013	0,0026 ± 0,0013	-3,31e-06 ± 4,77e-06
M3	0,0021 ± 0,0012	0,0021 ± 0,0013	-2,04e-07 ± 6,38e-06
A4	0,0015 ± 0,0012	0,0016 ± 0,0012	5,13e-06 ± 2,58e-05
M4	0,0016 ± 0,0011	0,0016 ± 0,0012	2,79e-06 ± 4,78e-06
A5	0,0017 ± 0,0011	0,0017 ± 0,0012	1,94e-06 ± 4,73e-06
M5	0,0020 ± 0,0013	0,0021 ± 0,0014	6.09e-06 ± 4.15e-06

Population	**F_{st}**					
	A3	**A4**	**A5**	**M1**	**M3**	**M4**
A1	0,17 / 0,32	0,19 / 0,39	0,26 / 0,47	0,14 / 0,28	–	–
M1	–	–	–	–	–	–
A3	–	0,16 / 0,35	0,24 / 0,47	–	–	–
M3	0,13 / 0,26	–	–	0,20 / 0,43	–	–
A4	–	–	0,28 / 0,56	–	–	–
M4	–	0,23 / 0,48	–	0,18 / 0,39	0,19 / 0,42	–
A5	–	–	–	–	–	–
M5	–	–	0,11 / 0,17	0,31 / 0,51	0,29 / 0,50	0,27 / 0,52

Table S3. Demographic inference for each model tested using Fastsimcoal2 in four population pairs of *Heliosperma pusillum*. **(a)** Delta Akaike Information Criterion (Δ AIC) across 60 maximum−likelihood runs for each scenario are given in the respective positions. Best scenarios are highlighted in bold. **(b)** Effective population size and time of divergence estimates of the best models. Each parameter is reported as the 95% confidence interval of the 30 best model estimates pulled from the top−10 estimates of the three best models in which these parameters were estimated. **(c)** Number of parameters, Maximum estimated likelihood (MaxEstL), maximum observed likelihood (MaxObsL), Delta likelihood (Δ L) and Delta Akaike Information Criterion (Δ AIC) of the best run of 60 maximum−likelihood runs for each scenario are given in the respective columns. **(d)** Effective population sizes, times of divergence (T1, T2 and T3), between and within localities migration parameters and mutation rate were estimated for each topology. For each parameter we report the 95% confidence interval of the top−10 best model estimates.

(a)

Ecotype pairs	Model	Δ AIC
1 − 3	1orSI	43137
	2orSI	**38247**
	1orIM	21315
	2orIM	**20440**
1 − 4	1orSI	24364
	2orSI	**12088**
	1orIM	14797
	2orIM	**13728**
1 − 5	1orSI	25054
	2orSI	**23736**
	1orIM	12726
	2orIM	**12127**
3 − 4	1orSI	74577
	2orSI	**74544**
	1orIM	**6910**
	2orIM	7343
3 − 5	1orSI	69843
	2orSI	**67772**
	1orIM	8985
	2orIM	**8460**
4 − 5	1orSI	8940
	2orSI	**8018**
	1orIM	4507
	2orIM	**4203**

(b)

		Pair 1	**Pair 3**	**Pair 4**	**Pair 5**
Ne alpine		5,705−8,474	6,053−9,533	4,366−6,547	1,577−4,854
Ne montane		1,561−2,416	1,105−2,143	3,500−4,776	3,392−5,027
TDiv alpine-montane		41,382−81,802	70,804−120,474	21,366−33,091	20,976−45,148
TDiv alpine -alpine	**Pair 3**	227,982−309,201			
	Pair 4	199,895−304,873	197,588−307,778		
	Pair 5	216,368−303,674	163,691−223,783	142,076−193,448	

(c)

Ecotype pairs	**Model**	**Divergence events**	**Parameters**	**Mean(MaxEstL)**	**MaxObsL**
1 − 3	1orSI	T2 > T3 / T3 > T2	8	-66607,159	-57240
	2orSI	**T2 > T3 / T3 > T3**	**8**	**-65545,331**	**-57240**
	1orIM	T2 > T3	20	-173081	-168452
		T3 > T2	20	-173129	-168452
	2orIM	T2 > T3	20	-174031	-168452
		T3 > T2	**20**	**-172891**	**-168452**
1 − 4	1orSI	T2 > T3 / T3 > T2	8	-36672,29	-31381,7
	2orSI	**T2 > T3 / T3 > T3**	**8**	**-34006,597**	**-31381,7**
	1orIM	T2 > T3	20	-125303	-122090
		T3 > T2	20	-125432	-122090
	2orIM	**T2 > T3**	**20**	**-125071**	**-122090**
		T3 > T2	20	-125153	-122090
1 − 5	1orSI	T2 > T3 / T3 > T2	8	-38626,209	-33185,8
	2orSI	**T2 > T3 / T3 > T3**	**8**	**-38340,069**	**-33185,8**
	1orIM	T2 > T3	20	-121743	-118980
		T3 > T2	20	-121849	-118980
	2orIM	**T2 > T3**	**20**	**-121613**	**-118980**
		T3 > T2	20	-121895	-118980
3 − 4	1orSI	T2 > T3 / T3 > T2	8	-57245,428	-41051,2
	2orSI	**T2 > T3 / T3 > T3**	**8**	**-57238,234**	**-41051,2**
	1orIM	**T2 > T3**	**20**	**-114566**	**-113066**
		T3 > T2	20	-114941	-113066
	2orIM	**T2 > T3**	**20**	**-114660**	**-113066**
		T3 > T2	20	-114760	-113066
3 − 5	1orSI	T2 > T3 / T3 > T2	8	-57939,726	-42773,5
	2orSI	**T2 > T3 / T3 > T3**	**8**	**-57489,966**	**-42773,5**
	1orIM	T2 > T3	20	-128150	-126199
		T3 > T2	20	-128187	-126199
	2orIM	**T2 > T3**	**20**	**-128036**	**-126199**
		T3 > T2	20	-128628	-126199
4 − 5	1orSI	T2 > T3 / T3 > T2	8	-19483,458	-17542,2
	2orSI	**T2 > T3 / T3 > T3**	**8**	**-19283,397**	**-17542,2**
	1orIM	T2 > T3	20	-90050	-88951,2
		T3 > T2	20	-89930	-88951,2
	2orIM	T2 > T3	20	-90003	-88951,2
		T3 > T2	**20**	**-89864**	**-88951,2**

(c) ...continued.

Ecotype pairs	**Δ L**	**AIC (MaxEstL)**	**AIC(MaxObsL)**	**Δ AIC**
1 – 3	9367,127	306753,3028	263.616	43.137
	8305,299	**301863,4042**	**263.616**	**38.247**
	4628,527	797107,461	775.792	21.315
	4676,527	797328,5091	775.792	21.536
	5578,527	801482,3726	775.792	25.690
	4438,527	**796232,4786**	**775.792**	**20.440**
1 – 4	5290,62	168898,1366	144.534	24.364
	2624,927	**156622,1666**	**144.534**	**12.088**
	3213,076	577081,6398	562.285	14.797
	3342,076	577675,7068	562.285	15.391
	2981,076	**576013,2403**	**562.285**	**13.728**
	3063,076	576390,8643	562.285	14.106
1 – 5	5440,453	177896,2661	152.842	25.054
	5154,313	**176578,5427**	**152.842**	**23.736**
	2763,403	560687,234	547.961	12.726
	2869,403	561175,382	547.961	13.214
	2633,403	**560088,5618**	**547.961**	**12.127**
	2915,403	561387,2198	547.961	13.426
3 – 4	16194,231	263640,9383	189.064	74.577
	16187,037	**263607,8087**	**189.064**	**74.544**
	1500,423	**527635,9275**	**520.726**	**6.910**
	1875,423	529362,8663	520.726	8.637
	1594,423	**528068,8135**	**520.726**	**7.343**
	1694,423	528529,3305	520.726	7.803
3 – 5	15166,214	266838,2988	196.995	69.843
	14716,454	**264767,0774**	**196.995**	**67.772**
	1951,153	590192,5593	581.207	8.985
	1988,153	590362,9506	581.207	9.156
	1837,153	**589667,5699**	**581.207**	**8.460**
	2429,153	592393,8307	581.207	11.187
4 – 5	1941,222	89740,6399	80.801	8.940
	1741,161	**88819,32495**	**80.801**	**8.018**
	1098,758	414735,5752	409.676	5.060
	978,758	414182,9548	409.676	4.507
	1051,758	414519,1322	409.676	4.844
	912,758	**413879,0136**	**409.676**	**4.203**

(d)

Ecotype pairs	**1 -3**		**1 - 4**		**1 - 5**	
Model	**2orIM**		**2orIM**		**2orIM**	
	NA1	5246-9592	NA1	5039-10473	NA1	3692-8496
Ne	NA3	5923-11480	NA4	3975-7142	NA5	1541-10180
	NM1	873-2526	NM1	2056-3146	NM1	928-2406
	NM3	1751-3444	NM4	2824-4806	NM5	3107-5690
Divergence time	Tp1-p3	227982-309201	Tp1-p4	199895-304873	Tp1-p5	216368-303674
	Ta1-m1	15601-27539	Ta1-m1	28366-59266	Ta1-m1	86116-152664
	Ta3-m3	76061-167326	Ta4-m4	17291-27455	Ta5-m5	16119-32568
Migration within	mA1M1	0–8.4e-04	mA1M1	1.1e-04–1.9e-04	mA1M1	1.7e-04-5.1e-04
	mM1A1	1.8e-04–1.4e-03	mM1A1	1.1e-04–1.8e-04	mM1A1	2.0e-04-5.9e-04
	mA3M3	3.6e-05–1.2e-04	mA4M4	1.8e-05–1.5e-04	mA5M5	3.1e-04-1.7e-03
	mM3A3	0–1.3e-03	mM4A4	3.8e-05–1.3e-04	mM5A5	0-2.9e-03
Migration between	mA1A3	0–1.0e-06	mA1A4	0–4.1e-07	mA1A5	1.7e-08-6.8e-08
	mA1M3	0–2.3e-05	mA1M4	1.5e-05–1.1e-04	mA1M5	0-8.6e-05
	mA3A1	0–1.9e-05	mA4A1	0–1.1e-06	mA5A1	0-3.9e-07
	mA3M1	0–3.8e-04	mA4M1	0–8.5e-05	mA5M1	0-1.3e-05
	mM1A3	9.4e-05–6.8e-04	mM1A4	2.5e-05–7.9e-05	mM1A5	0-6.7e-05
	mM1M3	0–7.7e-04	mM1M4	4.2e-05–1.2e-04	mM1M5	1.0e-04-3.2e-04
	mM3A1	0–4.6e-05	mM4A1	1.6e-05–1.2e-04	mM5A1	6.3e-06-4.2e-05
	mM3M1	1.0e-05–4.1e-05	mM4M1	0–5.2e-05	mM5M1	0-8.6e-04
Mutation rate		4.5e-09–6.7e-09		5.0e-09–6.8e-09		4.8e-09-7.1e-09

(d) . . . continued

Ecotype pairs	**3 - 4**		**3 - 5**		**4 - 5**	
Model	**2orIM**		**2orIM**		**2orIM**	
Ne	NA3	7661-13402	NA3	2127-6168	NA4	2212-4762
	NA4	5273-9375	NA5	826-3315	NA5	599-2832
	NM3	270-2192	NM3	451-1639	NM4	2026-4104
	NM4	4820-6246	NM5	2254-5831	NM5	2938-5438
Divergence time	Tp3-p4	197588-307778	Tp3-p5	163691-223783	Tp4-p5	142076-193448
	Ta3-m3	20200-86505	Ta3-m3	78278-145466	Ta4-m4	16949-43098
	Ta4-m4	19639-38940	Ta5-m5	13297-30639	Ta5-m5	22853-82898
Migration within	mA3M3	1.1e-04-2.4e-04	mA3M3	0-6.7e-04	mA4M4	0-5.7e-04
	mM3A3	4.4e-04-3.6e-03	mM3A3	5.3e-04-3.5e-03	mM4A4	0-5.1e-04
	mA4M4	0-4.2e-05	mA5M5	6.0e-04-6.1e-03	mA5M5	1.3e-03-1.5e-02
	mM4A4	1.1e-05-3.6e-05	mM5A5	1.3e-04-6.6e-04	mM5A5	0-2.2e-03
Migration between	mA3A4	0-2.9e-05	mA3A5	0-2.0e-07	mA4A5	0-1.6e-04
	mA3M4	0-1.6e-05	mA3M5	2.4e-05-4.9e-04	mA4M5	2.1e-05-1.3e-04
	mA4A3	1.2e-07-3.8e-07	mA5A3	5.2e-08-4.0e-07	mA5A4	0-5.7e-06
	mA4M3	4.1e-05-1.1e-04	mA5M3	0-1.2e-05	mA5M4	0-4.8e-05
	mM3A4	1.9e-04-9.0e-04	mM3A5	0-2.6e-04	mM4A5	0-2.6e-04
	mM3M4	1.7e-04-1.2e-03	mM3M5	0-6.8e-04	mM4M5	6.4e-06-4.5e-05
	mM4A3	1.5e-05-6.4e-05	mM5A3	2.2e-05-1.2e-04	mM5A4	6.6e-06-2.2e-04
	mM4M3	5.7e-06-6.4e-05	mM5M3	2.2e-06-8.4e-05	mM5M4	0-2.9e-04
Mutation rate		3.5e-09-6.4e-09		5.1e-09-7.8e-09		5.0e-09-7.9e-09

Table S4. Jaccard indexes of similarity of lists of DEGs over- (M > A) or underexpressed (M < A) in the montane ecotype.

Ecotype pairs	DEGs (M < A)	DEGs (A > M)
1 – 3	0.092	0,081
1 – 4	0,088	0,079
1 – 5	0,005	0,025
3 – 4	0,073	0,059
3 – 5	0,006	0,019
4 – 5	0,03	0,016

Table S5. Amount of DEGs found between geographically isolated populations in each ecotype.

Ecotype pairs	A	M
1 – 3	622	1043
1 – 4	1039	658
1 – 5	1892	1561
3 – 4	864	998
3 – 5	2727	1754
4 – 5	1896	1768

Table S6a. Full list of enriched GO terms enriched including all DEGs with complete IDs (adjusted p < 0.05). The GO terms are reported per locality (z-score > 0 and z-score < 0 indicate over- and underexpression in the montane ecotype, respectively).

Ecotype pair	Ontology	GO ID	GO Term	Gene number	adjusted p-val	z-score
1	BP	GO:0009751	response to salicylic acid	45	3,80E-08	-12,49019837
1	BP	GO:0042742	defense response to bacterium	88	1,80E-07	-12,86126922
1	BP	GO:0009864	induced systemic resistance, jasmonic ac,,,	8	1,90E-05	-4,927817481
1	BP	GO:0002229	defense response to oomycetes	15	3,80E-05	-4,835921203
1	BP	GO:0050832	defense response to fungus	47	0,00012	-8,276863062
1	BP	GO:0009627	systemic acquired resistance	22	0,00031	-9,817266238
1	BP	GO:0002237	response to molecule of bacterial origin	18	0,00037	-9,109275489
1	BP	GO:0016045	detection of bacterium	6	4,00E-04	-10,12498206
1	BP	GO:0009626	plant-type hypersensitive response	17	0,00056	-10,15182053
1	BP	GO:0000302	response to reactive oxygen species	43	0,00118	-10,24834434
1	BP	GO:0009742	brassinosteroid mediated signaling pathw,,,	18	0,00118	-0,623167257
1	BP	GO:0010193	response to ozone	13	0,0017	-2,62638338

Table S6a. ...continued.

1	BP	GO:0047484	regulation of response to osmotic stress	12	0,00176	-2,890841474
1	BP	GO:0010200	response to chitin	26	0,00195	-4,581183123
1	BP	GO:0015675	nickel cation transport	3	0,00302	-4,406268152
1	BP	GO:0010359	regulation of anion channel activity	8	0,00361	-6,70831401
1	BP	GO:0000373	Group II intron splicing	7	0,00362	-5,329779771
1	BP	GO:2000022	regulation of jasmonic acid mediated sig„,	9	0,00419	-1,89360817
1	BP	GO:0030007	cellular potassium ion homeostasis	6	0,00438	-0,197126271
1	BP	GO:0009695	jasmonic acid biosynthetic process	9	0,0047	-4,316329268
1	BP	GO:0009651	response to salt stress	76	0,00477	-6,998398132
1	BP	GO:0031129	inductive cell-cell signaling	3	0,00493	1,159790319
1	BP	GO:0007112	male meiosis cytokinesis	6	0,00522	-0,203772518
1	BP	GO:0042631	cellular response to water deprivation	12	0,00537	0,435658123
1	BP	GO:0009409	response to cold	54	0,00549	-5,832685934
1	BP	GO:0030026	cellular manganese ion homeostasis	4	0,00587	3,092657562
1	BP	GO:0009819	drought recovery	5	0,00602	0,222234251
1	BP	GO:0002758	innate immune response-activating signal„,	16	0,00637	-6,253515007
1	BP	GO:0046244	salicylic acid catabolic process	3	0,00757	-3,226365919
1	BP	GO:0010037	response to carbon dioxide	6	0,00765	-6,468663879
1	BP	GO:1902448	positive regulation of shade avoidance	4	0,00765	-1,153043912
1	BP	GO:0009620	response to fungus	66	0,00936	-11,45516926
1	BP	GO:0010600	regulation of auxin biosynthetic process	5	0,00975	-1,006185919
1	BP	GO:0006559	L-phenylalanine catabolic process	4	0,00977	0,488129848
1	BP	GO:0009057	macromolecule catabolic process	42	0,01131	-6,896897421
1	BP	GO:0010227	floral organ abscission	7	0,01227	-2,195127965
1	BP	GO:0031347	regulation of defense response	52	0,01271	-12,45681354
1	BP	GO:0046777	protein autophosphorylation	35	0,01381	-4,001326569
1	BP	GO:0009862	systemic acquired resistance, salicylic „,	6	0,01475	-4,291322631

Table S6a. ...continued.

1	BP	GO:0006015	5-phosphoribose 1-diphosphate biosynthet„,,	3	0,01493	2,120413348
1	BP	GO:2000039	regulation of trichome morphogenesis	4	0,01505	0,458488399
1	BP	GO:0002831	regulation of response to biotic stimulu„,,	17	0,01505	-5,162131093
1	BP	GO:0010152	pollen maturation	6	0,01673	-0,333348373
1	BP	GO:0032469	endoplasmic reticulum calcium ion homeos„,,	2	0,01688	-0,411456502
1	BP	GO:0010767	regulation of transcription from RNA pol„,,	2	0,01688	0,086754281
1	BP	GO:0001778	plasma membrane repair	2	0,01688	1,351012574
1	BP	GO:1990388	xylem-to-phloem iron transport	2	0,01688	-3,230559894
1	BP	GO:1904580	regulation of intracellular mRNA localiz„,,	2	0,01688	-0,849538844
1	BP	GO:0006816	calcium ion transport	7	0,01825	0,429196302
1	BP	GO:1900055	regulation of leaf senescence	10	0,01915	2,328018437
1	BP	GO:0048530	fruit morphogenesis	3	0,0197	1,159790319
1	BP	GO:0042814	monopolar cell growth	3	0,0197	1,159790319
1	BP	GO:0009556	microsporogenesis	9	0,01997	-3,595862338
1	BP	GO:0006164	purine nucleotide biosynthetic process	9	0,01998	6,045498026
1	BP	GO:0009611	response to wounding	40	0,0205	-8,850160556
1	BP	GO:0009813	flavonoid biosynthetic process	16	0,02078	1,893776149
1	BP	GO:0018108	peptidyl-tyrosine phosphorylation	7	0,02096	-3,115034389
1	BP	GO:0006952	defense response	177	0,02104	-19,82766889
1	BP	GO:0032456	endocytic recycling	4	0,02184	1,599051614
1	BP	GO:0045604	regulation of epidermal cell differentia„,,	4	0,02184	1,533929646
1	BP	GO:1901527	abscisic acid-activated signaling pathwa„,,	5	0,02267	-1,800835231
1	BP	GO:0009738	abscisic acid-activated signaling pathwa„,,	42	0,02337	-1,015885069
1	BP	GO:0016441	posttranscriptional gene silencing	12	0,02516	-1,390962596
1	BP	GO:0032101	regulation of response to external stimu„,,	17	0,02586	-5,162131093
1	BP	GO:0046283	anthocyanin-containing compound metaboli„,,	8	0,02594	-1,805518782
1	BP	GO:0009617	response to bacterium	115	0,02672	-15,1716453
1	BP	GO:1903800	positive regulation of production of miR„,,	2	0,02711	1,246200974

Table S6a. ...continued.

1	BP	GO:0010230	alternative respiration	2	0,02711	-0,317116762
1	BP	GO:1903335	regulation of vacuolar transport	2	0,02711	-0,849538844
1	BP	GO:0006007	glucose catabolic process	2	0,02711	4,759156981
1	BP	GO:0070291	N-acylethanolamine metabolic process	2	0,02711	5,932259987
1	BP	GO:0055072	iron ion homeostasis	13	0,02866	0,058153944
1	BP	GO:0033214	iron assimilation by chelation and trans,,,	3	0,03145	4,64621452
1	BP	GO:0046274	lignin catabolic process	3	0,03145	-0,428654627
1	BP	GO:0071577	zinc ion transmembrane transport	3	0,03145	-3,34745177
1	BP	GO:0080092	regulation of pollen tube growth	8	0,03267	-2,273740348
1	BP	GO:0050776	regulation of immune response	37	0,03278	-12,03679874
1	BP	GO:0008643	carbohydrate transport	15	0,0335	-1,087093154
1	BP	GO:0048367	shoot system development	95	0,03407	-2,252813979
1	BP	GO:0015692	lead ion transport	4	0,03505	2,90424887
1	BP	GO:0071483	cellular response to blue light	7	0,03831	-3,667063294
1	BP	GO:0007097	nuclear migration	3	0,03843	1,159790319
1	BP	GO:0009854	oxidative photosynthetic carbon pathway	3	0,03843	1,625990599
1	BP	GO:0071230	cellular response to amino acid stimulus	3	0,03843	-1,939620559
1	BP	GO:0008283	cell proliferation	10	0,03854	1,075920367
1	BP	GO:0019285	glycine betaine biosynthetic process fro,,,	2	0,03919	-2,371529437
1	BP	GO:0090449	phloem glucosinolate loading	2	0,03919	-0,917977795
1	BP	GO:1990619	histone H3-K9 deacetylation	2	0,03919	0,211450927
1	BP	GO:0009807	lignan biosynthetic process	2	0,03919	1,905722713
1	BP	GO:0015739	sialic acid transport	2	0,03919	-1,949218282
1	BP	GO:0002939	tRNA N1-guanine methylation	2	0,03919	-1,933157461
1	BP	GO:0006517	protein deglycosylation	2	0,03919	-1,560988075
1	BP	GO:0046740	transport of virus in host, cell to cell	2	0,03919	1,351012574
1	BP	GO:0009682	induced systemic resistance	12	0,0394	-4,372694751
1	BP	GO:0009306	protein secretion	5	0,04015	0,250554389

Table S6a. ...continued.

1	BP	GO:0010928	regulation of auxin mediated signaling p„,	8	0,04303	3,343391008
1	BP	GO:0000304	response to singlet oxygen	4	0,04595	-1,577109454
1	BP	GO:0002215	defense response to nematode	4	0,04595	-9,611652147
1	BP	GO:0009116	nucleoside metabolic process	9	0,04607	0,751080407
1	BP	GO:0042344	indole glucosinolate catabolic process	3	0,04613	-3,248139933
3	BP	GO:0010193	response to ozone	15	6,30E-06	-2,671655052
3	BP	GO:0009611	response to wounding	40	1,30E-05	-8,508301699
3	BP	GO:0009695	jasmonic acid biosynthetic process	9	0,00031	-3,777212534
3	BP	GO:0009409	response to cold	42	0,00037	-5,718785095
3	BP	GO:0009626	plant-type hypersensitive response	13	0,00049	1,504870979
3	BP	GO:0046256	2,4,6-trinitrotoluene catabolic process	4	0,00074	-7,489607891
3	BP	GO:0009617	response to bacterium	69	0,00089	-6,5457419
3	BP	GO:0031408	oxylipin biosynthetic process	6	0,00103	-4,35604368
3	BP	GO:0009407	toxin catabolic process	7	0,00145	-8,16044706
3	BP	GO:0010597	green leaf volatile biosynthetic process	6	0,00168	-3,192389519
3	BP	GO:0090333	regulation of stomatal closure	12	0,00185	1,964853525
3	BP	GO:0033617	mitochondrial respiratory chain complex „,	4	0,00243	5,014251034
3	BP	GO:0010224	response to UV-B	12	0,00345	-1,945822194
3	BP	GO:0009555	pollen development	38	0,00348	-8,335225105
3	BP	GO:0009630	gravitropism	11	0,00374	-3,82423485
3	BP	GO:0080187	floral organ senescence	4	0,00384	2,828312015
3	BP	GO:0006015	5-phosphoribose 1-diphosphate biosynthet„,	3	0,00507	3,692296162
3	BP	GO:0006749	glutathione metabolic process	7	0,00556	-8,16044706
3	BP	GO:0048443	stamen development	16	0,0066	-4,295822487
3	BP	GO:0006164	purine nucleotide biosynthetic process	5	0,00696	0,159080717
3	BP	GO:0010200	response to chitin	18	0,00726	-6,336074266
3	BP	GO:1901141	regulation of lignin biosynthetic proces„,	8	0,00757	-3,971785376
3	BP	GO:1990169	stress response to copper ion	3	0,00789	4,768711986
3	BP	GO:0009819	drought recovery	4	0,00817	-1,524976748
3	BP	GO:0002239	response to oomycetes	11	0,00924	-1,713223165
3	BP	GO:0009864	induced systemic resistance, jasmonic ac„,	4	9,60E-03	1,74371347

Table S6a. ...continued.

3	BP	GO:0048573	photoperiodism, flowering	15	9,62E-03	-4,019198892
3	BP	GO:0009698	phenylpropanoid metabolic process	30	1,03E-02	-9,361588641
3	BP	GO:0010540	basipetal auxin transport	6	0,01131	-4,538615925
3	BP	GO:0051083	de novo' cotranslational protein foldin„,,	2	0,01286	-1,893710345
3	BP	GO:0060919	auxin influx	4	0,01294	-4,991790199
3	BP	GO:1901703	protein localization involved in auxin p„,,	4	0,01294	-3,820993099
3	BP	GO:0071365	cellular response to auxin stimulus	17	0,01401	-5,465231084
3	BP	GO:0009629	response to gravity	15	0,01446	-7,142495957
3	BP	GO:0006468	protein phosphorylation	51	0,01486	-11,16715473
3	BP	GO:0071486	cellular response to high light intensit„,,	3	0,01675	-1,881238195
3	BP	GO:0006952	defense response	108	0,01683	-11,0021746
3	BP	GO:0009116	nucleoside metabolic process	5	0,01689	1,905173383
3	BP	GO:0042908	xenobiotic transport	5	0,01747	0,935614682
3	BP	GO:1990619	histone H3-K9 deacetylation	2	0,01881	-0,301772019
3	BP	GO:0009807	lignan biosynthetic process	2	0,01881	0,719319541
3	BP	GO:0006979	response to oxidative stress	54	0,01906	-7,636214635
3	BP	GO:1901347	negative regulation of secondary cell wa„,,	3	0,02005	-5,150447173
3	BP	GO:1901140	p-coumaryl alcohol transport	3	0,02005	0,756344556
3	BP	GO:0009644	response to high light intensity	15	0,02174	-2,750971738
3	BP	GO:0010262	somatic embryogenesis	3	0,02369	-1,089887758
3	BP	GO:0009753	response to jasmonic acid	24	0,0237	-3,420793547
3	BP	GO:0042631	cellular response to water deprivation	8	0,02389	-0,124290761
3	BP	GO:0042148	strand invasion	2	0,02569	-5,152757821
3	BP	GO:0015720	allantoin transport	2	0,02569	4,262761219
3	BP	GO:0090549	response to carbon starvation	2	0,02569	1,110644134
3	BP	GO:0042742	defense response to bacterium	47	0,02752	-2,955465908
3	BP	GO:0090332	stomatal closure	18	0,02778	-1,193851953
3	BP	GO:0009156	ribonucleoside monophosphate biosyntheti„,,	4	0,02826	4,995959665

Table S6a. ...continued.

3	BP	GO:0010187	negative regulation of seed germination	5	0,02986	-7,170533547
3	BP	GO:0009627	systemic acquired resistance	12	0,03085	-2,044188162
3	BP	GO:0008152	metabolic process	409	0,03103	-23,33156482
3	BP	GO:0010120	camalexin biosynthetic process	4	0,03185	-0,451942198
3	BP	GO:0010304	PSII associated light-harvesting complex„,,	3	0,03196	-3,777748169
3	BP	GO:0051307	meiotic chromosome separation	5	0,03317	-2,110933602
3	BP	GO:1902459	positive regulation of stem cell populat„,,	2	0,03342	-0,301772019
3	BP	GO:0006432	phenylalanyl-tRNA aminoacylation	2	0,03342	-2,970690924
3	BP	GO:0019605	butyrate metabolic process	2	0,03342	-11,5848056
3	BP	GO:0080151	positive regulation of salicylic acid me„,,	2	0,03342	-0,127871749
3	BP	GO:0046244	salicylic acid catabolic process	2	0,03342	-2,139384319
3	BP	GO:0043100	pyrimidine nucleobase salvage	2	0,03342	4,262761219
3	BP	GO:0071491	cellular response to red light	3	0,03346	-1,931528082
3	BP	GO:0071490	cellular response to far red light	3	0,03356	-1,931528082
3	BP	GO:0034063	stress granule assembly	4	0,03652	2,963296228
3	BP	GO:0000712	resolution of meiotic recombination inte„,,	3	0,03659	0,192861739
3	BP	GO:0009790	embryo development	39	0,03678	-8,616688875
3	BP	GO:0046521	sphingoid catabolic process	1	0,03726	-0,968471136
3	BP	GO:0050708	regulation of protein secretion	1	0,03726	-1,041610327
3	BP	GO:0000379	tRNA-type intron splice site recognition„,,	1	0,03726	-2,247933971
3	BP	GO:0034975	protein folding in endoplasmic reticulum	1	0,03726	-1,232064246
3	BP	GO:0019677	NAD catabolic process	1	0,03726	-0,775345796
3	BP	GO:0010845	positive regulation of reciprocal meioti„,,	1	0,03726	1,16626104
3	BP	GO:0006742	NADP catabolic process	1	0,03726	-0,775345796
3	BP	GO:0042543	protein N-linked glycosylation via argin„,,	1	0,03726	0,950155899
3	BP	GO:1990966	ATP generation from poly-ADP-D-ribose	1	0,03726	-0,871338067

Table S6a. ...continued.

3	BP	GO:0033499	galactose catabolic process via UDP-gala„,	1	0,03726	-0,966808519
3	BP	GO:0010344	seed oilbody biogenesis	3	0,04154	-1,929242485
3	BP	GO:0007263	nitric oxide mediated signal transductio„,	2	0,04192	2,164013673
3	BP	GO:0009423	chorismate biosynthetic process	2	0,04192	-1,387204523
3	BP	GO:0033198	response to ATP	2	0,04192	-2,949264484
3	BP	GO:0045332	phospholipid translocation	2	0,04192	-2,27041218
3	BP	GO:0009809	lignin biosynthetic process	16	0,04634	-7,061558035
3	BP	GO:0052542	defense response by callose deposition	5	0,04674	-3,607564749
3	BP	GO:0080051	cutin transport	3	0,04681	-1,669824621
3	BP	GO:0009862	systemic acquired resistance, salicylic „,	4	0,04771	-2,152395787
3	BP	GO:0009751	response to salicylic acid	21	0,04811	-5,216046223
3	BP	GO:0051603	proteolysis involved in cellular protein„,	18	0,04901	-0,878919927
3	BP	GO:0002237	response to molecule of bacterial origin	8	0,05052	-2,214295456
3	BP	GO:0080167	response to karrikin	19	0,05067	-10,07370556
3	BP	GO:0071492	cellular response to UV-A	2	0,05114	-1,645235893
3	BP	GO:0009800	cinnamic acid biosynthetic process	2	0,05114	-2,139384319
3	BP	GO:0043335	protein unfolding	2	0,05114	-1,893710345
3	BP	GO:0055047	generative cell mitosis	2	5,11E-02	-5,024800603
3	BP	GO:0015692	lead ion transport	3	5,24E-02	0,756344556
3	BP	GO:0009738	abscisic acid-activated signaling pathwa„,	22	0,05389	-4,098047032
4	BP	GO:0016126	sterol biosynthetic process	16	2,40E-05	-5,171059117
4	BP	GO:0042372	phylloquinone biosynthetic process	7	0,00035	2,016801259
4	BP	GO:0019287	isopentenyl diphosphate biosynthetic pro„,	8	0,00039	-8,868785004
4	BP	GO:0050832	defense response to fungus	69	0,00113	3,28980606
4	BP	GO:0006995	cellular response to nitrogen starvation	13	0,00125	3,483879277
4	BP	GO:0000160	phosphorelay signal transduction system	25	0,00206	-4,829033573

Table S6a. ...continued.

4	BP	GO:0018958	phenol-containing compound metabolic pro„,	33	0,0023	8,118516332
4	BP	GO:0009696	salicylic acid metabolic process	19	0,00238	6,354012994
4	BP	GO:0098869	cellular oxidant detoxification	20	0,00391	1,075168378
4	BP	GO:0009809	lignin biosynthetic process	25	0,00572	-2,911713886
4	BP	GO:0051289	protein homotetramerization	5	0,00721	3,682973483
4	BP	GO:0043562	cellular response to nitrogen levels	19	0,00828	4,614884628
4	BP	GO:0009863	salicylic acid mediated signaling pathwa„,	16	0,0085	2,757817916
4	BP	GO:0006824	cobalt ion transport	2	0,00891	-7,457471365
4	BP	GO:0000350	generation of catalytic spliceosome for „,	2	0,00891	-4,011131279
4	BP	GO:0000389	mRNA 3'-splice site recognition	2	0,00891	-4,011131279
4	BP	GO:1905516	positive regulation of fertilization	2	0,00891	-0,101860936
4	BP	GO:0010729	positive regulation of hydrogen peroxide„,	2	0,00891	1,373113433
4	BP	GO:0035444	nickel cation transmembrane transport	2	0,00891	-7,457471365
4	BP	GO:0051455	attachment of spindle microtubules to ki„,	2	0,00891	0,950344875
4	BP	GO:0055068	cobalt ion homeostasis	2	0,00891	-7,457471365
4	BP	GO:0010037	response to carbon dioxide	11	0,00991	-2,160504166
4	BP	GO:0006730	one-carbon metabolic process	5	0,01046	-1,064587723
4	BP	GO:0009617	response to bacterium	126	0,01107	0,894599965
4	BP	GO:0033617	mitochondrial respiratory chain complex „,	5	0,01341	6,489192685
4	BP	GO:0016106	sesquiterpenoid biosynthetic process	10	0,01344	-0,036892194
4	BP	GO:0010201	response to continuous far red light sti„,	3	0,0135	-1,947374571
4	BP	GO:0032889	regulation of vacuole fusion, non-autoph„,	3	0,0135	6,835681897
4	BP	GO:0044085	cellular component biogenesis	169	0,01366	-2,862134933
4	BP	GO:0010597	green leaf volatile biosynthetic process	8	0,01442	-4,816816127
4	BP	GO:0009695	jasmonic acid biosynthetic process	11	0,0169	-2,396283937

Table S6a. ...continued.

4	BP	GO:0050829	defense response to Gram-negative bacter„,,	9	0,01723	0,948076948
4	BP	GO:0051321	meiotic cell cycle	36	0,01723	4,755107712
4	BP	GO:0051555	flavonol biosynthetic process	8	0,01729	3,059012347
4	BP	GO:0080167	response to karrikin	44	0,01858	-1,148334779
4	BP	GO:0042744	hydrogen peroxide catabolic process	13	0,02024	-1,539504616
4	BP	GO:0010777	meiotic mismatch repair involved in reci„,	4	0,0211	-2,800784377
4	BP	GO:0006301	postreplication repair	7	0,02133	3,345043818
4	BP	GO:0010074	maintenance of meristem identity	9	0,02134	-2,04211288
4	BP	GO:0045471	response to ethanol	3	0,02198	2,246129899
4	BP	GO:0031542	positive regulation of anthocyanin biosy„,	3	0,02198	6,628660338
4	BP	GO:0035436	triose phosphate transmembrane transport	3	0,02198	-3,584840874
4	BP	GO:0015760	glucose-6-phosphate transport	3	0,02198	-3,584840874
4	BP	GO:0015713	phosphoglycerate transmembrane transport	3	0,02198	-3,584840874
4	BP	GO:0015714	phosphoenolpyruvate transport	3	0,02198	-3,584840874
4	BP	GO:0042353	fucose biosynthetic process	3	0,02198	3,150470479
4	BP	GO:0016104	triterpenoid biosynthetic process	3	0,02198	-3,491884252
4	BP	GO:0010053	root epidermal cell differentiation	47	0,02232	0,838532034
4	BP	GO:0010225	response to UV-C	5	0,02246	-1,269080355
4	BP	GO:0009969	xyloglucan biosynthetic process	5	0,02246	-0,908664337
4	BP	GO:0009753	response to jasmonic acid	46	0,0225	6,061189699
4	BP	GO:0009627	systemic acquired resistance	21	0,02285	4,223370747
4	BP	GO:0016180	snRNA processing	4	0,02503	-0,827374171
4	BP	GO:0006556	S-adenosylmethionine biosynthetic proces„,	2	0,02504	-1,60670299
4	BP	GO:0010203	response to very low fluence red light s„,	2	0,02504	-1,164601396
4	BP	GO:0009584	detection of visible light	2	0,02504	-1,164601396
4	BP	GO:1902916	positive regulation of protein polyubiqu„,	2	0,02504	0,785178635
4	BP	GO:1900486	positive regulation of isopentenyl dipho„,	2	0,02504	-4,926623268

Table S6a. ...continued.

4	BP	GO:1990052	ER to chloroplast lipid transport	2	0,02504	2,776824457
4	BP	GO:0015936	coenzyme A metabolic process	3	0,02505	-3,140645289
4	BP	GO:0060560	developmental growth involved in morphog„,	77	0,02506	3,999441762
4	BP	GO:0009751	response to salicylic acid	47	0,02641	0,529364515
4	BP	GO:0051026	chiasma assembly	7	0,02708	-3,945302481
4	BP	GO:0010337	regulation of salicylic acid metabolic p„,	8	0,02809	2,680269821
4	BP	GO:0008285	negative regulation of cell proliferatio„,	11	0,03246	-4,713011159
4	BP	GO:0106146	sideretin biosynthesis	3	0,03273	-0,401365176
4	BP	GO:0009957	epidermal cell fate specification	3	0,03273	8,514927288
4	BP	GO:1901045	negative regulation of oviposition	3	0,03273	-0,401365176
4	BP	GO:0060776	simple leaf morphogenesis	3	0,03273	-0,126903696
4	BP	GO:0007623	circadian rhythm	27	0,03443	3,739156872
4	BP	GO:0090333	regulation of stomatal closure	18	0,03498	1,520251839
4	BP	GO:0010411	xyloglucan metabolic process	12	0,03633	-1,29903474
4	BP	GO:0009854	oxidative photosynthetic carbon pathway	4	0,03667	1,947174238
4	BP	GO:0048767	root hair elongation	23	0,03707	4,122736709
4	BP	GO:0042273	ribosomal large subunit biogenesis	8	0,03739	-7,519344464
4	BP	GO:0006468	protein phosphorylation	93	0,03798	2,781675043
4	BP	GO:0010025	wax biosynthetic process	11	0,0392	-3,529081334
4	BP	GO:1900425	negative regulation of defense response „,	8	0,04031	3,035410965
4	BP	GO:0010026	trichome differentiation	23	0,04199	5,913896236
4	BP	GO:0080144	amino acid homeostasis	5	0,04215	-6,393256038
4	BP	GO:0070534	protein K63-linked ubiquitination	5	0,04215	4,24624604
4	BP	GO:0034614	cellular response to reactive oxygen spe„,	13	0,04544	-0,657784541
4	BP	GO:0071281	cellular response to iron ion	3	0,04572	-0,401365176
4	BP	GO:0051762	sesquiterpene biosynthetic process	3	0,04572	-6,694577975

Table S6a. ...continued.

4	BP	GO:2000104	negative regulation of DNA-dependent DNA,,,	4	0,0458	-6,100743462
4	BP	GO:0071495	cellular response to endogenous stimulus	146	0,04614	0,219160546
4	BP	GO:0031122	cytoplasmic microtubule organization	15	0,04617	0,941254453
4	BP	GO:1901979	regulation of inward rectifier potassium,,,	4	0,04637	14,17911471
4	BP	GO:0046885	regulation of hormone biosynthetic proce,,,	15	0,04669	0,206355314
4	BP	GO:1990169	stress response to copper ion	3	0,04694	2,938506285
4	BP	GO:0010325	raffinose family oligosaccharide biosynt,,,	2	0,04697	-0,101860936
4	BP	GO:0010479	stele development	2	0,04697	-1,339179928
4	BP	GO:0034757	negative regulation of iron ion transpor,,,	2	0,04697	-1,875478815
4	BP	GO:0001516	prostaglandin biosynthetic process	2	0,04697	0,104327577
4	BP	GO:0010142	farnesyl diphosphate biosynthetic proces,,,	2	0,04697	-5,646399658
4	BP	GO:0051639	actin filament network formation	2	0,04697	1,816792328
4	BP	GO:0090063	positive regulation of microtubule nucle,,,	2	0,04697	7,624280027
4	BP	GO:0015768	maltose transport	2	0,04697	-0,535004142
4	BP	GO:0046208	spermine catabolic process	2	0,04697	0,694799285
4	BP	GO:0006398	mRNA 3'-end processing by stem-loop bind,,,	2	0,04697	-1,109387365
5	BP	GO:0015995	chlorophyll biosynthetic process	10	3,00E-06	-0,540836627
5	BP	GO:1901259	chloroplast rRNA processing	7	4,30E-05	-3,292684166
5	BP	GO:0010206	photosystem II repair	6	0,00012	-1,912801605
5	BP	GO:0080167	response to karrikin	21	0,00018	1,588131075
5	BP	GO:0006816	calcium ion transport	6	2,00E-04	-1,873700218
5	BP	GO:0010207	photosystem II assembly	5	6,00E-04	-3,224890853
5	BP	GO:0006952	defense response	63	0,00064	5,734116651
5	BP	GO:0032594	protein transport within lipid bilayer	2	0,00065	-1,37291401
5	BP	GO:0009627	systemic acquired resistance	12	0,00095	4,056199882
5	BP	GO:0009409	response to cold	34	0,00102	2,539291295
5	BP	GO:0009249	protein lipoylation	3	0,00175	1,355034108
5	BP	GO:0010601	positive regulation of auxin biosyntheti,,,	3	0,00175	-3,476851029

Table S6a. ...continued.

5	BP	GO:1902458	positive regulation of stomatal opening	4	0,00179	2,986225306
5	BP	GO:0017126	nucleologenesis	3	0,00236	-12,80451125
5	BP	GO:0033169	histone H3-K9 demethylation	3	0,00308	2,531626668
5	BP	GO:0032544	plastid translation	4	0,00349	-2,457418427
5	BP	GO:0060862	negative regulation of floral organ absc„,,	2	0,00379	4,351468995
5	BP	GO:0048564	photosystem I assembly	4	0,00465	-2,272198137
5	BP	GO:1901562	response to paraquat	3	0,00602	5,770213908
5	BP	GO:1905011	transmembrane phosphate ion transport fr„,	2	0,00621	-3,388367519
5	BP	GO:0051083	de novo' cotranslational protein foldin„,	2	0,00621	-1,970525055
5	BP	GO:0010286	heat acclimation	9	0,0065	-0,622808565
5	BP	GO:0009773	photosynthetic electron transport in pho„,	3	0,00866	-3,353749952
5	BP	GO:0042793	plastid transcription	3	0,00866	-1,910633322
5	BP	GO:0009828	plant-type cell wall loosening	5	0,00882	-0,049739568
5	BP	GO:0045176	apical protein localization	2	0,00916	-2,404034422
5	BP	GO:0009662	etioplast organization	2	0,00916	-1,542701815
5	BP	GO:0045038	protein import into chloroplast thylakoi„,	2	0,00916	-1,37291401
5	BP	GO:0009610	response to symbiotic fungus	4	0,00962	0,32859803
5	BP	GO:0032502	developmental process	129	0,0111	3,265986401
5	BP	GO:0045454	cell redox homeostasis	4	0,01183	-5,385581176
5	BP	GO:0019464	glycine decarboxylation via glycine clea„,	2	0,0126	0,60847938
5	BP	GO:0034337	RNA folding	2	0,0126	1,890348862
5	BP	GO:0002240	response to molecule of oomycetes origin	3	0,01373	1,382372138
5	BP	GO:0009740	gibberellic acid mediated signaling path„,	6	0,01509	0,563968553
5	BP	GO:1990059	fruit valve development	3	0,01572	-0,1276856
5	BP	GO:0070919	production of siRNA involved in chromati„,	3	0,01572	1,476590653
5	BP	GO:0033500	carbohydrate homeostasis	4	0,01584	5,404595639
5	BP	GO:0009617	response to bacterium	42	0,01641	3,556298799
5	BP	GO:0061086	negative regulation of histone H3-K27 me„,	2	0,01652	-4,420768116

Table S6a. ...continued.

5	BP	GO:0042549	photosystem II stabilization	2	0,01652	-2,848494997
5	BP	GO:0090547	response to low humidity	2	0,01652	-4,420768116
5	BP	GO:0010258	NADH dehydrogenase complex (plastoquinon„,	2	0,01652	-1,659283332
5	BP	GO:0010027	thylakoid membrane organization	6	0,0166	0,179376701
5	BP	GO:0043903	regulation of symbiosis, encompassing mu„,	3	0,01786	4,459989314
5	BP	GO:0019538	protein metabolic process	106	0,01986	2,714813771
5	BP	GO:0009959	negative gravitropism	3	0,02016	2,603430921
5	BP	GO:0010047	fruit dehiscence	4	0,02031	1,230345426
5	BP	GO:0009607	response to biotic stimulus	60	0,02034	3,988621647
5	BP	GO:0009658	chloroplast organization	17	0,02083	-2,34318747
5	BP	GO:0034982	mitochondrial protein processing	2	0,02088	0,912694625
5	BP	GO:0033198	response to ATP	2	0,02088	2,986153388
5	BP	GO:0071586	CAAX-box protein processing	2	0,02088	-0,120050886
5	BP	GO:0010155	regulation of proton transport	2	0,02088	9,818660911
5	BP	GO:0048528	post-embryonic root development	7	0,02327	0,870198393
5	BP	GO:0071731	response to nitric oxide	3	0,02521	3,525227676
5	BP	GO:0006073	cellular glucan metabolic process	13	0,02537	0,823726431
5	BP	GO:0000453	enzyme-directed rRNA 2'-O-methylation	1	0,0256	-1,905171946
5	BP	GO:0048255	mRNA stabilization	1	0,0256	-0,905832346
5	BP	GO:0015825	L-serine transport	1	0,0256	-1,033025987
5	BP	GO:0033396	beta-alanine biosynthetic process via 3-„,	1	0,0256	1,220332571
5	BP	GO:0044070	regulation of anion transport	2	0,02563	-0,16442505
5	BP	GO:2001141	regulation of RNA biosynthetic process	42	0,02563	0,920796501
5	BP	GO:2000122	negative regulation of stomatal complex „,	2	0,02567	-4,558367893
5	BP	GO:0010377	guard cell fate commitment	2	0,02567	-4,420768116
5	BP	GO:0043335	protein unfolding	2	0,02567	-1,970525055

Table S6a. ...continued.

5	BP	GO:0046486	glycerolipid metabolic process	5	0,0257	2,620116861
5	BP	GO:0010119	regulation of stomatal movement	14	0,03004	-0,597748009
5	BP	GO:0002679	respiratory burst involved in defense re„,,	2	0,03085	2,986153388
5	BP	GO:0009615	response to virus	7	0,03448	4,372079847
5	BP	GO:0009750	response to fructose	4	0,03628	-0,40391424
5	BP	GO:0071366	cellular response to indolebutyric acid „,	2	0,0364	2,909030732
5	BP	GO:0071585	detoxification of cadmium ion	3	0,03718	-0,1276856
5	BP	GO:0007231	osmosensory signaling pathway	3	0,04055	4,335970431
5	BP	GO:0030968	endoplasmic reticulum unfolded protein r„,	4	0,04114	7,668723017
5	BP	GO:0009698	phenylpropanoid metabolic process	14	0,04157	5,984261033
5	BP	GO:0046104	thymidine metabolic process	2	0,04231	2,909030732
5	BP	GO:0071577	zinc ion transmembrane transport	2	0,04231	2,527539371
5	BP	GO:0009644	response to high light intensity	9	0,04255	-1,332362981
5	BP	GO:0042742	defense response to bacterium	31	0,04663	0,369954719
5	BP	GO:0031425	chloroplast RNA processing	5	0,04723	-3,697344325
5	BP	GO:1990748	cellular detoxification	9	0,04776	0,178441326
5	BP	GO:0010114	response to red light	8	0,04838	-1,205296517
5	BP	GO:0010412	mannan metabolic process	2	0,04854	1,696629278
5	BP	GO:0010239	chloroplast mRNA processing	2	0,04854	-1,447311088
5	BP	GO:0060866	leaf abscission	2	0,04854	-1,138562012
5	BP	GO:2000121	regulation of removal of superoxide radi„,	2	0,05042	-2,169378246
5	BP	GO:0010046	response to mycotoxin	1	0,05054	-0,795364594
5	BP	GO:0032194	ubiquinone biosynthetic process via 3,4-„,	1	0,05054	-1,118526211
5	BP	GO:0018117	protein adenylylation	1	0,05054	-0,795364594
5	BP	GO:0043157	response to cation stress	1	0,05054	-0,82662701
5	BP	GO:0010602	regulation of 1-aminocyclopropane-1-carb„,	1	0,05054	-1,719651936
5	BP	GO:0062034	L-pipecolic acid biosynthetic process	1	0,05054	-1,874096975

Table S6a. ...continued.

5	BP	GO:0000032	cell wall mannoprotein biosynthetic proc„,	1	0,05054	1,131852208
5	BP	GO:0070158	mitochondrial seryl-tRNA aminoacylation	1	0,05054	-1,728105129
5	BP	GO:0080169	cellular response to boron-containing su„,	1	0,05054	2,798628107
5	BP	GO:0030155	regulation of cell adhesion	1	0,05054	-3,054519656
5	BP	GO:0010234	anther wall tapetum cell fate specificat„,	1	0,05054	-1,198111972
5	BP	GO:0033355	ascorbate glutathione cycle	1	0,05054	-0,858897774
5	BP	GO:2000616	negative regulation of histone H3-K9 ace„,	1	0,05054	3,742965737

Table S6b. Full list of enriched GO terms enriched after excluding shared DEGs with complete IDs (adjusted $p < 0.05$). The GO terms are reported per locality (z-score > 0 and z-score < 0 indicate over- and underexpression in the montane ecotype, respectively). Note that the term root hair cell developement has a adjuste $p = 0{,}06$ but was reported because of its relevant function.

Ecotype pair	**Ontology**	**GO ID**	**GO Term**	**Gene number**	**adjusted p-val**	**z-score**
1	BP	GO:0009751	response to salicylic acid	24	0,00013	-11,957277
1	BP	GO:0042742	defense response to bacterium	50	0,00024	-13,099085
1	BP	GO:0016045	detection of bacterium	5	0,00036	-10,02394
1	BP	GO:0009864	induced systemic resistance, jasmonic ac„,	5	0,00093	-3,2950208
1	BP	GO:1902448	positive regulation of shade avoidance	4	0,00137	-1,1530439
1	BP	GO:0000302	response to reactive oxygen species	29	0,00142	-6,9370676
1	BP	GO:0030007	cellular potassium ion homeostasis	5	0,00277	-0,7201421
1	BP	GO:0002229	defense response to oomycetes	9	0,0034	-4,0557288
1	BP	GO:0002237	response to molecule of bacterial origin	13	0,0035	-8,5857227
1	BP	GO:0032456	endocytic recycling	4	0,00425	1,59905161
1	BP	GO:0055072	iron ion homeostasis	8	0,00429	1,89619043
1	BP	GO:0009742	brassinosteroid mediated signaling pathw„,	11	0,00548	-0,2000426
1	BP	GO:0009819	drought recovery	4	0,00608	0,67985504
1	BP	GO:0006816	calcium ion transport	5	0,00611	-0,5289693
1	BP	GO:0032469	endoplasmic reticulum calcium ion homeos„,	2	0,00671	-0,4114565

Table S6b. ...continued.

1	BP	GO:1904580	regulation of intracellular mRNA localiz„,	2	0,00671	-0,8495388
1	BP	GO:1990388	xylem-to-phloem iron transport	2	0,00671	-3,2305599
1	BP	GO:0001778	plasma membrane repair	2	0,00671	1,35101257
1	BP	GO:0010767	regulation of transcription from RNA pol„,	2	0,00671	0,08675428
1	BP	GO:0018108	peptidyl-tyrosine phosphorylation	6	0,00764	-0,7845371
1	BP	GO:0019722	calcium-mediated signaling	6	0,00809	-2,8306076
1	BP	GO:0010359	regulation of anion channel activity	6	0,0081	-9,9179842
1	BP	GO:0009306	protein secretion	4	0,0097	-0,1847458
1	BP	GO:0000304	response to singlet oxygen	4	0,0097	-1,5771095
1	BP	GO:0042023	DNA endoreduplication	5	0,00974	-0,3833989
1	BP	GO:1903335	regulation of vacuolar transport	2	0,01092	-0,8495388
1	BP	GO:0071230	cellular response to amino acid stimulus	3	0,01096	-1,9396206
1	BP	GO:0008283	cell proliferation	7	0,01101	-0,9438961
1	BP	GO:0042631	cellular response to water deprivation	8	0,01521	0,87115801
1	BP	GO:0010600	regulation of auxin biosynthetic process	4	0,01597	-0,3376651
1	BP	GO:0006517	protein deglycosylation	2	0,01602	-1,5609881
1	BP	GO:0015739	sialic acid transport	2	0,01602	-1,9492183
1	BP	GO:0046740	transport of virus in host, cell to cell	2	0,01602	1,35101257
1	BP	GO:0006559	L-phenylalanine catabolic process	3	0,01603	1,0617696
1	BP	GO:0009835	fruit ripening	3	0,01603	-1,4804119
1	BP	GO:0046777	protein autophosphorylation	24	0,0164	-4,2569335
1	BP	GO:0009620	response to fungus	34	0,01695	-5,0055244
1	BP	GO:0010200	response to chitin	16	0,0172	-2,0998471
1	BP	GO:1901527	abscisic acid-activated signaling pathwa„,	4	0,01838	-2,577109
1	BP	GO:0002758	innate immune response-activating signal„,	12	0,01842	-6,4396799
1	BP	GO:0047484	regulation of response to osmotic stress	7	0,0189	-1,3415395
1	BP	GO:0010216	maintenance of DNA methylation	3	0,01897	-0,6177637
1	BP	GO:0010227	floral organ abscission	5	0,01993	-3,3518189

Table S6b. ...continued.

1	BP	GO:0034220	ion transmembrane transport	25	0,02054	-4,3804356
1	BP	GO:0031347	regulation of defense response	31	0,02063	-11,803893
1	BP	GO:0031129	inductive cell-cell signaling	2	0,02192	2,51644709
1	BP	GO:0071332	cellular response to fructose stimulus	2	0,02192	-4,2611998
1	BP	GO:0002831	regulation of response to biotic stimulu„,,	9	0,02245	-6,9020304
1	BP	GO:0071472	cellular response to salt stress	6	0,02345	-1,4067661
1	BP	GO:0008643	carbohydrate transport	9	0,02376	-0,3409651
1	BP	GO:0006633	fatty acid biosynthetic process	12	0,02469	-0,2223835
1	BP	GO:0009626	plant-type hypersensitive response	9	0,02633	-9,7887832
1	BP	GO:0010365	positive regulation of ethylene biosynth„,,	2	0,02857	-0,0524983
1	BP	GO:0046244	salicylic acid catabolic process	2	0,02857	-3,3413981
1	BP	GO:0045604	regulation of epidermal cell differentia„,,	3	0,0295	2,66610951
1	BP	GO:0009934	regulation of meristem structural organi„,,	5	0,03204	-0,4024299
1	BP	GO:0010050	vegetative phase change	4	0,03347	-2,5076753
1	BP	GO:0006000	fructose metabolic process	3	0,03356	5,11551309
1	BP	GO:0032101	regulation of response to external stimu„,,	9	0,03395	-6,9020304
1	BP	GO:0016052	carbohydrate catabolic process	11	0,03414	4,10249373
1	BP	GO:0048609	multicellular organismal reproductive pr„,,	16	0,0342	-1,581616
1	BP	GO:0018142	protein-DNA covalent cross-linking	1	0,03424	2,14735154
1	BP	GO:0032780	negative regulation of ATPase activity	1	0,03424	3,54393121
1	BP	GO:0034089	establishment of meiotic sister chromati„,,	1	0,03424	2,68857836
1	BP	GO:0015727	lactate transport	1	0,03424	3,47009177
1	BP	GO:0010446	response to alkaline pH	1	0,03424	3,54393121
1	BP	GO:1902553	positive regulation of catalase activity	1	0,03424	-0,7625815
1	BP	GO:0034421	post-translational protein acetylation	1	0,03424	2,68857836

Table S6b. ...continued.

1	BP	GO:0006780	uroporphyrinogen III biosynthetic proces„,	1	0,03424	-0,8453566
1	BP	GO:0006655	phosphatidylglycerol biosynthetic proces„,	2	0,03591	1,149142
1	BP	GO:2000214	regulation of proline metabolic process	2	0,03591	-2,7835411
1	BP	GO:0005987	sucrose catabolic process	2	0,03591	-1,5129398
1	BP	GO:0031663	lipopolysaccharide-mediated signaling pa„,	2	0,03591	0,89915785
1	BP	GO:0009057	macromolecule catabolic process	24	0,03715	-9,5788807
1	BP	GO:0080170	hydrogen peroxide transmembrane transpor„,	3	0,0379	0,35561092
1	BP	GO:2000762	regulation of phenylpropanoid metabolic „,	4	0,03819	-3,8712885
1	BP	GO:0010152	pollen maturation	4	0,04004	-1,2518328
1	BP	GO:0009556	microsporogenesis	6	0,04095	-1,5000734
1	BP	GO:0002221	pattern recognition receptor signaling p„,	6	0,04194	0,38118278
1	BP	GO:0035335	peptidyl-tyrosine dephosphorylation	3	0,04251	-0,753138
1	BP	GO:0006875	cellular metal ion homeostasis	14	0,04282	0,56326348
1	BP	GO:0010090	trichome morphogenesis	9	0,04344	1,35830244
1	BP	GO:0000165	MAPK cascade	5	0,04345	-0,3654709
1	BP	GO:0006829	zinc ion transport	4	0,04365	-2,9138117
1	BP	GO:0006491	N-glycan processing	2	0,04389	-1,5609881
1	BP	GO:0006145	purine nucleobase catabolic process	2	0,04389	-1,2392164
1	BP	GO:2000022	regulation of jasmonic acid mediated sig„,	5	0,04793	0,95745956
3	BP	GO:0009555	pollen development	24	0,0037	-2,1399173
3	BP	GO:0009626	plant-type hypersensitive response	8	0,0059	4,10811907
3	BP	GO:0071365	cellular response to auxin stimulus	12	0,0066	-5,0791027
3	BP	GO:0009819	drought recovery	3	0,0086	-1,0038707
3	BP	GO:0090333	regulation of stomatal closure	7	0,0095	5,03150392
3	BP	GO:0060919	auxin influx	3	0,0123	-4,2356659
3	BP	GO:0009611	response to wounding	19	0,0151	-2,4236531
3	BP	GO:0010540	basipetal auxin transport	4	0,0173	-3,2924426
3	BP	GO:0071493	cellular response to UV-B	2	0,0186	-2,9207568
3	BP	GO:0019677	NAD catabolic process	1	0,0195	-0,7753458

Table S6b. ...continued.

3	BP	GO:1990966	ATP generation from poly-ADP-D-ribose	1	0,0195	-0,8713381
3	BP	GO:0006742	NADP catabolic process	1	0,0195	-0,7753458
3	BP	GO:0034975	protein folding in endoplasmic reticulum	1	0,0195	-1,2320642
3	BP	GO:0010845	positive regulation of reciprocal meioti„,,	1	0,0195	1,16626104
3	BP	GO:0042543	protein N-linked glycosylation via argin„,,	1	0,0195	0,9501559
3	BP	GO:0000379	tRNA-type intron splice site recognition„,,	1	0,0195	-2,247934
3	BP	GO:0009790	embryo development	17	0,0195	-4,233979
3	BP	GO:0046256	2,4,6-trinitrotoluene catabolic process	2	0,022	-4,3534757
3	BP	GO:0009630	gravitropism	7	0,023	-3,3961645
3	BP	GO:0009269	response to desiccation	3	0,026	1,54803191
3	BP	GO:0016444	somatic cell DNA recombination	2	0,0295	-0,1021922
3	BP	GO:0001676	long-chain fatty acid metabolic process	2	0,0337	0,09823426
3	BP	GO:0010417	glucuronoxylan biosynthetic process	2	0,038	-2,5056326
3	BP	GO:0071994	phytochelatin transmembrane transport	1	0,0386	-0,9011357
3	BP	GO:0032049	cardiolipin biosynthetic process	1	0,0386	-2,1757312
3	BP	GO:0019424	sulfide oxidation, using siroheme sulfit„,,	1	0,0386	-1,5946931
3	BP	GO:0043619	regulation of transcription from RNA pol„,,	1	0,0386	-2,5630667
3	BP	GO:0090617	mitochondrial mRNA 5'-end processing	1	0,0386	1,49469508
3	BP	GO:0006592	ornithine biosynthetic process	1	0,0386	-0,8344083
3	BP	GO:0019240	citrulline biosynthetic process	1	0,0386	-1,741924
3	BP	GO:0044648	histone H3-K4 dimethylation	1	0,0386	-2,6774119
3	BP	GO:1990570	GDP-mannose transmembrane transport	1	0,0386	-3,9118025
3	BP	GO:0051070	galactomannan biosynthetic process	1	0,0386	-2,9772173
3	BP	GO:0036290	protein trans-autophosphorylation	1	0,0386	-3,1183377
3	BP	GO:0048205	COPI coating of Golgi vesicle	1	0,0386	-0,9719947
3	BP	GO:0071457	cellular response to ozone	1	0,0386	-0,9316852

Table S6b. ...continued.

3	BP	GO:0006154	adenosine catabolic process	1	0,0386	-3,7770262
3	BP	GO:0010392	galactoglucomannan metabolic process	1	0,0386	-2,9772173
3	BP	GO:0006114	glycerol biosynthetic process	1	0,0386	0,81586834
3	BP	GO:0008152	metabolic process	207	0,0476	-17,470531
3	BP	GO:0009750	response to fructose	4	0,0479	-1,2491012
3	BP	GO:0080147	root hair cell development	6	6,37E-02	1,2311631
4	BP	GO:0016126	sterol biosynthetic process	14	1,70E-05	-8,6360107
4	BP	GO:0019287	isopentenyl diphosphate biosynthetic pro„,	8	7,90E-05	-8,868785
4	BP	GO:0042372	phylloquinone biosynthetic process	6	0,00054	2,48909597
4	BP	GO:0006995	cellular response to nitrogen starvation	11	0,00123	3,57485244
4	BP	GO:0000160	phosphorelay signal transduction system	18	0,00179	-2,707364
4	BP	GO:0051289	protein homotetramerization	5	0,00208	3,68297348
4	BP	GO:0009696	salicylic acid metabolic process	16	0,00391	5,69279782
4	BP	GO:0000350	generation of catalytic spliceosome for „,	2	0,00503	-4,0111313
4	BP	GO:0000389	mRNA 3'-splice site recognition	2	0,00503	-4,0111313
4	BP	GO:1905516	positive regulation of fertilization	2	0,00503	-0,1018609
4	BP	GO:0010729	positive regulation of hydrogen peroxide„,	2	0,00503	1,37311343
4	BP	GO:0016106	sesquiterpenoid biosynthetic process	9	0,00602	-0,5177353
4	BP	GO:0010074	maintenance of meristem identity	8	0,00796	-3,6002968
4	BP	GO:0098869	cellular oxidant detoxification	15	0,00836	1,16776199
4	BP	GO:0050829	defense response to Gram-negative bacter„,	8	0,00979	0,44008211
4	BP	GO:0045471	response to ethanol	3	0,01004	2,2461299
4	BP	GO:0031542	positive regulation of anthocyanin biosy„,	3	0,01004	6,62866034
4	BP	GO:0035436	triose phosphate transmembrane transport	3	0,01004	-3,5848409
4	BP	GO:0015760	glucose-6-phosphate transport	3	0,01004	-3,5848409

Table S6b. ...continued.

4	BP	GO:0015713	phosphoglycerate transmembrane transport	3	0,01004	-3,5848409
4	BP	GO:0015714	phosphoenolpyruvate transport	3	0,01004	-3,5848409
4	BP	GO:0016104	triterpenoid biosynthetic process	3	0,01004	-3,4918843
4	BP	GO:0043562	cellular response to nitrogen levels	16	0,01095	4,62268938
4	BP	GO:0010026	trichome differentiation	18	0,01391	3,71083323
4	BP	GO:0070534	protein K63-linked ubiquitination	5	0,01394	4,24624604
4	BP	GO:0010305	leaf vascular tissue pattern formation	13	0,01395	0,55494353
4	BP	GO:0015936	coenzyme A metabolic process	3	0,01438	-3,1406453
4	BP	GO:1902916	positive regulation of protein polyubiqu„,,	2	0,01438	0,78517863
4	BP	GO:1900486	positive regulation of isopentenyl dipho„,,	2	0,01438	-4,9266233
4	BP	GO:1990052	ER to chloroplast lipid transport	2	0,01438	2,77682446
4	BP	GO:0106146	sideretin biosynthesis	3	0,01522	-0,4013652
4	BP	GO:1901045	negative regulation of oviposition	3	0,01522	-0,4013652
4	BP	GO:0080167	response to karrikin	35	0,01625	1,20361655
4	BP	GO:0009624	response to nematode	14	0,01625	-9,0082309
4	BP	GO:0051321	meiotic cell cycle	23	0,02071	2,46562981
4	BP	GO:0071281	cellular response to iron ion	3	0,02165	-0,4013652
4	BP	GO:0051762	sesquiterpene biosynthetic process	3	0,02165	-6,694578
4	BP	GO:2000104	negative regulation of DNA-dependent DNA„,,	4	0,02167	-6,1007435
4	BP	GO:0018958	phenol-containing compound metabolic pro„,,	28	0,0219	6,5345917
4	BP	GO:0006301	postreplication repair	6	0,02672	2,61590701
4	BP	GO:0010325	raffinose family oligosaccharide biosynt„,,	2	0,02741	-0,1018609
4	BP	GO:0010479	stele development	2	0,02741	-1,3391799
4	BP	GO:0034757	negative regulation of iron ion transpor„,,	2	0,02741	-1,8754788
4	BP	GO:0001516	prostaglandin biosynthetic process	2	0,02741	0,10432758
4	BP	GO:0010142	farnesyl diphosphate biosynthetic proces„,,	2	0,02741	-5,6463997

Table S6b. ...continued.

4	BP	GO:0051639	actin filament network formation	2	0,02741	1,81679233
4	BP	GO:0015768	maltose transport	2	0,02741	-0,5350041
4	BP	GO:0046208	spermine catabolic process	2	0,02741	0,69479928
4	BP	GO:0015671	oxygen transport	2	0,02741	2,7995286
4	BP	GO:0033512	L-lysine catabolic process to acetyl-CoA,,,	2	0,02741	3,42912468
4	BP	GO:0030245	cellulose catabolic process	4	0,0285	-0,9327613
4	BP	GO:0048767	root hair elongation	19	0,03434	4,56584571
4	BP	GO:0050832	defense response to fungus	48	0,03461	6,41391477
4	BP	GO:0010225	response to UV-C	4	0,03464	-1,0196469
4	BP	GO:0009969	xyloglucan biosynthetic process	4	0,03464	-0,3625891
4	BP	GO:0042744	hydrogen peroxide catabolic process	10	0,03558	-3,04061
4	BP	GO:0010345	suberin biosynthetic process	7	0,03782	-8,9620512
4	BP	GO:0009867	jasmonic acid mediated signaling pathway	15	0,03788	4,48016583
4	BP	GO:0010190	cytochrome b6f complex assembly	3	0,03823	5,86987902
4	BP	GO:0051016	barbed-end actin filament capping	3	0,03823	-2,3671118
4	BP	GO:0071475	cellular hyperosmotic salinity response	3	0,03823	-2,8658764
4	BP	GO:0010102	lateral root morphogenesis	16	0,03902	-5,0104684
4	BP	GO:0042273	ribosomal large subunit biogenesis	7	0,03936	-6,9922127
4	BP	GO:0010337	regulation of salicylic acid metabolic p,,,	7	0,0413	3,89696987
4	BP	GO:0046885	regulation of hormone biosynthetic proce,,,	10	0,04343	0,90135859
4	BP	GO:0045338	farnesyl diphosphate metabolic process	4	0,04344	-5,7865767
4	BP	GO:2000029	regulation of proanthocyanidin biosynthe,,,	2	0,04355	6,19895459
4	BP	GO:0009745	sucrose mediated signaling	2	0,04355	2,94703061
4	BP	GO:0010025	wax biosynthetic process	9	0,04687	-6,3460285
4	BP	GO:0009863	salicylic acid mediated signaling pathwa,,,	12	0,04894	3,41225258
4	BP	GO:0042127	regulation of cell proliferation	15	0,04916	-3,4590997
5	BP	GO:1901259	chloroplast rRNA processing	7	3,80E-06	-3,2926842

Table S6b. ...continued.

5	BP	GO:0006816	calcium ion transport	6	3,30E-05	-1,8737002
5	BP	GO:0010207	photosystem II assembly	5	0,00014	-3,2248909
5	BP	GO:0015995	chlorophyll biosynthetic process	8	0,00025	-1,8698656
5	BP	GO:0032594	protein transport within lipid bilayer	2	0,00031	-1,372914
5	BP	GO:0032544	plastid translation	4	0,00088	-2,4574184
5	BP	GO:0009409	response to cold	27	0,00104	-1,0186984
5	BP	GO:0010286	heat acclimation	8	0,0029	-2,4066805
5	BP	GO:1905011	transmembrane phosphate ion transport fr„,,	2	0,00296	-3,3883675
5	BP	GO:0051083	de novo' cotranslational protein foldin„,,	2	0,00296	-1,9705251
5	BP	GO:0042793	plastid transcription	3	0,00303	-1,9106333
5	BP	GO:0009773	photosynthetic electron transport in pho„,,	3	0,00303	-3,35375
5	BP	GO:0009658	chloroplast organization	15	0,00304	-3,7029748
5	BP	GO:0032502	developmental process	88	0,00306	-1,3467013
5	BP	GO:0009740	gibberellic acid mediated signaling path„,,	6	0,00318	0,56396855
5	BP	GO:0009662	etioplast organization	2	0,0044	-1,5427018
5	BP	GO:0045176	apical protein localization	2	0,0044	-2,4040344
5	BP	GO:0045038	protein import into chloroplast thylakoi„,,	2	0,0044	-1,372914
5	BP	GO:0070919	production of siRNA involved in chromati„,,	3	0,00563	1,47659065
5	BP	GO:0043903	regulation of symbiosis, encompassing mu„,,	3	0,00644	4,45998931
5	BP	GO:0080167	response to karrikin	13	0,00704	0,63589336
5	BP	GO:0009959	negative gravitropism	3	0,00731	2,60343092
5	BP	GO:0090547	response to low humidity	2	0,00802	-4,4207681
5	BP	GO:0042549	photosystem II stabilization	2	0,00802	-2,848495
5	BP	GO:0061086	negative regulation of histone H3-K27 me„,,	2	0,00802	-4,4207681
5	BP	GO:0048528	post-embryonic root development	5	0,0096	2,41661312
5	BP	GO:0010155	regulation of proton transport	2	0,01019	9,81866091
5	BP	GO:0006952	defense response	31	0,01214	0,22676158
5	BP	GO:0010377	guard cell fate commitment	2	0,01259	-4,4207681
5	BP	GO:0043335	protein unfolding	2	0,01259	-1,9705251

Table S6b. ...continued.

5	BP	GO:0009249	protein lipoylation	2	0,01259	0,10279133
5	BP	GO:0017126	nucleologenesis	2	0,01521	-12,820166
5	BP	GO:0010206	photosystem II repair	3	0,01673	-2,3165151
5	BP	GO:0046486	glycerolipid metabolic process	5	0,01754	2,62011686
5	BP	GO:0000453	enzyme-directed rRNA 2'-O-methylation	1	0,01756	-1,9051719
5	BP	GO:0015825	L-serine transport	1	0,01756	-1,033026
5	BP	GO:0048255	mRNA stabilization	1	0,01756	-0,9058323
5	BP	GO:0044070	regulation of anion transport	2	0,01756	-0,1644251
5	BP	GO:0031425	chloroplast RNA processing	5	0,01791	-3,6973443
5	BP	GO:0033169	histone H3-K9 demethylation	2	0,01804	0,45392032
5	BP	GO:0009610	response to symbiotic fungus	3	0,0198	4,45998931
5	BP	GO:0045454	cell redox homeostasis	3	0,02315	-2,705304
5	BP	GO:0010239	chloroplast mRNA processing	2	0,02431	-1,4473111
5	BP	GO:0009615	response to virus	6	0,02542	2,70617227
5	BP	GO:0051260	protein homooligomerization	3	0,02679	-0,6647874
5	BP	GO:0009089	lysine biosynthetic process via diaminop„,	2	0,02773	-1,9279527
5	BP	GO:0010268	brassinosteroid homeostasis	2	0,03133	2,76354856
5	BP	GO:0070158	mitochondrial seryl-tRNA aminoacylation	1	0,0348	-1,7281051
5	BP	GO:0080169	cellular response to boron-containing su„,	1	0,0348	2,79862811
5	BP	GO:0043157	response to cation stress	1	0,0348	-0,826627
5	BP	GO:0010234	anther wall tapetum cell fate specificat„,	1	0,0348	-1,198112
5	BP	GO:0035524	proline transmembrane transport	1	0,0348	-1,033026
5	BP	GO:0030155	regulation of cell adhesion	1	0,0348	-3,0545197
5	BP	GO:0033355	ascorbate glutathione cycle	1	0,0348	-0,8588978
5	BP	GO:0055062	phosphate ion homeostasis	3	0,03494	-2,3780523
5	BP	GO:0010047	fruit dehiscence	3	0,03494	0,54759987
5	BP	GO:2000039	regulation of trichome morphogenesis	2	0,03905	0,45392032
5	BP	GO:0045597	positive regulation of cell differentiat„,	3	0,04289	-2,0611759

Table S6b. ...continued.

5	BP	GO:0032776	DNA methylation on cytosine	2	0,0474	0,45392032

Table S7. Full list of enriched GO terms enriched in cRDA analysis with complete IDs (adjusted $p < 0.05$). (z-score > 0 and z-score < 0 indicate over- and underexpression in the montane ecotype, respectively).

Ontology	**GO ID**	**GO Term**	**Gene number**	**adjusted p-val**	**z-score**
BP	GO:0009751	response to salicylic acid	31	1,00E-06	-5,78546
BP	GO:0042742	defense response to bacterium	60	1,10E-06	-3,93038
BP	GO:0010193	response to ozone	15	1,20E-06	-2,36985
BP	GO:0050832	defense response to fungus	34	9,50E-05	-4,29654
BP	GO:0000302	response to reactive oxygen species	37	0,00012	-6,05236
BP	GO:0031408	oxylipin biosynthetic process	7	0,00013	-2,93799
BP	GO:0009695	jasmonic acid biosynthetic process	9	0,00026	-4,11923
BP	GO:0009620	response to fungus	51	3,00E-04	-5,73248
BP	GO:0016126	sterol biosynthetic process	9	0,00054	-3,73295
BP	GO:0006468	protein phosphorylation	51	0,00133	-4,13121
BP	GO:0009627	systemic acquired resistance	14	0,00164	-3,85289
BP	GO:0019287	isopentenyl diphosphate biosynthetic pro...	4	0,00173	-4,71045
BP	GO:0002215	defense response to nematode	5	0,00183	-3,59285
BP	GO:0033617	mitochondrial respiratory chain complex ...	4	0,00224	-0,44218
BP	GO:0016255	attachment of GPI anchor to protein	3	0,00343	-1,16939
BP	GO:0080187	floral organ senescence	4	0,00355	2,05834
BP	GO:0042425	choline biosynthetic process	2	0,00388	-3,54106
BP	GO:0016045	detection of bacterium	4	0,00437	-2,18247
BP	GO:0090059	protoxylem development	3	0,00477	-3,93511
BP	GO:0042221	response to chemical	230	0,00493	-9,77326
BP	GO:0048443	stamen development	14	0,00604	-2,76376
BP	GO:1901348	positive regulation of secondary cell wa...	3	0,00638	-3,93511
BP	GO:0071555	cell wall organization	31	0,0064	-3,55127
BP	GO:1990169	stress response to copper ion	3	0,00756	3,94319
BP	GO:0090431	alkyl caffeate ester biosynthetic proces...	2	0,00758	-3,07301
BP	GO:0010142	farnesyl diphosphate biosynthetic proces...	2	0,00758	-3,29363
BP	GO:0033494	ferulate metabolic process	2	0,00758	-3,07301
BP	GO:0010074	maintenance of meristem identity	6	0,00832	-1,88086
BP	GO:1990110	callus formation	6	0,00844	-3,61033
BP	GO:0048235	pollen sperm cell differentiation	7	0,00848	0,74722
BP	GO:0006722	triterpenoid metabolic process	5	0,01039	-4,9346
BP	GO:0034508	centromere complex assembly	3	0,01048	1,14821
BP	GO:0045338	farnesyl diphosphate metabolic process	5	0,01221	-5,14713

Table S7. ...continued.

BP	GO:0006863	purine nucleobase transport	3	0,0123	1,29322
BP	GO:0071365	cellular response to auxin stimulus	15	0,01301	-5,01283
BP	GO:0009626	plant-type hypersensitive response	11	0,01352	-2,01483
BP	GO:0009737	response to abscisic acid	62	0,01573	-0,59483
BP	GO:0010037	response to carbon dioxide	5	0,01575	0,61507
BP	GO:0010150	leaf senescence	22	0,01592	-2,06192
BP	GO:0055062	phosphate ion homeostasis	5	0,01604	0,93
BP	GO:0042744	hydrogen peroxide catabolic process	7	0,01804	-1,0833
BP	GO:0051665	membrane raft localization	2	0,01805	3,23347
BP	GO:1990619	histone H3-K9 deacetylation	2	0,01805	-0,16587
BP	GO:0034394	protein localization to cell surface	2	0,01805	0,00578
BP	GO:0051174	regulation of phosphorus metabolic proce...	6	0,01818	-2,22716
BP	GO:0009835	fruit ripening	3	0,01893	-1,17375
BP	GO:0009735	response to cytokinin	10	0,02148	-2,94014
BP	GO:0042148	strand invasion	2	0,02466	-3,38291
BP	GO:0016104	triterpenoid biosynthetic process	2	0,02466	-3,24372
BP	GO:0006651	diacylglycerol biosynthetic process	2	0,02466	-3,54106
BP	GO:0009742	brassinosteroid mediated signaling pathw...	10	0,02471	-5,78873
BP	GO:0098869	cellular oxidant detoxification	9	0,02508	-3,7613
BP	GO:0010359	regulation of anion channel activity	6	0,02518	-0,04875
BP	GO:0009555	pollen development	35	0,02541	-2,88542
BP	GO:0031667	response to nutrient levels	17	0,0263	-0,49221
BP	GO:0098542	defense response to other organism	99	0,02723	-6,81946
BP	GO:0012501	programmed cell death	21	0,02844	-5,26967
BP	GO:0006656	phosphatidylcholine biosynthetic process	3	0,03022	-1,70913
BP	GO:0010304	PSII associated light-harvesting complex...	3	0,03022	-1,11872
BP	GO:0048759	xylem vessel member cell differentiation	3	0,03022	-3,93511
BP	GO:0006083	acetate metabolic process	2	0,0321	0,20018
BP	GO:1902459	positive regulation of stem cell populat...	2	0,0321	-0,16587
BP	GO:0019605	butyrate metabolic process	2	0,0321	0,20018
BP	GO:0046244	salicylic acid catabolic process	2	0,0321	-3,03952
BP	GO:0080151	positive regulation of salicylic acid me...	2	0,0321	-3,37643
BP	GO:0009789	positive regulation of abscisic acid-act...	9	0,03434	2,31957
BP	GO:0010623	programmed cell death involved in cell d...	4	0,03451	2,18801
BP	GO:0006779	porphyrin-containing compound biosynthet...	7	0,03452	-5,72762
BP	GO:0009863	salicylic acid mediated signaling pathwa...	6	0,03474	-3,80743
BP	GO:0042543	protein N-linked glycosylation via argin...	1	0,03645	2,00368

Table S7. ...continued.

BP	GO:0033499	galactose catabolic process via UDP-gala...	1	0,03645	-2,33299
BP	GO:0080092	regulation of pollen tube growth	6	0,03721	3,76725
BP	GO:0052325	cell wall pectin biosynthetic process	4	0,03744	0,01643
BP	GO:0009856	pollination	26	0,03975	-1,69253
BP	GO:0006097	glyoxylate cycle	2	0,04028	0,20018
BP	GO:0005987	sucrose catabolic process	2	0,04028	-3,12779
BP	GO:0009611	response to wounding	32	0,04472	-7,50861
BP	GO:0010183	pollen tube guidance	5	0,04624	-3,17634
BP	GO:0002229	defense response to oomycetes	7	0,04824	-4,629
BP	GO:0009686	gibberellin biosynthetic process	4	0,04851	-2,46939
BP	GO:0006873	cellular ion homeostasis	11	0,04881	-0,58991
BP	GO:1905177	tracheary element differentiation	6	0,04913	-3,74898
BP	GO:0006360	transcription by RNA polymerase I	2	0,04916	0,10709
BP	GO:0009813	flavonoid biosynthetic process	8	0,04961	0,15958

Table S8. Functional annotation of genes containing outlier SNPs that were found to be diverged in both ecotype pairs 1 and 3.

Gene ID	**Tair Homolog Gene ID**	**Protein**	**GO IDs**	**GO Names**
HELPU_000905	At5g57940	cyclic nucleotide-gated channel 6	GO:0005886, GO:0016021, GO:0035618, GO:0090406, GO:0005223, GO:0005249, GO:0005262, GO:0005516, GO:0030552, GO:0030553, GO:0009860, GO:0046686, GO:0070588, GO:0071805	plasma membrane, integral component of membrane, root hair, pollen tube,intracellular cGMP-activated cation channel activity, voltage-gated potassium channel activity, calcium channel activity, calmodulin binding, cAMP binding,cGMP binding, pollen tube growth, response to cadmium ion, calcium ion transmembrane transport, potassium ion transmembrane transport
HELPU_022172	At1g18540	Putative 60S ribosomal protein L6	GO:0005730, GO:0005783, GO:0005886, GO:0009506, GO:0022625, GO:0003729, GO:0003735, GO:0000027, GO:0002181	nucleolus, endoplasmic reticulum, plasma membrane, plasmodesma, cytosolic large ribosomal subunit, mRNA binding, structural constituent of ribosome, ribosomal large subunit assembly, cytoplasmic translation
HELPU_006410	At5g61560	U-box domain-containing protein kinase family protein	GO:0005886, GO:0009507, GO:0004674, GO:0005515, GO:0044237	plasma membrane, chloroplast,protein serine/threonine kinase activity, protein binding, cellular metabolic process
HELPU_006411	At4g25610	C2H2-like zinc finger protein	no GO terms	no GO terms

Table S8. ...continued.

HELPU_006413	At1g53570	mitogen-activated protein kinase kinase kinase 3	GO:2000071, GO:1900150, GO:0010098, GO:0046777, GO:1900424, GO:0002221, GO:0005886, GO:0000165, GO:0005524, GO:0005515, GO:0010229, GO:0005938, GO:0045088, GO:0005829, GO:0004709, GO:0106311, GO:0010103, GO:0106310	regulation of defense response by callose deposition, regulation of defense response to fungus, suspensor development, protein autophosphorylation, regulation of defense response to bacterium, pattern recognition receptor signaling pathway, plasma membrane, MAPK cascade, ATP binding, protein binding, inflorescence development, cell cortex,regulation of innate immune response, cytosol, MAP kinase kinase kinase activity,p rotein threonine kinase activity, stomatal complex morphogenesis, protein serine kinase activity
HELPU_003040	At5g52882	P-loop containing nucleoside triphosphate hydrolases superfamily protein	GO:0005524, GO:0016787, GO:0048235	ATP binding, hydrolase activity, pollen sperm cell differentiation
HELPU_012632	At2g19240	Ypt/Rab-GAP domain of gyp1p superfamily protein	no GO terms	no GO terms
HELPU_012633	At3g25520	ribosomal protein L5	GO:0005654, GO:0005730, GO:0005773, GO:0005886, GO:0009507, GO:0022625, GO:0042788, GO:0003729, GO:0003735, GO:0008097, GO:0000027, GO:0006412, GO:0006913, GO:0009704, GO:0009955, GO:0009965, GO:0010015, GO:0051301, GO:0071277, GO:0090333	nucleoplasm, nucleolus,vacuole, plasma membrane, chloroplast, cytosolic large ribosomal subunit, polysomal ribosome, mRNA binding, structural constituent of ribosome, 5S rRNA binding, ribosomal large subunit assembly, translation, nucleocytoplasmic transport, de-etiolation, adaxial/abaxial pattern specification, leaf morphogenesis, root morphogenesis, cell division, cellular response to calcium ion, regulation of stomatal closure

Table S8. ...continued.

HELPU_005422	At5g53160	regulatory components of ABA receptor 3	GO:0042803, GO:0080163, GO:0038023, GO:0005886, GO:0009789, GO:0005634, GO:0004864, GO:0005524, GO:0009507, GO:0003723, GO:0003724, GO:0043086, GO:0010427, GO:0046872, GO:0005829, GO:0016740, GO:0016787	protein homodimerization activity, regulation of protein serine/threonine phosphatase activity, signaling receptor activity, plasma membrane, positive regulation of abscisic acid-activated signaling pathway, nucleus, protein phosphatase inhibitor activity, ATP binding, chloroplast, RNA binding, RNA helicase activity, negative regulation of catalytic activity, abscisic acid binding, metal ion binding, cytosol, transferase activity, hydrolase activity
HELPU_008709	At4g39170	Sec14p-like phosphatidylinositol transfer family protein	GO:0005886, GO:0009506	plasma membrane, plasmodesma
HELPU_016528	At3g18100	myb domain protein 4r1	GO:0000976, GO:0003700, GO:0005515, GO:0006974, GO:0008285, GO:0009723, GO:0009733, GO:0009751, GO:0009753, GO:0045892	transcription cis-regulatory region binding, DNA-binding transcription factor activity, protein binding, cellular response to DNA damage stimulus,negative regulation of cell population proliferation, response to ethylene, response to auxin, response to salicylic acid, response to jasmonic acid, negative regulation of transcription, DNA-templated
HELPU_007977	At1g22250	E3 ubiquitin-protein ligase	no GO terms	no GO terms

Table S8. ...continued.

HELPU_007983	At1g10210	mitogen-activated protein kinase 1	GO:0005634, GO:0005829, GO:0005874, GO:0009504, GO:0016021, GO:0004707, GO:0005515, GO:0005524, GO:0106310, GO:0106311, GO:0000165, GO:0000911, GO:0006468, GO:0006972, GO:0007112, GO:0009409, GO:0009555, GO:0009620, GO:0009734, GO:0009737, GO:0009862, GO:0009868, GO:0042539, GO:0042542, GO:0043622, GO:0045087, GO:0071244, GO:0090333	nucleus, cytosol, microtubule, cell plate, integral component of membrane, MAP kinase activity, protein binding, ATP binding, protein serine kinase activity, protein threonine kinase activity, MAPK cascade, cytokinesis by cell plate formation, protein phosphorylation, hyperosmotic response, male meiosis cytokinesis, response to cold, pollen development, response to fungus, auxin-activated signaling pathway, response to abscisic acid, systemic acquired resistance, salicylic acid mediated signaling pathway, jasmonic acid and ethylene-dependent systemic resistance, jasmonic acid mediated signaling pathway, hypotonic salinity response, response to hydrogen peroxide, cortical microtubule organization, innate immune response, cellular response to carbon dioxide, regulation of stomatal closure
HELPU_014489	At1g34220	Regulator of Vps4 activity in the MVB pathway protein	GO:0005739, GO:0015031	mitochondrion, protein transport
HELPU_010671	At2g37730	glycosyltransferase (DUF604)	GO:0005794, GO:0008375	Golgi apparatus, acetylglucosaminyltransferase activity
HELPU_010672	At2g37730	glycosyltransferase (DUF604)	GO:0005794, GO:0008376	Golgi apparatus, acetylglucosaminyltransferase activity
HELPU_007496	At4g27580	SPFH/Band 7/PHB domain-containing membrane-associated protein family	GO:0005739, GO:0005794, GO:0005886, GO:0009506, GO:0009705, GO:0043424, GO:0002239	mitochondrion, Golgi apparatus, plasma membrane, plasmodesma, plant-type vacuole membrane, protein histidine kinase binding, response to oomycetes
HELPU_007501	At1g06250	alpha/beta-Hydrolases superfamily protein;	GO:0005737	cytoplasm

2. Parallel adaptation to lower altitudes is associated with enhanced plasticity

Authors: **Szukala A**, Bertel C, Frajman B, Schoenswetter P & Paun O.

Reference: **Szukala A**, Bertel C, Frajman B, Schoenswetter P & Paun O. 2022. Parallel adaptation to lower altitudes is associated with enhanced plasticity in *Heliosperma pusillum* (Caryophyllaceae).

Status: submitted to *New Phytologist*.

Own contribution: performed parts of the wet lab work; performed bioinformatics analyses including differential expression analysis, GxE interaction, estimations of genetic diversity and private alleles, and GO terms enrichment; derived the analytical results, and prepared result visualizations; wrote the first draft of the manuscript; revised the manuscript.

2.1. Summary

- High levels of phenotypic plasticity are thought to be inherently costly in stable or extreme environments, but enhanced expression plasticity may evolve as a response to novel environments and foster adaptation.

- *Heliosperma pusillum* forms pubescent montane and glabrous alpine ecotypes that diverged recurrently and polytopically (*parallel evolution*). To disentangle the relative contribution of constitutive versus plastic gene expression to altitudinal divergence, we analyze the transcriptomic profiles of two parallely evolved ecotype pairs grown in reciprocal transplantations at native altitudinal sites.

- Only a minor proportion of genes appear constitutively differentially expressed between the ecotypes regardless of the growing environment. The montane populations bear higher plasticity of gene expression than the alpine populations that can be considered in this system as 'ancestor-proxies'. Genes that change expression plastically and constitutively underlie similar ecologically relevant pathways, related to response to drought and trichome formation. Other relevant processes, such as photosynthesis, seem to rely mainly on plastic changes.

- The enhanced plasticity in the montane ecotype likely evolved as a response to the newly colonized environment. Our findings confirm that directional changes in gene expression plasticity can shape initial stages of phenotypic evolution, likely fostering adaptation to novel environments.

Keywords: altitudinal adaptation; drought tolerance; ecotypes; gene expression plasticity; *Heliosperma pusillum*; local adaptation; parallel evolution; RNA-seq.

2.2. Introduction

How phenotypic divergence between conspecific populations arises, possibly leading to local adaptation, stable differentiation and ultimately speciation, is a central question in evolutionary biology. A property of organisms, which can determine population differentiation across heterogeneous environments, is plasticity, i.e., the capacity of a genotype to change the expression of its phenotype upon exposure to differing environmental conditions (Schlichting & Pigliucci, 1998). It is still poorly investigated if phenotypic plasticity can lead to long-term phenotypic change, and what are the mechanisms behind translating short-term environmental responses into long-term evolutionary states (Sommer, 2020; Stearns, 1989; Stotz et al., 2021).

Despite being a necessary property to survive in variable environments, especially for sessile organisms, plasticity was hypothesized to be inherently evolutionarily costly when the population reached an adaptive optimum (DeWitt et al., 1998; Pál & Miklós, 1999). Moreover, some authors advanced the hypothesis that plasticity might reduce the power of natural selection, representing a dead end of evolution (Charlesworth et al., 1982). In stark contrast, phenotypic plasticity has been advanced as a primary object of selection by others (Levis & Pfennig, 2016; Stotz et al., 2021; Waddington, 1942), who called for a reconsideration of its importance for the evolutionary process. Adaptive benefits of plasticity have been documented, at least for some traits, related to biotic responses (Auld & Relyea, 2011) and abiotic stress (Dudley & Schmitt, 1996; Nicotra et al., 2015; Solé Medina et al., 2022; Stotz et al., 2021). However, plastic components of some traits can also be neutral or even maladaptive (Arnold, Kruuk, & Nicotra, 2019; Van Kleunen & Fischer, 2005). How and under which conditions plasticity supplies the phenotypic variation later refined by selection remains debated (Arnold, Nicotra, & Kruuk, 2019; Flatscher et al., 2012; Fox et al., 2019; Levis & Pfennig, 2016; Wund, 2012).

Evidence for a link between plasticity and local adaptation has been reported. Corl et al. (2018) showed for example how plasticity at genes controlling skin coloration of the common side-blotched lizard facilitated colonization of dark-soil environments,

and suggested that genetic changes in the same genes were shaped by natural selection refining a pre-existing plastic phenotype. Similarly, Levis et al. (2018) reported that in spadefoot toad tadpoles adaptive novelty can arise from pre-existing plasticity in diet-related morphological and molecular features. However, the study also uncovered diet-induced maladaptive plasticity affecting mouthpart formation, but also expression of a diet-relevant gene. Selection can also promote enhanced plasticity in certain conditions but not in others, as shown for example in the waxy bluebell *Wahlenbergia ceracea* Lothian (Campanulaceae; Nicotra et al. 2015). In this plant, low-elevation populations show enhanced temperature-induced plasticity, which was found to be more often adaptive compared to populations from higher elevations.

Evidence from natural study systems is required to clarify under which conditions plasticity is favored or hindered by evolution. A meta-study by Barley et al. (2021) quantified thermal acclimation capacity across 19 species including arthropods, molluscs, and chordates, showing that within species, marginal populations experiencing the highest thermal conditions had decreased plasticity and acclimation capacity. Similarly, a negative relationship between plasticity and adaptation to heat extremes was found in laboratory experiments (Kelly et al., 2017; Sasaki & Dam, 2021). These results suggest that there is a trade-off for plasticity at ecological extremes (Chevin & Hoffmann, 2017), such that extreme environments favor phenotypic robustness through *canalization* (Waddington, 1942). On the other hand, evolve and resequence studies on *Drosophila melanogaster* have shown that after 60 generations of adaptation to hot temperatures 75% of genes evolved higher plasticity (Mallard et al., 2020), suggesting that adaptation to novel environments leads to an increase in plasticity, at least in initial stages. Altogether, it is still unclear if plasticity precedes and facilitates adaptation to novel environments, or, in contrast, adaptation to novel conditions initially fosters increased plasticity (Fig. 1), followed by a progressive loss of plastic potential through *genetic assimilation* (Ehrenreich & Pfennig, 2016). Despite their contrasting nature, both scenarios suggest that plasticity plays a pivotal role during initial phases of adaptation.

Here, we investigate gene expression plasticity vs. genetically encoded expression

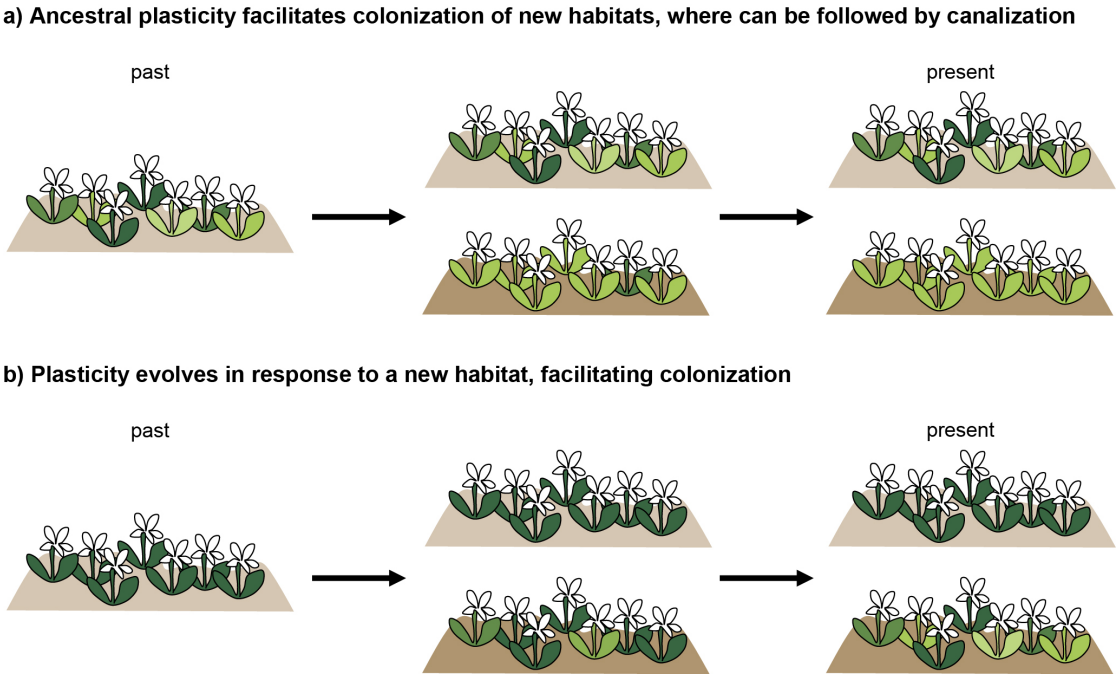

Figure 1. Two hypotheses about the role of phenotypic plasticity during evolution of different ecotypes. The heterogeneity in plant color symbolizes here the degree of plasticity at different stages, whereas light and dark brown indicate an ancestral and a derived niche, respectively. Other aspects, for example the amount of genetic variation in the population, its size, or the temporal and spatial environmental heterogeneity, are not taken into account in these simplified scenarios. **(a)** Pre-existing plasticity in an ancestral population (e.g. in a heterogeneous environment) may facilitate colonization of new habitats. The phenotype is ultimately refined in the newly occupied habitat, where plasticity could be lost over time, due to genetic assimilation. **(b)** The ancestral population bears little plasticity, which evolves in response to a newly colonized environment. This scenario has been coined 'plasticity-led evolution' (Levis et al., 2018; Schwander & Leimar, 2011).

differentiation during initial stages of parallel divergence in the plant *Heliosperma pusillum* (Waldst. and Kit.) Rchb. (Caryophyllaceae). This species forms altitudinal ecotypes previously shown to bear cross-generations phenotypic differentiation and a fitness advantage in their native niches (Bertel, Hülber, et al., 2016; Bertel et al., 2018). The alpine ecotype is widely distributed from the Spanish Cordillera Cantabrica to the Romanian and Ukrainian Carpathians, inhabiting wet screes, rock faces and open grasslands above the timberline, typically at elevations between 1,400 and 2,300 m. By contrast, the montane ecotype (previously referred to as *H. veselskyi* Janka; Bertel, Buchner, et al. 2016; Bertel

et al. 2018, 2017; Frajman & Oxelman 2007) is restricted to the south-eastern Alps, being represented by isolated and typically small populations, mostly below overhanging cliffs

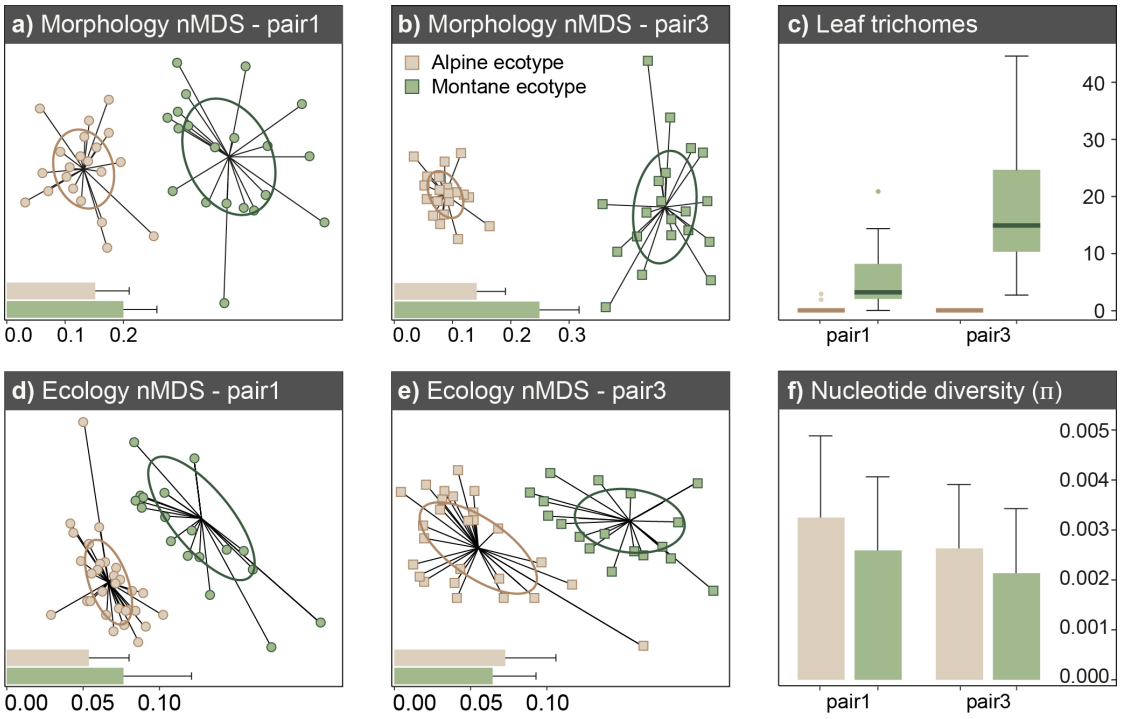

Figure 2. Summary of within-population morphological, ecological and genetic diversity within the two population pairs of *Heliosperma pussilum* investigated here, drawn from previously published data. Green- and brown-filled elements represent the montane and alpine ecotypes, respectively, while circles and squares represent pair 1 and 3, respectively. **(a-b)** Non-metric multidimensional scaling (nMDS) showing increased morphological variability in the montane ecotype among 16 morphometric characters measured on 20 individuals per population in each ecotype and ecotype pair, newly calculated using the data from Bertel, Buchner, et al. (2016). Confidence ellipses around treatment centroids represent the standard deviation of the measurements of the respective group. The bar charts on the lower left corner are the mean and SD of the dissimilarity matrices based on Bray-Curtis distances for each population. **(c)** Pronounced variation in the amount of glandular trichomes measured in the montane ecotype, as compared to the alpine, potentially suggestive of increased plasticity in the former. Boxplots drawn from data from Bertel et al. (2018). **(d-e)** Non-metric multidimensional scaling (nMDS) of ecological differentiation. Ordinations are based on dissimilarity matrices of mean Landolt indicator values of species growing within a circular area of 0.2 m radius centered on individuals, drawn from data from Bertel et al. (2018). **(f)** Estimates of within-population nucleotide diversity (π) in each pair, calculated using RNA-seq data from Szukala et al. (2022).

in poor light conditions and shaded from rain in the montane belt (500–1,300 m). The lack (alpine) or presence (montane) of a dense indumentum with long multicellular sticky glandular hairs on stem and leaves is the most divergent morphological trait (Fig. 2; Bertel, Buchner, et al. 2016; Bertel et al. 2018, 2017).

Phenotypic divergence is most strongly correlated with temperature and soil humidity differences between the two altitudinal sites, whereas humidity and light availability show higher temporal variability at the montane sites compared to the alpine ones (Bertel et al., 2018). Along the same lines, typically montane traits such as multicellular trichomes and physiological response to low light (Bertel, Buchner, et al., 2016) show greater variability across and within montane populations (Fig. 2a-c; Bertel et al. 2018). This variability is likely at least in part due to plasticity, given that reduced genetic variation was found in the small montane populations (Fig. 2f; Szukala et al. 2022; Trucchi et al. 2017). Reciprocal transplantation experiments performed at the native altitudinal sites (Bertel et al., 2018) demonstrated a home-site advantage of each ecotype in terms of establishment success (i.e. measured as the proportion of plants alive one year after germination). Higher survival rates of either ecotype in its respective native environment are strong indicators that the morphological and physiological differentiation has adaptive value.

Pairs of geographically clustered montane and alpine ecotypes in the south-eastern Alps were shown to have diverged at least four times independently, representing a case of parallel evolution (Szukala et al., 2022; Trucchi et al., 2017) and can be regarded as natural evolutionary replicates. Here, we investigate the role of gene expression shaping ecotype divergence in *H. pusillum*. More specifically, we address two hypotheses on the role of phenotypic plasticity in initial phases of divergence (Fig. 1). We quantify gene expression divergence in two parallely evolved ecotype pairs upon reciprocal transplantations at natural growing sites, to identify genes that i) diverge in expression between the two ecotypes regardless of the growing environment (*constitutive component of gene expression divergence*), and ii) change their expression plastically as a function of the environment (*plastic component of gene expression divergence*), and quantify and characterize these two components of ecotype expression differentiation. To reinforce our interpretation of

the observed patterns, we investigate the amount of private genetic variation and minor allele frequencies in the ecotypes. Finally, we discuss how plasticity might aid adaptation during early stages of ecological divergence.

2.3. Materials and Methods

2.3.1. Reciprocal transplantations and plant material

To be able to investigate the interaction between altitude and gene expression, we isolated RNA from leaves of both ecotypes grown at either the alpine or the montane natural sites (Fig. 3a). The two altitudinal niches are characterized by stark differences in average and amplitude of temperature, water and light availability (Bertel et al., 2018), but also by distinct biotic environments (Bertel et al., 2018; Trucchi et al., 2017). Reciprocal transplantations were carried out in 2017 in Lienzer Dolomiten, Kärnten (Austria; alpine site: 46.762 N 12.877 E, 2,055 m; montane site: 46.774 N 12.901 E, 790 m). Seeds were collected from wild populations of both ecotypes at these two localities and in the Puez-Geisler region, Trentino-Südtirol/Alto Adige (Italy; alpine site: 46.601 N 11.768 E, 2290 m; montane site: 46.564 N 11.77 E, 1690 m). We use the same acronyms as in Bertel et al. (2018) and Szukala et al. (2022), and name the ecotype pair from Puez-Geisler as pair 1, and that from Lienzer Dolomiten as pair 3, to facilitate comparisons between studies. Seeds were first germinated in a common garden in the Botanical Garden of the University of Innsbruck, Austria, and young seedlings were then transferred to the transplantation sites and grown for one season before sampling leaves in early autumn 2017. This approach was necessary, as transplantation trials attempting germination directly at the native sites showed insufficient and erratic germination rates, especially in the dry montane habitats (Bertel et al., 2018).

Our approach included hundreds of individuals, and originally aimed to finally investigate with RNA-seq a total of 40 individuals: two ecotypes × two pairs × two elevations × five individuals. However, due to the death of individuals during the course of the experiment (i.e., the alpine site experienced pronounced damage by chamois, among

others), only two individuals remained available for the group of montane individuals from pair 3 transplanted to the alpine site. For this reason, our final analyses comprise a total of 37 individuals with five biological replicates per group, and one group with only two biological replicates.

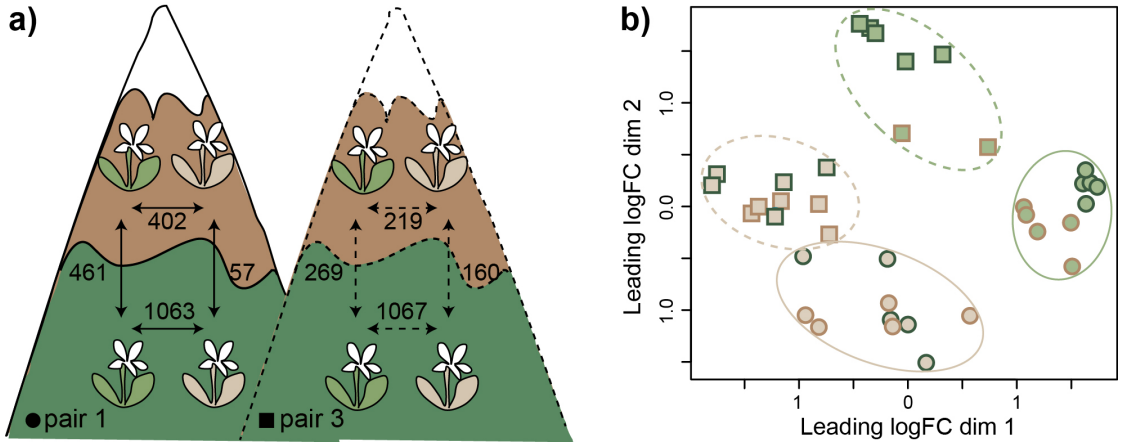

Figure 3. Study design and summary of its results. (a) Setup of the reciprocal transplantations between alpine (symbolized with brown areas of the mountains) and montane sites (shown with dark green areas). Brown plants represent the alpine ecotype, green plants the montane one. The numbers represent differentially expressed genes in different comparisons (adjusted $p < 0.05$). For simplicity the two ecotype pairs are here shown on different mountains, but they have been both reared together at the native localities of pair 1. **(b)** Multidimensional scaling plot of distances between gene expression profiles of individuals of the two ecotypes grown at different altitudes. Circles and continuous lines represent the ecotype pair 1, squares and dashed lines the ecotype pair 3. Green- and brown-filled symbols show the montane and alpine ecotypes, respectively, while green and brown symbol margins represent the low and high growing sites, respectively.

2.3.2. Library preparation and sequencing

Fresh vegetative shoots from transplanted and control plants were fixed in RNAlater (Sigma) on the same day and time of the day (ca. 2:00 pm) and stored at -80 °C until further processing. Total RNA was extracted from ca. 90 mg leaves using the mirVana miRNA Isolation Kit (Ambion) following the manufacturer's instructions, and it was further depleted of residual DNA with a RNase-Free DNase Set (Qiagen) and of the

abundant ribosomal RNA by using a Ribo-Zero rRNA Removal Kit (Illumina). RNA was quantified with a NanoDrop2000 spectrophotometer (Thermo Scientific), and its quality assessed using a 2100 Bioanalyzer (Agilent). NEBNext Ultra Directional RNA Library Prep Kit (New England Biolabs) was used to prepare strand-specific libraries. Individually-indexed libraries were pooled together and sequenced with single-end reads (100 bp) on two runs of Illumina NovaSeq S1 at the Vienna Biocenter Core Facilities (`VBCF;https://www.viennabiocenter.org/facilities/`).

2.3.3. Differential expression analyses

After demultiplexing using BamIndexDecoder v.1.03 (available from `http://wtsi-npg.github.io/illumina2bam/#BamIndexDecoder`), bam files were converted to fastq using samtools v.1.3 (Li et al., 2009) and quality and adapter trimmed using trimmomatic v.0.36 (Bolger et al., 2014). The individual samples were aligned against the reference genome for *Heliosperma pusillum* v.1.0 (Szukala et al., 2022) using the available .gff file for gene annotations and STAR v.2.6.0c (Dobin et al., 2013). A table of counts was produced using FeatureCounts v.2.0.3 from Rsubread package (Liao et al., 2014) including only uniquely mapping reads. After filtering count matrices retaining genes with an average count per million higher than 1, data normalization and differential expression (DE) analyses were performed using the Bioconductor package EdgeR v.3.24.3 (Robinson et al., 2010) implementing a generalized linear model of the type *expression = pair + altitude + ecotype + pair×altitude×ecotype* to account for the effects of the covariates altitude, ecotype pair and ecotype on gene expression. Gene-wise dispersion was estimated over all genes using the *estimateDisp()* function and specifying *robust=T* to robustify the estimation against potential outliers. We fitted a gene-wise negative binomial generalized log-linear model (EdgeR function *glmFit*), again with the option *robust=T* to decrease the informativeness of outlier genes. A likelihood ratio test (EdgeR function *glmLRT*) was used to test for DE genes and the significance was adjusted using Benjamini-Hochberg correction of p-values to account for multiple testing. Spearman correlation tests between gene expression changes at different altitudes were also performed.

First, we looked for DE genes between ecotypes in one environment and across both environments (i.e., *constitutive expression divergence*). Second, we aimed to detect plastic expression changes due to the component altitude in each of the ecotypes in each pair. We checked which genes are DE between altitudes in each ecotype, and additionally identified the genes showing a minimum mean fold change (FC) in expression of 1.5 across biological replicates when the growing environment is changed. The FC threshold was set to detect genes showing a strong association with the environmental change. Finally, we tested the statistical significance of the overlap between lists of DE genes using the genes retained after trimming low counts as background and the hypergeometric test of the Bioconductor package SuperExactTest (M. Wang et al., 2015).

2.3.4. Biological interpretation of DE genes

To retrieve functional annotations of the genes, we updated the functional annotations of the gene models for the reference genome v.1.0 for *Heliosperma pusillum* (Szukala et al., 2022) by blasting against the latest *Arabidopsis thaliana* database using Blast2GO v.5.2.5 (Götz et al., 2008). Fisher's exact tests implemented in the Bioconductor package topGO v.2.34.0 (`https://bioconductor.org/packages/release/bioc/html/topGO.html`) was used to identify significantly overrepresented functions (adjusted $p < 0.05$).

2.3.5. Detection of population-wise private alleles

We sorted mapped files according to the mapping position, and marked and removed duplicates using Picard v.2.9.2 (`https://broadinstitute.github.io/picard/`). Variant calling was then performed following standard practices for RNA as implemented in GATK v.4.1.8.1 (Van der Auwera & O'Connor, 2020). First, reads with Ns in the CIGAR string were split using the *split'N'trim* function and overhangs were trimmed. HaplotypeCaller was used to call variants with the option *-ERC GVCF*. Subsequently, multiple samples in gvcf format were merged using the GenomicsDBImport utility with the *-L* option to operate in parallel on multiple genomic intervals. Finally, we used GenotypeGVCFs to perform joint genotyping. We filtered the obtained vcf file first using the vcfallelicprimit-

ives modality implemented in vcflib v.1.0.2 (`https://github.com/vcflib/vcflib`) with the options *–keep-info –keep-geno* to split multiple nucleotide polymorphisms (MNPs) into multiple SNPs. VCFtools v.0.1.16 (Danecek et al., 2011) was used to keep only high-quality biallelic SNPs with the options *–max-alleles 2 –min-alleles 2 –minDP 4 –minGQ 20 –minQ 30 –remove-indels*. Additionally, we filtered using the *–max-missing 1* option to discard all loci with missing genotypes and test for consistency of the results when missingness was not allowed. To detect population-wise private alleles we used the vcf-contrast module of VCFtools with the options *-n -f -d 5* and specifying the population samples using *–indv*. Raw numbers of private alleles per population were normalized by the number of samples in each ecotype and population (i.e., ten individuals, except for the montane ecotype of pair 3 with seven individuals). Finally, VCFtools was run on the output files of vcf-contrast with the option *–freq* and specifying the population samples using *–indv* to obtain major and minor allele frequencies for the private alleles.

2.4. Results

2.4.1. Gene expression differences are driven by origin (ecotype pair) and ecotype divergence

After filtering out genes with low normalized expression counts we searched a total of 15,591 genes for genetically vs. environmentally-driven expression divergence between ecotypes and environments. Multidimensional scaling (MDS, Fig 3b) and principal component analysis (PCA, Supplementary Fig. S1) of normalized read counts showed that gene expression clusters the samples by ecotype pair (i.e., pair 1 shown with circles in Fig. 3b versus pair 3 shown with squares; in Supplementary Fig. S1 PC1 explaining 17.0% of variance), as well as by ecotype (i.e., alpine shown with brown-filled symbols in Fig. 3b versus montane shown with green-filled symbols; in Supplementary Fig. S1 PC2 explaining 10.4% of variance). The variable growing environment explained less variance of the data (montane environment shown with symbols with green margins versus alpine environment shown with symbols with brown margins; in Supplementary Fig. S1 PC5

explaining 4.7% of variance). This clustering shows that the locality of origin of each plant and the divergence between ecotypes explain most of the expression patterns recovered.

We observed that gene expression differences between ecotypes upon reciprocal transplantation showed similar patterns in both pairs analyzed (Figs. 3–4). In the montane environment, we found 1,063 DE genes between the two ecotypes of pair 1 (652 under- and 411 overexpressed in the montane ecotype compared to the alpine one) and 1,067 DE genes between the two ecotypes of pair 3 (483 under- and 584 overexpressed in the montane ecotype compared to the alpine one; green and grey symbols in Fig. 4). By contrast, significantly fewer genes were found to be DE in the alpine environment (brown and grey symbols in Fig. 4) with 402 DE genes between ecotypes in pair 1 (246 under- and 156 overexpressed in the montane ecotype compared to the alpine one) and 219 in pair 3 (83 under- and 136 overexpressed in the montane ecotype compared to the alpine one). Despite these differences in expression patterns observed when comparing the situation between the growing environments, in both ecotype pairs the expression patterns at either altitude were positively correlated (Spearman's correlation 0.49 and 0.36 in pair 1 and 3, respectively, Fig. 4), implying that an important proportion of gene expression networks is under genetic control and does not change substantially upon environmental change.

2.4.2. Constitutive evolutionary changes in gene expression

Among the DE genes 216 (more than expected by chance; hypergeometric $p < 1e\text{-}147$) and 118 (more than chance expectations; hypergeometric $p < 2.6e\text{-}79$) genes (grey symbols in Fig. 4) were always DE between ecotypes in the same direction in pair 1 and 3, respectively, regardless of the growing environment. These genes that do not show significant environmental sensitivity represent constitutive expression divergence and are most likely relevant in shaping stable trait differences between ecotypes. Moreover, the genes with constitutive expression divergence appeared to shape a considerable proportion of expression differences in the alpine conditions – i.e., representing consistently ca. 54% of overall expression differences between ecotypes in this environment in both pairs. Among the constitutive genes identified in each pair, 26 genes (Supplementary Table S1) were

shared by both ecotype pairs (more than chance expectations; hypergeometric p < 3e-24). Finally, eight of these genes (Supplementary Table S1) were also found to be DE in both ecotype pairs in a non-native, common garden environment in a previous study (Szukala et al., 2022), despite the different growing conditions and developmental stage.

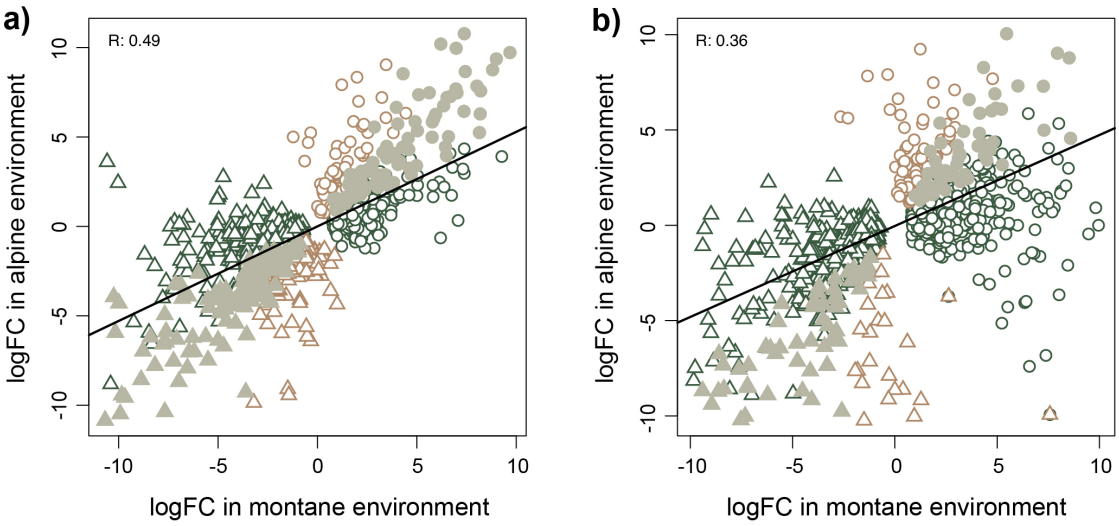

Figure 4. Differentially expressed (DE) genes between ecotypes in different environments. The X- and Y-axis show log fold-change values for genes with differential expression between ecotypes when these are grown in the montane (green and grey symbols) and alpine (brown and grey symbols) environment, respectively, for ecotype pair 1 **(a)** and 3 **(b)**. Triangles and circles represent genes under- and over-expressed in the montane ecotype compared to the alpine, respectively. Grey filled symbols show genes with stable, non-plastic expression divergence between ecotypes, independent of the environment. The black line shows the correlation between gene expression changes in the montane and alpine environments.

2.4.3. Environmentally sensitive gene expression

We also looked for environmentally induced expression changes within each ecotype, when these are grown at different elevations (i.e. G×E interaction). We found 461 (pair 1) and 269 (pair 3) DE genes in the montane ecotype versus 57 (pair 1) and 160 (pair 3) DE genes in the alpine ecotype that were explained by the variable "altitude" of the generalized linear model (Figs. 3a and 5). These results suggest that gene expression in the montane ecotype is strongly modified depending on the altitude, implying more

pronounced expression plasticity than in the alpine ecotype. This pattern was particularly pronounced in pair 1. In both pairs, the amount of genes showing significant expression plasticity in the montane ecotype is more than double the amount of constitutive DE genes shaping ecotype differentiation. We did not observe a clear pattern of down- or

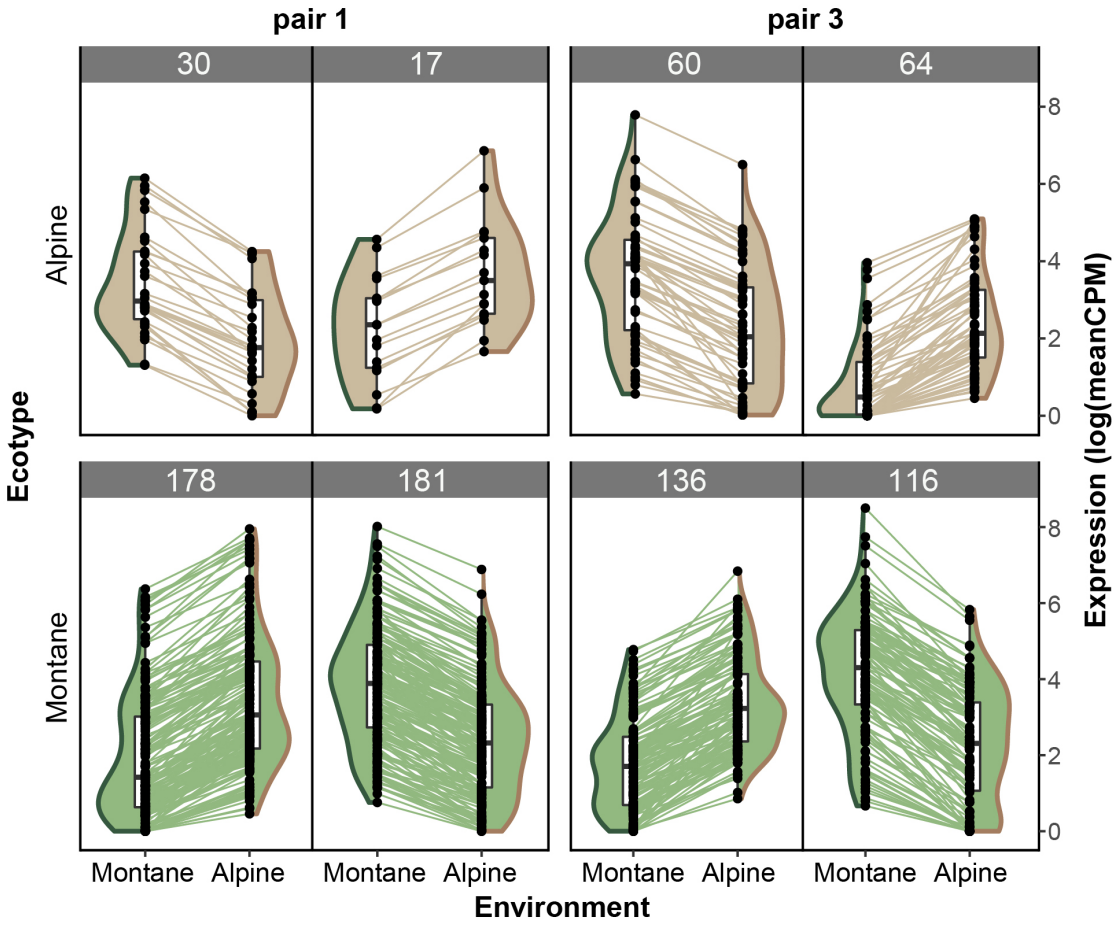

Figure 5. Genotype by environment interactions are more pronounced in the montane ecotype, as exemplified by environmentally driven gene expression changes. Brown- and green-filled violinplots represent the montane and alpine ecotypes, whereas green and brown violinplot margins represent the montane and alpine environment, respectively. Genes DE (adjusted $p < 0.05$, logFC > 1.5) when alpine (upper row) or montane (lower row) ecotypes are grown at different altitudes are reported. The numbers on top of each plot give the number of genes in the respective category. Each dot represents the average expression of a gene in a given environment, while lines connecting two dots show the expression change of a particular gene at different altitudes.

up-regulation of gene expression in the non-native environment that was consistent across both pairs. Also, in both ecotypes, the amount of down- vs. up-regulated genes in the non-native environment was similar.

2.4.4. Biological significance of constitutive DE genes

The 26 genes always DE between ecotypes regardless of the environment and shared by both ecotype pairs are reported with GO term annotations in Supplementary Table S1. The genes overexpressed in the montane ecotype (positive logFC in both pairs) are involved in response to salt-stress and water deprivation (BSK11, CER1), epigenetic regulation of gene expression by methylation (DNMT2), and protein phosphorylation (LRR-RLK, RPS20B), while underexpressed genes (negative logFC in both pairs) play roles in immunity (FUC1, At4g35733, CYP83B1) and enhanced drought and salt tolerance by loss-of-function (CLB, see de Silva et al., 2011 for increased salt tolerance in knock-out mutants of *Arabidopsis thaliana*).

Additionally, we performed GO terms enrichment of the genes that were always DE between ecotypes regardless of the environment (i.e. constitutive DE genes) in each ecotype pair separately, to clarify if different sets of constitutive genes do underlie similar functional networks and adaptive responses (Fig. 6a-b, Supplementary Tables S2 and S3). In both pairs we found significant enrichment (adjusted $p < 0.05$, Fisher-exact test) of response to water deficit and salinity, as well as responses to abscisic acid (ABA), probably related to different stress conditions (Fig. 6a-b). Despite the convergence of GO terms enriched, the number of genes underlying each term, as well as the z-score exemplifying the overall expression direction change differed in the two evolutionary replicates (Wolfe et al., 2021). Ecologically relevant enriched functions that were not shared by the two pairs have also been identified. In pair 1, DE genes overexpressed in the montane ecotype were enriched for root hair elongation (i.e., a pathway representative also for multicellular trichome development in plants) and epidermal cell differentiation, as well as stomatal closure and negative regulation of gene expression (Fig. 6a). In pair 3, genes overexpressed in the montane ecotype were involved in negative regulation of

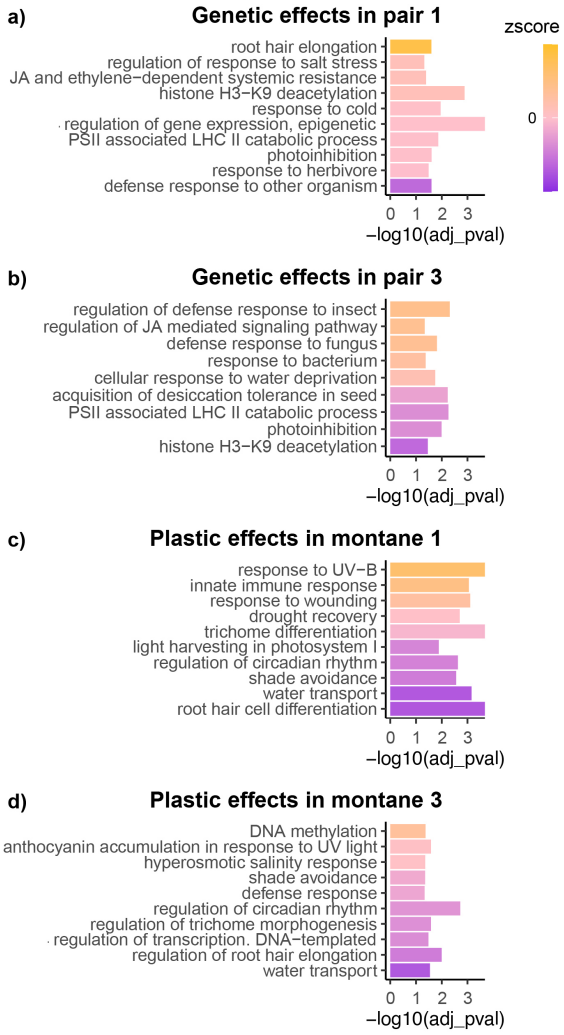

Figure 6. GO terms enrichment (biological processes) of constitutive vs. plastic DE genes. Enriched functions in constitutive expression differentiation between ecotypes in pair 1 **(a)** and 3 **(b)**. Enriched functions in genes changing their expression plastically between altitudes in the montane ecotype 1 **(c)** and 3 **(d)**. Each bar corresponds to a GO term (y axis), while the size of the bars corresponds to the significance of the enrichment (adjusted $p < 0.05$). The color scale represents the z-score, which is computed based on the logFC of expression of each gene underlying a specific GO term with orange shades corresponding to overexpression in the montane ecotype **(a-b)** or the montane environment **(c-d)**, and violet shades indicate an underexpression in the montane ecotype **(a-b)** or the montane environment **(c-d)**. GO terms reported were selected because of their ecological relevance from a larger list of significant GO terms, fully reported in the Supplementary Tables 2-5. JA, jasmonic acid; LHC, light-harvesting complex; PSII, photosystem II.

defense responses, as well as jasmonic acid-mediated signaling (Fig. 6b). The full lists of GO terms enriched in pair 1 and, respectively, pair 3 for genes constitutively DE between ecotypes are reported in the Supplementary Tables S2-S3.

2.4.5. Biological significance of plastic DE genes

We report in Fig. 6c-d, and Supplementary Tables S4 and S5 the GO terms enriched in genes changing expression plastically in the montane ecotype of both pairs, and in Supplementary Tables S6 and S7 the GO enrichment of the genes changing expression plastically in the alpine ecotype. Terms enriched in plastic DE genes in the montane ecotype were similar among the two ecotype pairs, including response to high light intensity (such as photosynthesis, anthocyanin biosynthesis, response to UV-B and shade avoidance), trichome or root hair differentiation, regulation of circadian rhythm, response to salinity and water transport, and regulation of transcription and methylation. Plastic differential gene expression in the montane ecotype tended to be characterized by pronounced downregulation in the alpine environment in both pairs (Fig. 6c). The direction of expression changes underlying the same function were often inconsistent between pairs, likely depending on the function of different genes affecting the same pathway (Fig. 6c-d). As mentioned above, the alpine ecotype showed reduced plasticity of gene expression compared to the montane one, especially in pair 1. Despite the lower number of differentially expressed genes underlying enriched function, we found some similar functions to be enriched as in the montane ecotype (e.g. regulation of circadian rhythm and response to light).

2.4.6. Population-wise private alleles

After calling and filtering high quality private single nucleotide polymorphisms (SNPs) in each one of the four studied populations we observed an excess of private polymorphisms in the alpine populations compared to the montane ones (Fig. S2a and S3). Additionally, we observed that minor allele frequencies (MAFs) among private alleles tend to be quite high (i.e., mean(MAF) > 0.2 in all populations, Fig. S2b), suggesting that a majority of them

did not accumulate during recent population expansion. We also observed that MAFs of private alleles tend to be similar between montane and alpine populations, suggesting that private variation is not strongly affected by opposite trends in the evolution of the effective population size between ecotypes (i.e. larger alpine populations vs smaller montane ones). Taken together, these results suggest that the alpine ecotype could be considered as a proxy for the ancestral form within the species.

2.5. Discussion

To date, a handful of studies have investigated the evolution of plasticity during early stages of adaptation in natural (Corl et al., 2018; Levis et al., 2018; Passow et al., 2017; Scoville & Pfrender, 2010) or experimental populations (Brennan et al., 2021; Huang & Agrawal, 2016; Mallard et al., 2020; Sikkink et al., 2019). Here, we have investigated both constitutive and plastic changes in gene expression of altitudinally segregated ecotypes upon reciprocal transplantations in their natural growing sites.

Our results suggest that a combination of constitutive expression divergence and different degrees of expression plasticity underlying the same ecologically relevant functions plays an important role in shaping ecotype divergence. More specifically, the alpine ecotype is characterized by reduced expression plasticity. This ecotype is possibly closer to the ancestral genotype state according to the higher amount of private variation detected in our analyses, which is generally used as a proxy for ancestral state (Paun et al., 2008; Schönswetter & Tribsch, 2005). It also experiences extreme environmental factors (e.g. higher amplitude of seasonal temperature fluctuations, low temperatures and enhanced solar irradiation), consistent with the hypothesis that extremes lead to enhanced robustness of gene expression and lack of plasticity (Chevin & Hoffmann, 2017; Lande, 2009). The inability of the alpine ecotype to react plastically to the altitudinal transplantation is possibly consistent with a (albeit not significantly) lower establishment success of alpine plants transplanted to the montane environment compared to transplanted plants of montane origin at non-native elevation (Bertel et al., 2018).

2. Parallel adaptation to lower altitudes is associated with enhanced plasticity

By contrast, the montane ecotype bears higher plastic potential of gene expression. As a consequence of this enhanced plasticity, the expression profiles of the ecotypes were more similar in the alpine environment, while they differed strongly in the montane one, except for a minor proportion of constitutive expression changes. Similar to our results, enhanced phenotypic plasticity in low-elevation individuals compared to high-elevation ones was found in *Wahlenbergia ceracea* by Nicotra et al. (2015). In this species, higher plasticity in low-elevation plants was shown to be adaptive, whereas plasticity in high-elevation plants was more likely to be maladaptive. In the same study, higher epigenetic diversity in response to growth temperature detected in seedlings from low elevation suggested a role for DNA methylation in shaping adaptive plastic responses. Possibly in line with these results, our GO terms enrichments (Fig. 6, Supplementary Tables S2-6) showed that both constitutive gene expression divergence, as well as gene expression plasticity are enriched in epigenetic processes (e.g. histone H3-K9 deacetylation and methylation in constitutive and plastic DE genes, respectively). However, a previous proof-of-concept study did not reveal significantly different within-ecotype levels of DNA methylation variation between the two ecotypes (Trucchi et al., 2016).

Similarly as many alpine plant species (Giesecke et al., 2017), *H. pusillum* likely migrated upslope after the Last Glacial Maximum (LGM); the few montane populations present today could represent relicts of the original LGM populations. The alpine ecotype was resolved as ancestral in the study of Frajman & Oxelman (2007) and the time of divergence between ecotypes was estimated around LGM (Trucchi et al., 2017), albeit older in another study (Szukala et al., 2022). The relict montane populations likely adapted to the specific niche under overhanging cliffs with lack of competition and high levels of abiotic stress (Davis, 1951; García & Zamora, 2003; Minuto et al., 2012), as this progressively became warmer and the original alpine habitats at low elevations strongly reduced due to the advancement of forests during the Holocene. The alpine ecotype, on the other hand, enlarged its distribution range throughout the southern European mountain ranges, where its habitats are abundant. Despite both habitats likely differing from the ancestral environment preceding ecotype divergence, we hypothesize that the

alpine niche resembles more the ancestral one with regard to temperature and humidity, as well as biotic interactions. Under this scenario, the montane ecotype would have enhanced expression plasticity as a consequence of the adaptation to the very specific niche in the montane environment, starting from an ancestral state, in which plasticity was lacking. Alternatively, the alpine ecotype might have lost ancestral plasticity through canalization. Although this second hypothesis appears less likely, it cannot be safely ruled out.

Despite some differences in the magnitude of the patterns found, our results were consistent between the two ecotype pairs analyzed, which represent independent instances of ecotype formation (Szukala et al., 2022; Trucchi et al., 2017), and can therefore be considered natural evolutionary replicates. It is important to notice that we could sample only two biological replicates of the montane ecotype from pair 3 transplanted to the alpine site. Interpretations of the results regarding this group should therefore be considered with caution. Still, while differences in the absolute numbers observed between ecotype pairs might have been driven by these differences in sampling density, the overall patterns of evolutionary vs. plastic expression changes should not be affected severely.

Since evolution favored the maintenance of enhanced plasticity in the montane environment in at least two independent divergence events, we hypothesize that enhanced plasticity leads to a fitness advantage in the montane habitat and is therefore adaptive (Bertel et al., 2018). Plasticity might indeed be beneficial in the stressful montane niche under overhanging cliffs which is characterized by heterogeneous light and water availability, longer periods of drought, and higher average temperatures (Bertel et al., 2018). Our results align with experimental studies showing that adaptation to novel conditions (e.g. high temperature) involves an increase in gene expression plasticity (Brennan et al., 2021; Mallard et al., 2020). Moreover, exposure to abiotic stress, such as drought, salinity, and heat, induced high gene expression plasticity in *Brachypodium distachyon* (Priest et al., 2014). Like in *Heliosperma*, convergence in the evolution of plasticity was found in two parallelly evolved zinc-tolerant lineages of *Silene uniflora* (Wood et al., 2021). Nevertheless, zinc-tolerant *Silene* derived populations appeared to

have decreased plasticity due to genetic assimilation of ancestral plasticity. Future studies should aim to directly assess if expression plasticity in the montane ecotype changes the phenotype deterministically in such a way that fitness is increased, in order to drive stronger conclusions about the impact of natural selection on plasticity in this system. Understanding the importance of phenotypic plasticity for fast adaptation to abiotic stress is very timely also for crops and breeding (Dalal et al., 2017; Fox et al., 2019; Shao et al., 2007).

We found that over 50% of the genes DE between ecotypes in the alpine environment were also DE in the montane environment, implying that an important part of expression divergence in the alpine environment is driven by evolutionary change, while a major additional proportion of divergence in the montane environment is plastic. Consistent with a previous investigation of ecotype-specific gene expression profiles in a common garden (Szukala et al., 2022), we found a significant, but still limited amount of constitutive DE genes shared by the two ecotype pairs. This result confirms the previously observed heterogeneity of DE genes in parallely evolved ecotype pairs, suggesting alternative adaptive solutions to cope with altitudinal differentiation. Interestingly, eight among these 26 genes were previously found to be DE in both pairs in Szukala et al. (2022), even if the seeds were collected in a different year and RNA extracted from leaves at a different developmental stage. Notably, we recovered similar biological functions enriched for constitutive DE genes, especially related to (a-)biotic defense responses, such as herbivory, temperature, water deprivation and salt-stress (note that these two stressors are functionally strongly interconnected; Y. Ma et al. (2020)), light availability, and epigenetic regulation, despite the limited overlap of specific constitutive genes. Similar functions related to the morphological (i.e. differences in hairiness) and ecological (i.e. differences in temperature, and water and light availability) divergence of the populations were underlied by both plastic and constitutive gene expression divergence.

In summary, the comparison of gene expression patterns between ecotypes upon reciprocal transplantations provided insights into the relative roles of expression plasticity and evolution in shaping gene expression divergence in nature. Similarly as in precedent

studies (McCairns & Bernatchez, 2010; Narum & Campbell, 2015), our findings point to an intricate interaction of evolutionary changes and plasticity, and to an important role of expression plasticity favoring the colonization of novel habitats during early stages of divergence. Future studies should aim for a better understanding of the regulatory patterns behind plasticity and its role in shaping adaptation.

2.6. Acknowledgements

This work was financially supported by the Austrian Science Fund (FWF) through the doctoral programme (DK) grant W1225-B20 to a faculty team including O.P., and through grant Y661-B16 to O.P. We thank Nicholas Barton, Andrew Clark, Virginie Courtier-Orgogozo, Joachim Hermisson, Thibault Leroy, Magnus Nordborg, John Parsch, and Christian Schlötterer for insightful comments and feedback. We thank Marie Huber and Daniela Paun for their support during laboratory work and data acquisition, Pau Cornicero Campmany for help during setting up of the reciprocal transplantations, as well as Martina Imhiavan and Daniel Schlorhaufer from the Botanical Garden of the University of Innsbruck for the germination of the plants. Computational resources were provided by the Vienna Scientific Cluster (VSC) and the Life Science Compute Cluster (LiSC) of the University of Vienna. A permit to conduct the presented research activities was granted by the Parco Naturale Dolomiti Friulane (no. 1943); for the Austrian federal state Tirol no such permit was necessary.

2.7. Authors contributions

OP, **PS**, and **BF** designed the study concept; **AS** and **OP** performed laboratory work; **PS**, **OP** and **BF** performed seeds sampling; **AS** performed bioinformatic analyses; **AS** derived the analytical results, and prepared the first figure drafts that were than improved together with **OP**; **CB** adapted the morphometric analyses from previous work; **AS** wrote the first draft of the manuscript; **OP** and **AS** revised the manuscript with contributions from all other authors.

2.8. Data availability

All raw read data was uploaded to NCBI and can be found under Bioproject ID PRJNA760819.

Supporting information - Chapter 2

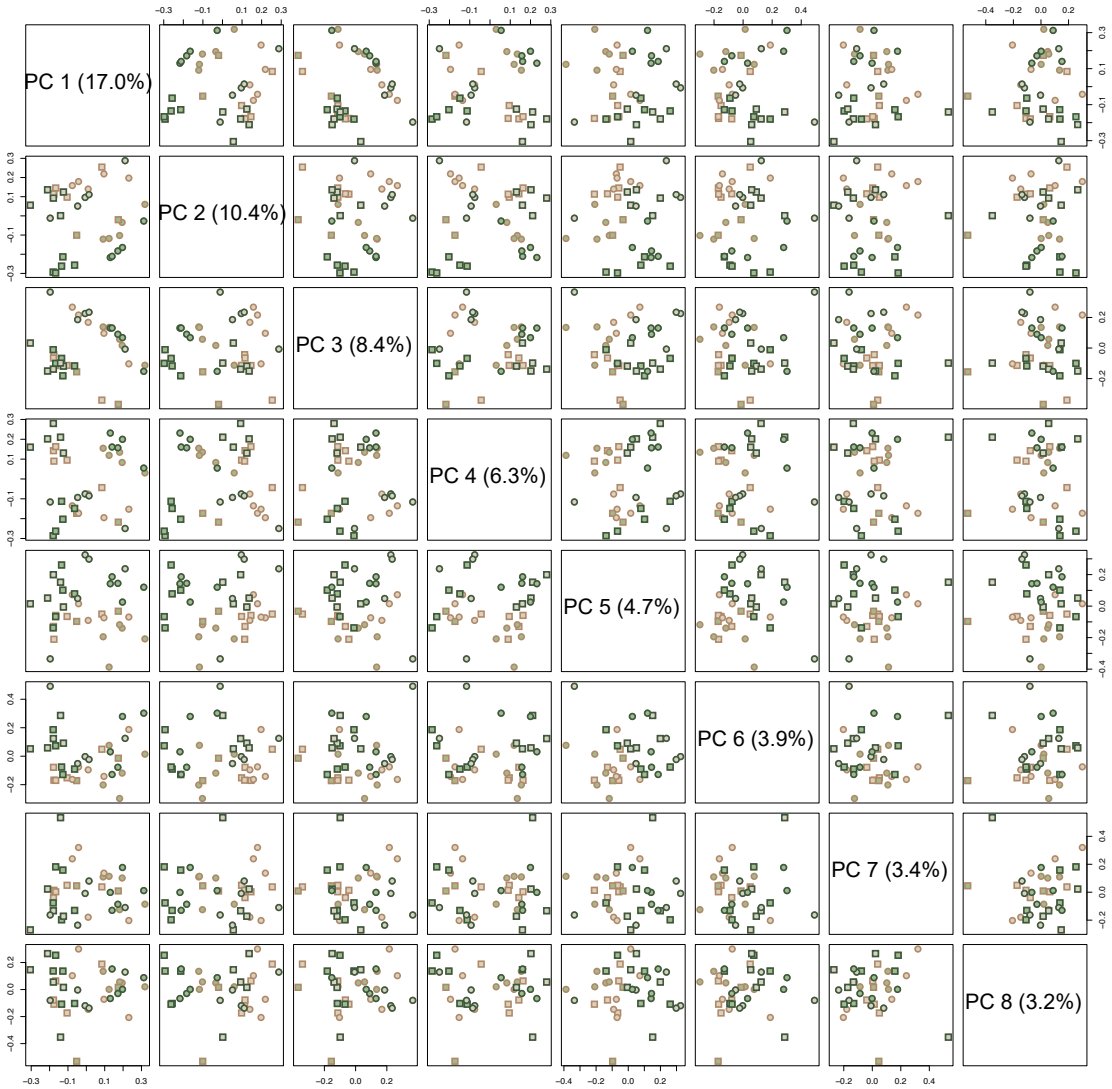

Supplementary Figure S1. Main trends in normalized gene expression counts. Principal component analysis of normalized gene expression counts. Visualization of the components 1 to 8. Circles represent the ecotype pair 1, squares the ecotype pair 3. Green- and brown-filled symbols show the montane and alpine ecotypes, respectively, while green and brown symbol margins represent the low and high growing sites, respectively.

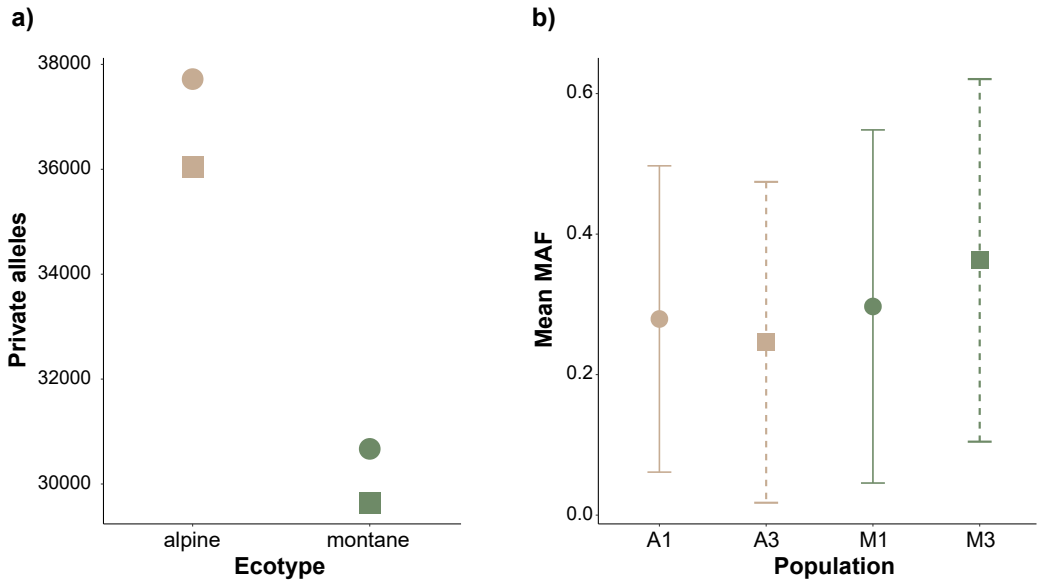

Supplementary Figure S2. Population private alleles and their minor allele frequency (MAF). **(a)** Total amount of private alleles by population after normalization by sample size and considering only biallelic SNPs (no missing data allowed). **(b)** MAF of private alleles by population. Bars represent the standard deviation.

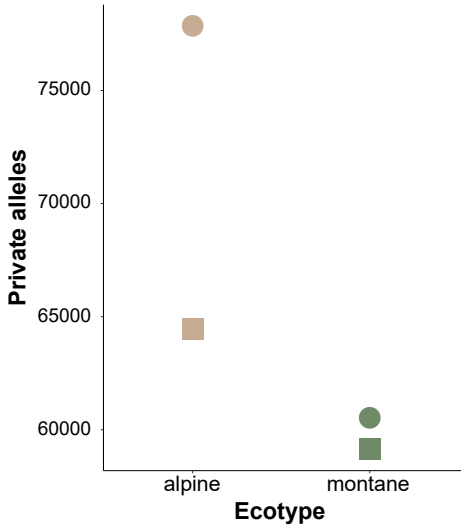

Supplementary Figure S3. Per population private allele statistics when allowing missing data.

Table S1. Ten constitutive genes always DE between ecotypes regardless of the environment and shared by both ecotype pairs are reported with UniProt database gene and protein IDs, selected GO term annotations, expression logFC, logCPM, and adjusted p-value. The three IDs in bold are the genes that were found to be DE also in a previous common garden experiment in Szukala et al. (2022)

Gene ID	**UniProt Gene ID**	**Protein Name**	**GO Names**
HELPU_007500	RPS20B	Ribosomal protein S10p/ S20e family protein	mRNA binding, phosphorylation
HELPU_007047	LRR-RLK	Leucine-rich repeat protein kinase family protein	protein binding, phosphorylation
HELPU_012215	At4g35733	F-box protein At4g35733	protein ubiquitination
HELPU_015501	BSK11	kinase with tetratricopeptide repeat domain-containing protein	response to cold, response to salt stress, defense response to bacterium, defense response to fungus
HELPU_014337	FUC1	alpha-L-fucosidase 1	glycoprotein catabolic process, glycoside catabolic process
HELPU_005982	CYP83B1	cytochrome P450	response to insect, response to red light, adventitious root development, defense response to fungus
HELPU_015351	DNMT2	DNA methyltransferase-2 / tRNA (cytosine38-C5) -methyltransferase isoforms	negative regulation of gene expression,epigenetic
HELPU_015352	DNMT2	DNA methyltransferase-2 / tRNA (cytosine38-C5) -methyltransferase isoforms	negative regulation of gene expression,epigenetic
HELPU_017295	CER1	Fatty acid hydroxylase superfamily	response to water deprivation, wax biosynthetic process, defense response to bacterium, defense response to fungus
HELPU_008737	CLB	Calcium-dependent lipid-binding (CaLB domain) family protein	negative regulation of transcription, response to salt stress,response to water deprivation
HELPU_012594	no ann	no ann	no ann
HELPU_023944	At1g58400	NB-ARC domain-containing disease resistance protein	defense response to other organism

Table S1. ...continued.

HELPU_012627	LOX2	PLAT/LH2 domain -containing lipoxygenase family protein	response to wounding, response to high light intensity,response to JA, response to ozone, response to herbivore, negative regulation of defense response to insect
HELPU_018186	Q8LKJ5	histone deacetylase	JA and ethylene-dependent systemic resistance, defense response to bacterium, posttranscriptional gene silencing,histone H3-K9 deacetylation
HELPU_020540	NFYA8	nuclear factor Y, subunit A8	regulation of transcription by RNA polymerase II, response to water deprivation, blue light signaling pathway
HELPU_023783	CBSX5	Cystathionine beta -synthase (CBS) family protein	response to wounding
HELPU_018816	At1g12320	ankyrin repeat/KH domain protein (DUF1442)	no ann
HELPU_019469	no ann	no ann	no ann
HELPU_015500	VAR2	FtsH extracellular protease family	photoinhibition, photosystem II repair, PSII associated light -harvesting complex II catabolic process
HELPU_010242	At1g03400	2-oxoglutarate (2OG) and Fe(II)-dependent oxygenase superfamily protein	regulation of glucosinolate biosynthetic process, 3-butenylglucosinolate 2-hydroxylase activity
HELPU_014336	RH3	DEAD box RNA helicase (RH3)	group II intron splicing, response to cold, response to water deprivation
HELPU_015886	VAR2	FtsH extracellular protease family	photoinhibition, photosystem II repair,PSII associated light-harvesting complex II catabolic process
HELPU_004631	At2g34740	Protein phosphatase 2C family protein	protein dephosphorylation, red light signaling pathway

Table S1. ...continued.

HELPU_014328	KT1	K+ transporter 1	response to water deprivation, response to salt stress, root hair elongation, regulation of stomatal closure
HELPU_002185	IRK	Leucine-rich repeat protein kinase family protein	phosphorylation, root development, regulation of cell division
HELPU_007086	no ann	no ann	no ann

Table S1. ...continued: expression logFC, logCPM, and adjusted p-value.

GeneID	**logFC**	**logCPM**	**padj**	**logFC**	**logCPM**	**padj**
	pair 1			**pair 3**		
HELPU_007500	4,54	2,41	2,52E-03	4,77	2,410	4,24E-03
HELPU_007047	1,73	2,41	1,31E-02	2,30	2,412	2,16E-03
HELPU_012215	-9,92	3,02	3,91E-08	-7,32	3,020	1,42E-06
HELPU_015501	2,80	4,44	1,07E-03	3,56	4,440	9,84E-05
HELPU_014337	-7,36	8,12	4,82E-04	-4,06	8,120	1,83E-02
HELPU_005982	-2,19	7,24	2,81E-04	-1,43	7,240	1,05E-02
HELPU_015351	3,97	2,55	1,88E-02	8,52	2,548	7,54E-06
HELPU_015352	4,32	2,55	1,33E-02	8,48	2,548	3,79E-04
HELPU_017295	6,90	6,63	1,52E-04	3,64	6,627	2,94E-02
HELPU_008737	-4,58	0,90	1,77E-03	-4,11	0,898	1,03E-02
HELPU_012594	6,44	0,44	1,09E-05	-3,43	0,439	2,45E-02
HELPU_023944	-9,99	1,84	7,58E-08	-7,18	1,845	1,53E-03
HELPU_012627	1,65	5,78	3,02E-02	2,86	5,783	3,99E-05
HELPU_018186	-4,14	4,43	9,04E-04	-6,08	4,426	4,77E-06
HELPU_020540	-8,78	1,83	9,63E-07	-8,36	1,834	7,13E-05
HELPU_023783	-3,27	1,20	1,27E-04	-3,77	1,196	2,82E-05
HELPU_018816	-7,61	1,86	8,38E-06	-9,40	1,855	1,32E-06
HELPU_019469	-2,70	6,07	2,30E-03	-3,51	6,074	4,43E-05
HELPU_015500	3,49	8,76	3,97E-06	3,44	8,756	5,04E-06
HELPU_010242	-3,76	5,66	2,49E-04	-3,98	5,662	9,17E-05
HELPU_014336	-2,77	1,97	1,22E-04	-2,96	1,972	2,13E-04
HELPU_015886	-3,60	8,85	8,50E-03	-8,39	8,855	1,25E-08
HELPU_004631	-3,19	6,92	1,00E-06	-1,94	6,922	4,74E-03
HELPU_014328	9,69	2,07	4,62E-12	8,59	2,072	4,45E-09
HELPU_002185	0,93	5,48	2,07E-02	1,22	5,479	1,21E-03
HELPU_007086	-4,86	2,35	2,74E-06	2,20	2,346	4,99E-02

Table S2. Go terms enriched in genes constitutively DE between ecotypes regardless of the environment in pair 1.

GO category	GO ID	GO term	Genes	adj p-val	z-score
BP	GO:0045814	negative regulation of gene expression, epigenetic	5	0,00017	-0,031583
BP	GO:0010262	somatic embryogenesis	3	0,00051	-9,373425
BP	GO:0043048	dolichyl monophosphate biosynthetic process	2	0,00087	0,603341
BP	GO:1990619	histone H3-K9 deacetylation	2	0,0013	1,277652
BP	GO:1902459	positive regulation of stem cell population maintenance	2	0,00239	1,277652
BP	GO:0048510	regulation of timing of transition from vegetative to reproductive phase	5	0,00246	-1,59796
BP	GO:1900459	positive regulation of brassinosteroid mediated signaling pathway	3	0,00366	-3,00703
BP	GO:1901979	regulation of inward rectifier potassium channel activity	2	0,00859	12,59766
BP	GO:0006012	galactose metabolic process	2	0,00859	-5,880042
BP	GO:0010941	regulation of cell death	4	0,00966	6,017344
BP	GO:1990573	potassium ion import across plasma membrane	3	0,00988	4,60195
BP	GO:0048497	maintenance of floral organ identity	2	0,01098	2,382966
BP	GO:0009409	response to cold	14	0,01111	0,292383
BP	GO:0009969	xyloglucan biosynthetic process	2	0,01228	0,380847
BP	GO:0010304	PSII associated light-harvesting complex II catabolic process	2	0,01364	-0,082117
BP	GO:0009785	blue light signaling pathway	3	0,01441	-5,088842
BP	GO:0016441	posttranscriptional gene silencing	3	0,01514	-0,355673
BP	GO:0006004	fucose metabolic process	3	0,01826	-3,122503
BP	GO:0009809	lignin biosynthetic process	5	0,01908	6,624553
BP	GO:2000033	regulation of seed dormancy process	2	0,01969	2,382966
BP	GO:1900426	positive regulation of defense response to bacterium	3	0,02082	-0,687084
BP	GO:0043410	positive regulation of MAPK cascade	2	0,02135	0,754056
BP	GO:0009558	embryo sac cellularization	2	0,02135	8,49218
BP	GO:0010205	photoinhibition	2	0,02484	-0,082117
BP	GO:0098542	defense response to other organism	23	0,02501	-6,071123
BP	GO:0048767	root hair elongation	5	0,02527	8,391519
BP	GO:0048564	photosystem I assembly	2	0,02666	-0,082117
BP	GO:0060560	developmental growth involved in morphogenesis	12	0,02736	7,01919
BP	GO:0015689	molybdate ion transport	1	0,02808	2,187129

Table S2. ...continued.

BP	GO:0009061	anaerobic respiration	1	0,02808	-3,224367
BP	GO:0071323	cellular response to chitin	2	0,03046	0,754056
BP	GO:0007112	male meiosis cytokinesis	2	0,03244	8,49218
BP	GO:0080027	response to herbivore	2	0,03244	-0,152999
BP	GO:0010582	floral meristem determinacy	2	0,03447	1,01123
BP	GO:0010206	photosystem II repair	2	0,03447	-0,082117
BP	GO:0051555	flavonol biosynthetic process	2	0,03654	5,333168
BP	GO:0060862	negative regulation of floral organ abscission	1	0,03726	-2,583243
BP	GO:0090241	negative regulation of histone H4 acetylation	1	0,03726	1,955849
BP	GO:0006384	transcription initiation from RNA polymerase III promoter	1	0,03726	-5,996127
BP	GO:0032197	transposition, RNA-mediated	1	0,03726	1,955849
BP	GO:0009611	response to wounding	11	0,03967	-5,227318
BP	GO:0010027	thylakoid membrane organization	3	0,04004	1,687194
BP	GO:0009861	jasmonic acid and ethylene-dependent systemic resistance	2	0,04083	1,277652
BP	GO:0010053	root epidermal cell differentiation	9	0,04277	3,72292
BP	GO:0010597	green leaf volatile biosynthetic process	2	0,04304	5,7576
BP	GO:0070482	response to oxygen levels	3	0,04624	0,283895
BP	GO:0019632	shikimate metabolic process	1	0,04636	3,038437
BP	GO:0006516	glycoprotein catabolic process	1	0,04636	-4,579726
BP	GO:1901001	negative regulation of response to salt stress	2	0,0476	1,277652

Table S3. GO terms enriched in genes constitutively DE between ecotypes regardless of the environment in pair 3.

GO category	**GO ID**	**GO term**	**Genes**	**adj p-val**	**z-score**
BP	GO:1900366	negative regulation of defense response to insect	2	0,0049	4,25
BP	GO:0010304	PSII associated light-harvesting complex II catabolic process	2	0,0055	-3,50
BP	GO:0048700	acquisition of desiccation tolerance in seed	1	0,0059	-2,13
BP	GO:0010205	photoinhibition	2	0,0102	-3,50
BP	GO:0048564	photosystem I assembly	2	0,011	-3,50
BP	GO:0072718	response to cisplatin	1	0,0118	-2,13
BP	GO:0009698	phenylpropanoid metabolic process	3	0,0137	-3,49
BP	GO:1900865	chloroplast RNA modification	2	0,0143	4,32
BP	GO:0010206	photosystem II repair	2	0,0143	-3,50

Table S3. ...continued.

BP	GO:0050832	defense response to fungus	8	0,0154	3,81
BP	GO:0009971	anastral spindle assembly involved in male meiosis	1	0,0176	1,47
BP	GO:0071345	cellular response to cytokine stimulus	1	0,0176	5,25
BP	GO:0009722	detection of cytokinin stimulus	1	0,0176	5,25
BP	GO:0006422	aspartyl-tRNA aminoacylation	1	0,0176	-3,93
BP	GO:0060560	developmental growth involved in morphogenesis	5	0,0177	3,71
BP	GO:0042631	cellular response to water deprivation	3	0,0181	1,59
BP	GO:0016139	glycoside catabolic process	2	0,0231	-1,31
BP	GO:0009134	nucleoside diphosphate catabolic process	1	0,0234	7,26
BP	GO:0033528	S-methylmethionine cycle	1	0,0234	4,38
BP	GO:0015967	diadenosine tetraphosphate catabolic process	1	0,0234	-1,31
BP	GO:0010951	negative regulation of endopeptidase activity	1	0,0234	1,86
BP	GO:0006516	glycoprotein catabolic process	1	0,0291	-4,10
BP	GO:0043048	dolichyl monophosphate biosynthetic process	1	0,0291	4,73
BP	GO:0010187	negative regulation of seed germination	2	0,0313	-7,50
BP	GO:1990619	histone H3-K9 deacetylation	1	0,0349	-6,08
BP	GO:0015813	L-glutamate transmembrane transport	2	0,0402	-4,41
BP	GO:0016126	sterol biosynthetic process	2	0,0404	-1,56
BP	GO:0015720	allantoin transport	1	0,0406	4,34
BP	GO:1900000	regulation of anthocyanin catabolic process	1	0,0406	2,25
BP	GO:0042353	fucose biosynthetic process	1	0,0406	4,38
BP	GO:1901695	tyramine biosynthetic process	1	0,0406	4,50
BP	GO:0018874	benzoate metabolic process	1	0,0406	-2,00
BP	GO:0010821	regulation of mitochondrion organization	1	0,0406	-3,90
BP	GO:0010192	mucilage biosynthetic process	3	0,041	7,48
BP	GO:0009553	embryo sac development	4	0,0414	-4,02
BP	GO:0009617	response to bacterium	13	0,0424	2,93
BP	GO:0010431	seed maturation	3	0,0454	-3,74
BP	GO:2000022	regulation of jasmonic acid mediated signaling pathway	2	0,0459	3,99
BP	GO:0042276	error-prone translesion synthesis	1	0,0462	1,93
BP	GO:1903401	L-lysine transmembrane transport	1	0,0462	-8,95
BP	GO:1902459	positive regulation of stem cell population maintenance	1	0,0462	-6,08
BP	GO:0043100	pyrimidine nucleobase salvage	1	0,0462	4,34
BP	GO:0006432	phenylalanyl-tRNA aminoacylation	1	0,0462	-2,72

Table S3. ...continued.

BP	GO:0009695	jasmonic acid biosynthetic process	2	0,0474	1,03

Table S4. GO terms enriched in genes DE between altitudes in the montane ecotype of pair 1.

GO category	GO ID	GO term	Genes	adj p-val	z-score
BP	GO:0010026	trichome differentiation	11	5,20E-07	-0,79
BP	GO:0010224	response to UV-B	12	1,90E-05	6,38
BP	GO:0032091	negative regulation of protein binding	4	2,50E-05	-2,27
BP	GO:0010482	regulation of epidermal cell division	5	4,70E-05	-6,64
BP	GO:0080110	sporopollenin biosynthetic process	4	7,30E-05	5,04
BP	GO:0016045	detection of bacterium	5	8,50E-05	6,18
BP	GO:0048765	root hair cell differentiation	17	1,70E-04	-7,33
BP	GO:0080170	hydrogen peroxide transmembrane transport	5	1,80E-04	-7,24
BP	GO:0010359	regulation of anion channel activity	7	2,70E-04	6,54
BP	GO:0002237	response to molecule of bacterial origin	10	4,20E-04	4,94
BP	GO:0031542	positive regulation of anthocyanin biosynthetic process	3	5,10E-04	5,17
BP	GO:0051792	medium-chain fatty acid biosynthetic process	2	6,30E-04	6,14
BP	GO:0006833	water transport	6	7,00E-04	-7,26
BP	GO:0009611	response to wounding	25	7,90E-04	2,84
BP	GO:0009957	epidermal cell fate specification	3	8,00E-04	4,29
BP	GO:0046244	salicylic acid catabolic process	3	8,00E-04	3,63
BP	GO:0002758	innate immune response-activating signal transduction	9	8,90E-04	4,82
BP	GO:0051567	histone H3-K9 methylation	6	1,29E-03	-5,61
BP	GO:0010200	response to chitin	15	1,44E-03	-3,12
BP	GO:0009800	cinnamic acid biosynthetic process	3	1,66E-03	3,13
BP	GO:0046680	response to DDT	2	1,86E-03	1,86
BP	GO:0043433	negative regulation of DNA-binding trans...	2	1,86E-03	-3,94
BP	GO:0033591	response to L-ascorbic acid	2	1,86E-03	1,86
BP	GO:0080127	fruit septum development	2	1,86E-03	-2,89
BP	GO:0009819	drought recovery	4	2,00E-03	0,20
BP	GO:0042752	regulation of circadian rhythm	11	2,38E-03	-4,36
BP	GO:0080167	response to karrikin	18	2,38E-03	6,78
BP	GO:0009641	shade avoidance	5	2,78E-03	-4,82
BP	GO:0060919	auxin influx	4	3,27E-03	-1,34
BP	GO:0002215	defense response to nematode	4	3,27E-03	6,50
BP	GO:0009629	response to gravity	12	3,66E-03	2,59

Table S4. ...continued.

BP	GO:0015700	arsenite transport	3	3,73E-03	-4,10
BP	GO:0009407	toxin catabolic process	5	5,74E-03	5,85
BP	GO:0000086	G2/M transition of mitotic cell cycle	3	5,98E-03	-1,26
BP	GO:0070995	NADPH oxidation	2	5,99E-03	3,21
BP	GO:2000029	regulation of proanthocyanidin biosynthe...	2	5,99E-03	4,02
BP	GO:0006121	mitochondrial electron transport, succin...	2	5,99E-03	1,95
BP	GO:0031540	regulation of anthocyanin biosynthetic p...	7	6,25E-03	5,32
BP	GO:0009718	anthocyanin-containing compound biosynth...	11	6,82E-03	4,17
BP	GO:0046685	response to arsenic-containing substance	4	8,18E-03	-4,75
BP	GO:0009733	response to auxin	29	8,19E-03	-3,05
BP	GO:1900384	regulation of flavonol biosynthetic process	3	8,79E-03	4,08
BP	GO:0030639	polyketide biosynthetic process	2	8,83E-03	3,96
BP	GO:0032025	response to cobalt ion	2	8,83E-03	1,86
BP	GO:0080191	secondary thickening	2	8,83E-03	-2,89
BP	GO:0035865	cellular response to potassium ion	2	8,83E-03	-3,17
BP	GO:0001736	establishment of planar polarity	2	8,83E-03	-2,38
BP	GO:0031347	regulation of defense response	26	9,53E-03	1,62
BP	GO:0009863	salicylic acid mediated signaling pathway	6	1,30E-02	1,32
BP	GO:0009768	photosynthesis, light harvesting in photosystem I	3	1,31E-02	-4,11
BP	GO:0006952	defense response	75	1,36E-02	2,88
BP	GO:0009753	response to jasmonic acid	20	1,54E-02	0,85
BP	GO:0006631	fatty acid metabolic process	16	1,57E-02	3,74
BP	GO:1902975	mitotic DNA replication initiation	2	1,60E-02	1,83
BP	GO:0032922	circadian regulation of gene expression	3	1,70E-02	-1,12
BP	GO:0000162	tryptophan biosynthetic process	3	1,70E-02	0,56
BP	GO:0071215	cellular response to abscisic acid stimulus	19	1,79E-02	0,37
BP	GO:0050776	regulation of immune response	16	1,84E-02	3,05
BP	GO:0010214	seed coat development	8	1,90E-02	-1,44
BP	GO:2000214	regulation of proline metabolic process	2	2,02E-02	-2,27
BP	GO:0009413	response to flooding	2	2,02E-02	-0,32
BP	GO:0009644	response to high light intensity	10	2,13E-02	-4,75
BP	GO:0048317	seed morphogenesis	3	2,15E-02	-3,47
BP	GO:0050829	defense response to Gram-negative bacterium	4	2,24E-02	-0,92
BP	GO:0010311	lateral root formation	9	2,29E-02	-3,83
BP	GO:0051716	cellular response to stimulus	129	2,32E-02	-2,83

Table S4. ...continued.

BP	GO:1901703	protein localization involved in auxin p...	3	2,40E-02	0,13
BP	GO:0006730	one-carbon metabolic process	3	2,47E-02	0,23
BP	GO:0035445	borate transmembrane transport	2	2,48E-02	-3,77
BP	GO:0043335	protein unfolding	2	2,48E-02	2,91
BP	GO:0030638	polyketide metabolic process	3	2,50E-02	2,32
BP	GO:0072708	response to sorbitol	2	2,51E-02	-0,76
BP	GO:0006742	NADP catabolic process	1	2,51E-02	1,29
BP	GO:0010062	negative regulation of trichoblast fate specification	1	2,51E-02	1,59
BP	GO:0019677	NAD catabolic process	1	2,51E-02	1,29
BP	GO:0018142	protein-DNA covalent cross-linking	1	2,51E-02	2,09
BP	GO:0043111	replication fork arrest	1	2,51E-02	1,56
BP	GO:0018293	protein-FAD linkage	1	2,51E-02	1,46
BP	GO:0071280	cellular response to copper ion	1	2,51E-02	-2,91
BP	GO:0071286	cellular response to magnesium ion	1	2,51E-02	-2,91
BP	GO:0031115	negative regulation of microtubule polym...	1	2,51E-02	-2,91
BP	GO:0031117	positive regulation of microtubule depol...	1	2,51E-02	-2,91
BP	GO:0016118	carotenoid catabolic process	1	2,51E-02	-2,50
BP	GO:0072709	cellular response to sorbitol	1	2,51E-02	-2,91
BP	GO:0010350	cellular response to magnesium starvatio...	1	2,51E-02	-2,91
BP	GO:0034553	mitochondrial respiratory chain complex ...	1	2,51E-02	1,46
BP	GO:0033611	oxalate catabolic process	1	2,51E-02	-1,96
BP	GO:0016576	histone dephosphorylation	1	2,51E-02	-0,95
BP	GO:0071325	cellular response to mannitol stimulus	1	2,51E-02	-2,91
BP	GO:0071327	cellular response to trehalose stimulus	1	2,51E-02	1,41
BP	GO:0072423	response to DNA damage checkpoint signal...	1	2,51E-02	-1,88
BP	GO:0010315	auxin efflux	3	2,67E-02	-0,88
BP	GO:0000160	phosphorelay signal transduction system	7	2,68E-02	-3,59
BP	GO:0010380	regulation of chlorophyll biosynthetic p...	4	2,80E-02	2,85
BP	GO:0009734	auxin-activated signaling pathway	12	2,86E-02	-4,93
BP	GO:0016132	brassinosteroid biosynthetic process	3	0,02946	-2,45
BP	GO:0035435	phosphate ion transmembrane transport	3	0,02946	-0,47
BP	GO:0048829	root cap development	3	0,02946	-1,39
BP	GO:0042754	negative regulation of circadian rhythm	2	0,02981	-3,94

Table S4. ...continued.

BP	GO:0009735	response to cytokinin	9	0,03068	-5,79

Table S5. GO terms enriched in genes DE between altitudes in the montane ecotype of pair 3.

GO category	GO ID	GO term	Genes	adj p-val	z-score
BP	GO:0032091	negative regulation of protein binding	4	2,60E-06	-2,38
BP	GO:0035445	borate transmembrane transport	3	3,10E-04	-7,28
BP	GO:0015700	arsenite transport	3	7,20E-04	-7,28
BP	GO:0042752	regulation of circadian rhythm	7	1,91E-03	-3,11
BP	GO:0080170	hydrogen peroxide transmembrane transpor...	3	3,52E-03	-7,28
BP	GO:0046685	response to arsenic-containing substance	3	3,52E-03	-7,28
BP	GO:0080029	cellular response to boron-containing su...	3	3,52E-03	-7,28
BP	GO:0031129	inductive cell-cell signaling	2	3,99E-03	-3,40
BP	GO:0010031	circumnutation	2	3,99E-03	-0,49
BP	GO:0010258	NADH dehydrogenase complex (plastoquinon...	2	5,27E-03	3,24
BP	GO:0005992	trehalose biosynthetic process	3	5,70E-03	-4,34
BP	GO:0009740	gibberellic acid mediated signaling path...	5	8,49E-03	-0,86
BP	GO:0048530	fruit morphogenesis	2	1,01E-02	-3,40
BP	GO:1902890	regulation of root hair elongation	2	1,01E-02	-4,78
BP	GO:0042814	monopolar cell growth	2	1,01E-02	-3,40
BP	GO:0034063	stress granule assembly	3	1,21E-02	-3,67
BP	GO:0045338	farnesyl diphosphate metabolic process	2	1,40E-02	3,34
BP	GO:0015871	choline transport	1	1,41E-02	1,33
BP	GO:0042794	plastid rRNA transcription	1	1,41E-02	2,05
BP	GO:0015990	electron transport coupled proton transp...	1	1,41E-02	-2,71
BP	GO:0033611	oxalate catabolic process	1	1,41E-02	-2,76
BP	GO:0007097	nuclear migration	2	1,62E-02	-3,40
BP	GO:0065007	biological regulation	95	1,70E-02	-6,89
BP	GO:0080001	mucilage extrusion from seed coat	3	1,75E-02	2,14
BP	GO:0048358	mucilage pectin biosynthetic process	2	1,85E-02	-0,55
BP	GO:0006744	ubiquinone biosynthetic process	3	1,88E-02	8,21
BP	GO:0010482	regulation of epidermal cell division	2	2,35E-02	-3,40
BP	GO:2000039	regulation of trichome morphogenesis	2	2,62E-02	-3,40
BP	GO:0043481	anthocyanin accumulation in tissues in response to UV light	2	2,62E-02	0,43

Table S5. ...continued.

BP	GO:0043619	regulation transcription from RNA polymerase II promoter	1	2,81E-02	3,37
BP	GO:1902389	ceramide 1-phosphate transport	1	2,81E-02	2,20
BP	GO:0006557	S-adenosylmethioninamine biosynthetic pr...	1	2,81E-02	-2,83
BP	GO:0006833	water transport	3	2,87E-02	-7,28
BP	GO:0015995	chlorophyll biosynthetic process	4	3,01E-02	-2,11
BP	GO:0010214	seed coat development	5	3,12E-02	-4,43
BP	GO:0045604	regulation of epidermal cell differentia...	2	3,20E-02	-3,40
BP	GO:0045892	negative regulation of transcription, DNA-templated	10	3,31E-02	-3,69
BP	GO:0006465	signal peptide processing	2	3,50E-02	-1,82
BP	GO:0006446	regulation of translational initiation	2	3,50E-02	-5,35
BP	GO:0001932	regulation of protein phosphorylation	3	3,51E-02	-1,55
BP	GO:0009834	plant-type secondary cell wall biogenesi...	5	3,99E-02	-5,28
BP	GO:0055088	lipid homeostasis	4	4,05E-02	1,55
BP	GO:0016126	sterol biosynthetic process	3	4,08E-02	5,10
BP	GO:0010381	peroxisome-chloroplast membrane tetherin...	1	4,18E-02	1,63
BP	GO:0009443	pyridoxal 5'-phosphate salvage	1	4,18E-02	2,97
BP	GO:0043433	negative regulation of DNA-binding transcription factor activity	1	4,18E-02	-3,85
BP	GO:0080127	fruit septum development	1	4,18E-02	-2,67
BP	GO:0046680	response to DDT	1	4,18E-02	1,47
BP	GO:0030643	cellular phosphate ion homeostasis	1	4,18E-02	1,35
BP	GO:0033591	response to L-ascorbic acid	1	4,18E-02	1,47
BP	GO:0045792	negative regulation of cell size	1	4,18E-02	-2,46
BP	GO:0015970	guanosine tetraphosphate biosynthetic pr...	1	4,18E-02	-2,32
BP	GO:0032259	methylation	10	4,29E-02	3,27
BP	GO:0042538	hyperosmotic salinity response	5	4,39E-02	0,37
BP	GO:0009641	shade avoidance	3	4,45E-02	-1,57
BP	GO:0006085	acetyl-CoA biosynthetic process	2	4,48E-02	2,74
BP	GO:0006952	defense response	32	4,62E-02	-1,86
BP	GO:0002215	defense response to nematode	2	4,82E-02	8,93
BP	GO:0031347	regulation of defense response	10	4,93E-02	-4,96

Table S6. Genes DE between altitudes in alpine ecotype of pair 1 and relative functional annotation.

GO category	**GO ID**	**GO term**	**Genes**	**adj p-val**	**z-score**
BP	GO:0010482	regulation of epidermal cell division	3	1,30E-05	4,885

Table S6. ...continued.

BP	GO:0010501	RNA secondary structure unwinding	2	2,00E-04	2,098
BP	GO:0032091	negative regulation of protein binding	2	2,00E-04	-0,112
BP	GO:0051567	histone H3-K9 methylation	3	0,00043	4,885
BP	GO:0042752	regulation of circadian rhythm	4	0,00074	-1,523
BP	GO:0048765	root hair cell differentiation	4	0,00133	4,997
BP	GO:0000380	alternative mRNA splicing, via spliceoso...	2	0,00196	2,098
BP	GO:0010043	response to zinc ion	3	0,00198	0,58
BP	GO:0035616	histone H2B conserved C-terminal lysine ...	1	0,00275	-1,438
BP	GO:0010099	regulation of photomorphogenesis	3	0,00311	2,013
BP	GO:0019853	L-ascorbic acid biosynthetic process	2	0,00538	0,153
BP	GO:1902455	negative regulation of stem cell populat...	1	0,00549	-1,912
BP	GO:0046680	response to DDT	1	0,00822	-1,963
BP	GO:0033591	response to L-ascorbic acid	1	0,00822	-1,963
BP	GO:0042246	tissue regeneration	1	0,00822	-2,587
BP	GO:1902006	negative regulation of proline biosynthe...	1	0,00822	1,569
BP	GO:0007623	circadian rhythm	7	0,00843	0,564
BP	GO:0051791	medium-chain fatty acid metabolic proces...	1	0,01094	-1,673
BP	GO:1902395	regulation of 1-deoxy-D-xylulose-5-phosp...	1	0,01094	1,606
BP	GO:0032508	DNA duplex unwinding	2	0,01255	2,098
BP	GO:0006308	DNA catabolic process	1	0,01637	2,572
BP	GO:0010322	regulation of isopentenyl diphosphate bi...	1	0,01637	1,606
BP	GO:0032025	response to cobalt ion	1	0,01637	-1,963
BP	GO:0010026	trichome differentiation	3	0,01671	4,885
BP	GO:0010031	circumnutation	1	0,01908	-1,537
BP	GO:0033540	fatty acid beta-oxidation using acyl-CoA...	1	0,01908	-1,673
BP	GO:0042549	photosystem II stabilization	1	0,02177	2,397
BP	GO:0048026	positive regulation of mRNA splicing, vi...	1	0,02446	1,346
BP	GO:0016120	carotene biosynthetic process	1	0,02446	-2,244
BP	GO:0019310	inositol catabolic process	1	0,02446	2,18
BP	GO:0015995	chlorophyll biosynthetic process	2	0,02745	1,989
BP	GO:0016973	poly(A)+ mRNA export from nucleus	1	0,02982	-1,438
BP	GO:0010228	vegetative to reproductive phase transit...	4	0,03107	1,313
BP	GO:0010114	response to red light	3	0,03121	-0,087
BP	GO:0031539	positive regulation of anthocyanin metab...	1	0,03515	-4,772

Table S6. ...continued.

BP	GO:0010224	response to UV-B	2	0,03603	-5,726
BP	GO:0010017	red or far-red light signaling pathway	4	0,03907	0,879
BP	GO:0034059	response to anoxia	1	0,04571	1,451
BP	GO:1905157	positive regulation of photosynthesis	1	0,04571	1,57
BP	GO:0006355	regulation of transcription, DNA-templat...	11	0,04591	1,062
BP	GO:0080187	floral organ senescence	1	0,04834	2,572

Table S7. Genes DE between altitudes in alpine ecotype of pair 3 and relative functional annotation.

GO category	**GO ID**	**GO term**	**Genes**	**adj p-val**	**z-score**
BP	GO:1901430	positive regulation of syringal lignin b...	3	0,0014	-6,939
BP	GO:0010501	RNA secondary structure unwinding	2	0,0017	2,156
BP	GO:0006624	vacuolar protein processing	2	0,0022	-6,364
BP	GO:0009739	response to gibberellin	7	0,0023	3,074
BP	GO:0035445	borate transmembrane transport	2	0,0028	3,799
BP	GO:0016579	protein deubiquitination	4	0,0038	-4,432
BP	GO:0015700	arsenite transport	2	0,0047	3,799
BP	GO:0034508	centromere complex assembly	2	0,0047	-7,929
BP	GO:0008283	cell proliferation	3	0,0055	2,186
BP	GO:0080167	response to karrikin	8	0,0061	-4,437
BP	GO:0046685	response to arsenic-containing substance	3	0,0079	4,216
BP	GO:0007623	circadian rhythm	7	0,0111	-1,97
BP	GO:0080029	cellular response to boron-containing su...	2	0,0133	3,799
BP	GO:0080170	hydrogen peroxide transmembrane transpor...	2	0,0133	3,799
BP	GO:0048235	pollen sperm cell differentiation	3	0,0148	-10,88
BP	GO:0000122	negative regulation of transcription by ...	2	0,0158	-0,088
BP	GO:0048317	seed morphogenesis	2	0,0158	2,905
BP	GO:0000380	alternative mRNA splicing, via spliceoso...	2	0,0158	2,156
BP	GO:1902455	negative regulation of stem cell populat...	1	0,016	-1,606
BP	GO:0006580	ethanolamine metabolic process	1	0,016	1,434
BP	GO:0010252	auxin homeostasis	3	0,0161	3,586
BP	GO:0031347	regulation of defense response	9	0,0162	-0,837
BP	GO:1901703	protein localization involved in auxin p...	2	0,017	-0,422
BP	GO:0002215	defense response to nematode	2	0,017	-9,676
BP	GO:0051307	meiotic chromosome separation	2	0,0211	-7,929

Table S7. ...continued.

BP	GO:0031540	regulation of anthocyanin biosynthetic p...	3	0,0237	-4,328
BP	GO:0033591	response to L-ascorbic acid	1	0,0239	-1,989
BP	GO:2001294	malonyl-CoA catabolic process	1	0,0239	-8,632
BP	GO:0046680	response to DDT	1	0,0239	-1,989
BP	GO:0042425	choline biosynthetic process	1	0,0239	-1,469
BP	GO:0015970	guanosine tetraphosphate biosynthetic pr...	1	0,0239	1,625
BP	GO:0015938	coenzyme A catabolic process	1	0,0239	-8,632
BP	GO:0051973	positive regulation of telomerase activi...	1	0,0239	2,555
BP	GO:0009567	double fertilization forming a zygote an...	3	0,0249	-5,412
BP	GO:0009753	response to jasmonic acid	8	0,0255	-1,849
BP	GO:0006355	regulation of transcription, DNA-templat...	22	0,028	4,228
BP	GO:0009970	cellular response to sulfate starvation	2	0,0288	0,433
BP	GO:0010214	seed coat development	4	0,0299	-6,38
BP	GO:2000469	negative regulation of peroxidase activi...	1	0,0318	1,481
BP	GO:0006104	succinyl-CoA metabolic process	1	0,0318	-8,632
BP	GO:0090697	post-embryonic plant organ morphogenesis	3	0,0319	0,823
BP	GO:0009733	response to auxin	11	0,0319	2,822
BP	GO:0009737	response to abscisic acid	16	0,0322	1,806
BP	GO:0010150	leaf senescence	7	0,0328	-1,629
BP	GO:0010043	response to zinc ion	3	0,037	0,612
BP	GO:0009637	response to blue light	5	0,0381	-3,627
BP	GO:0071365	cellular response to auxin stimulus	5	0,0386	5,242
BP	GO:0071722	detoxification of arsenic-containing sub...	1	0,0396	1,929
BP	GO:0007141	male meiosis I	1	0,0396	1,807
BP	GO:0009745	sucrose mediated signaling	1	0,0396	-2,154
BP	GO:1900057	positive regulation of leaf senescence	2	0,0429	0,031
BP	GO:0009908	flower development	10	0,045	-4,569
BP	GO:0031669	cellular response to nutrient levels	8	0,0455	1,013
BP	GO:0032508	DNA duplex unwinding	3	0,0462	2,804
BP	GO:1903508	positive regulation of nucleic acid-temp...	8	0,0463	0,785
BP	GO:0031539	positive regulation of anthocyanin metab...	2	0,0469	-4,822
BP	GO:1900864	mitochondrial RNA modification	2	0,0471	-4,226
BP	GO:1905615	positive regulation of developmental veg...	1	0,0473	2,775
BP	GO:0019285	glycine betaine biosynthetic process fro...	1	0,0473	7,837

Table S7. ...continued.

BP	GO:0080162	intracellular auxin transport	1	0,0473	1,897
BP	GO:0032025	response to cobalt ion	1	0,0473	-1,989
BP	GO:0010089	xylem development	4	0,0494	-4,885

3. A small RNA perspective on recurrent altitudinal adaptation

Authors: **Szukala A**, Mederake M, Bielke A, Frajman B, Schoenswetter P & Paun O.

Reference: **Szukala A**, Mederake M, Bielke A, Frajman B, Schoenswetter P, Paun O. 2022. A small RNA perspective on recurrent altitudinal adaptation in *Heliosperma pusillum* (Caryophyllaceae). (in preparation).

Status: in preparation for submission to *Molecular Biology and Evolution.*

Own contribution: performed parts of the wet lab work; performed bioinformatics analyses including differential targeting analyses and GO terms enrichments; derived the analytical results; prepared result visualizations; wrote the first draft of the manuscript; revised the manuscript.

3.1. Abstract

Small RNAs (smRNAs) are non-coding RNAs that play key roles in controlling genome stability and regulate plastic phenotypic responses to changing environments. Variation in smRNAs activity can also be transmitted from parents to offspring (non-genetic inheritance). Still, it is unclear to what extent short-term changes in smRNA networks might affect long-term phenotypic and ecological divergence. Here, we analyze smRNA profiles of multiple pairs of ecotypes of the plant *Heliosperma pusillum* in common garden, as well as in reciprocal transplantations settings. The ecotype pairs adapted to different altitudes multiple times in parallel and thus offer powerful insights into the evolution of smRNAs divergence in natural evolutionary replicates. Our results show that between 12% and 27% of all differentially targeted genomic regions (DTRs) by smRNAs include genic regions, depending on the growing environment and the ecotype pair analyzed, while a major proportion of DTRs are intergenic. We recover little similarity of smRNAs targeting genes across ecotype pairs, suggesting that evolutionary replicates can evolve in largely different directions in regard to smRNA activity. In all ecotype pairs and growing environments diverging smRNA profiles appear linked to important biological processes, regulating differential responses to multiple (a-)biotic stressors, including herbivory and differing bacterial communities, drought and shade, and are tightly connected to various epigenetic modifications. Concordant patterns of plasticity recovered in DTRs and differential gene expression suggest that smRNAs are a driving force shaping differences in gene expression plasticity between ecotypes. A part of differentially expressed genes underlying phenotypic differentiation appears to be also differentially targeted by smRNAs. Overall, the clear link between smRNAs profiles and different gene expression states and plasticity suggests that smRNAs should be given more attention as an important driver of ecological divergence.

Keywords: small RNAs; ecotypes; ecological divergence; plasticity; *Heliosperma pusillum*; parallel evolution; post-transcriptional regulation

3.2. Introduction

Small non-coding RNAs (smRNAs) play key roles in regulatory networks and impact a number of developmental processes (Bourc'his & Voinnet, 2010; Eriksson et al., 2020), as well as responses to (a-)biotic stress and diseases (Bartel, 2004; Cabrera et al., 2016; Dowen et al., 2012; Hewezi, 2020). For example, smRNAs mediated responses to osmotic stress have been reported in plants (Z. Sun et al., 2016), molluscs (Zhao et al., 2016), and fishes (e.g. Su et al., 2021). Still, transcriptional and post-transcriptional rewiring by smRNAs is generally thought to be short-lived and reversible, affecting maximally a few generations after removal of a stressor (Beltran et al., 2020; Heard & Martienssen, 2014). Thus, it is still unclear if and to what extent smRNAs mediated (epi-)genetic inheritance (X. Feng & Guang, 2013) may contribute to ecological processes and evolutionary change.

It has been documented that small RNAs can induce transgenerational gene silencing and enhanced rates of epimutation, lasting up to ten generations in absence of selection, likely representing an important source of phenotypic variation on short time scales (Beltran et al., 2020; X. Feng & Guang, 2013; Xu et al., 2018). In sticklebacks, small RNAs expression and targeting was shown to differ in sympatric species, especially related to distinct sex chromosomal states (Kitano et al., 2013), suggesting an important role of these regulatory elements in shaping trait divergence in incipient speciation. Moreover, smRNAs can induce morphological divergence, such as shell pigmentation in bivalves (D. Feng et al., 2020), and were proposed to induce transgenerational improvements of water-deficit stress tolerance in durum wheat (Liu et al., 2021). Interestingly, a yellow spot marking the site of pollinator entry in magenta snapdragon flowers is controlled by a smRNA repressing pigment biosynthesis, and the inverted gene duplication generating the smRNA was found to be under selection (Bradley et al., 2017).

In plants, smRNAs are 20–24 nucleotide (nt) long non-coding RNA molecules (Borges & Martienssen, 2015). Two main classes have been described based on the RNA precursor from which they are generated: (a) those derived from a single-stranded RNA folding into a hairpin-like structure (micro RNAs, miRNAs) usually 20–22 nt in length and (b) the

double-stranded RNA-derived (small interfering RNAs, siRNAs) usually 21–24 nt in length. Both miRNAs and siRNAs target in trans either RNA or DNA affecting transcription and translation (Borges & Martienssen, 2015; Guleria et al., 2011; Moss, 2001), at the transcriptional level through DNA methylation or histone modification (siRNAs), and post-transcriptionally through mRNA degradation or translational repression (miRNAs and siRNAs). Some authors noticed that the diversification and specialization of gene-silencing networks in plants probably reflect an important role for smRNAs in the adaptation to a sessile lifestyle (Borges & Martienssen, 2015; Formey et al., 2014). Indeed, the role of smRNAs shaping phenotypic plasticity under e.g. varying temperatures (Campos et al., 2014; Q. Wang et al., 2016; Zuo et al., 2021), and drought stress (Gelaw & Sanan, 2021; Zheng et al., 2019) has been shown in several studies.

Here, we investigate smRNAs-mediated regulatory divergence of gene expression in altitudinal ecotypes of the plant *Heliosperma pusillum* (Waldst. and Kit.) Rchb. (Caryophyllaceae). Glabrous alpine and glandular-pubescent montane ecotypes in this species have diverged multiple times in parallel in the South-Eastern Alps (Bertel et al., 2018; Szukala et al., 2022; Trucchi et al., 2017), offering natural replicates of incipient (Bertel, Hülber, et al., 2016) but stable (Bertel et al., 2018, 2017) ecological and morphological divergence. Reciprocal transplantation experiments at the natural growing sites confirmed a fitness advantage of each ecotype in its native environment (Bertel et al., 2018), and uncovered enhanced phenotypic plasticity in the derived montane ecotype compared to the alpine (Bertel et al. 2018; Chapter 2 of this thesis). After growing plants from different ecotype pairs in a common garden (CG) and in reciprocal transplantations (RT), we aim here to identify ecotype-specific targeting of genes by smRNAs affecting ecological divergence and different degrees of gene expression plasticity. We particularly investigate if smRNAs are involved in guiding the increased phenotypic plasticity reported in the derived ecotypes (Bertel et al. 2018; Chapter 2 of this thesis). Further, we compare the detected patterns of smRNAs differential targeting (DT) with previous findings on between-ecotypes gene expression diversification under the same experimental conditions (Szukala et al. 2022; Chapter 2 of this thesis).

3.3. Materials and Methods

3.3.1. Experimental designs and plant material

We sampled and sequenced 60 smRNA libraries from the leaves of montane and alpine ecotypes of *H. pusillum*. Our aim was to detect differences between the ecotypes in regard to the activity of smRNAs, in particular when targeting genic regions. To achieve a comprehensive picture of genotypic and environmental effects on smRNA activity we grew plants from both ecotypes in two different experimental settings: (i) a common garden (CG), and (ii) reciprocal transplantations (RT) at natural sites of occurrence (Fig. 1a, b, and d). For the CG design we grew 23 plants in uniform conditions at the Botanical Garden of the University of Innsbruck, Austria, aiming for three biological replicates for each population (Fig. 1; Table S1). Wild seeds were collected from four alpine/montane ecotype pairs in the south-eastern Alps (Table S1). To stabilize levels of smRNAs and gene expression, the plants have been grown in a climate chamber (Percival PGC6L set to 16 h 25 °C three lamps/8 h 15 °C no lamps) one week before fixation of the plant material. Fresh stalk-leaf material, sampled at a vegetative, similar developmental stage across accessions, was fixed in RNAlater (Sigma Aldrich) in the same morning and kept at -80 °C until extraction.

RT were performed in the alpine/montane localities of occurence of the ecotypes of pair 3 (Table S1) using seeds from ecotype pairs 1 and 3 (Fig. 1). In this experiment we investigated 37 accessions, aiming for five biological replicates per population. With few exceptions, the accessions and tissue fixations used in this study were also used for transcriptome analyses in two previous works (Szukala et al. 2022; Chapter 2 of this thesis) as indicated in Table S1 and S2. In this way, we were able to directly compare patterns of differential targeting by small RNAs with gene expression patterns in the same experimental setup and the same individuals.

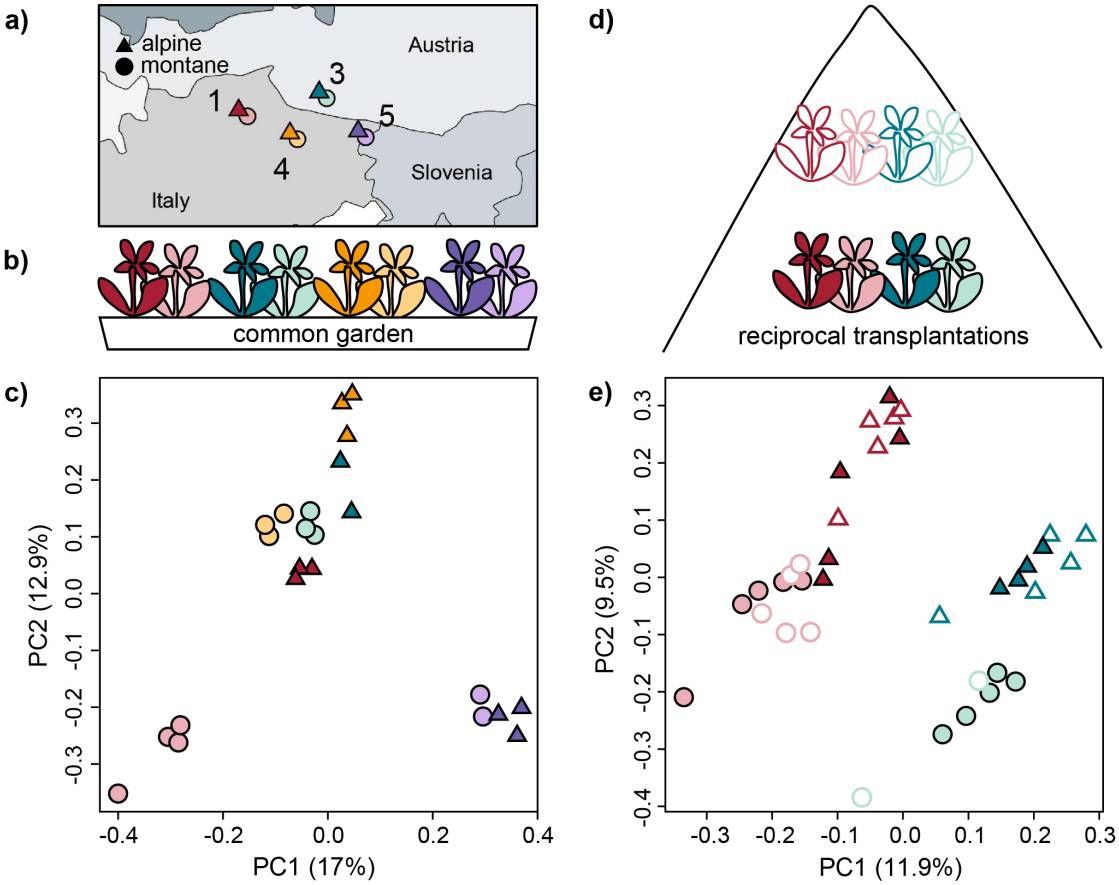

Figure 1. Geographic localization of the four ecotype pairs analyzed (a), experimental designs (CG, b, and RT, d), and clustering of individuals based on smRNAs targeting activity in CG (c) and RT (e). As in the map **(a)**, red, green, orange, and violet color shades represent ecotype pairs 1, 3, 4, and 5, respectively, while darker triangles and brighter circles represent the alpine and montane ecotype, respectively. Principal component analysis of normalized smRNAs read counts of individual samples from four ecotype pairs (1, 3, 4, and 5) grown in CG **(c)** and from two ecotype pairs (1 and 3) grown in RT **(e)**. Filled and empty symbols in **(d-e)** represent the montane and alpine growing sites, respectively. The numbering of the ecotype pairs is the same used in Bertel et al. (2018) and Szukala et al. (2022).

3.3.2. Library preparation and sequencing

Total RNA was extracted from c. 90 mg leaf tissue using the mirVana miRNA Isolation Kit (Ambion) following the manufacturer's instructions, which allows for small RNA extraction in parallel to total RNA isolation. Residual DNA has been digested with the

RNase-Free DNase Set (Qiagen). Size selection of small RNAs (20–24 nt) was performed on a vertical TBE-Urea gel (life Technologies) with the help of a micro RNA marker (New England Biolabs), following the protocol explained in detail in Balao et al. (2017). Strand-specific libraries were prepared with the NEBNext Multiplex small RNA Library Prep Set for Illumina (New England Biolabs). Twelve (CG data) and twenty (RT data) individually-indexed smRNA-seq libraries were pooled and sequenced per Illumina HiSeq 2500 lane with single-end reads (50 bp) at the Vienna Biocenter Core Facilities (VBCF; `https://www.viennabiocenter.org`).

3.3.3. Reads alignment and definition of genomic regions of interest

smRNA data was demultiplexed using BamIndexDecoder v.1.03 (`http://wtsi-npg.github.io/illumina2bam/#BamIndexDecoder`). The raw reads were then cleaned to remove adaptors and quality filtered using trimmomatic v.0.32 (Bolger et al., 2014). We retained only reads between 20 and 24 nt using AWK. Individual reads were aligned to the *Heliosperma* reference genome v.1.0 (NCBI accession number JAIUZE010000000; Szukala et al. 2022) using STAR v.2.7.9a (Dobin et al., 2013) with the options *–alignIntronMax 1 –outFilterMismatchNoverLmax 0.05*. Mapped files were sorted by leftmost coordinates using samtools sort (Danecek et al., 2011). We then aimed to identify genomic windows targeted by smRNAs in an approach unconstrained by already available structural information. We used the bamCoverage tool of deepTools2 v.3.5.1 (Ramìrez et al., 2016) to track per sample smRNA read coverage along the genome using a window size of 100 bp and ignoring windows below a threshold of ten reads aligned. We then merged the filtered regions across samples using bedtools merge v.2.30.0 (Quinlan & Hall, 2010), combining adjacent features into a single bed file. The resulting bed file containing peak regions of small RNAs alignment was then converted to gff format using the R package rtracklayer v.1.42.2.

3.3.4. Counting reads aligned to genomic features

FeatureCounts v.2.0.3 from Rsubread package (Liao et al., 2014) was used to produce a count table with the option *-M –fraction* to allow fractional counts for multi mapping reads (i.e., 1 / no. of mapping positions), as smRNAs are known to frequently target members of gene or TE families (Axtell, 2013; Borges & Martienssen, 2015). First, we aimed to investigate the amount of targeting of different genomic regions by different length classes of smRNAs. We thus produced multiple tables of counts for different length classes of smRNAs (i.e. 20, 21, 22, 23, and 24 nt separately) and using the option *-t* to specify different genomic regions of interest, i.e. genes (defined to include exons and introns), exons, introns, 'promoters' (broadly defined as potentially regulatory regions 1,000 bp up- and downstream of genes), and intergenic regions (defined as all genomic regions excluding genes as above defined). Second, we aimed to identify differentially targeted regions (DTRs) between ecotypes and growing environments. For this task, we used as genomic regions of interest (i.e. the *-t* option in FeatureCounts) the previously produced gff file containing peak regions of small RNAs alignment, without separation of smRNAs reads based on length (i.e. 20–24 nt long smRNAs reads were treated the same way while counting).

3.3.5. Analysis of differential targeting by smallRNAs

DT analysis was performed using the Bioconductor package EdgeR v.3.24.3 (Robinson et al., 2010). Given that all five length classes of smRNAs are known to target genic regions (i.e. the main focus of our investigation), we performed DT analysis by treating different read lengths equally. Peak regions with low levels of targeting by small RNAs across samples were discarded using the *filterByExpr* function setting minimum count equal to 8. We analyzed CG and RT data separately, since the year of seed collection, the growing environment, and the developmental stage at which RNA was fixed, differed. By using too many predictors in our regression model, we would run the risk of inflating the standard errors and make results uninterpretable, as well as lowering statistical power. Therefore, we implemented a generalized linear model to account for the effects of the

covariates ecotype pair and ecotype on small RNA profiles of CG data ($y_{CG} \sim$ ecotype + pair + ecotype × pair), and of the covariates altitude, ecotype pair, and ecotype on small RNA profiles of RT data ($y_{RT} \sim$ ecotype + pair + altitude + ecotype × pair × altitude). Peak-wise dispersion was estimated over all peaks using the *estimateDisp* function and specifying *robust=T* to robustify the estimation against potential outliers. We fitted a quasi-likelihood negative binomial generalized log-linear model (EdgeR function *glmQLFit*), again with the option *robust=T* to lower the effect of outlier peaks. A quasi-likelihood test (EdgeR function *glmQLFTest*) was used to test for differential targeting of regions (DTR) and the significance was adjusted using Benjamini-Hochberg correction of p-values to account for multiple testing. We tested the statistical significance of the overlap between lists of DTR using the hypergeometric test of the Bioconductor package SuperExactTest (M. Wang et al., 2015).

3.3.6. GO terms enrichment of targeted genes

Upon identification of DTRs, we gave particular attention to those overlapping with genic regions, including proximal regulatory and promoter sites, defined as the 1,000 bp region up- and downstream of genes. We used bedtools intersect to extract lists of genes overlapping DTRs and defined those as differentially targeted genes (DTGs). We then performed GO terms enrichment of DTGs using Fisher's exact tests implemented in the Bioconductor package topGO v.2.34.0 (`https://bioconductor.org/packages/release/bioc/html/topGO.html`) to identify significantly overrepresented functions (FDR adjusted $p < 0.05$). Where more then one DTR would overlap the same gene, we randomly retained one DTR and its differential targeting values to perform GO terms enrichment, since this analysis allows only unique values for each gene in the DTGs list. This choice would not affect the GO terms resulting as enriched, but would partly affect the underlying logFC and resulting z-score. Finally, we compared the information gained about differential targeting of genes (DTG) in CG and RT against GO terms enrichment results from Szukala et al. (2022) and Chapter 2 of this thesis.

3.4. Results

3.4.1. Targeting of genomic regions by different smRNAs length classes

All length classes of smRNAs predominantly aligned to intergenic regions across datasets and samples (Fig. S1a). Genes, and particularly exonic regions within genes, were characterized by enhanced targeting by 21 nt long smRNAs, whereas 'promoters', introns and intergenic regions by 23–24 nt long smRNAs (Fig. S1a and b). Intergenic regions showed an enhanced targeting by 20 nt long smRNAs compared to the other genomic regions analyzed, while exonic regions within genes were less targeted by 24 nt long smRNAs (Fig. S1b).

3.4.2. Genes and pathways differentially targeted by smRNAs across evolutionary replicates (CG)

After excluding regions with low counts, we retained 290,335 out of 719,317 genomic regions of interest in the CG data. The PCA of normalized read counts (Fig. 1c) shows that smRNAs alignments cluster the ecotypes and ecotype pairs consistently with previously observed patterns based on genetic variation and gene expression (Szukala et al., 2022). Accordingly, ecotype pair 5 is most diverged from the other three (PC1, 17.0% of variation). Also, between-ecotypes divergence is least pronounced in pair 5, while most pronounced in 1 and intermediate in pairs 3 and 4 (PC2, 12.9% of variation).

Pairs 1 and 4 showed strong between-ecotype differentiation in smRNAs targeting (Fig. 2a and c), with 37,402 (21,559 and 15,843 up- and down-targeted peaks in the montane ecotype, respectively) and 33,147 (16,194 and 16,953 up- and down-targeted peaks in the montane ecotype, respectively) DTRs found in each pair, respectively (Table 1a). Among these DTRs, 5,000 (2,987 and 2,013 up- and down-targeted peaks in the montane ecotype, respectively) and 4,192 (2,490 and 1,702 up- and down-targeted peaks in the montane ecotype, respectively) overlapped with or were included within genes in pair 1 and 4, respectively (Fig. 2a; Table 1a). By contrast, we detected 5,930 (2,846 and 3,084 up- and down-targeted peaks in the montane ecotype, respectively) and 1,189 (793 and 396 up-

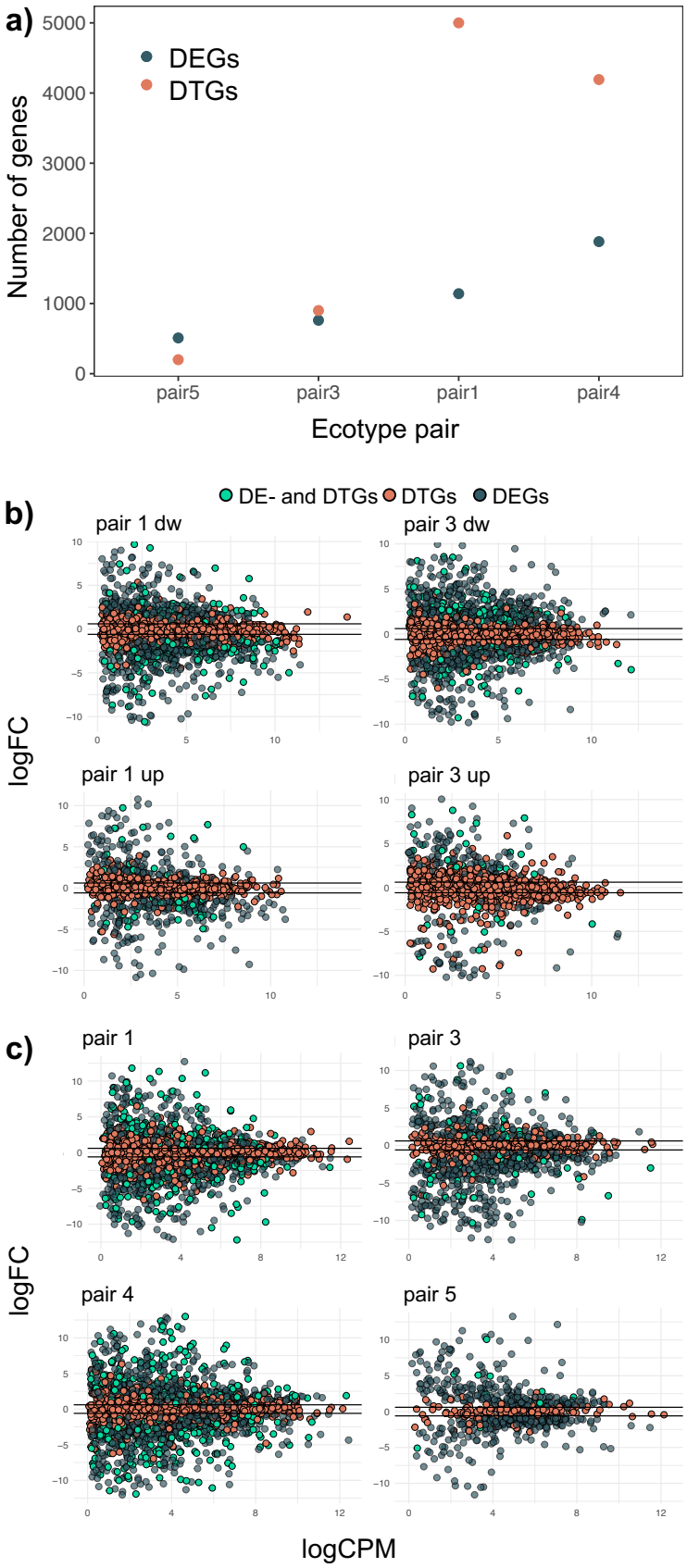
a)
Number of genes
5000
4000
3000
2000
1000
0
DEGs
DTGs
pair5
pair3
pair1
pair4
Ecotype pair
b)
DE- and DTGs
DTGs
DEGs
pair 1 dw
pair 3 dw
pair 1 up
pair 3 up
logFC
c)
pair 1
pair 3
pair 4
pair 5
logFC
logCPM

Figure 2. Comparison between the amount of differentially expressed (DEGs) and targeted (DTGs) in the four ecotype pairs grown in CG and pair 1 and 3 grown in RT. (a) Numbers of DEGs vs DTGs in each ecotype pair in CG. Dark green dots, DEGs; orange dots, DTGs. **(b)** MA plots of DEGs (dark green dots), with DTGs marked with orange dots, and both DTG and DEGs with light green dots.Patterns in pair 1 are shown on the left, and 3 on the right at both montane growing site ("dw", upper row) and alpine site ("up", bottom row). **(c)** MA plots of DEGs (dark green dots), with DTGs marked with orange dots, and both DTG and DEGs with light-blues dots, detected in pairs 1, 3, 4, and 5 grown in CG. In **(b)** and **(c)**, the genes that are neither DE or DT have been excluded.

and down-targeted peaks in the montane ecotype, respectively) DTRs and 900 (536 and 364 up- and down-targeted genes in the montane ecotype, respectively) and 199 (165 and 34 up- and down-targeted genes in the montane ecotype, respectively) DTGs in pairs 3 and 5, respectively (Fig. 2a and c, Table 1a). The MA plots reported in Fig. 2c show that in general only a minor proportion of differential targeting involves differentially expressed genes. The amount of shared DTRs among all four ecotype pairs was equal to 0 for both DTRs up- and down-targeted in the montane ecotype (Fig. S2a and d), as was the amount of shared DTGs down-targeted in the montane ecotype (Fig. S3d). Three genes up-targeted in the montane ecotype were shared across all ecotype pairs (Fig. S3a), whereas the absence of shared DTRs indicates that different portions of these three genes are affected by differential targeting in the ecotype pairs.

3.4.3. Altitudinal effects on smRNAs targeting activity (RT)

After filtering low counts regions we retained 166,776 out of 576,675 genomic regions of interest in the RT data. The first PC of the normalized read counts (Fig. 1e, 11.9% of variation) separates the two pairs analyzed (i.e. pair 1 and 3), while the second PC (9.5% of variation) the ecotypes. This pattern resembles the clustering observed for gene expression data (Chapter 2 of this thesis).

Table 1. Numbers of differentially expressed (DEGs) and differentially targeted (DTGs) genes, as well as overlapping genes between these two groups (i.e. being both DE and DT) in each comparison and experimental setup. Genes detected in alpine-montane ecotype comparison **(a)**, and genes detected in the growing site comparisons **(b)**.

(a)

Ecotype pair	Common garden (CG)			Reciprocal transplantations (RT)			
	DEGs (Szukala et al., 2022)	DTGs	genes DE and DT (proportion of DEGs)	growing site	DEGs (Chapter 2)	DTGs	genes DE and DT (proportion of DEGs)
1	1140	5000	359 (31.5%)	montane	1063	2359	196 (18.4%)
				alpine	402	1244	48 (12%)
3	761	900	87 (11.4%)	montane	1067	1989	172 (16.1%)
				alpine	219	2112	36 (16.4%)
4	1882	4192	546 (29%)				
5	509	199	12 (39%)				

(b)

Reciprocal transplantations (RT)				
ecotype pair	ecotype	DEGs (Chapter 2)	DTGs	genes DE and DT (proportion of DEGs)
1	alpine	57	243	1 (1,75%)
	montane	461	435	14 (3%)
3	alpine	160	28	0 (0%)
	montane	269	1206	12 (4,5%)

We detected 15,862 (among those 7,561 and 8,301 up- and down-targeted peaks in the montane, respectively) and 8,009 (among those 4,129 and 3,880 up- and down-targeted peaks in the montane, respectively) DTRs between ecotypes in pair 1 when grown at the montane and alpine sites, respectively (Table 1a), including 2,359 (1,144 and 1,215 up- and down-targeted peaks in the montane ecotype) and 1,234 (643 and 591 up- and down-targeted peaks in the montane) DTGs at the montane and alpine sites, respectively. Similarly, in pair 3 we detected less regions being DT at the higher altitude even if the difference was less pronounced, with 13,610 (6,044 and 7,566 up- and down-targeted peaks in the montane, respectively) and 11,370 (8,241 and 3,129 up- and down-targeted peaks in the montane, respectively) DTRs found at the montane and alpine site, respectively (Table 1a). These DTRs included 1,989 (1,135 and 854 up- and down-targeted peaks in

the montane, respectively) and 2,112 (1,762 and 350 up- and down-targeted peaks in the montane, respectively) DTGs at the montane and alpine sites, respectively. Accordingly, lower gene expression differentiation between ecotypes at the higher altitudinal site was observed previously (Chapter 2 of this thesis), and similarly this pattern was more pronounced in pair 1. Nevertheless, despite overall DTGs numbers being always higher in the montane environment, the amounts of DTGs in pair 3 at the two elevations are similar. Interestingly, differential targeting appeared to be largely dominated by enhanced targeting of the montane ecotype compared to the alpine (Chapter 2 of this thesis). Thirtyeight DTGs were shared by both environments and both pairs (Fig. S4b and e), an overlap significantly higher than chance expectations (hypergeometric p = 1.8e-23). By contrast, the amount of shared DTRs across all four comparisons was within chance expectation (i.e. 249 shared DTRs, hypergeometric p = 0, Fig. S4a and d).

We also searched for regions DT between altitudes in each ecotype in RT, thus showing plasticity in the activity of the targeting smRNAs. Consistent with higher plasticity of gene expression in the montane ecotype reported in Chapter 2 of this thesis, we detected enhanced plasticity in smRNAs activity in the montane ecotype. We reported 1,910 and 5,070 DTRs in this ecotype for pair 1 and 3, respectively, overlapping 435 DTGs (202 and 233 up- and down-targeted in the non-native alpine environment) and 1,206 DTGs (1,110 and 96 up- and down-targeted in the non-native alpine environment), respectively. By contrast, we detected 956 and 236 DTRs in the alpine ecotype of pair 1 and 3, respectively (Table 1b), overlapping 243 (110 and 133 up- and down-targeted in the non-native montane environment) and 28 (18 and 19 up- and down-targeted in the non-native montane environment) DTGs, respectively (Table 1b).

Finally, a relevant portion of the DTGs did not appear to be affected by the growing environment. In both ecotype pairs studied in RT the overlap of DTGs detected at both altitudes with DTGs detected in CG was significantly higher than chance expectation, i.e. 299 in pair 1 (hypergeometric p = 2.35e-32), and 94 in pair 3 (hypergeometric p = 0.007), whereas this overlap was particularly pronounced in pair 1 (Fig. S3b,c,e and f).

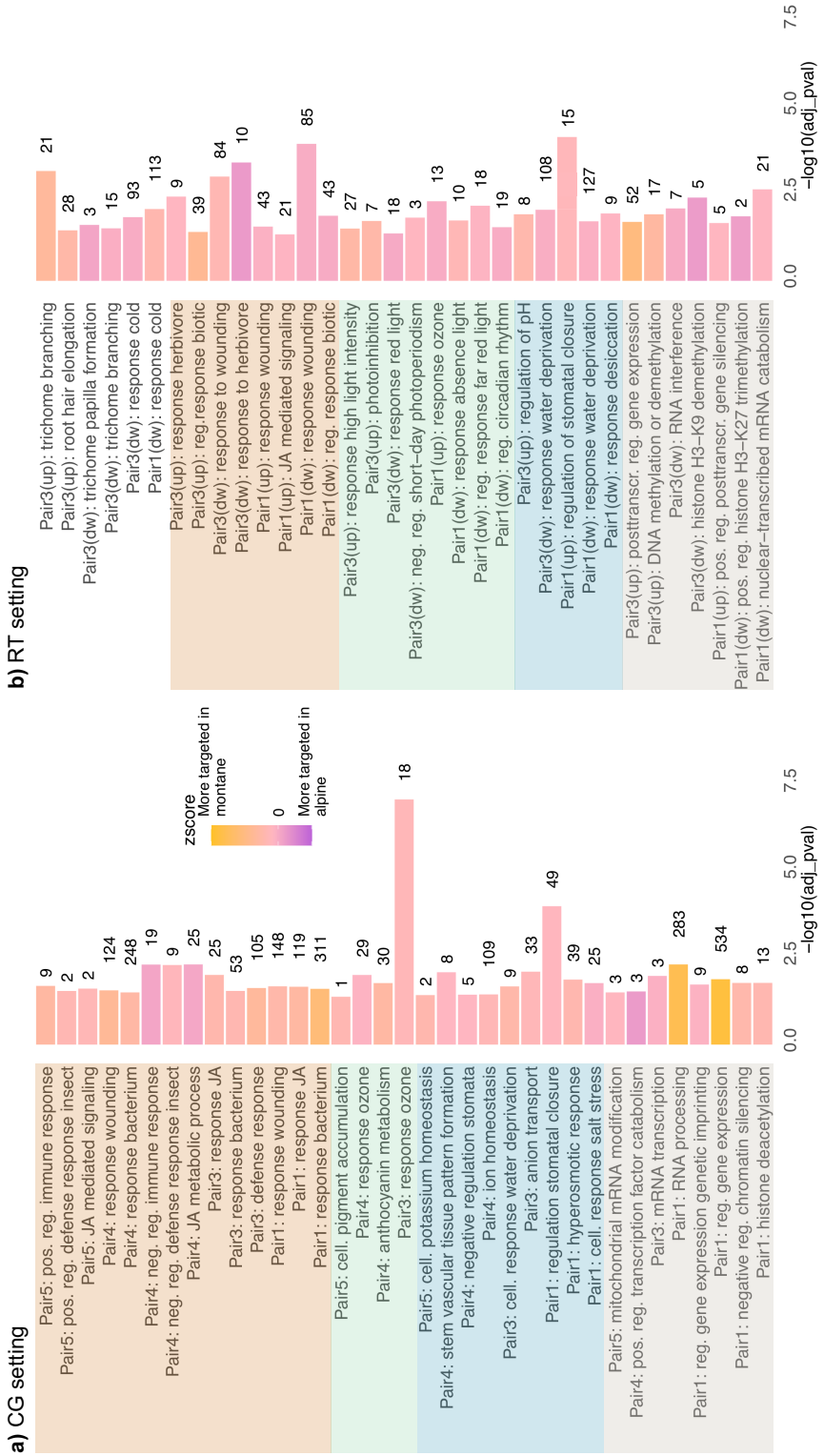
a) CG setting
Pair5: pos. reg. immune response
Pair5: pos. reg. defense response insect
Pair5: JA mediated signaling
Pair4: response wounding
Pair4: response bacterium
Pair4: neg. reg. immune response
Pair4: neg. reg. defense response insect
Pair4: JA metabolic process
Pair3: response JA
Pair3: response bacterium
Pair3: defense response
Pair1: response wounding
Pair1: response JA
Pair1: response bacterium
Pair5: cell. pigment accumulation
Pair4: response ozone
Pair4: anthocyanin metabolism
Pair3: response ozone
Pair5: cell. potassium homeostasis
Pair4: stem vascular tissue pattern formation
Pair4: negative regulation stomata
Pair4: ion homeostasis
Pair3: cell. response water deprivation
Pair3: anion transport
Pair1: regulation stomatal closure
Pair1: hyperosmotic response
Pair1: cell. response salt stress
Pair5: mitochondrial mRNA modification
Pair4: pos. reg. transcription factor catabolism
Pair3: mRNA transcription
Pair1: RNA processing
Pair1: reg. gene expression genetic imprinting
Pair1: reg. gene expression
Pair1: negative reg. chromatin silencing
Pair1: histone deacetylation
9
2
2
124
248
19
9
25
25
53
105
148
119
311
1
29
30
18
2
8
5
109
9
33
49
39
25
3
3
3
283
9
534
8
13
0.0
2.5
5.0
7.5
−log10(adj_pval)
zscore
More targeted in montane
0
More targeted in alpine
b) RT setting
Pair3(up): trichome branching
Pair3(up): root hair elongation
Pair3(dw): trichome papilla formation
Pair3(dw): trichome branching
Pair3(dw): response cold
Pair1(dw): response cold
Pair3(up): response herbivore
Pair3(up): reg.response biotic
Pair3(dw): response to wounding
Pair3(dw): response to herbivore
Pair1(up): response wounding
Pair1(up): JA mediated signaling
Pair1(dw): response wounding
Pair1(dw): reg. response biotic
Pair3(up): response high light intensity
Pair3(up): photoinhibition
Pair3(dw): response red light
Pair3(dw): neg. reg. short−day photoperiodism
Pair1(up): response ozone
Pair1(dw): response absence light
Pair1(dw): reg. response far red light
Pair1(dw): reg. circadian rhythm
Pair3(up): regulation of pH
Pair3(dw): response water deprivation
Pair1(up): regulation of stomatal closure
Pair1(dw): response water deprivation
Pair1(dw): response desiccation
Pair3(up): posttranscr. reg. gene expression
Pair3(up): DNA methylation or demethylation
Pair3(dw): RNA interference
Pair3(dw): histone H3−K9 demethylation
Pair1(up): pos. reg. posttranscr. gene silencing
Pair1(dw): pos. reg. histone H3−K27 trimethylation
Pair1(dw): nuclear−transcribed mRNA catabolism
21
28
3
15
93
113
9
39
84
10
43
21
85
43
27
7
18
3
13
10
18
19
8
108
15
127
9
52
17
7
5
5
2
21
0.0
2.5
5.0
7.5
−log10(adj_pval)

Figure 3. Biological processes enriched in DTGs are similar across environmental conditions. GO terms (biological processes) enriched in DTGs detected in four ecotype pairs grown in CG **(a)**, and in RT **(b)**. The pair in which a GO term is enriched is reported in front of the term id, whereas in **(b)** the growing site is additionally indicated as "up" (alpine) or "dw" (montane). The X-axis shows the significance of the enrichment, the color of the bars shows the z-score (i.e. in which ecotype, enhanced targeting of the genes underlying a specific term was detected), and the numbers on the side of the bars display the number of DTGs underlying a GO term. The colors highlighting groups of GO terms correspond to four functional categories (i.e. orange, response to biotic stress; green, response to light; blue, response to drought; and grey, (epi-)genetic modifications). GO terms not highlighted with colors are found only in RT, but not in CG. GO term names were shortened for visual clarity.

3.4.4. Biological implications of smRNAs targeting

We report in the first place biological processes that were found enriched in DTGs detected in the between-ecotypes comparison across ecotype pairs and environments (i.e. in CG, Fig. 3a and Table S2, but also montane and alpine sites in RT, Fig. 3b and Table S3). Indeed, we recovered processes that were similar among environmental setups (highlighted with the same colors in Fig. 3). A large number of functions were involved in the response to biotic stressors (in particular bacteria, insects, and fungi) and damage (see e.g. the recurrent term "response to wounding"), but also to water availability, drought and salinity. Also, we reported several enriched functions related to the epigenetic regulation of gene expression and silencing (e.g. histone acetylation and methylation, as well as DNA methylation). Responses to light were enriched in both CG and RT experimental settings, but we observe a plastic component of this response in RT, given that responses to low light and shade were enriched in the montane sites, while responses to higher light intensity were enriched in CG and the alpine site of RT. Similarly, the response to temperature was enriched in the RT montane environment, but not in the CG and RT alpine environments, showing a more plastic behavior. We also found an enrichment of terms related to trichome formation in pair 3 in the RT setting, both in the montane and alpine sites.

We observed that the montane ecotype plastically targets genes related to photoinhibition, water deprivation, epigenetic modifications (Fig. 4b and Table S4, pair 1 and 3), and trichome development (Fig. 4b, pair 3 only). Similar functions were targeted plastically also in the alpine ecotype (Fig. 4a), but the number of genes behaving plastically was strongly reduced. Also, while in the alpine ecotype the plasticity in drought response seems to be lacking (Fig. 4a), we reported plasticity in several abiotic stress responses (Fig. 4a). Finally, no functions related to trichomes or hair development were detected in CG, despite high numbers of DTGs found. Multiple genes related to trichomes were differently expressed in the same CG setting (Szukala et al., 2022), and this lack of trichomes related functions in DTGs would suggest that the specific genes detected related to this trait are not affected by smRNAs activity.

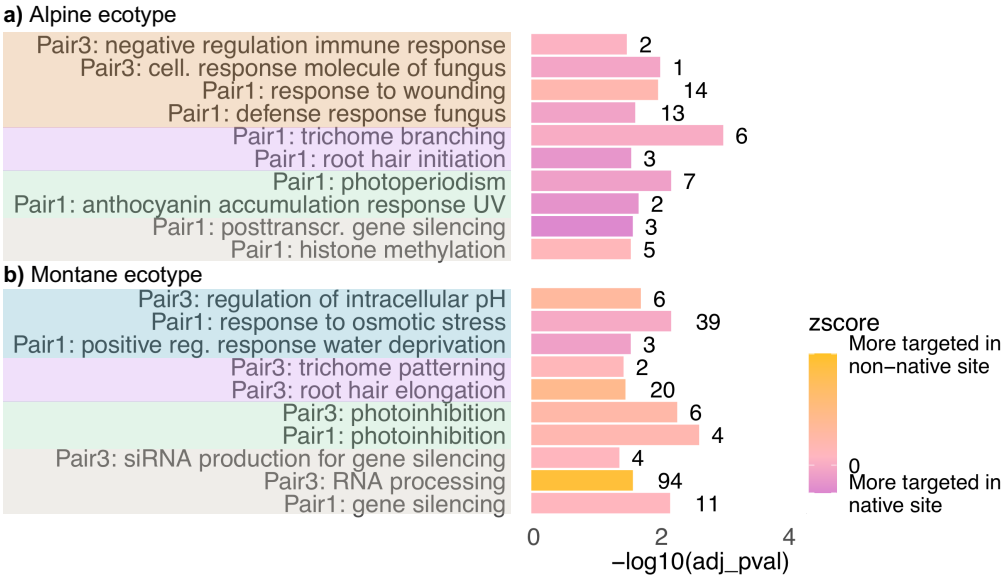

Figure 4. Biological significance of plastic DTGs. GO terms (biological processes) enriched in genes DT at different altitudes in the alpine **(a)**, and montane **(b)** ecotype. The X-axis shows the significance of the enrichment, the color of the bars shows the z-score (i.e. if smRNAs targeting is enhanced in the native or non-native environment), and the numbers on the side of the bars display the number of DTGs underlying a GO term. The colors highlighting groups of GO terms correspond to Fig. 3, with the addition of trichomes related functions in pink. GO term names were shortened for visual clarity.

3.4.5. Differentially expressed genes associated with differential targeting by smRNAs

The differentially expressed genes detected in previous studies using plants grown in the same experimental settings (Szukala et al. 2022; Chapter 2 of this thesis) that were also DT by smRNAs are reported in Table 1a. In the CG data, we found that 359, 87, 546, and 12 genes were both DT and differentially expressed in the pairs 1, 3, 4, and 5, respectively (Table 1a). In pair 5, smRNAs seem therefore to play a minor role in shaping gene expression divergence, compared to the other pairs. In accordance with previously observed GO term enrichments of DTGs in CG, these differentially expressed and targeted genes play a role in shaping responses to biotic (pair 1, 3, 4, and 5) and abiotic stressors (especially drought, heat, and light, pair 1, 3, and 4) and epigenetic modifications (pair 1) (Table S5). A few of these genes were involved in trichome morphogenesis (in pairs 1, 3, and 4, Fig. 5 and Table S6).

In the RT experiment, 196 (montane site) and 48 (alpine site), and 172 (montane site) and 36 (alpine site) DTGs detected were also differentially expressed between ecotypes in the pairs 1 and 3, respectively (Table 1b). We detected no effects of small RNAs on the limited number of genes differentially expressed at different altitudes in the alpine ecotype, consistent with overall low plasticity of expression in this ecotype. In the montane ecotype, we reported 14 and 12 genes DT and differentially expressed at different altitudes in pair 1 and 3, respectively (Table 1b). Also in RT data, differentially expressed and targeted genes included trichome related genes (Fig. 5, Table S6), that were partly shared with those found in GC data. A high number of differentially expressed and targeted genes were enriched in previously observed responses to biotic and abiotic stressors at the montane site (Table S7). Similar enriched processes were recovered at the alpine site, but the number of underlying genes was rather low, given the small number of genes differentially expressed and targeted found in this environment.

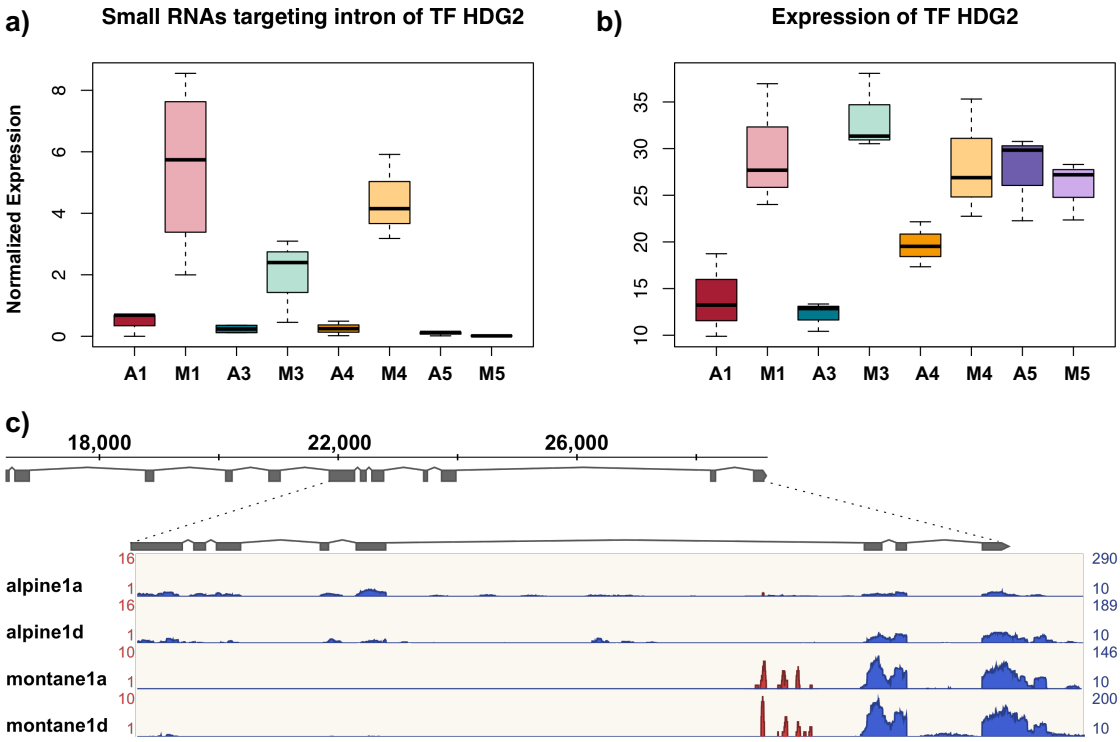

Figure 5. Differential targeting of a differentially expressed transcription factor putatively related to trichomes. **(a)** Normalized counts of 23-24 nt long smRNAs aligned to a portion of a long intronic region (4,260 nt) of HDG2, depicted in **(c)**. smRNAs targeting is significantly higher (FDR < 0.05) in the montane ecotype of pair 1, 3, and 4. **(b)** Normalized expression levels of the homeodomain GLABROUS 2 (HDG2), a transcription factor of the homeobox-leucine zipper family proteins related to trichomes formation and development in several plants. Expression is significantly higher (FDR < 0.05) in the montane ecotype of pair 1, 3 (CG data). **(c)** Gene model of HDG2 showing exons (gray boxes) and introns (gray lines connecting gray boxes). RNA-seq and smRNAs reads coverage is shown overlaid in blue and red, respectively, for two alpine and two montane individuals of pair 1. Numbers in red on the left refer to smRNAs, while black numbers on the right to RNA. The Y-axis has been scaled proportional to the respective library size of the different accessions for RNA-seq data, and separately for smRNA-seq data. Note the difference in expression rates between the alpine and montane, but also the expression of different splicing variants.

3.5. Discussion

We analyzed smRNAs profiles of ecologically diverged plants grown in CG and RT. Our study was designed to explore smRNAs genome targeting in parallelly evolved pairs of

ecotypes, with the aim to investigate degree of smRNAs divergence and plasticity in evolutionary replicates of early phases of divergence. A second aim was to detect genes potentially affected by smRNAs regulatory activity and shown previously to underlie ecotype divergence, as well as different degrees of ecotype plasticity (Szukala et al. 2022; Chapter 2 of this thesis). Being key modulators of gene expression and TE activity, epigenetic markers, and phenotypic plasticity (Voskarides, 2017), smRNAs have been most often investigated from a molecular biology point of view (reviewed in e.g. Borges & Martienssen 2015). Also, several studies have shown that smRNAs underlie stable morphological variation in natural populations (Arif et al., 2013; Bradley et al., 2017; Clop et al., 2006; Nair et al., 2010). Nevertheless, we only have little understanding of the ecological and evolutionary significance of smRNAs-driven divergence (Silva et al., 2021).

We observed that a high proportion of smRNAs in our datasets target intergenic regions, suggesting a major role of smRNAs in targeting repetitive elements (Cantu et al., 2010; Hollister et al., 2011; Wendel et al., 2016). Consistently, the *Heliosperma* genome was found to be rich in repetitive fragments, which make up 71% of the assembled reference (Szukala et al., 2022). Twenty-one nt long smRNAs represented the length-class most aligned to genes, and particularly exons; they are known to reduce protein levels, either at the transcriptional or post-transcriptional stage (Borges & Martienssen, 2015; Wendel et al., 2016). In turn, 20 nt smRNAs appeared to target more intergenic fragments, and 22 nt ones were more equally distributed among genomic regions. In line with their known role as key regulators of transposons (Cantu et al., 2010; Hollister et al., 2011; Wendel et al., 2016), from which they are also encoded (Borges & Martienssen, 2015; Hoffmann et al., 2015), 23-24 nt long smRNAs were more often aligned to intergenic, intronic and 'promoter' regions. Despite these observed differences, all length classes appear to be involved in gene targeting, likely affecting the rate of both transcription and translation. Indeed, a redundant functionality of smRNAs length classes was observed in other studies (Wendel et al., 2016).

Read counts of smRNAs alignments clustered the analyzed populations in a similar way as genetic variation and gene expression (Szukala et al. 2022; Chapter 2 of this thesis),

with pair 5 clearly separated from the other pairs. The similarity observed between how smRNAs, as well as genetic variation and gene expression patterns cluster the populations analyzed, suggests that smRNAs activity evolved in concordance with genetic divergence. Nevertheless, the amount of DTGs detected in each pair in CG setting was highly variable, partly exceeding the differences previously observed in gene expression (Szukala et al., 2022) by several orders of magnitude (Fig. 2a), suggesting that smRNAs may evolve at faster rates than gene expression. This pattern is possibly consistent with higher rates of epimutations compared to genetic mutations (Tal et al., 2010) and rapid evolution of smRNAs in bacteria (Dutcher et al., 2018), likely due to only partial complementarity to their mRNA targets, their fast production, and high amounts in cells (Reichholf et al., 2019). Indeed, we observed that the number of DTGs strongly exceeded that of differentially expressed genes in more divergent ecotypes (pair 1 and 4), while the numbers were not so different in less diverged ecotypes (pair 5 and 3), suggesting that the accumulation of divergence in smRNAs increases more rapidly than gene expression divergence over longer time laces or under more divergent ecological conditions (Fig. S2). The patterns observed in pairs 1 and 4 may be also consistent with segregating mutations between the respective alpine and montane populations at one or several master regulators of the smRNA processing pathways, resulting in rapid divergence between ecotypes.

We recovered very little amounts of DTGs shared by different ecotype pairs (in particular between pair 5 and the other pairs) in CG (Fig. 2a and b). This result is consistent with little amounts of shared differentially expressed genes observed previously (Szukala et al., 2022), indicating that also smRNAs seem to follow diverse routes of divergence and possibly are one driving force behind little repeatability in evolutionary replicates. It is known that smRNAs with different sequences and structures can exert similar functions (Tsai et al., 2014), suggesting that smRNAs-driven regulatory mechanisms can be highly redundant. Moreover, strong differences in smRNAs regulatory efficacy were observed in closely related species, such as transposons silencing by small RNAs in *Arabidopsis thaliana* and *A. lyrata* (Hollister et al., 2011). Thus, it is possible that smRNAs are enhancing the little repeatability of gene expression divergence previously observed.

Congruent with the enhanced potential for expression plasticity in the montane ecotype (Chapter 2 of this thesis), we reported enhanced altitudinal diversification of DTR in the montane ecotype, compared to the alpine. This result suggests that different degrees of gene expression plasticity in the two ecotypes are likely enhanced by differences in regulatory activity via smRNAs. Interestingly, we recovered functions related to trichomes in plastic DTGs (RT) of the montane (pair 3) and alpine (pair 1) ecotype, suggesting that a part of the processes related to the trichome pathway are affected by smRNAs targeting, following different modalities in the two ecotype pairs analyzed. Despite the observed connection between plasticity of gene expression and DTR in the montane ecotype, the amount of shared DTRs and DTGs between different environments but within ecotype pair (i.e. pairs 1 and 3 in CG and RT at different altitudes) was significantly higher than chance expectation (in contrast to the low overlap across evolutionary replicates in CG). This result suggests that despite being important drivers of plasticity, a portion of smRNAs pathways are relatively stable across environments and could be involved in transcriptional regulation.

Despite low overlap of DTGs across ecotype pairs, we found conserved biological processes to be targeted differentially between ecotypes (Fig. 3). More specifically, smRNAs appeared to be strongly involved in differential responses to biotic stress, driven mainly by herbivores, fungi, and bacteria. The alpine and montane ecological niches were previously hypothesized to bear different herbivory pressures (Bertel et al., 2018), and were shown to have highly differing bacterial and competitor communities (Bertel et al., 2018; Trucchi et al., 2017). Also abiotic stressors seemed to trigger differential smRNAs responses. A reaction to water deprivation and desiccation was particularly apparent at the montane growing site in RT, but different responses to water availability were also found in CG and the alpine site in RT. Plastic responses in DTGs seemed also associated with different light availability in the RT montane site compared to the alpine site and the CG. Several functions related to gene silencing, expression regulation, and epigenetics were also enriched in DTGs, suggesting that the smRNA regulatory machinery is tightly linked to epigenetic modifications, and likely represent important drivers of gene

expression plasticity in RT (Szukala et al., 2022).

As already mentioned, we found that some genes related to trichome formation are differentially targeted between ecotypes and show a plastic targeting reaction upon RT. For instance, our analyses detected a peak of smRNAs differentially targeting the longest intronic region of a gene homologous to the *Arabidopsis* homeodomain glabrous 2 (HDG2) transcription factor, which appeared to be differentially spliced between ecotypes, with the isoforms also differently expressed in three out of four ecotype pairs (Fig. 5, Szukala et al. 2022). It was shown that alternative splicing can be driven by smRNAs targeting exons or branch point sequences of intronic regions (Alló et al., 2009; Kelemen et al., 2013). Moreover, mutations in HD-zipper transcription factors via e.g. TEs insertions were shown to affect trichome phenotypes in cucumber (Pan et al., 2015) and cotton (M. Ding et al., 2015). We believe that the concurrence of differential targeting by smRNAs and differential expression of the same gene has the potential to reveal hundreds of genetic loci underlying phenotypic divergence. Thus, future analyses should focus on genes such as HDG2 in *Heliosperma* and aim for functional validations of such targets.

Overall, our results show that smRNAs play a pivotal role in regulating specific ecotype responses to ecological stressors in *Heliosperma*. Given their high evolutionary rates, smRNAs have the potential to be an important driver of evolution, which was given only limited attention up to now. Further, the high redundancy of smRNAs functions and regulatory solutions, might affect the repeatability of molecular patterns during parallel ecological diversification. More investigations on natural and laboratory populations are needed to further explain these aspects and their overall role as drivers of evolutionary change.

3.6. Acknowledgements

This work was financially supported by the Austrian Science Fund (FWF) through the doctoral programme (DK) grant W1225-B20 to a faculty team including O.P., and through grant Y661-B16 to O.P. We thank Nicholas Barton, Andrew Clark, Virginie Courtier-

Orgogozo, Joachim Hermisson, Magnus Nordborg, John Parsch, Christian Schlötterer, and Daniel Schubert for insightful comments and feedback. Special thanks go to Arezoo Fani for support during preliminary investigations. We thank Marie Huber and Daniela Paun, Carles Ortega for their support during laboratory work and data acquisition, Pau Carnicero Campmany for help during setting up of the reciprocal transplantations, as well as Martina Imhiavan and Daniel Schlorhaufer from the Botanical Garden of the University of Innsbruck for the germination of the plants. Computational resources were provided by the Vienna Scientific Cluster (VSC) and the Life Science Compute Cluster (LiSC) of the University of Vienna. A permit to conduct the presented research activities was granted by the Parco Naturale Dolomiti Friulane (no. 1943); for the Austrian federal state Tirol no such permit was necessary.

3.7. Authors contributions

OP designed the study concept; **AS** and **OP**performed laboratory work; **PS** and **BF** supported seeds sampling and cultivation of the plants; **AS** performed bioinformatic analyses with contributions form **MM** and **AB**; **AS** derived the analytical results, and prepared the first figure drafts that were than improved together with **OP**; **OP** provided feed-back on the analyses; **AS** wrote the first draft of the manuscript; **OP** and **AS** revised the manuscript with contributions from all other authors.

Supporting information - Chapter 3

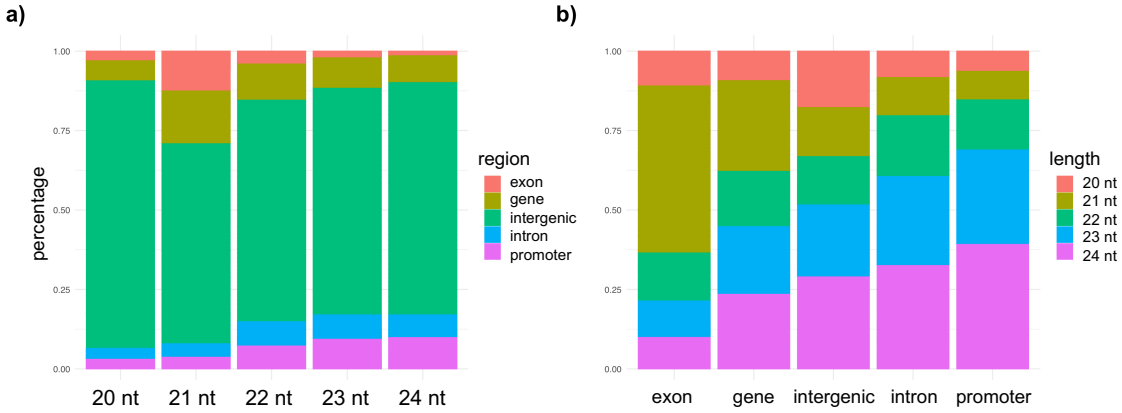

Figure S1. Patterns of smRNAs targeting different genomic regions based on read length. The genomic regions considered here are intergenic regions, 'promoters' (including regulatory regions 1,000 bp up- and downstream of genes), genes, and within the latter exons and introns. **(a)** Amount of genomic regions targeted by different read length classes of smRNAs (i.e. 20-24 nt), given as the percentage of the read aligning to a specific region for each length class. **(b)** Amount of reads aligned to each genomic region of interest depending on read length.

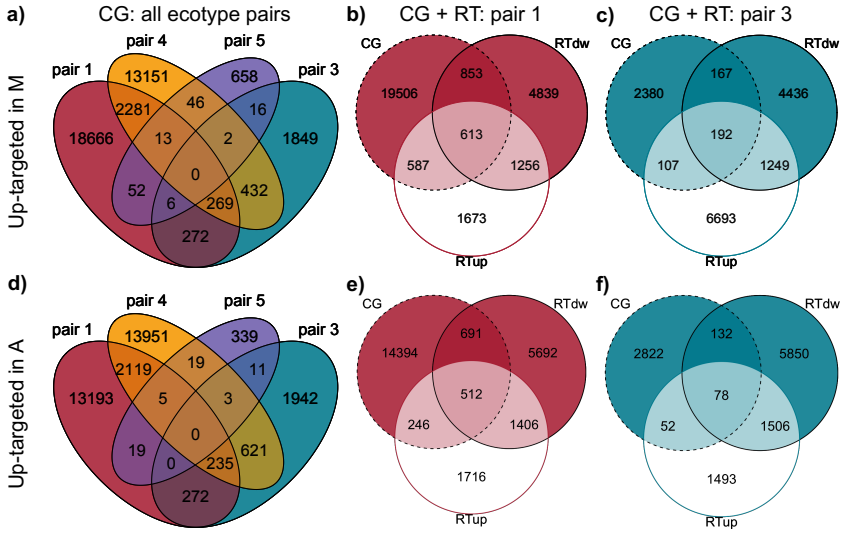

Figure S2. Overlap of differentially targeted regions by smRNAs (DTRs). (a-c) Venn diagrams showing the amount of regions up-targeted in the montane ecotype (M). **(d-g)** Venn diagrams showing the amount of regions up-targeted in the alpine ecotype (A). **(a,d)** Shared DTRs among four ecotype pairs grown in CG. **(b,e)** and **(c,f)** show DTRs shared across different environments (i.e. CG, and RT at alpine (up) and montane (dw) sites) in pair 1 and 3, respectively. Colors of areas and borders as in Fig. 1b (CG) and d (RT).

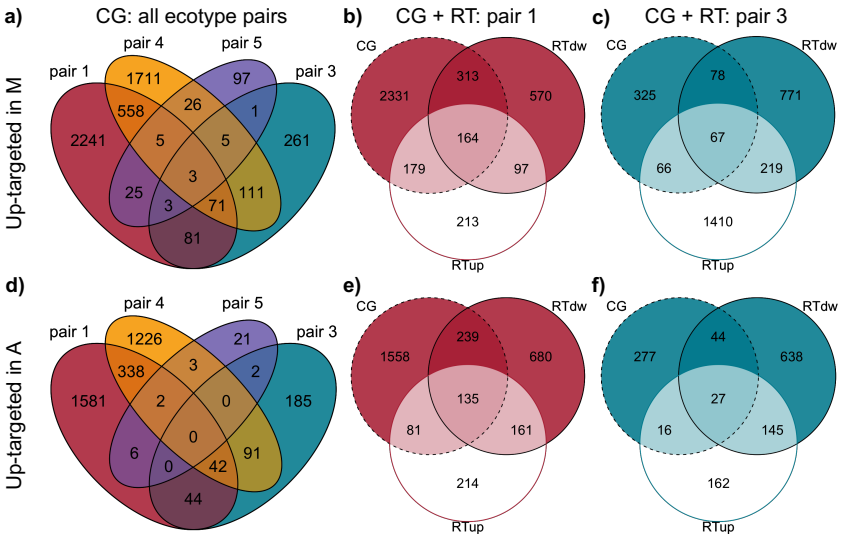

Figure S3. Overlap of differentially targeted genes by smRNAs (DTGs). (a-c) Venn diagrams showing the amount of genes up-targeted in the montane ecotype (M). **(d-g)** Venn diagrams showing the amount of genes up-targeted in the alpine ecotype (A). (a,d) Shared DTGs among four ecotype pairs grown in CG. **(b,e)** and **(c,f)** show DTGs shared across different environments (i.e. CG, and RT at alpine (up) and montane (dw) sites) in pair 1 and 3, respectively. Colors of areas and borders as in Fig. 1b (CG) and d (RT).

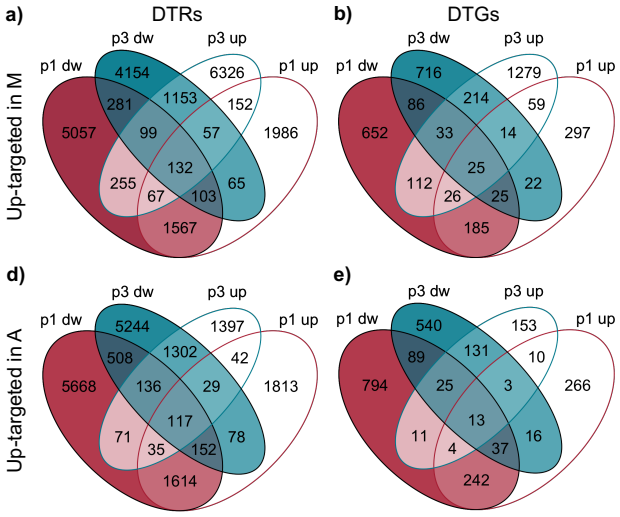

Figure S4. Overlap of differentially targeted regions (DTRs) and genes (DTGs) in pair 1 and 3 in the RT experiment. (a-c) Venn diagrams showing the amount of regions up- **(a)** and down-targeted **(c)** in the montane ecotype (M). **(b,d)** Venn diagrams showing the amount of genes up- **(b)** and down-targeted **(d)** in the montane ecotype (M). Colors of areas and borders as in Fig. 1b (CG) and d (RT).

Table S1. Details regarding the accessions included in the present study. The growing site referes to the experimental set-up (CG = common garden, RT (790 m) = reciprocal transplantations (montane site), RT (2055 m) = reciprocal transplantations (alpine site)), while the locality, longitude, latitude, and altitude refer to the original population from which the seeds for the experiment were collected.

Sample ID	**Growing site**	**Ecotype**	**Ecotype Pair**	**Locality (original population)**	**Longitude**	**Latitude**	**Altitude (m)**
A1A	CG	alpine	1	Italy: Trentino-Alto Adige: Dolomiti di Gardena/Grödner Dolomiten	11.768 E	46.601 N	2290
A1C	CG	alpine	1	Italy: Trentino-Alto Adige: Dolomiti di Gardena/Grödner Dolomiten	11.768 E	46.601 N	2290
A1D	CG	alpine	1	Italy: Trentino-Alto Adige: Dolomiti di Gardena/Grödner Dolomiten	11.768 E	46.601 N	2290
A3A	CG	alpine	3	Austria: Kärnten: Lienzer Dolomiten	12.877 E	46.762 N	2055
A3B	CG	alpine	3	Austria: Kärnten: Lienzer Dolomiten	12.877 E	46.762 N	2055
A4A	CG	alpine	4	Italy: Friuli-Venezia Giulia: Val Cimoliana	12.48 E	46.391 N	1700
A4B	CG	alpine	4	Italy: Friuli-Venezia Giulia: Val Cimoliana	12.48 E	46.391 N	1700
A4C	CG	alpine	4	Italy: Friuli-Venezia Giulia: Val Cimoliana	12.48 E	46.391 N	1700
A5B	CG	alpine	5	Italy: Friuli-Venezia Giulia: Alpi Giulie	13.459 E	46.376 N	1820
A5C	CG	alpine	5	Italy: Friuli-Venezia Giulia: Alpi Giulie	13.459 E	46.376 N	1820
A5D	CG	alpine	5	Italy: Friuli-Venezia Giulia: Alpi Giulie	13.459 E	46.376 N	1820
M1A	CG	montane	1	Italy: Trentino-Alto Adige: Dolomiti di Gardena/Grödner Dolomiten	11.77 E	46.564 N	1690
M1B	CG	montane	1	Italy: Trentino-Alto Adige: Dolomiti di Gardena/Grödner Dolomiten	11.77 E	46.564 N	1690
M1C	CG	montane	1	Italy: Trentino-Alto Adige: Dolomiti di Gardena/Grödner Dolomiten	11.77 E	46.564 N	1690
M1D	CG	montane	3	Austria: Kärnten: Lienzer Dolomiten	12.901 E	46.774 N	790
M3A	CG	montane	3	Austria: Kärnten: Lienzer Dolomiten	12.901 E	46.774 N	790
M3B	CG	montane	3	Austria: Kärnten: Lienzer Dolomiten	12.901 E	46.774 N	790
M3C	CG	montane	3	Austria: Kärnten: Lienzer Dolomiten	12.901 E	46.774 N	790

Table S1. ...continued.

M4A	CG	montane	4	Italy: Friuli-Venezia Giulia: Val Cimoliana	12.489 E	46.38 N	1180
M4B	CG	montane	4	Italy: Friuli-Venezia Giulia: Val Cimoliana	12.489 E	46.38 N	1180
M4C	CG	montane	4	Italy: Friuli-Venezia Giulia: Val Cimoliana	12.489 E	46.38 N	1180
M5C	CG	montane	5	Italy: Friuli-Venezia Giulia: Alpi Giulie	13.459 E	46.388 N	1170
M5E	CG	montane	5	Italy: Friuli-Venezia Giulia: Alpi Giulie	13.459 E	46.388 N	1170
A1_DA	RT (790 m)	alpine	1	Italy: Trentino-Alto Adige: Dolomiti di Gardena/Grödner Dolomiten	11.768 E	46.601 N	2290
A1_DB	RT (790 m)	alpine	1	Italy: Trentino-Alto Adige: Dolomiti di Gardena/Grödner Dolomiten	11.768 E	46.601 N	2290
A1_DD	RT (790 m)	alpine	1	Italy: Trentino-Alto Adige: Dolomiti di Gardena/Grödner Dolomiten	11.768 E	46.601 N	2290
A1_DE	RT (790 m)	alpine	1	Italy: Trentino-Alto Adige: Dolomiti di Gardena/Grödner Dolomiten	11.768 E	46.601 N	2290
A1_DF	RT (790 m)	alpine	1	Italy: Trentino-Alto Adige: Dolomiti di Gardena/Grödner Dolomiten	11.768 E	46.601 N	2290
A1_UA	RT (2055 m)	alpine	1	Italy: Trentino-Alto Adige: Dolomiti di Gardena/Grödner Dolomiten	11.768 E	46.601 N	2290
A1_UB	RT (2055 m)	alpine	1	Italy: Trentino-Alto Adige: Dolomiti di Gardena/Grödner Dolomiten	11.768 E	46.601 N	2290
A1_UC	RT (2055 m)	alpine	1	Italy: Trentino-Alto Adige: Dolomiti di Gardena/Grödner Dolomiten	11.768 E	46.601 N	2290
A1_UD	RT (2055 m)	alpine	1	Italy: Trentino-Alto Adige: Dolomiti di Gardena/Grödner Dolomiten	11.768 E	46.601 N	2290
A1_UE	RT (2055 m)	alpine	1	Italy: Trentino-Alto Adige: Dolomiti di Gardena/Grödner Dolomiten	11.768 E	46.601 N	2290
A3_DB	RT (790 m)	alpine	3	Austria: Kärnten: Lienzer Dolomiten	12.877 E	46.762 N	2055
A3_DC	RT (790 m)	alpine	3	Austria: Kärnten: Lienzer Dolomiten	12.877 E	46.762 N	2055
A3_DD	RT (790 m)	alpine	3	Austria: Kärnten: Lienzer Dolomiten	12.877 E	46.762 N	2055
A3_DG	RT (790 m)	alpine	3	Austria: Kärnten: Lienzer Dolomiten	12.877 E	46.762 N	2055
A3_DJ	RT (790 m)	alpine	3	Austria: Kärnten: Lienzer Dolomiten	12.877 E	46.762 N	2055

Table S1. ...continued.

A3_UA	RT (2055 m)	alpine	3	Austria: Kärnten: Lienzer Dolomiten	12.877 E	46.762 N	2055
A3_UB	RT (2055 m)	alpine	3	Austria: Kärnten: Lienzer Dolomiten	12.877 E	46.762 N	2055
A3_UC	RT (2055 m)	alpine	3	Austria: Kärnten: Lienzer Dolomiten	12.877 E	46.762 N	2055
A3_UD	RT (2055 m)	alpine	3	Austria: Kärnten: Lienzer Dolomiten	12.877 E	46.762 N	2055
A3_UF	RT (2055 m)	alpine	3	Austria: Kärnten: Lienzer Dolomiten	12.877 E	46.762 N	2055
M1_DA	RT (790 m)	montane	1	Italy: Trentino-Alto Adige: Dolomiti di Gardena/Grödner Dolomiten	11.77 E	46.564 N	1690
M1_DB	RT (790 m)	montane	1	Italy: Trentino-Alto Adige: Dolomiti di Gardena/Grödner Dolomiten	11.77 E	46.564 N	1690
M1_DC	RT (790 m)	montane	1	Italy: Trentino-Alto Adige: Dolomiti di Gardena/Grödner Dolomiten	11.77 E	46.564 N	1690
M1_DE	RT (790 m)	montane	1	Italy: Trentino-Alto Adige: Dolomiti di Gardena/Grödner Dolomiten	11.77 E	46.564 N	1690
M1_DF	RT (790 m)	montane	1	Italy: Trentino-Alto Adige: Dolomiti di Gardena/Grödner Dolomiten	11.77 E	46.564 N	1690
M1_UA	RT (2055 m)	montane	1	Italy: Trentino-Alto Adige: Dolomiti di Gardena/Grödner Dolomiten	11.77 E	46.564 N	1690
M1_UB	RT (2055 m)	montane	1	Italy: Trentino-Alto Adige: Dolomiti di Gardena/Grödner Dolomiten	11.77 E	46.564 N	1690
M1_UC	RT (2055 m)	montane	1	Italy: Trentino-Alto Adige: Dolomiti di Gardena/Grödner Dolomiten	11.77 E	46.564 N	1690
M1_UE	RT (2055 m)	montane	1	Italy: Trentino-Alto Adige: Dolomiti di Gardena/Grödner Dolomiten	11.77 E	46.564 N	1690
M1_UF	RT (2055 m)	montane	1	Italy: Trentino-Alto Adige: Dolomiti di Gardena/Grödner Dolomiten	11.77 E	46.564 N	1690
M3_DA	RT (790 m)	montane	3	Austria: Kärnten: Lienzer Dolomiten	12.901 E	46.774 N	790
M3_DB	RT (790 m)	montane	3	Austria: Kärnten: Lienzer Dolomiten	12.901 E	46.774 N	790
M3_DC	RT (790 m)	montane	3	Austria: Kärnten: Lienzer Dolomiten	12.901 E	46.774 N	790
M3_DE	RT (790 m)	montane	3	Austria: Kärnten: Lienzer Dolomiten	12.901 E	46.774 N	790
M3_DF	RT (790 m)	montane	3	Austria: Kärnten: Lienzer Dolomiten	12.901 E	46.774 N	790

Table S1. ...continued.

M3_UA	RT (2055 m)	montane	3	Austria: Kärnten: Lienzer Dolomiten	12.901 E	46.774 N	790
M3_UB	RT (2055 m)	montane	3	Austria: Kärnten: Lienzer Dolomiten	12.901 E	46.774 N	790

Table S2. Enriched GO terms (adjusted $p < 0.05$) in DTGs detected in CG settings in different ecotype pairs (i.e. 1,3,4, and 5).

Ecotype pair	**GO category**	**GO ID**	**GO term**	**DTGs number**	**adjusted p**	**z-score**
1	BP	GO:0070417	cellular response to cold	24	4,13E-03	11,38
1	BP	GO:0009793	embryo development ending in seed dormanancy	221	1,88E-02	19,52
4	BP	GO:0010220	positive regulation of vernalization response	5	3,60E-04	5,50
1	BP	GO:0090333	regulation of stomatal closure	49	1,00E-04	3,76
1	BP	GO:0015700	arsenite transport	10	1,20E-04	9,17
1	BP	GO:0006826	iron ion transport	23	1,52E-03	-0,90
1	BP	GO:0030026	cellular manganese ion homeostasis	9	2,02E-03	-5,04
1	BP	GO:0015690	aluminum cation transport	4	3,79E-03	10,16
1	BP	GO:0055070	copper ion homeostasis	9	5,36E-03	4,12
1	BP	GO:0080170	hydrogen peroxide transmembrane transport	11	9,35E-03	3,62
1	BP	GO:0070574	cadmium ion transmembrane transport	6	9,59E-03	-6,08
1	BP	GO:0034765	regulation of ion transmembrane transport	22	1,19E-02	2,81
1	BP	GO:0071421	manganese ion transmembrane transport	10	1,31E-02	-9,79
1	BP	GO:1990573	potassium ion import across plasma membrane	19	1,32E-02	0,20
1	BP	GO:0006972	hyperosmotic response	39	1,32E-02	8,06
1	BP	GO:0071472	cellular response to salt stress	25	1,67E-02	1,08
1	BP	GO:0007231	osmosensory signaling pathway	13	2,02E-02	-0,25
1	BP	GO:0008272	sulfate transport	12	2,73E-02	2,13

Table S2. ...continued.

1	BP	GO:0071475	cellular hyperosmotic salinity response	6	3,31E-02	-1,86
3	BP	GO:0032594	protein transport within lipid bilayer	2	1,88E-03	-0,94
3	BP	GO:1901140	p-coumaryl alcohol transport	4	4,22E-03	11,42
3	BP	GO:0006820	anion transport	33	7,80E-03	5,56
3	BP	GO:1905177	tracheary element differentiation	5	1,61E-02	1,80
3	BP	GO:0015692	lead ion transport	4	1,62E-02	11,42
3	BP	GO:0030026	cellular manganese ion homeostasis	3	2,07E-02	7,76
3	BP	GO:0042631	cellular response to water deprivation	9	2,08E-02	9,36
3	BP	GO:0010496	intercellular transport	5	2,47E-02	11,50
3	BP	GO:0070072	vacuolar proton-transporting V-type ATPa...	2	2,51E-02	1,80
3	BP	GO:0098739	import across plasma membrane	9	2,78E-02	13,01
3	BP	GO:0015871	choline transport	1	4,34E-02	2,89
3	BP	GO:0080168	abscisic acid transport	4	3,53E-02	11,42
4	BP	GO:1905177	tracheary element differentiation	18	7,40E-04	1,68
4	BP	GO:0006892	post-Golgi vesicle-mediated transport	17	3,47E-03	10,87
4	BP	GO:1902476	chloride transmembrane transport	5	5,20E-03	1,62
4	BP	GO:0070778	L-aspartate transmembrane transport	4	7,35E-03	2,19
4	BP	GO:0015808	L-alanine transport	9	7,80E-03	1,18
4	BP	GO:0033214	siderophore-dependent iron import into cell	7	8,01E-03	4,51
4	BP	GO:0010222	stem vascular tissue pattern formation	8	8,11E-03	3,10
4	BP	GO:0030026	cellular manganese ion homeostasis	7	1,32E-02	2,69
4	BP	GO:0070588	calcium ion transmembrane transport	18	1,70E-02	3,34
4	BP	GO:0015839	cadaverine transport	4	1,85E-02	-8,22
4	BP	GO:0010496	intercellular transport	17	2,70E-02	3,74
4	BP	GO:0010268	brassinosteroid homeostasis	7	3,01E-02	-1,63
4	BP	GO:0055078	sodium ion homeostasis	10	3,14E-02	-3,29

Table S2. ...continued.

4	BP	GO:1904278	positive regulation of wax biosynthetic ...	6	3,35E-02	9,51
4	BP	GO:0016197	endosomal transport	17	3,36E-02	6,24
4	BP	GO:0050801	ion homeostasis	109	3,54E-02	6,05
4	BP	GO:2000122	negative regulation of stomatal complex development	5	3,61E-02	3,09
5	BP	GO:0042938	dipeptide transport	4	7,70E-03	2,55
5	BP	GO:0015871	choline transport	1	1,05E-02	5,29
5	BP	GO:0090160	Golgi to lysosome transport	1	1,05E-02	-1,81
5	BP	GO:0030007	cellular potassium ion homeostasis	2	3,71E-02	8,40
5	BP	GO:1901527	abscisic acid-activated signaling pathway involved in stomatal movement	2	3,95E-02	8,40
1	BP	GO:0046685	response to arsenic-containing substance	12	5,80E-04	7,39
1	BP	GO:0010167	response to nitrate	25	3,17E-03	6,97
1	BP	GO:0009751	response to salicylic acid	112	4,31E-03	5,83
1	BP	GO:0042221	response to chemical	1248	4,63E-03	39,26
1	BP	GO:0010042	response to manganese ion	10	1,36E-02	-9,66
1	BP	GO:0009787	regulation of abscisic acid-activated signaling pathway	83	1,66E-02	7,35
1	BP	GO:2000022	regulation of jasmonic acid mediated signaling pathway	22	1,82E-02	7,88
1	BP	GO:0010104	regulation of ethylene-activated signaling pathway	14	1,89E-02	7,54
1	BP	GO:1901672	positive regulation of systemic acquired resistance	6	1,90E-02	2,53
1	BP	GO:0009611	response to wounding	148	2,07E-02	9,31
1	BP	GO:0009753	response to jasmonic acid	119	2,13E-02	11,60
1	BP	GO:0009617	response to bacterium	311	2,44E-02	22,69
1	BP	GO:0009727	detection of ethylene stimulus	8	2,59E-02	2,88
1	BP	GO:0080151	positive regulation of salicylic acid mediated signaling pathway	5	2,64E-02	6,85
1	BP	GO:0012501	programmed cell death	88	3,40E-02	10,30

Table S2. ...continued.

1	BP	GO:0010597	green leaf volatile biosynthetic process	14	3,41E-02	-3,21
1	BP	GO:0050829	defense response to Gram-negative bacterium	17	2,33E-02	10,29
3	BP	GO:0009751	response to salicylic acid	24	2,59E-03	6,43
3	BP	GO:0009753	response to jasmonic acid	25	9,68E-03	8,44
3	BP	GO:0009610	response to symbiotic fungus	5	1,32E-02	2,71
3	BP	GO:1902290	positive regulation of defense response to oomycetes	3	1,34E-02	-8,95
3	BP	GO:0009694	jasmonic acid metabolic process	11	1,35E-02	-8,61
3	BP	GO:0009695	jasmonic acid biosynthetic process	7	1,36E-02	-7,56
3	BP	GO:0012501	programmed cell death	21	1,66E-02	9,49
3	BP	GO:0009620	response to fungus	42	1,68E-02	4,28
3	BP	GO:0000304	response to singlet oxygen	4	2,16E-02	4,93
3	BP	GO:0006952	defense response	105	2,32E-02	13,12
3	BP	GO:0009617	response to bacterium	53	2,81E-02	7,53
3	BP	GO:0034059	response to anoxia	3	3,52E-02	3,54
3	BP	GO:1900366	negative regulation of defense response to insect	3	4,09E-02	4,83
3	BP	GO:1990451	cellular stress response to acidic pH	1	4,34E-02	4,45
3	BP	GO:1902347	response to strigolactone	2	4,43E-02	2,64
4	BP	GO:0009627	systemic acquired resistance	41	3,82E-03	5,20
4	BP	GO:0009694	jasmonic acid metabolic process	25	4,82E-03	-1,16
4	BP	GO:0050777	negative regulation of immune response	19	4,87E-03	-1,68
4	BP	GO:1900366	negative regulation of defense response to insect	9	5,01E-03	4,69
4	BP	GO:0009624	response to nematode	33	5,34E-03	-2,90
4	BP	GO:0043069	negative regulation of programmed cell death	17	1,30E-02	5,31

Table S2. ...continued.

4	BP	GO:2001020	regulation of response to DNA damage stimulus	9	1,32E-02	1,23
4	BP	GO:1990110	callus formation	17	1,46E-02	3,83
4	BP	GO:1900425	negative regulation of defense response to bacterium	15	1,60E-02	-3,83
4	BP	GO:1902289	negative regulation of defense response to oomycetes	4	1,85E-02	2,41
4	BP	GO:0009611	response to wounding	124	2,70E-02	14,69
4	BP	GO:0080027	response to herbivore	11	3,01E-02	4,26
4	BP	GO:0009617	response to bacterium	248	3,10E-02	10,72
4	BP	GO:0016104	triterpenoid biosynthetic process	4	3,62E-02	3,53
4	BP	GO:0043562	cellular response to nitrogen levels	21	3,64E-02	3,47
4	BP	GO:0010508	positive regulation of autophagy	12	3,82E-02	2,78
5	BP	GO:0002218	activation of innate immune response	7	1,00E-03	14,89
5	BP	GO:0010350	cellular response to magnesium starvation	1	1,05E-02	3,62
5	BP	GO:0071280	cellular response to copper ion	1	1,05E-02	3,62
5	BP	GO:0071286	cellular response to magnesium ion	1	1,05E-02	3,62
5	BP	GO:0072709	cellular response to sorbitol	1	1,05E-02	3,62
5	BP	GO:0050778	positive regulation of immune response	9	2,01E-02	11,43
5	BP	GO:0009864	induced systemic resistance, jasmonic acid mediated signaling pathway	2	2,41E-02	5,97
5	BP	GO:1900367	positive regulation of defense response to insect	2	2,82E-02	6,83
5	BP	GO:0098869	cellular oxidant detoxification	4	3,05E-02	8,33
5	BP	GO:1905036	positive regulation of antifungal innate immune response	1	3,12E-02	4,51
5	BP	GO:0002833	positive regulation of response to biotic stimulus	5	4,06E-02	5,31

Table S2. ...continued.

5	BP	GO:2000786	positive regulation of autophagosome assembly	1	4,14E-02	7,25
5	BP	GO:0071325	cellular response to mannitol stimulus	1	1,05E-02	3,62
1	BP	GO:0010214	seed coat development	53	2,85E-02	3,59
1	BP	GO:0048825	cotyledon development	48	2,91E-02	9,62
3	BP	GO:0061387	regulation of extent of cell growth	2	1,07E-02	4,95
3	BP	GO:0010187	negative regulation of seed germination	6	1,55E-02	-3,53
3	BP	GO:1990110	callus formation	6	1,87E-02	0,51
3	BP	GO:0009828	plant-type cell wall loosening	6	2,05E-02	5,99
3	BP	GO:0009901	anther dehiscence	5	2,33E-02	1,62
3	BP	GO:0080086	stamen filament development	4	2,46E-02	3,33
3	BP	GO:0010102	lateral root morphogenesis	16	2,73E-02	4,65
3	BP	GO:0010227	floral organ abscission	6	3,42E-02	0,15
3	BP	GO:0048497	maintenance of floral organ identity	3	3,52E-02	8,73
3	BP	GO:0090470	shoot organ boundary specification	1	4,34E-02	3,16
3	BP	GO:2000114	regulation of establishment of cell polarity	4	4,84E-02	1,31
3	BP	GO:0071555	cell wall organization	32	4,96E-02	4,68
4	BP	GO:0007164	establishment of tissue polarity	9	1,40E-03	5,78
4	BP	GO:0009828	plant-type cell wall loosening	19	3,28E-03	5,24
4	BP	GO:0010077	maintenance of inflorescence meristem id...	9	5,01E-03	4,61
4	BP	GO:0048438	floral whorl development	102	7,22E-03	10,48
4	BP	GO:0009911	positive regulation of flower developmen...	29	8,26E-03	4,12
4	BP	GO:0060560	developmental growth involved in morphog...	160	8,65E-03	9,89
4	BP	GO:0080086	stamen filament development	11	9,45E-03	8,68
4	BP	GO:0009827	plant-type cell wall modification	50	1,70E-02	5,59

Table S2. ...continued.

4	BP	GO:0010311	lateral root formation	45	1,94E-02	9,83
4	BP	GO:0042659	regulation of cell fate specification	6	2,16E-02	-1,30
4	BP	GO:0009832	plant-type cell wall biogenesis	72	2,85E-02	4,80
4	BP	GO:0051639	actin filament network formation	3	2,91E-02	1,93
4	BP	GO:0061387	regulation of extent of cell growth	3	2,91E-02	6,96
4	BP	GO:0048833	specification of floral organ number	4	3,62E-02	3,29
4	BP	GO:0010076	maintenance of floral meristem identity	4	3,62E-02	2,49
4	BP	GO:0080172	petal epidermis patterning	4	3,62E-02	6,59
5	BP	GO:0051510	regulation of unidimensional cell growth	5	3,86E-02	0,72
1	BP	GO:0033617	mitochondrial respiratory chain complex ...	9	7,06E-03	0,29
1	BP	GO:1903866	palisade mesophyll development	3	1,53E-02	2,64
1	BP	GO:0009902	chloroplast relocation	15	1,89E-02	0,33
3	BP	GO:0010193	response to ozone	18	8,20E-08	5,42
3	BP	GO:0000266	mitochondrial fission	5	6,10E-04	10,05
3	BP	GO:0007623	circadian rhythm	21	2,91E-03	1,94
3	BP	GO:0042754	negative regulation of circadian rhythm	3	1,04E-02	6,27
3	BP	GO:0009853	photorespiration	8	1,48E-02	-8,59
3	BP	GO:0009638	phototropism	5	4,81E-02	2,21
4	BP	GO:0010193	response to ozone	29	9,71E-03	2,13
4	BP	GO:0046283	anthocyanin-containing compound metabolic process	30	1,67E-02	11,16
5	BP	GO:0043482	cellular pigment accumulation	1	4,14E-02	7,25
1	BP	GO:0022414	reproductive process	809	3,77E-03	35,74
1	BP	GO:0019953	sexual reproduction	74	2,67E-02	6,58
1	BP	GO:0090567	reproductive shoot system development	232	2,36E-02	21,25
3	BP	GO:0048229	gametophyte development	40	3,18E-02	11,34
4	BP	GO:0010584	pollen exine formation	18	7,51E-03	2,94

Table S2. ...continued.

5	BP	GO:0080173	male-female gamete recognition during double fertilization forming a zygote and endosperm	1	3,12E-02	5,14
1	BP	GO:0006396	RNA processing	283	4,82E-03	31,96
1	BP	GO:0006390	mitochondrial transcription	5	1,24E-02	4,02
1	BP	GO:0010468	regulation of gene expression	534	1,29E-02	35,94
1	BP	GO:0006406	mRNA export from nucleus	13	1,40E-02	1,70
1	BP	GO:0006264	mitochondrial DNA replication	3	1,53E-02	6,27
1	BP	GO:0002926	tRNA wobble base 5-methoxycarbonylmethyl...	3	1,53E-02	10,13
1	BP	GO:0018216	peptidyl-arginine methylation	5	1,53E-02	12,82
1	BP	GO:0016575	histone deacetylation	13	1,64E-02	7,64
1	BP	GO:0031936	negative regulation of chromatin silencing	8	1,65E-02	8,88
1	BP	GO:0006349	regulation of gene expression by genetic imprinting	9	1,84E-02	1,98
1	BP	GO:0010587	miRNA catabolic process	6	1,90E-02	1,76
1	BP	GO:0080009	mRNA methylation	6	1,90E-02	-0,69
1	BP	GO:0000727	double-strand break repair via break-ind...	5	2,64E-02	6,69
1	BP	GO:0072355	histone H3-T3 phosphorylation	5	2,64E-02	0,81
1	BP	GO:0045596	negative regulation of cell differentiation	14	3,30E-02	3,96
1	BP	GO:0000381	regulation of alternative mRNA splicing, via spliceosome	6	3,31E-02	-1,71
3	BP	GO:0009299	mRNA transcription	3	1,04E-02	1,45
3	BP	GO:0032968	positive regulation of transcription elongation from RNA polymerase II promoter	4	3,15E-02	-1,28
3	BP	GO:0070816	phosphorylation of RNA polymerase II C-terminal domain	4	3,94E-02	2,23
3	BP	GO:0070537	histone H2A K63-linked deubiquitination	1	4,34E-02	2,50

Table S2. ...continued.

3	BP	GO:0000379	tRNA-type intron splice site recognition and cleavage	1	4,34E-02	-3,19
3	BP	GO:0016480	negative regulation of transcription by RNA polymerase III	1	4,34E-02	1,25
3	BP	GO:0006432	phenylalanyl-tRNA aminoacylation	2	4,43E-02	-5,30
3	BP	GO:0006260	DNA replication	9	4,52E-02	9,08
4	BP	GO:1901485	positive regulation of transcription factor catabolic process	3	2,91E-02	-4,46
5	BP	GO:0071528	tRNA re-export from nucleus	1	1,05E-02	1,72
5	BP	GO:0006307	DNA dealkylation involved in DNA repair	1	2,09E-02	3,35
5	BP	GO:0035511	oxidative DNA demethylation	1	3,12E-02	3,35
5	BP	GO:0080156	mitochondrial mRNA modification	3	3,10E-02	3,64
1	BP	GO:0043170	macromolecule metabolic process	1780	2,26E-03	63,88
1	BP	GO:0044237	cellular metabolic process	2495	9,44E-03	67,58
1	BP	GO:0044238	primary metabolic process	2278	2,87E-02	68,78
1	BP	GO:0010411	xyloglucan metabolic process	18	1,08E-02	7,72
1	BP	GO:0046110	xanthine metabolic process	3	1,53E-02	-0,15
1	BP	GO:0006102	isocitrate metabolic process	6	1,90E-02	6,28
1	BP	GO:0072593	reactive oxygen species metabolic proces...	97	2,48E-02	7,35
1	BP	GO:0048359	mucilage metabolic process involved in s...	24	2,62E-02	2,74
1	BP	GO:0010310	regulation of hydrogen peroxide metaboli...	8	3,31E-02	1,82
3	BP	GO:0046110	xanthine metabolic process	2	5,48E-03	4,52
3	BP	GO:0046655	folic acid metabolic process	3	1,04E-02	-7,53
3	BP	GO:0048363	mucilage pectin metabolic process	3	2,51E-02	0,75
3	BP	GO:0005976	polysaccharide metabolic process	29	4,32E-02	3,80

Table S2. ...continued.

4	BP	GO:0006000	fructose metabolic process	10	4,85E-03	4,41
4	BP	GO:0015936	coenzyme A metabolic process	5	8,60E-03	2,32
4	BP	GO:0032268	regulation of cellular protein metabolic...	88	1,18E-02	0,14
4	BP	GO:0019222	regulation of metabolic process	649	1,39E-02	19,42
4	BP	GO:0048363	mucilage pectin metabolic process	6	1,85E-02	-0,86
4	BP	GO:0048359	mucilage metabolic process involved in s...	16	3,26E-02	5,97
5	BP	GO:0046110	xanthine metabolic process	1	3,12E-02	3,55
5	BP	GO:0006541	glutamine metabolic process	2	4,69E-02	5,67
1	BP	GO:0006624	vacuolar protein processing	7	1,27E-03	6,94
1	BP	GO:0048511	rhythmic process	64	1,32E-03	13,99
1	BP	GO:0006145	purine nucleobase catabolic process	7	3,34E-03	1,91
1	BP	GO:0007186	G protein-coupled receptor signaling pat...	10	3,34E-03	4,16
1	BP	GO:0010264	myo-inositol hexakisphosphate biosynthet...	8	5,36E-03	0,38
1	BP	GO:0009686	gibberellin biosynthetic process	13	6,75E-03	4,92
1	BP	GO:0006635	fatty acid beta-oxidation	25	1,06E-02	2,18
1	BP	GO:0097577	sequestering of iron ion	9	1,24E-02	-9,05
1	BP	GO:0051131	chaperone-mediated protein complex assem...	5	1,24E-02	10,21
1	BP	GO:1902000	homogentisate catabolic process	5	1,24E-02	8,82
1	BP	GO:0009657	plastid organization	133	1,35E-02	20,76
1	BP	GO:0034052	positive regulation of plant-type hypers...	7	1,36E-02	2,99
1	BP	GO:0009959	negative gravitropism	11	1,40E-02	4,35
1	BP	GO:0042908	xenobiotic transport	17	1,40E-02	10,38
1	BP	GO:0042761	very long-chain fatty acid biosynthetic ...	12	1,45E-02	4,00
1	BP	GO:0009294	DNA mediated transformation	32	1,47E-02	5,65

Table S2. ...continued.

1	BP	GO:2001295	malonyl-CoA biosynthetic process	4	1,52E-02	-6,11
1	BP	GO:0002103	endonucleolytic cleavage of tetracistron...	4	1,52E-02	6,05
1	BP	GO:0042554	superoxide anion generation	4	1,53E-02	-1,25
1	BP	GO:0006422	aspartyl-tRNA aminoacylation	3	1,53E-02	7,71
1	BP	GO:0006750	glutathione biosynthetic process	3	1,53E-02	7,82
1	BP	GO:0006623	protein targeting to vacuole	20	1,68E-02	10,79
1	BP	GO:0010581	regulation of starch biosynthetic proces...	6	1,90E-02	4,88
1	BP	GO:0071244	cellular response to carbon dioxide	15	1,94E-02	7,93
1	BP	GO:0010182	sugar mediated signaling pathway	27	2,01E-02	5,64
1	BP	GO:0080175	phragmoplast microtubule organization	8	2,64E-02	12,45
1	BP	GO:0006267	pre-replicative complex assembly involve...	5	2,64E-02	6,69
1	BP	GO:0006694	steroid biosynthetic process	21	2,65E-02	5,86
1	BP	GO:0035825	homologous recombination	20	2,66E-02	1,28
1	BP	GO:0045492	xylan biosynthetic process	17	2,71E-02	7,20
1	BP	GO:0009660	amyloplast organization	6	3,31E-02	1,59
1	BP	GO:0071732	cellular response to nitric oxide	6	3,31E-02	-1,94
3	BP	GO:0006564	L-serine biosynthetic process	3	1,48E-03	4,50
3	BP	GO:0070179	D-serine biosynthetic process	3	1,48E-03	4,50
3	BP	GO:0034440	lipid oxidation	7	1,84E-03	3,13
3	BP	GO:0031408	oxylipin biosynthetic process	6	2,26E-03	-0,68
3	BP	GO:0051260	protein homooligomerization	7	2,64E-03	0,31
3	BP	GO:0006565	L-serine catabolic process	3	3,87E-03	-7,53
3	BP	GO:0097054	L-glutamate biosynthetic process	2	5,48E-03	-0,31
3	BP	GO:1901259	chloroplast rRNA processing	6	5,52E-03	-0,46

Table S2. ...continued.

3	BP	GO:0019264	glycine biosynthetic process from serine	3	5,62E-03	-7,53
3	BP	GO:0035999	tetrahydrofolate interconversion	4	9,79E-03	-7,37
3	BP	GO:0007064	mitotic sister chromatid cohesion	4	1,62E-02	8,52
3	BP	GO:0016559	peroxisome fission	3	1,68E-02	7,14
3	BP	GO:0006110	regulation of glycolytic process	2	1,73E-02	0,62
3	BP	GO:0042554	superoxide anion generation	2	1,73E-02	4,52
3	BP	GO:0006516	glycoprotein catabolic process	2	1,73E-02	-5,54
3	BP	GO:0006542	glutamine biosynthetic process	2	1,73E-02	0,52
3	BP	GO:2001295	malonyl-CoA biosynthetic process	2	1,73E-02	-9,11
3	BP	GO:0006890	retrograde vesicle-mediated transport, G...	6	2,05E-02	5,22
3	BP	GO:1901959	positive regulation of cutin biosyntheti...	2	2,51E-02	0,62
3	BP	GO:0019676	ammonia assimilation cycle	2	2,51E-02	-0,31
3	BP	GO:0045038	protein import into chloroplast thylakoi...	2	2,51E-02	-0,94
3	BP	GO:0010037	response to carbon dioxide	4	2,52E-02	-1,47
3	BP	GO:0072755	cellular response to benomyl	1	4,34E-02	4,45
3	BP	GO:0010352	lithium ion export across the plasma mem...	1	4,34E-02	8,21
3	BP	GO:0051262	protein tetramerization	5	2,97E-02	-4,44
3	BP	GO:0042372	phylloquinone biosynthetic process	3	2,99E-02	-0,10
3	BP	GO:0010417	glucuronoxylan biosynthetic process	3	2,99E-02	2,53
3	BP	GO:0010047	fruit dehiscence	5	3,13E-02	-0,89
3	BP	GO:0000737	DNA catabolic process, endonucleolytic	1	4,34E-02	7,22
3	BP	GO:0036258	multivesicular body assembly	1	4,34E-02	2,93
3	BP	GO:1901141	regulation of lignin biosynthetic proces...	7	4,39E-02	6,60
3	BP	GO:0034497	protein localization to phagophore assem...	2	4,43E-02	-0,17

Table S2. ...continued.

3	BP	GO:0032790	ribosome disassembly	2	4,43E-02	5,05
3	BP	GO:0042147	retrograde transport, endosome to Golgi	3	4,70E-02	4,11
3	BP	GO:0006809	nitric oxide biosynthetic process	3	4,70E-02	3,03
4	BP	GO:0010182	sugar mediated signaling pathway	26	6,70E-04	1,91
4	BP	GO:0009969	xyloglucan biosynthetic process	10	1,10E-03	4,46
4	BP	GO:0070301	cellular response to hydrogen peroxide	15	3,82E-03	2,61
4	BP	GO:1901601	strigolactone biosynthetic process	7	4,48E-03	6,04
4	BP	GO:0006110	regulation of glycolytic process	4	7,35E-03	5,97
4	BP	GO:0007229	integrin-mediated signaling pathway	4	7,35E-03	2,72
4	BP	GO:0035653	cargo loading into clathrin-coated vesic...	4	7,35E-03	-2,53
4	BP	GO:0009838	abscission	14	8,59E-03	3,83
4	BP	GO:0046835	carbohydrate phosphorylation	15	9,94E-03	3,53
4	BP	GO:0009744	response to sucrose	39	1,26E-02	7,27
4	BP	GO:0009251	glucan catabolic process	14	1,31E-02	2,77
4	BP	GO:0010345	suberin biosynthetic process	16	1,37E-02	3,82
4	BP	GO:0007030	Golgi organization	17	1,80E-02	3,65
4	BP	GO:0016106	sesquiterpenoid biosynthetic process	20	1,84E-02	5,65
4	BP	GO:0080171	lytic vacuole organization	5	1,85E-02	3,93
4	BP	GO:0019285	glycine betaine biosynthetic process fro...	4	1,85E-02	2,41
4	BP	GO:1901959	positive regulation of cutin biosyntheti...	4	1,85E-02	5,97
4	BP	GO:0045176	apical protein localization	4	1,85E-02	0,62
4	BP	GO:0046166	glyceraldehyde-3-phosphate biosynthetic ...	4	1,85E-02	7,34
4	BP	GO:0090449	phloem glucosinolate loading	4	1,85E-02	2,30
4	BP	GO:0061062	regulation of nematode larval developmen...	7	2,05E-02	-4,69

Table S2. ...continued.

4	BP	GO:0034614	cellular response to reactive oxygen spe...	28	2,14E-02	0,25
4	BP	GO:0080167	response to karrikin	85	2,20E-02	11,50
4	BP	GO:0046294	formaldehyde catabolic process	11	2,32E-02	-0,37
4	BP	GO:0000162	tryptophan biosynthetic process	9	2,33E-02	5,88
4	BP	GO:0010089	xylem development	35	2,34E-02	0,57
4	BP	GO:0016311	dephosphorylation	74	2,63E-02	2,13
4	BP	GO:0006659	phosphatidylserine biosynthetic process	3	2,91E-02	-0,11
4	BP	GO:0034058	endosomal vesicle fusion	3	2,91E-02	-1,15
4	BP	GO:0010581	regulation of starch biosynthetic proces...	5	3,61E-02	3,11
4	BP	GO:1904821	chloroplast disassembly	5	3,61E-02	-0,19
4	BP	GO:1900039	positive regulation of cellular response...	6	3,35E-02	1,34
4	BP	GO:0010321	regulation of vegetative phase change	6	3,35E-02	3,86
4	BP	GO:0019432	triglyceride biosynthetic process	12	3,24E-02	3,70
4	BP	GO:0045723	positive regulation of fatty acid biosyn...	5	3,61E-02	4,75
4	BP	GO:0045053	protein retention in Golgi apparatus	4	3,62E-02	9,06
4	BP	GO:0018026	peptidyl-lysine monomethylation	4	3,62E-02	2,39
4	BP	GO:0006633	fatty acid biosynthetic process	56	3,64E-02	8,36
4	BP	GO:0000280	nuclear division	52	3,66E-02	7,81
4	BP	GO:0009958	positive gravitropism	22	3,77E-02	9,01
5	BP	GO:0046512	sphingosine biosynthetic process	2	3,00E-03	0,58
5	BP	GO:0031115	negative regulation of microtubule polymerization	1	1,05E-02	3,62
5	BP	GO:0031117	positive regulation of microtubule depol...	1	1,05E-02	3,62
5	BP	GO:1902440	protein localization to mitotic spindle ...	1	1,05E-02	5,09
5	BP	GO:0009051	pentose-phosphate shunt, oxidative branch	2	1,06E-02	5,95
5	BP	GO:0030245	cellulose catabolic process	2	1,35E-02	2,95
5	BP	GO:1901181	negative regulation of cellular response to caffeine	1	4,14E-02	2,61

Table S2. ...continued.

5	BP	GO:0006218	uridine catabolic process	1	4,14E-02	7,96
5	BP	GO:0006499	N-terminal protein myristoylation	1	3,12E-02	3,62
5	BP	GO:0046177	D-gluconate catabolic process	1	3,12E-02	5,14
5	BP	GO:0019427	acetyl-CoA biosynthetic process from ace...	1	2,09E-02	4,90
5	BP	GO:0016121	carotene catabolic process	1	2,09E-02	2,70
5	BP	GO:0051484	isopentenyl diphosphate biosynthetic pro...	1	2,09E-02	-4,29
5	BP	GO:0000769	syncytium formation by mitosis without c...	1	2,09E-02	-6,71
5	BP	GO:0050665	hydrogen peroxide biosynthetic process	2	2,21E-02	6,58
5	BP	GO:0010497	plasmodesmata-mediated intercellular tra...	2	4,19E-02	7,87
5	BP	GO:0042744	hydrogen peroxide catabolic process	3	4,31E-02	7,94

Table S3. Enriched GO terms (adjusted $p < 0.05$) in DTGs detected in RT settings in the ecotype pairs 1 and 3.

Ecotype pair	**Growing site**	**GO category**	**GO ID**	**GO term**	**DTGs number**	**adjusted p**	**z-score**
1	dw	BP	GO:0009409	response to cold	113	8,42E-03	7,91
3	dw	BP	GO:0009409	response to cold	93	1,44E-02	0,09
1	dw	BP	GO:0015690	aluminum cation transport	4	1,90E-04	8,01
1	dw	BP	GO:0009651	response to salt stress	141	1,76E-03	0,78
1	dw	BP	GO:0090333	regulation of stomatal closure	25	3,10E-03	1,14
1	dw	BP	GO:0035445	borate transmembrane transport	5	3,29E-03	4,23
1	dw	BP	GO:0006820	anion transport	84	3,90E-03	-0,10
1	dw	BP	GO:0009269	response to desiccation	9	1,13E-02	2,54
1	dw	BP	GO:0070588	calcium ion transmembrane transport	12	1,28E-02	1,58
1	dw	BP	GO:0006863	purine nucleobase transport	4	1,33E-02	0,02
1	dw	BP	GO:0055085	transmembrane transport	188	1,33E-02	-1,58

Table S3. ...continued.

1	dw	BP	GO:0070574	cadmium ion transmembrane transport	4	1,44E-02	-3,79
1	dw	BP	GO:0042128	nitrate assimilation	13	1,48E-02	-0,50
1	dw	BP	GO:0009414	response to water deprivation	127	1,91E-02	1,35
1	dw	BP	GO:0071421	manganese ion transmembrane transport	6	2,30E-02	-2,90
1	dw	BP	GO:0071249	cellular response to nitrate	6	2,30E-02	1,97
1	dw	BP	GO:0055070	copper ion homeostasis	6	2,30E-02	-1,03
1	up	BP	GO:0015690	aluminum cation transport	4	1,50E-05	7,50
1	up	BP	GO:1990069	stomatal opening	8	4,31E-02	4,21
1	up	BP	GO:0090333	regulation of stomatal closure	15	8,35E-03	5,03
1	up	BP	GO:0015700	arsenite transport	3	4,34E-02	5,52
3	dw	BP	GO:0015706	nitrate transport	16	2,04E-03	5,81
3	dw	BP	GO:0009414	response to water deprivation	108	8,84E-03	0,78
3	dw	BP	GO:0042631	cellular response to water deprivation	17	9,24E-03	-3,80
3	dw	BP	GO:0010166	wax metabolic process	16	2,40E-02	0,73
3	dw	BP	GO:0015914	phospholipid transport	7	4,10E-02	-2,67
3	dw	BP	GO:0010025	wax biosynthetic process	13	4,79E-02	0,04
3	up	BP	GO:0071705	nitrogen compound transport	153	1,30E-03	30,36
3	up	BP	GO:1902476	chloride transmembrane transport	4	3,79E-03	7,83
3	up	BP	GO:1904278	positive regulation of wax biosynthetic ...	5	9,39E-03	3,97
3	up	BP	GO:0006885	regulation of pH	8	1,19E-02	8,58
3	up	BP	GO:1902600	proton transmembrane transport	19	3,10E-02	14,52
3	up	BP	GO:0034220	ion transmembrane transport	79	4,55E-02	20,94
3	up	BP	GO:0006813	potassium ion transport	25	4,77E-02	10,38
1	dw	BP	GO:0016973	poly(A)+ mRNA export from nucleus	6	6,90E-04	-0,64
1	dw	BP	GO:0000956	nuclear-transcribed mRNA catabolic process	21	2,27E-03	2,79
1	dw	BP	GO:0006367	transcription initiation from RNA polyme...	10	5,73E-03	-0,36

Table S3. ...continued.

1	dw	BP	GO:1904281	positive regulation of transcription by RNA polymerase V	2	1,37E-02	-3,41
1	dw	BP	GO:0006307	DNA dealkylation involved in DNA repair	2	1,37E-02	2,08
1	dw	BP	GO:0006435	threonyl-tRNA aminoacylation	2	1,37E-02	0,40
1	dw	BP	GO:1990280	RNA localization to chromatin	2	1,37E-02	-3,41
1	dw	BP	GO:1902466	positive regulation of histone H3-K27 trimethylation	2	1,37E-02	-3,41
1	up	BP	GO:0060148	positive regulation of posttranscriptional gene silencing	5	2,14E-02	3,31
1	up	BP	GO:0010032	meiotic chromosome condensation	2	2,15E-02	-6,03
1	up	BP	GO:0051754	meiotic sister chromatid cohesion, centr...	2	2,15E-02	-6,14
1	up	BP	GO:0009294	DNA mediated transformation	11	2,42E-02	-2,41
1	up	BP	GO:0016441	posttranscriptional gene silencing	16	3,46E-02	0,35
1	up	BP	GO:0010608	posttranscriptional regulation of gene e...	28	4,89E-02	-0,68
1	up	BP	GO:0070734	histone H3-K27 methylation	5	4,94E-02	-0,49
3	dw	BP	GO:0070918	primary sncRNA processing	14	1,17E-03	-4,12
3	dw	BP	GO:0033169	histone H3-K9 demethylation	5	3,93E-03	-4,25
3	dw	BP	GO:0016246	RNA interference	7	8,09E-03	-0,06
3	dw	BP	GO:0006432	phenylalanyl-tRNA aminoacylation	3	3,60E-02	-0,81
3	dw	BP	GO:0006303	double-strand break repair via nonhomolo...	5	3,98E-02	1,72
3	up	BP	GO:0006336	DNA replication-independent nucleosome a...	2	3,32E-02	4,77
3	up	BP	GO:0035279	mRNA cleavage involved in gene silencing...	2	3,32E-02	4,59
3	up	BP	GO:0044728	DNA methylation or demethylation	17	1,20E-02	11,95
3	up	BP	GO:0031936	negative regulation of chromatin silencing	5	1,82E-02	7,65

Table S3. ...continued.

3	up	BP	GO:0010608	posttranscriptional regulation of gene expression	52	1,98E-02	21,04
1	dw	BP	GO:0031347	regulation of defense response	79	2,42E-03	1,32
1	dw	BP	GO:0009737	response to abscisic acid	185	6,00E-03	0,58
1	dw	BP	GO:0009727	detection of ethylene stimulus	6	7,15E-03	-1,52
1	dw	BP	GO:0002239	response to oomycetes	30	9,02E-03	4,26
1	dw	BP	GO:0051365	cellular response to potassium ion starv...	9	1,13E-02	0,27
1	dw	BP	GO:0002831	regulation of response to biotic stimulus	43	1,32E-02	-0,19
1	dw	BP	GO:0050776	regulation of immune response	37	1,35E-02	2,03
1	dw	BP	GO:0046685	response to arsenic-containing substance	11	4,10E-06	2,12
1	dw	BP	GO:0015700	arsenite transport	8	2,60E-05	3,48
1	dw	BP	GO:0009611	response to wounding	85	1,10E-04	0,38
1	dw	BP	GO:1900425	negative regulation of defense response ...	10	2,04E-02	-0,70
1	dw	BP	GO:0043562	cellular response to nitrogen levels	14	2,29E-02	-1,59
1	dw	BP	GO:0080029	cellular response to boron-containing su...	7	2,30E-02	2,78
1	dw	BP	GO:1902289	negative regulation of defense response ...	3	2,43E-02	1,16
1	dw	BP	GO:0032101	regulation of response to external stimu...	43	2,85E-02	-0,19
1	dw	BP	GO:0050777	negative regulation of immune response	9	2,93E-02	2,82
1	up	BP	GO:0080029	cellular response to boron-containing su...	6	1,83E-03	-0,48
1	up	BP	GO:0009695	jasmonic acid biosynthetic process	10	3,30E-03	-2,10
1	up	BP	GO:0009620	response to fungus	57	1,62E-02	1,76
1	up	BP	GO:0051410	detoxification of nitrogen compound	2	2,15E-02	-4,93
1	up	BP	GO:2000022	regulation of jasmonic acid mediated sig...	8	2,69E-02	-1,50
1	up	BP	GO:0009611	response to wounding	43	2,71E-02	1,51
1	up	BP	GO:0031349	positive regulation of defense response	18	2,74E-02	3,10

Table S3. ...continued.

1	up	BP	GO:0043066	negative regulation of apoptotic process	3	2,75E-02	1,99
1	up	BP	GO:2000071	regulation of defense response by callos...	4	2,76E-02	7,40
1	up	BP	GO:0034052	positive regulation of plant-type hypers...	3	3,49E-02	-2,25
1	up	BP	GO:0009741	response to brassinosteroid	12	4,25E-02	0,82
1	up	BP	GO:0009867	jasmonic acid mediated signaling pathway	21	4,56E-02	2,49
1	up	BP	GO:0010817	regulation of hormone levels	47	4,89E-02	-0,78
3	dw	BP	GO:0080027	response to herbivore	10	3,80E-04	-4,72
3	dw	BP	GO:0009620	response to fungus	95	4,30E-04	1,63
3	dw	BP	GO:1990110	callus formation	13	6,50E-04	5,14
3	dw	BP	GO:0009871	jasmonic acid and ethylene-dependent sys...	5	8,00E-04	-0,18
3	dw	BP	GO:0009611	response to wounding	84	9,70E-04	6,87
3	dw	BP	GO:0009627	systemic acquired resistance	28	1,28E-03	-2,23
3	dw	BP	GO:0009695	jasmonic acid biosynthetic process	13	4,01E-03	2,47
3	dw	BP	GO:0042128	nitrate assimilation	12	4,04E-03	1,96
3	dw	BP	GO:0009864	induced systemic resistance, jasmonic ac...	7	5,10E-03	2,44
3	dw	BP	GO:0010597	green leaf volatile biosynthetic process	9	5,43E-03	1,55
3	dw	BP	GO:0071215	cellular response to abscisic acid stimu...	79	5,52E-03	6,51
3	dw	BP	GO:0009751	response to salicylic acid	49	9,51E-03	5,86
3	dw	BP	GO:0033674	positive regulation of kinase activity	4	9,57E-03	0,47
3	dw	BP	GO:0019236	response to pheromone	2	9,58E-03	3,23
3	dw	BP	GO:0009866	induced systemic resistance, ethylene me...	6	1,01E-02	2,63
3	dw	BP	GO:0042221	response to chemical	527	1,71E-02	7,30
3	dw	BP	GO:1900425	negative regulation of defense response ...	9	1,85E-02	0,39
3	dw	BP	GO:0006950	response to stress	565	1,87E-02	3,73
3	dw	BP	GO:0010167	response to nitrate	13	2,41E-02	5,69
3	dw	BP	GO:0043069	negative regulation of programmed cell d...	10	4,27E-02	0,01
3	dw	BP	GO:0009753	response to jasmonic acid	59	4,89E-02	3,22

Table S3. ...continued.

3	up	BP	GO:0071395	cellular response to jasmonic acid stimu...	23	1,77E-03	13,25
3	up	BP	GO:0009807	lignan biosynthetic process	4	1,78E-03	1,72
3	up	BP	GO:0080027	response to herbivore	9	3,68E-03	2,92
3	up	BP	GO:0080029	cellular response to boron-containing su...	7	7,13E-03	6,30
3	up	BP	GO:0050776	regulation of immune response	50	8,96E-03	15,96
3	up	BP	GO:0010226	response to lithium ion	3	3,25E-02	-4,20
3	up	BP	GO:1900150	regulation of defense response to fungus	18	3,66E-02	14,55
3	up	BP	GO:0002831	regulation of response to biotic stimulus	39	3,87E-02	15,46
3	up	BP	GO:2001020	regulation of response to DNA damage sti...	6	4,80E-02	2,13
3	up	BP	GO:0048583	regulation of response to stimulus	163	4,80E-02	32,96
1	dw	BP	GO:0031542	positive regulation of anthocyanin biosy...	4	4,86E-03	-0,56
1	dw	BP	GO:2000030	regulation of response to red or far red...	18	6,74E-03	2,36
1	dw	BP	GO:0010380	regulation of chlorophyll biosynthetic p...	10	1,89E-02	2,06
1	dw	BP	GO:0042752	regulation of circadian rhythm	19	2,82E-02	0,09
1	up	BP	GO:0010193	response to ozone	13	5,02E-03	0,17
1	up	BP	GO:0031542	positive regulation of anthocyanin biosy...	3	7,03E-03	-2,23
1	dw	BP	GO:0009646	response to absence of light	10	1,80E-02	6,11
1	up	BP	GO:0010099	regulation of photomorphogenesis	7	3,28E-02	1,29
1	up	BP	GO:2000029	regulation of proanthocyanidin biosynthe...	2	3,43E-02	-0,40
1	up	BP	GO:0010220	positive regulation of vernalization res...	2	3,43E-02	4,39
3	dw	BP	GO:0048577	negative regulation of short-day photoperiodism, flowering	3	1,49E-02	3,26
3	dw	BP	GO:0010193	response to ozone	16	1,79E-02	0,95
3	dw	BP	GO:0010114	response to red light	18	4,28E-02	-0,41

Table S3. ...continued.

3	up	BP	GO:0010205	photoinhibition	7	1,87E-02	9,63
3	up	BP	GO:0009644	response to high light intensity	27	3,09E-02	10,46
3	up	BP	GO:0022900	electron transport chain	24	3,17E-02	12,89
1	dw	BP	GO:0010072	primary shoot apical meristem specificat...	7	7,76E-03	1,64
1	dw	BP	GO:0009957	epidermal cell fate specification	4	8,82E-03	-3,08
1	dw	BP	GO:0007275	multicellular organism development	572	9,31E-03	-3,31
1	dw	BP	GO:0040009	regulation of growth rate	6	9,98E-03	-3,65
1	dw	BP	GO:0046622	positive regulation of organ growth	3	1,33E-02	-2,34
1	dw	BP	GO:0071555	cell wall organization	84	1,59E-02	2,09
1	dw	BP	GO:0010252	auxin homeostasis	14	1,87E-02	-1,92
1	dw	BP	GO:0009826	unidimensional cell growth	91	1,95E-02	2,84
1	dw	BP	GO:0048527	lateral root development	44	2,09E-02	1,62
1	dw	BP	GO:0010030	positive regulation of seed germination	10	2,78E-02	1,87
1	dw	BP	GO:0009926	auxin polar transport	27	2,82E-02	-1,97
1	dw	BP	GO:0010344	seed oilbody biogenesis	6	2,91E-02	8,25
1	up	BP	GO:0048443	stamen development	18	2,00E-04	-3,37
1	up	BP	GO:0051301	cell division	47	6,35E-03	-4,70
1	up	BP	GO:0048480	stigma development	4	1,50E-02	-2,67
1	up	BP	GO:0051211	anisotropic cell growth	4	1,50E-02	-7,24
1	up	BP	GO:0010252	auxin homeostasis	9	2,09E-02	-3,74
1	up	BP	GO:0009911	positive regulation of flower developmen...	11	2,80E-02	-3,87
1	up	BP	GO:0042127	regulation of cell proliferation	10	2,94E-02	-1,21
1	up	BP	GO:0051512	positive regulation of unidimensional ce...	5	4,13E-02	5,08
3	dw	BP	GO:0009911	positive regulation of flower developmen...	19	1,29E-03	3,86
3	dw	BP	GO:0010183	pollen tube guidance	13	1,74E-03	5,26
3	dw	BP	GO:0009828	plant-type cell wall loosening	12	2,65E-03	-0,04
3	dw	BP	GO:1990059	fruit valve development	7	2,88E-03	0,57
3	dw	BP	GO:0009555	pollen development	76	6,67E-03	7,40
3	dw	BP	GO:0046622	positive regulation of organ growth	3	8,05E-03	0,99
3	dw	BP	GO:0010311	lateral root formation	26	9,31E-03	-2,08

Table S3. ...continued.

3	dw	BP	GO:0010315	auxin efflux	7	1,05E-02	0,83
3	dw	BP	GO:0080086	stamen filament development	7	1,05E-02	2,13
3	dw	BP	GO:0040009	regulation of growth rate	5	2,03E-02	-2,57
3	dw	BP	GO:0010930	negative regulation of auxin mediated si...	4	2,38E-02	1,12
3	dw	BP	GO:0009826	unidimensional cell growth	80	2,40E-02	4,08
3	dw	BP	GO:0010540	basipetal auxin transport	10	2,43E-02	4,21
3	dw	BP	GO:0048527	lateral root development	44	3,47E-02	1,71
3	dw	BP	GO:0051511	negative regulation of unidimensional ce...	3	3,60E-02	-0,43
3	dw	BP	GO:0048443	stamen development	26	4,77E-02	2,70
3	up	BP	GO:0051017	actin filament bundle assembly	9	1,20E-03	9,90
3	up	BP	GO:0060560	developmental growth involved in morphog...	105	1,27E-03	27,04
3	up	BP	GO:0009926	auxin polar transport	31	6,91E-03	11,28
3	up	BP	GO:0010311	lateral root formation	26	3,31E-02	9,26
3	up	BP	GO:0010449	root meristem growth	11	4,84E-02	8,86
1	dw	BP	GO:0022414	reproductive process	392	2,25E-02	-2,23
1	up	BP	GO:0048467	gynoecium development	19	4,60E-03	0,77
3	dw	BP	GO:1905499	trichome papilla formation	3	2,42E-02	-1,65
3	dw	BP	GO:0010091	trichome branching	15	3,04E-02	0,86
3	up	BP	GO:0010091	trichome branching	21	6,70E-04	13,30
3	up	BP	GO:0048767	root hair elongation	28	3,48E-02	9,88
3	up	BP	GO:0042147	retrograde transport, endosome to Golgi	5	4,89E-02	8,83
3	up	BP	GO:0015808	L-alanine transport	5	4,89E-02	5,11
1	dw	BP	GO:0042343	indole glucosinolate metabolic process	14	2,70E-07	5,18
1	dw	BP	GO:0071732	cellular response to nitric oxide	7	6,30E-05	-0,65
1	dw	BP	GO:0006012	galactose metabolic process	8	1,00E-04	-0,63
1	dw	BP	GO:0019432	triglyceride biosynthetic process	11	1,19E-03	-1,57
1	dw	BP	GO:1901141	regulation of lignin biosynthetic proces...	20	2,18E-03	4,82
1	dw	BP	GO:0009686	gibberellin biosynthetic process	9	4,50E-03	-0,60

Table S3. ...continued.

1	dw	BP	GO:1902000	homogentisate catabolic process	4	4,86E-03	-1,48
1	dw	BP	GO:0048511	rhythmic process	37	4,89E-03	1,40
1	dw	BP	GO:0009740	gibberellic acid mediated signaling path...	15	5,13E-03	-1,79
1	dw	BP	GO:0006659	phosphatidylserine biosynthetic process	3	5,82E-03	-4,03
1	dw	BP	GO:0032886	regulation of microtubule-based process	4	5,85E-03	-3,02
1	dw	BP	GO:0006559	L-phenylalanine catabolic process	6	7,15E-03	-1,62
1	dw	BP	GO:0080167	response to karrikin	55	7,17E-03	-0,21
1	dw	BP	GO:0032091	negative regulation of protein binding	4	8,82E-03	-2,51
1	dw	BP	GO:0030705	cytoskeleton-dependent intracellular tra...	9	1,24E-02	-2,52
1	dw	BP	GO:0018107	peptidyl-threonine phosphorylation	5	1,33E-02	2,41
1	dw	BP	GO:2001295	malonyl-CoA biosynthetic process	3	1,33E-02	0,38
1	dw	BP	GO:0071398	cellular response to fatty acid	3	1,33E-02	4,30
1	dw	BP	GO:0009250	glucan biosynthetic process	23	1,34E-02	-0,61
1	dw	BP	GO:0007031	peroxisome organization	11	1,35E-02	-5,32
1	dw	BP	GO:0052573	UDP-D-galactose metabolic process	2	1,37E-02	4,22
1	dw	BP	GO:0006557	S-adenosylmethioninamine biosynthetic pr...	2	1,37E-02	-3,80
1	dw	BP	GO:0010247	detection of phosphate ion	2	1,37E-02	4,15
1	dw	BP	GO:0030833	regulation of actin filament polymerizat...	10	1,44E-02	0,65
1	dw	BP	GO:0033198	response to ATP	4	1,44E-02	-2,20
1	dw	BP	GO:0010906	regulation of glucose metabolic process	4	1,44E-02	-4,85
1	dw	BP	GO:0044794	positive regulation by host of viral pro...	2	1,37E-02	-5,57
1	dw	BP	GO:0005975	carbohydrate metabolic process	160	1,84E-02	-1,38
1	dw	BP	GO:0071244	cellular response to carbon dioxide	9	2,00E-02	5,43
1	dw	BP	GO:0048583	regulation of response to stimulus	184	2,03E-02	5,17
1	dw	BP	GO:0009750	response to fructose	11	2,04E-02	-1,71

Table S3. ...continued.

1	dw	BP	GO:0019748	secondary metabolic process	101	2,07E-02	4,69
1	dw	BP	GO:0009308	amine metabolic process	28	2,16E-02	-4,61
1	dw	BP	GO:0090615	mitochondrial mRNA processing	6	2,18E-02	-0,67
1	dw	BP	GO:0043335	protein unfolding	4	2,18E-02	-3,13
1	dw	BP	GO:0009800	cinnamic acid biosynthetic process	4	2,18E-02	-4,91
1	dw	BP	GO:0006108	malate metabolic process	5	2,38E-02	2,63
1	dw	BP	GO:1903086	negative regulation of sinapate ester bi...	3	2,43E-02	-3,85
1	dw	BP	GO:0080162	intracellular auxin transport	3	2,43E-02	-2,82
1	dw	BP	GO:0032025	response to cobalt ion	3	2,43E-02	-3,00
1	dw	BP	GO:0010273	detoxification of copper ion	3	2,43E-02	0,34
1	dw	BP	GO:0006656	phosphatidylcholine biosynthetic process	5	3,12E-02	-2,67
1	dw	BP	GO:0009647	skotomorphogenesis	4	3,12E-02	-1,59
1	up	BP	GO:0032091	negative regulation of protein binding	5	4,50E-05	-4,68
1	up	BP	GO:0031408	oxylipin biosynthetic process	9	1,10E-04	-0,35
1	up	BP	GO:0019432	triglyceride biosynthetic process	9	1,80E-04	-0,54
1	up	BP	GO:0009920	cell plate formation involved in plant-t...	9	2,80E-04	0,68
1	up	BP	GO:0006048	UDP-N-acetylglucosamine biosynthetic pro...	4	4,50E-04	6,03
1	up	BP	GO:0006011	UDP-glucose metabolic process	5	8,60E-04	7,15
1	up	BP	GO:0030187	melatonin biosynthetic process	3	9,30E-04	-3,92
1	up	BP	GO:0007064	mitotic sister chromatid cohesion	7	1,40E-03	-1,74
1	up	BP	GO:0071732	cellular response to nitric oxide	4	3,50E-03	-5,94
1	up	BP	GO:2000694	regulation of phragmoplast microtubule o...	4	3,50E-03	-2,67
1	up	BP	GO:0019500	cyanide catabolic process	2	3,90E-03	-4,93
1	up	BP	GO:0052573	UDP-D-galactose metabolic process	2	3,90E-03	3,48
1	up	BP	GO:0044794	positive regulation by host of viral pro...	2	3,90E-03	-6,29

Table S3. ...continued.

1	up	BP	GO:0032025	response to cobalt ion	3	4,21E-03	-2,25
1	up	BP	GO:0006535	cysteine biosynthetic process from serin...	4	4,99E-03	-7,69
1	up	BP	GO:0072318	clathrin coat disassembly	3	7,03E-03	2,26
1	up	BP	GO:0031648	protein destabilization	5	8,26E-03	-2,41
1	up	BP	GO:0010152	pollen maturation	7	8,33E-03	-6,32
1	up	BP	GO:0030100	regulation of endocytosis	6	9,08E-03	-2,14
1	up	BP	GO:0046685	response to arsenic-containing substance	5	1,02E-02	3,07
1	up	BP	GO:0035825	homologous recombination	6	1,08E-02	1,73
1	up	BP	GO:0018343	protein farnesylation	2	1,12E-02	5,91
1	up	BP	GO:0051315	attachment of mitotic spindle microtubul...	2	1,12E-02	-4,72
1	up	BP	GO:1900386	positive regulation of flavonol biosynth...	2	1,12E-02	-2,49
1	up	BP	GO:0046506	sulfolipid biosynthetic process	2	1,12E-02	5,05
1	up	BP	GO:1905952	regulation of lipid localization	4	1,19E-02	-2,67
1	up	BP	GO:0061025	membrane fusion	9	1,50E-02	-1,79
1	up	BP	GO:0072659	protein localization to plasma membrane	8	1,50E-02	3,38
1	up	BP	GO:0080157	regulation of plant-type cell wall organ...	4	1,50E-02	-2,67
1	up	BP	GO:0048354	mucilage biosynthetic process involved i...	6	1,52E-02	-2,07
1	up	BP	GO:0009856	pollination	39	1,53E-02	2,43
1	up	BP	GO:0071586	CAAX-box protein processing	3	1,54E-02	6,31
1	up	BP	GO:0070574	cadmium ion transmembrane transport	3	1,54E-02	-2,71
1	up	BP	GO:0046940	nucleoside monophosphate phosphorylation	4	2,29E-02	-2,67
1	up	BP	GO:0010241	ent-kaurene oxidation to kaurenoic acid	2	2,15E-02	3,30
1	up	BP	GO:0000266	mitochondrial fission	4	1,87E-02	-2,67
1	up	BP	GO:0007094	mitotic spindle assembly checkpoint	3	2,09E-02	-6,47
1	up	BP	GO:0055046	microgametogenesis	6	2,44E-02	4,18
1	up	BP	GO:0006635	fatty acid beta-oxidation	10	2,54E-02	5,30

Table S3. ...continued.

1	up	BP	GO:0006207	'de novo' pyrimidine nucleobase biosynth...	4	3,28E-02	-2,67
1	up	BP	GO:0018107	peptidyl-threonine phosphorylation	3	3,43E-02	3,06
1	up	BP	GO:0005991	trehalose metabolic process	4	3,43E-02	-0,47
1	up	BP	GO:0006516	glycoprotein catabolic process	2	3,43E-02	-2,77
1	up	BP	GO:0002100	tRNA wobble adenosine to inosine editing	2	3,43E-02	-3,59
1	up	BP	GO:0098734	macromolecule depalmitoylation	2	3,43E-02	5,27
1	up	BP	GO:0072660	maintenance of protein location in plasm...	2	3,43E-02	-0,09
1	up	BP	GO:0007076	mitotic chromosome condensation	2	3,43E-02	-6,03
1	up	BP	GO:0006110	regulation of glycolytic process	2	3,43E-02	0,54
1	up	BP	GO:0045903	positive regulation of translational fid...	2	3,43E-02	-1,29
1	up	BP	GO:0006285	base-excision repair, AP site formation	2	3,43E-02	4,62
1	up	BP	GO:0033542	fatty acid beta-oxidation, unsaturated, ...	2	3,43E-02	2,49
1	up	BP	GO:0110102	chloroplast ribulose bisphosphate carbox...	3	3,49E-02	2,10
1	up	BP	GO:0051726	regulation of cell cycle	17	4,13E-02	-3,02
1	up	BP	GO:0060151	peroxisome localization	4	4,49E-02	1,03
1	up	BP	GO:1901959	positive regulation of cutin biosyntheti...	2	4,94E-02	0,54
1	up	BP	GO:0043132	NAD transport	2	4,94E-02	-0,55
1	up	BP	GO:0046398	UDP-glucuronate metabolic process	2	4,94E-02	3,48
1	up	BP	GO:1903086	negative regulation of sinapate ester bi...	2	4,94E-02	-2,49
1	up	BP	GO:1900186	negative regulation of clathrin-dependen...	2	4,94E-02	0,08
1	up	BP	GO:0002943	tRNA dihydrouridine synthesis	2	4,94E-02	1,45
3	dw	BP	GO:0071555	cell wall organization	72	3,30E-04	2,57
3	dw	BP	GO:0009696	salicylic acid metabolic process	15	2,91E-03	5,00

Table S3. ...continued.

3	dw	BP	GO:0042547	cell wall modification involved in multi...	10	2,92E-03	-0,02
3	dw	BP	GO:0010150	leaf senescence	49	3,22E-03	1,87
3	dw	BP	GO:0009694	jasmonic acid metabolic process	20	3,76E-03	0,42
3	dw	BP	GO:0007389	pattern specification process	42	3,93E-03	2,03
3	dw	BP	GO:0009738	abscisic acid-activated signaling pathwa...	63	7,63E-03	4,10
3	dw	BP	GO:0016560	protein import into peroxisome matrix, d...	4	7,70E-03	2,66
3	dw	BP	GO:0048575	short-day photoperiodism, flowering	8	8,37E-03	-0,33
3	dw	BP	GO:0009687	abscisic acid metabolic process	10	8,39E-03	-1,96
3	dw	BP	GO:0000105	histidine biosynthetic process	5	8,41E-03	1,84
3	dw	BP	GO:0048205	COPI coating of Golgi vesicle	2	9,58E-03	4,47
3	dw	BP	GO:0070407	oxidation-dependent protein catabolic pr...	2	9,58E-03	6,52
3	dw	BP	GO:0072718	response to cisplatin	2	9,58E-03	1,09
3	dw	BP	GO:0033473	indoleacetic acid conjugate metabolic pr...	2	9,58E-03	-2,43
3	dw	BP	GO:0032979	protein insertion into mitochondrial inn...	2	9,58E-03	1,83
3	dw	BP	GO:0031408	oxylipin biosynthetic process	8	1,03E-02	2,75
3	dw	BP	GO:0019748	secondary metabolic process	71	1,16E-02	2,66
3	dw	BP	GO:0006145	purine nucleobase catabolic process	4	1,19E-02	1,02
3	dw	BP	GO:0010143	cutin biosynthetic process	10	1,24E-02	-1,04
3	dw	BP	GO:0032889	regulation of vacuole fusion, non-autoph...	3	1,49E-02	-6,04
3	dw	BP	GO:0032501	multicellular organismal process	531	1,66E-02	4,87
3	dw	BP	GO:0016540	protein autoprocessing	4	1,72E-02	2,37
3	dw	BP	GO:0030245	cellulose catabolic process	5	2,03E-02	1,88
3	dw	BP	GO:0016042	lipid catabolic process	27	2,41E-02	0,98
3	dw	BP	GO:0080088	spermidine hydroxycinnamate conjugate bi...	3	2,42E-02	-3,32

Table S3. ...continued.

3	dw	BP	GO:0018874	benzoate metabolic process	3	2,42E-02	1,99
3	dw	BP	GO:0010031	circumnutation	3	2,42E-02	0,28
3	dw	BP	GO:0009686	gibberellin biosynthetic process	7	2,51E-02	1,88
3	dw	BP	GO:0045493	xylan catabolic process	5	2,59E-02	-0,76
3	dw	BP	GO:1904975	response to bleomycin	2	2,69E-02	2,45
3	dw	BP	GO:0046110	xanthine metabolic process	2	2,69E-02	3,48
3	dw	BP	GO:1900486	positive regulation of isopentenyl dipho...	2	2,69E-02	-0,60
3	dw	BP	GO:2000685	positive regulation of cellular response...	2	2,69E-02	2,45
3	dw	BP	GO:2000601	positive regulation of Arp2/3 complexme...	2	2,69E-02	-4,41
3	dw	BP	GO:0007154	cell communication	245	3,10E-02	4,34
3	dw	BP	GO:0006722	triterpenoid metabolic process	6	3,17E-02	-3,10
3	dw	BP	GO:0060919	auxin influx	7	3,23E-02	-1,48
3	dw	BP	GO:0000272	polysaccharide catabolic process	19	3,57E-02	-1,39
3	dw	BP	GO:0010731	protein glutathionylation	3	3,60E-02	-4,27
3	dw	BP	GO:0019605	butyrate metabolic process	3	3,60E-02	3,47
3	dw	BP	GO:0046244	salicylic acid catabolic process	3	3,60E-02	4,43
3	dw	BP	GO:0048579	negative regulation of long-day photoper...	6	4,29E-02	4,62
3	up	BP	GO:0006432	phenylalanyl-tRNA aminoacylation	5	6,50E-04	1,16
3	up	BP	GO:0007018	microtubule-based movement	15	1,11E-03	11,59
3	dw	BP	GO:0010047	fruit dehiscence	8	4,26E-02	1,53
3	up	BP	GO:0019566	arabinose metabolic process	5	4,78E-03	10,35
3	up	BP	GO:0034058	endosomal vesicle fusion	3	4,79E-03	5,71
3	up	BP	GO:0016236	macroautophagy	8	4,79E-03	8,57
3	up	BP	GO:0006515	protein quality control for misfolded or...	9	6,31E-03	7,92
3	up	BP	GO:0006574	valine catabolic process	5	9,39E-03	0,58
3	up	BP	GO:0016567	protein ubiquitination	63	1,00E-02	17,48

Table S3. ...continued.

3	up	BP	GO:0006110	regulation of glycolytic process	3	1,10E-02	5,11
3	up	BP	GO:1905933	regulation of cell fate determination	3	1,10E-02	5,03
3	up	BP	GO:0006542	glutamine biosynthetic process	3	1,10E-02	3,42
3	up	BP	GO:0016560	protein import into peroxisome matrix, d...	4	1,14E-02	6,54
3	up	BP	GO:0006661	phosphatidylinositol biosynthetic proces...	8	1,19E-02	4,31
3	up	BP	GO:0009685	gibberellin metabolic process	7	1,19E-02	8,47
3	up	BP	GO:0046398	UDP-glucuronate metabolic process	3	1,19E-02	6,13
3	up	BP	GO:0033674	positive regulation of kinase activity	4	1,19E-02	0,56
3	up	BP	GO:0052573	UDP-D-galactose metabolic process	2	1,19E-02	5,10
3	up	BP	GO:0044794	positive regulation by host of viral pro...	2	1,19E-02	5,05
3	up	BP	GO:1990116	ribosome-associated ubiquitin-dependent ...	2	1,19E-02	1,43
3	up	BP	GO:0044528	regulation of mitochondrial mRNA stabili...	2	1,19E-02	6,10
3	up	BP	GO:0070407	oxidation-dependent protein catabolic pr...	2	1,19E-02	6,20
3	up	BP	GO:0006784	heme a biosynthetic process	2	1,19E-02	6,48
3	up	BP	GO:0006617	SRP-dependent cotranslational protein ta...	2	1,19E-02	7,78
3	up	BP	GO:0010014	meristem initiation	6	1,19E-02	9,33
3	up	BP	GO:0071230	cellular response to amino acid stimulus	5	1,33E-02	0,35
3	up	BP	GO:0007015	actin filament organization	22	1,56E-02	12,36
3	up	BP	GO:1904821	chloroplast disassembly	4	1,74E-02	5,20
3	up	BP	GO:0010540	basipetal auxin transport	11	1,99E-02	5,51
3	up	BP	GO:1901959	positive regulation of cutin biosyntheti...	3	2,02E-02	5,11
3	up	BP	GO:0010201	response to continuous far red light sti...	3	2,02E-02	6,72
3	up	BP	GO:0009880	embryonic pattern specification	9	2,15E-02	6,72

Table S3. ...continued.

3	up	BP	GO:0007064	mitotic sister chromatid cohesion	7	2,16E-02	5,45
3	up	BP	GO:0000723	telomere maintenance	8	2,16E-02	6,16
3	up	BP	GO:0080157	regulation of plant-type cell wall organ...	5	2,42E-02	6,46
3	up	BP	GO:2000694	regulation of phragmoplast microtubule o...	4	2,50E-02	5,29
3	up	BP	GO:0048229	gametophyte development	109	2,96E-02	27,34
3	up	BP	GO:0000266	mitochondrial fission	5	3,12E-02	5,95
3	up	BP	GO:0010371	regulation of gibberellin biosynthetic p...	5	3,25E-02	7,12
3	up	BP	GO:0000913	preprophase band assembly	3	3,25E-02	6,29
3	up	BP	GO:0051131	chaperone-mediated protein complex assem...	3	3,25E-02	6,59
3	up	BP	GO:0045017	glycerolipid biosynthetic process	22	3,30E-02	9,78
3	up	BP	GO:0010364	regulation of ethylene biosynthetic proc...	6	3,31E-02	6,05
3	up	BP	GO:0006429	leucyl-tRNA aminoacylation	2	3,32E-02	5,63
3	up	BP	GO:0006231	dTMP biosynthetic process	2	3,32E-02	0,55
3	up	BP	GO:2000636	positive regulation of primary miRNA pro...	2	3,32E-02	4,37
3	up	BP	GO:2000601	positive regulation of Arp2/3 complex-me...	2	3,32E-02	1,09
3	up	BP	GO:1905036	positive regulation of antifungal innate...	2	3,32E-02	6,55
3	up	BP	GO:0009257	10-formyltetrahydrofolate biosynthetic p...	2	3,32E-02	0,55
3	up	BP	GO:0019265	glycine biosynthetic process, by transam...	2	3,32E-02	4,81
3	up	BP	GO:0071368	cellular response to cytokinin stimulus	5	3,34E-02	6,11
3	up	BP	GO:1905393	plant organ formation	42	3,38E-02	14,58
3	up	BP	GO:0000911	cytokinesis by cell plate formation	28	3,95E-02	16,81
3	up	BP	GO:0006221	pyrimidine nucleotide biosynthetic proce...	10	4,53E-02	8,53

Table S3. ...continued.

3	up	BP	GO:0010165	response to X-ray	4	4,53E-02	2,43
3	up	BP	GO:0007154	cell communication	250	4,66E-02	38,26
3	up	BP	GO:0033036	macromolecule localization	157	4,71E-02	28,37
3	up	BP	GO:0034484	raffinose catabolic process	3	4,79E-02	4,77
3	up	BP	GO:0090058	metaxylem development	3	4,79E-02	4,79
3	up	BP	GO:0080119	ER body organization	3	4,79E-02	5,29
3	up	BP	GO:0031396	regulation of protein ubiquitination	5	4,79E-02	2,89
3	up	BP	GO:0032544	plastid translation	6	4,84E-02	4,98

Table S4. Enriched GO terms in DTGs that change plastically between environments in RT settings.

Ecotype pair	**ecotype**	**GO category**	**GO ID**	**GO term**	**DTGs number**	**adjp-val**	**z-score**
1	**montane**	**BP**	**GO:0016458**	**gene silencing**	**11**	**6,72E-03**	**3,81**
1	**montane**	**BP**	**GO:0010608**	**posttranscriptional regulation of gene expression**	**11**	**6,79E-03**	**6,82**
1	montane	BP	GO:0045014	carbon catabolite repression of transcription by glucose	2	6,85E-03	-2,50
1	montane	BP	GO:0006346	DNA methylation-dependent heterochromatin assembly	3	1,53E-02	-0,08
1	montane	BP	GO:0006307	DNA dealkylation involved in DNA repair	1	4,36E-02	-4,85
3	montane	BP	GO:1905642	negative regulation of DNA methylation	2	4,10E-03	7,29
3	montane	BP	GO:0044528	regulation of mitochondrial mRNA stability	2	4,10E-03	6,92
3	montane	BP	GO:1901259	chloroplast rRNA processing	7	9,50E-03	11,35
3	**montane**	**BP**	**GO:0008380**	**RNA splicing**	**32**	**1,00E-02**	**22,52**
3	**montane**	**BP**	**GO:0051570**	**regulation of histone H3-K9 methylation**	**5**	**1,17E-02**	**9,38**
3	montane	BP	GO:0035279	miRNA-mediated gene silencing by mRNA destabilization	2	1,18E-02	6,08
3	montane	BP	GO:0006336	DNA replication-independent chromatin assembly	2	1,18E-02	4,55

Table S4. ...continued.

3	montane	BP	GO:0006429	leucyl-tRNA aminoacylation	2	1,18E-02	5,89
3	montane	BP	GO:2000636	positive regulation of primary miRNA processing	2	1,18E-02	6,31
3	montane	BP	GO:0045727	positive regulation of translation	6	1,26E-02	10,17
3	**montane**	**BP**	**GO:0031936**	**negative regulation of chromatin silencing**	**4**	**1,29E-02**	**9,09**
3	montane	BP	GO:1900871	chloroplast mRNA modification	3	1,64E-02	6,59
3	**montane**	**BP**	**GO:0006396**	**RNA processing**	**94**	**2,57E-02**	**36,76**
3	**montane**	**BP**	**GO:0070919**	**production of siRNA involved in gene silencing by small RNA**	**4**	**4,18E-02**	**3,81**
1	alpine	BP	GO:0035066	positive regulation of histone acetylation	2	1,52E-03	2,26
1	alpine	BP	GO:0060195	negative regulation of antisense RNA transcription	1	1,25E-02	-4,80
1	alpine	BP	GO:1990258	histone glutamine methylation	1	2,49E-02	1,80
1	alpine	BP	GO:0045948	positive regulation of translational ini...	1	2,49E-02	-3,19
1	alpine	BP	GO:0000494	box C/D snoRNA 3'-end processing	1	2,49E-02	1,80
1	alpine	BP	GO:0016441	posttranscriptional gene silencing	3	2,58E-02	-9,53
1	**alpine**	**BP**	**GO:0016571**	**histone methylation**	**5**	**2,77E-02**	**4,98**
1	alpine	BP	GO:0006346	methylation-dependent chromatin silencin...	2	3,60E-02	-7,76
1	alpine	BP	GO:0009301	snRNA transcription	1	3,71E-02	-4,31
1	montane	BP	GO:1902358	sulfate transmembrane transport	3	5,50E-04	-3,88
1	montane	BP	GO:0098721	uracil import across plasma membrane	2	4,64E-03	-3,12
1	montane	BP	GO:0098710	guanine import across plasma membrane	2	4,64E-03	-3,12
1	**montane**	**BP**	**GO:0006970**	**response to osmotic stress**	**39**	**6,48E-03**	**-0,36**
1	montane	BP	GO:0010184	cytokinin transport	2	1,24E-02	3,40
1	montane	BP	GO:0015692	lead ion transport	3	1,36E-02	1,25
1	**montane**	**BP**	**GO:0071475**	**cellular hyperosmotic salinity response**	**2**	**2,34E-02**	**6,29**

Table S4. ...continued.

1	montane	BP	GO:0080168	abscisic acid transport	3	2,54E-02	-0,88
1	**montane**	**BP**	**GO:1902584**	**positive regulation of response to water deprivation**	**3**	**2,78E-02**	**-3,01**
1	**montane**	**BP**	**GO:0010335**	**response to non-ionic osmotic stress**	**1**	**4,36E-02**	**-3,53**
1	montane	BP	GO:0010268	brassinosteroid homeostasis	2	4,74E-02	1,02
1	montane	BP	GO:0010222	stem vascular tissue pattern formation	2	4,74E-02	3,40
1	montane	BP	GO:1903288	positive regulation of potassium ion import across plasma membrane	2	9,46E-03	-5,98
1	montane	BP	GO:0080051	cutin transport	3	1,20E-02	3,45
1	montane	BP	GO:0042908	xenobiotic transport	4	1,24E-02	1,47
1	montane	BP	GO:0015910	peroxisomal long-chain fatty acid import	1	2,21E-02	3,64
3	montane	BP	GO:1902476	chloride transmembrane transport	3	7,50E-03	7,60
3	**montane**	**BP**	**GO:0051453**	**regulation of intracellular pH**	**6**	**1,93E-02**	**12,63**
3	**montane**	**BP**	**GO:0006886**	**intracellular protein transport**	**46**	**3,63E-02**	**27,08**
3	montane	BP	GO:0015867	ATP transport	4	4,86E-02	10,00
1	alpine	BP	GO:0006820	anion transport	9	2,31E-02	3,25
1	alpine	BP	GO:0010025	wax biosynthetic process	4	1,15E-02	-5,67
1	montane	BP	GO:0010205	photoinhibition	4	2,36E-03	7,63
1	montane	BP	GO:0010228	vegetative to reproductive phase transit...	15	1,14E-02	-3,74
1	montane	BP	GO:0048571	long-day photoperiodism	3	4,23E-02	-5,42
3	montane	BP	GO:0010205	photoinhibition	6	5,20E-03	10,05
3	montane	BP	GO:0048564	photosystem I assembly	6	6,30E-03	9,53
1	**alpine**	**BP**	**GO:0009648**	**photoperiodism**	**7**	**6,48E-03**	**-3,05**
1	alpine	BP	GO:0062055	photosynthetic state transition	1	1,25E-02	1,52
1	alpine	BP	GO:0043481	anthocyanin accumulation in tissues in r...	2	2,09E-02	-6,88
3	montane	BP	GO:1905036	positive regulation of antifungal innate...	2	1,18E-02	4,63
3	montane	BP	GO:0043434	response to peptide hormone	3	2,24E-02	7,25

Table S4. ...continued.

3	**montane**	**BP**	**GO:0002239**	**response to oomycetes**	**16**	**3,49E-02**	**15,83**
1	alpine	BP	GO:0009970	cellular response to sulfate starvation	3	8,01E-03	5,05
1	**alpine**	**BP**	**GO:0009611**	**response to wounding**	**14**	**1,04E-02**	**8,07**
1	alpine	BP	GO:1900366	negative regulation of defense response ...	2	2,09E-02	-3,02
1	alpine	BP	GO:0034976	response to endoplasmic reticulum stress	4	2,23E-02	-2,78
1	**alpine**	**BP**	**GO:0050832**	**defense response to fungus**	**13**	**2,36E-02**	**-2,37**
1	alpine	BP	GO:0050829	defense response to Gram-negative bacter...	3	1,66E-02	0,99
3	alpine	BP	GO:0071226	cellular response to molecule of fungal ...	1	9,61E-03	-1,65
3	**alpine**	**BP**	**GO:0050777**	**negative regulation of immune response**	**2**	**3,20E-02**	**1,97**
1	montane	BP	GO:0034976	response to endoplasmic reticulum stress	5	2,14E-02	-3,42
3	**montane**	**BP**	**GO:0048767**	**root hair elongation**	**20**	**3,36E-02**	**16,98**
3	**montane**	**BP**	**GO:0048629**	**trichome patterning**	**2**	**3,60E-02**	**5,01**
1	**alpine**	**BP**	**GO:0010091**	**trichome branching**	**6**	**9,90E-04**	**0,23**
1	**alpine**	**BP**	**GO:2000039**	**regulation of trichome morphogenesis**	**2**	**2,09E-02**	**3,62**
1	**alpine**	**BP**	**GO:0048766**	**root hair initiation**	**3**	**2,73E-02**	**-6,06**
1	montane	BP	GO:0048443	stamen development	8	1,33E-02	-5,53
1	montane	BP	GO:0009826	unidimensional cell growth	22	2,00E-02	1,54
1	montane	BP	GO:0009734	auxin-activated signaling pathway	10	3,59E-02	0,01
1	montane	BP	GO:0010777	meiotic mismatch repair involved in reciprocal meiotic recombination	4	1,00E-04	4,90
1	montane	BP	GO:0045934	negative regulation of nucleobase-containing compound metabolic process	20	4,60E-04	-0,97
1	montane	BP	GO:0006431	methionyl-tRNA aminoacylation	2	1,43E-03	-3,15

Table S4. ...continued.

1	montane	BP	GO:0098702	adenine import across plasma membrane	2	4,64E-03	-3,12
1	montane	BP	GO:0006285	base-excision repair, AP site formation	2	4,64E-03	-1,06
1	montane	BP	GO:0051026	chiasma assembly	4	5,12E-03	4,90
1	montane	BP	GO:1901183	positive regulation of camalexin biosynt...	2	9,46E-03	4,05
1	montane	BP	GO:0043248	proteasome assembly	3	1,05E-02	1,93
1	montane	BP	GO:0010047	fruit dehiscence	4	1,24E-02	-2,95
1	montane	BP	GO:0010483	pollen tube reception	2	1,24E-02	0,88
1	montane	BP	GO:0007059	chromosome segregation	8	1,50E-02	7,02
1	montane	BP	GO:0006552	leucine catabolic process	2	1,57E-02	-0,97
1	montane	BP	GO:1903578	regulation of ATP metabolic process	2	1,57E-02	4,37
1	montane	BP	GO:0006102	isocitrate metabolic process	2	1,94E-02	4,00
1	montane	BP	GO:0043419	urea catabolic process	1	2,21E-02	-2,47
1	montane	BP	GO:0042760	very long-chain fatty acid catabolic pro...	1	2,21E-02	3,64
1	montane	BP	GO:0097359	UDP-glucosylation	1	2,21E-02	3,88
1	montane	BP	GO:0016099	monoterpenoid biosynthetic process	1	2,21E-02	-1,80
1	montane	BP	GO:1901430	positive regulation of syringal lignin b...	3	2,31E-02	-3,05
1	montane	BP	GO:0010158	abaxial cell fate specification	2	2,34E-02	-5,98
1	montane	BP	GO:0052543	callose deposition in cell wall	4	2,54E-02	-1,99
1	montane	BP	GO:0006631	fatty acid metabolic process	12	2,60E-02	4,62
1	montane	BP	GO:0046482	para-aminobenzoic acid metabolic process	2	3,22E-02	6,29
1	montane	BP	GO:0070301	cellular response to hydrogen peroxide	3	3,29E-02	7,87
1	montane	BP	GO:0042325	regulation of phosphorylation	7	3,65E-02	3,22
1	montane	BP	GO:0080024	indolebutyric acid metabolic process	2	3,70E-02	6,29
1	montane	BP	GO:0019375	galactolipid biosynthetic process	2	3,70E-02	6,38
1	montane	BP	GO:0033674	positive regulation of kinase activity	2	4,35E-02	-0,35
1	montane	BP	GO:0031407	oxylipin metabolic process	2	4,36E-02	2,07
1	montane	BP	GO:0071433	cell wall repair	1	4,36E-02	-1,92

Table S4. ...continued.

1	montane	BP	GO:0006069	ethanol oxidation	1	4,36E-02	-2,23
1	montane	BP	GO:0006673	inositol phosphoceramide metabolic proce...	1	4,36E-02	-4,04
1	montane	BP	GO:0006435	threonyl-tRNA aminoacylation	1	4,36E-02	-4,01
1	montane	BP	GO:2000640	positive regulation of SREBP signaling p...	1	4,36E-02	-2,28
1	montane	BP	GO:0010605	negative regulation of macromolecule met...	32	4,50E-02	-0,32
1	montane	BP	GO:0051211	anisotropic cell growth	2	4,74E-02	-1,80
1	montane	BP	GO:1901140	p-coumaryl alcohol transport	2	4,74E-02	-0,13
3	montane	BP	GO:0010133	proline catabolic process to glutamate	3	1,00E-03	7,62
3	montane	BP	GO:0042776	mitochondrial ATP synthesis coupled prot...	3	2,40E-03	6,72
3	montane	BP	GO:0070995	NADPH oxidation	3	2,40E-03	1,93
3	montane	BP	GO:0007015	actin filament organization	14	2,90E-03	15,50
3	montane	BP	GO:0106074	aminoacyl-tRNA metabolism involved in tr...	5	3,50E-03	8,62
3	montane	BP	GO:0006661	phosphatidylinositol biosynthetic proces...	7	4,10E-03	5,69
3	montane	BP	GO:0033674	positive regulation of kinase activity	5	4,10E-03	1,03
3	montane	BP	GO:0006617	SRP-dependent cotranslational protein ta...	2	4,10E-03	9,32
3	montane	BP	GO:0044794	positive regulation by host of viral pro...	2	4,10E-03	4,44
3	montane	BP	GO:0019441	tryptophan catabolic process to kynureni...	2	4,10E-03	5,87
3	montane	BP	GO:0006784	heme a biosynthetic process	2	4,10E-03	8,30
3	montane	BP	GO:0099636	cytoplasmic streaming	3	4,50E-03	8,36
3	montane	BP	GO:0009807	lignan biosynthetic process	3	4,50E-03	1,96
3	montane	BP	GO:0051014	actin filament severing	3	4,50E-03	8,36
3	montane	BP	GO:0051017	actin filament bundle assembly	6	5,20E-03	9,56
3	montane	BP	GO:0000913	preprophase band assembly	3	7,50E-03	9,76
3	montane	BP	GO:0009846	pollen germination	15	8,30E-03	12,98

Table S4. ...continued.

3	montane	BP	GO:0010731	protein glutathionylation	3	1,15E-02	3,85
3	montane	BP	GO:0019265	glycine biosynthetic process, by transam...	2	1,18E-02	6,60
3	montane	BP	GO:0034645	cellular macromolecule biosynthetic proc...	207	1,26E-02	55,56
3	montane	BP	GO:0048317	seed morphogenesis	5	1,64E-02	8,57
3	montane	BP	GO:0005982	starch metabolic process	9	1,96E-02	11,74
3	montane	BP	GO:0048497	maintenance of floral organ identity	4	2,04E-02	8,08
3	montane	BP	GO:0008202	steroid metabolic process	13	2,22E-02	14,29
3	montane	BP	GO:0080163	regulation of protein serine/threonine p...	3	2,24E-02	4,49
3	montane	BP	GO:0071588	hydrogen peroxide mediated signaling pat...	4	2,25E-02	8,86
3	montane	BP	GO:0061936	fusion of sperm to egg plasma membrane i...	3	2,25E-02	5,91
3	montane	BP	GO:0035024	negative regulation of Rho protein signa...	2	2,25E-02	1,90
3	montane	BP	GO:0051639	actin filament network formation	2	2,25E-02	3,06
3	montane	BP	GO:0031022	nuclear migration along microfilament	2	2,25E-02	7,63
3	montane	BP	GO:0010951	negative regulation of endopeptidase act...	2	2,25E-02	5,08
3	montane	BP	GO:0051645	Golgi localization	5	2,28E-02	9,41
3	montane	BP	GO:0080187	floral organ senescence	4	2,49E-02	7,66
3	montane	BP	GO:0030050	vesicle transport along actin filament	5	2,65E-02	10,18
3	montane	BP	GO:0007018	microtubule-based movement	8	3,07E-02	14,91
3	montane	BP	GO:0071323	cellular response to chitin	5	3,51E-02	6,36
3	montane	BP	GO:0010115	regulation of abscisic acid biosynthetic...	5	3,56E-02	10,17
3	montane	BP	GO:0032958	inositol phosphate biosynthetic process	4	3,59E-02	4,08
3	montane	BP	GO:2000029	regulation of proanthocyanidin biosynthe...	2	3,60E-02	4,65
3	montane	BP	GO:1904966	positive regulation of vitamin E biosynt...	2	3,60E-02	4,63

Table S4. ...continued.

3	montane	BP	GO:2000693	positive regulation of seed maturation	2	3,60E-02	7,55
3	montane	BP	GO:0080121	AMP transport	2	3,60E-02	6,96
3	montane	BP	GO:0051052	regulation of DNA metabolic process	14	3,60E-02	11,70
3	montane	BP	GO:0002221	pattern recognition receptor signaling p...	8	3,66E-02	9,20
3	montane	BP	GO:2000082	regulation of L-ascorbic acid biosynthet...	3	3,73E-02	6,72
3	montane	BP	GO:0006116	NADH oxidation	3	3,73E-02	1,93
3	montane	BP	GO:0031648	protein destabilization	4	4,18E-02	7,36
3	montane	BP	GO:0015866	ADP transport	4	4,18E-02	10,00
3	montane	BP	GO:0048825	cotyledon development	14	4,19E-02	11,96
3	montane	BP	GO:0000184	nuclear-transcribed mRNA catabolic proce...	6	4,51E-02	8,75
3	montane	BP	GO:0016559	peroxisome fission	3	4,62E-02	8,04
3	montane	BP	GO:0043489	RNA stabilization	3	4,62E-02	6,55
3	montane	BP	GO:0006574	valine catabolic process	3	4,62E-02	6,88
3	montane	BP	GO:0010165	response to X-ray	3	4,62E-02	5,01
3	montane	BP	GO:0060151	peroxisome localization	4	4,86E-02	8,28
3	montane	BP	GO:0009750	response to fructose	7	4,95E-02	8,57
1	alpine	BP	GO:0010777	meiotic mismatch repair involved in reciprocal meiotic recombination	4	1,10E-05	-8,04
1	alpine	BP	GO:0019252	starch biosynthetic process	6	6,90E-05	-7,67
1	alpine	BP	GO:0006000	fructose metabolic process	4	1,20E-04	-3,61
1	alpine	BP	GO:0045934	negative regulation of nucleobase-containing compound metabolic process	10	1,50E-04	-9,03
1	alpine	BP	GO:0006557	S-adenosylmethioninamine biosynthetic pr...	2	1,60E-04	5,07
1	alpine	BP	GO:0007010	cytoskeleton organization	14	1,90E-04	-6,40
1	alpine	BP	GO:0042814	monopolar cell growth	3	3,00E-04	1,07
1	alpine	BP	GO:0051973	positive regulation of telomerase activi...	2	4,60E-04	-1,37
1	alpine	BP	GO:0051026	chiasma assembly	4	6,50E-04	-8,04

Table S4. ...continued.

1	alpine	BP	GO:0030187	melatonin biosynthetic process	2	9,20E-04	-0,98
1	alpine	BP	GO:0006633	fatty acid biosynthetic process	9	1,71E-03	-6,45
1	alpine	BP	GO:0099636	cytoplasmic streaming	2	2,27E-03	-5,61
1	alpine	BP	GO:0051014	actin filament severing	2	2,27E-03	-5,61
1	alpine	BP	GO:0046686	response to cadmium ion	20	2,67E-03	-7,69
1	alpine	BP	GO:0007064	mitotic sister chromatid cohesion	3	2,85E-03	-2,22
1	alpine	BP	GO:0009686	gibberellin biosynthetic process	5	3,14E-03	-6,58
1	alpine	BP	GO:0006597	spermine biosynthetic process	2	3,15E-03	5,07
1	alpine	BP	GO:0031129	inductive cell-cell signaling	2	3,15E-03	3,62
1	alpine	BP	GO:0006085	acetyl-CoA biosynthetic process	3	4,13E-03	-8,59
1	alpine	BP	GO:0045793	positive regulation of cell size	2	4,16E-03	-6,88
1	alpine	BP	GO:0006565	L-serine catabolic process	2	4,16E-03	3,88
1	alpine	BP	GO:0008295	spermidine biosynthetic process	2	4,16E-03	5,07
1	alpine	BP	GO:0019264	glycine biosynthetic process from serine	2	5,31E-03	3,88
1	alpine	BP	GO:0019915	lipid storage	2	5,31E-03	0,13
1	alpine	BP	GO:0009734	auxin-activated signaling pathway	8	5,81E-03	2,16
1	alpine	BP	GO:0006730	one-carbon metabolic process	4	6,46E-03	-2,74
1	alpine	BP	GO:0046835	carbohydrate phosphorylation	4	7,90E-03	-1,46
1	alpine	BP	GO:2000694	regulation of phragmoplast microtubule o...	2	7,97E-03	-5,24
1	alpine	BP	GO:0046655	folic acid metabolic process	2	7,97E-03	3,88
1	alpine	BP	GO:0071732	cellular response to nitric oxide	2	7,97E-03	-3,02
1	alpine	BP	GO:0048530	fruit morphogenesis	2	7,97E-03	3,62
1	alpine	BP	GO:0009920	cell plate formation involved in plant-t...	3	1,02E-02	-6,41
1	alpine	BP	GO:0080167	response to karrikin	10	1,05E-02	-1,23
1	alpine	BP	GO:0010152	pollen maturation	3	1,18E-02	-6,17
1	alpine	BP	GO:0016477	cell migration	1	1,25E-02	-2,37
1	alpine	BP	GO:0030866	cortical actin cytoskeleton organization	1	1,25E-02	-2,37

Table S4. ...continued.

1	alpine	BP	GO:0033611	oxalate catabolic process	1	1,25E-02	3,52
1	alpine	BP	GO:0034286	response to maltose	1	1,25E-02	-3,19
1	alpine	BP	GO:0007097	nuclear migration	2	1,29E-02	3,62
1	alpine	BP	GO:0033353	S-adenosylmethionine cycle	2	1,29E-02	-7,76
1	alpine	BP	GO:0019079	viral genome replication	2	1,29E-02	5,07
1	alpine	BP	GO:1905952	regulation of lipid localization	2	1,47E-02	-5,24
1	alpine	BP	GO:0010605	negative regulation of macromolecule met...	19	1,58E-02	-5,41
1	alpine	BP	GO:0048480	stigma development	2	1,67E-02	-5,24
1	alpine	BP	GO:0009835	fruit ripening	2	1,67E-02	-3,02
1	alpine	BP	GO:0080157	regulation of plant-type cell wall organ...	2	1,67E-02	-5,24
1	alpine	BP	GO:0009727	detection of ethylene stimulus	2	1,67E-02	-3,02
1	alpine	BP	GO:0010030	positive regulation of seed germination	3	1,76E-02	-0,43
1	alpine	BP	GO:0008360	regulation of cell shape	3	1,76E-02	0,12
1	alpine	BP	GO:0010482	regulation of epidermal cell division	2	1,88E-02	3,62
1	alpine	BP	GO:0000266	mitochondrial fission	2	1,88E-02	-5,24
1	alpine	BP	GO:0009738	abscisic acid-activated signaling pathwa...	9	2,07E-02	0,74
1	alpine	BP	GO:0046940	nucleoside monophosphate phosphorylation	2	2,09E-02	-5,24
1	alpine	BP	GO:0080187	floral organ senescence	2	2,09E-02	3,84
1	alpine	BP	GO:0051603	proteolysis involved in cellular protein...	7	2,16E-02	4,20
1	alpine	BP	GO:0010150	leaf senescence	8	2,25E-02	2,15
1	alpine	BP	GO:0009693	ethylene biosynthetic process	3	2,31E-02	0,16
1	alpine	BP	GO:0042128	nitrate assimilation	3	2,34E-02	6,20
1	alpine	BP	GO:0071994	phytochelatin transmembrane transport	1	2,49E-02	-3,61
1	alpine	BP	GO:0098653	centromere clustering	1	2,49E-02	-4,18
1	alpine	BP	GO:0060178	regulation of exocyst localization	1	2,49E-02	-3,26
1	alpine	BP	GO:0035999	tetrahydrofolate interconversion	2	2,56E-02	3,88
1	alpine	BP	GO:0043447	alkane biosynthetic process	2	2,56E-02	0,80

Table S4. ...continued.

1	alpine	BP	GO:0045604	regulation of epidermal cell differentia...	2	2,56E-02	3,62
1	alpine	BP	GO:0006207	'de novo' pyrimidine nucleobase biosynth...	2	2,56E-02	-5,24
1	alpine	BP	GO:0000712	resolution of meiotic recombination inte...	2	2,56E-02	-5,82
1	alpine	BP	GO:0030100	regulation of endocytosis	2	2,81E-02	-5,24
1	alpine	BP	GO:0080029	cellular response to boron-containing su...	2	3,06E-02	-5,24
1	alpine	BP	GO:0009740	gibberellic acid mediated signaling path...	4	3,44E-02	-5,65
1	alpine	BP	GO:0007568	aging	12	3,68E-02	-2,29
1	alpine	BP	GO:0015970	guanosine tetraphosphate biosynthetic pr...	1	3,71E-02	4,36
1	alpine	BP	GO:0019483	beta-alanine biosynthetic process	1	3,71E-02	-2,20
1	alpine	BP	GO:1902418	(+)-abscisic acid D-glucopyranosyl ester...	1	3,71E-02	-3,61
1	alpine	BP	GO:1900060	negative regulation of ceramide biosynth...	1	3,71E-02	-2,89
1	alpine	BP	GO:2000601	positive regulation of Arp2/3 complex-me...	1	3,71E-02	4,92
1	alpine	BP	GO:0010266	response to vitamin B1	1	3,71E-02	3,01
1	alpine	BP	GO:0006212	uracil catabolic process	1	3,71E-02	-2,20
3	alpine	BP	GO:0051865	protein autoubiquitination	2	9,10E-04	6,10
3	alpine	BP	GO:0000028	ribosomal small subunit assembly	2	1,59E-03	6,39
3	alpine	BP	GO:1905691	lipid droplet disassembly	1	6,42E-03	-1,88
3	alpine	BP	GO:0035627	ceramide transport	1	9,61E-03	-3,34
3	alpine	BP	GO:0120009	intermembrane lipid transfer	1	1,12E-02	-3,34
3	alpine	BP	GO:0019605	butyrate metabolic process	1	1,28E-02	1,60
3	alpine	BP	GO:0006083	acetate metabolic process	1	1,28E-02	1,60
3	alpine	BP	GO:0006097	glyoxylate cycle	1	1,44E-02	1,60
3	alpine	BP	GO:0043066	negative regulation of apoptotic process	1	1,76E-02	4,44

Table S4. ...continued.

3	alpine	BP	GO:0006574	valine catabolic process	1	2,07E-02	5,50
3	alpine	BP	GO:0034051	negative regulation of plant-type hypers...	1	2,07E-02	-1,65
3	alpine	BP	GO:0010366	negative regulation of ethylene biosynth...	1	2,07E-02	4,18
3	alpine	BP	GO:0019375	galactolipid biosynthetic process	1	2,23E-02	3,42
3	alpine	BP	GO:0000105	histidine biosynthetic process	1	2,23E-02	-2,39
3	alpine	BP	GO:0009938	negative regulation of gibberellic acid ...	1	3,01E-02	9,20
3	alpine	BP	GO:0010072	primary shoot apical meristem specificat...	1	3,33E-02	9,20
3	alpine	BP	GO:0031648	protein destabilization	1	3,33E-02	4,44
3	alpine	BP	GO:0046854	phosphatidylinositol phosphorylation	1	3,33E-02	5,26
3	alpine	BP	GO:0006551	leucine metabolic process	1	3,48E-02	5,50
3	alpine	BP	GO:0010336	gibberellic acid homeostasis	1	4,72E-02	9,20

Table S5. Enriched GO terms in differentially targeted genes detected in CG and that are also differentially expressed in the same environment (Szukala et al., 2022).

Ecotype pair	**GO ID**	**GO term**	**DTGs number**	**adjp-val**	**z-score**
1	GO:0009751	response to salicylic acid	19	7,60E-05	4,54
1	GO:0002229	**defense response to oomycetes**	8	3,60E-04	4,57
1	GO:0042742	**defense response to bacterium**	31	8,00E-04	5,74
1	GO:0016441	**posttranscriptional gene silencing**	5	1,18E-03	7,02
1	GO:0030026	**cellular manganese ion homeostasis**	3	1,88E-03	1,04
1	GO:1990388	xylem-to-phloem iron transport	2	1,94E-03	1,60
1	GO:0009627	**systemic acquired resistance**	10	2,12E-03	0,01
1	GO:0010037	response to carbon dioxide	4	2,31E-03	-3,30
1	GO:0033617	mitochondrial respiratory chain complex „,	3	2,81E-03	1,60

Table S5. ...continued.

1	GO:0009626	**plant-type hypersensitive response**	8	2,90E-03	3,48
1	GO:0047484	**regulation of response to osmotic stress**	5	3,36E-03	4,74
1	GO:1990619	**histone H3-K9 deacetylation**	2	4,73E-03	8,69
1	GO:0009807	lignan biosynthetic process	2	4,73E-03	-0,39
1	GO:0042908	xenobiotic transport	4	6,44E-03	7,84
1	GO:0010193	**response to ozone**	6	7,05E-03	7,20
1	GO:0080170	hydrogen peroxide transmembrane transpor,,,	3	7,14E-03	-1,85
1	GO:0042631	**cellular response to water deprivation**	6	7,42E-03	0,49
1	GO:0015692	lead ion transport	3	8,10E-03	4,77
1	GO:1902459	positive regulation of stem cell populat,,,	2	8,62E-03	8,69
1	GO:0006875	cellular metal ion homeostasis	8	1,32E-02	6,57
1	GO:0006145	purine nucleobase catabolic process	2	1,35E-02	5,11
1	GO:2000122	**negative regulation of stomatal complex ,,,**	2	1,35E-02	-2,04
1	GO:0080168	abscisic acid transport	3	1,54E-02	4,77
1	GO:0071732	cellular response to nitric oxide	2	1,63E-02	-3,72
1	GO:0016052	carbohydrate catabolic process	8	1,81E-02	4,34
1	GO:0015727	lactate transport	1	1,82E-02	1,29
1	GO:1902553	positive regulation of catalase activity	1	1,82E-02	-3,68
1	GO:0031347	**regulation of defense response**	15	1,83E-02	9,64
1	GO:0009409	**response to cold**	21	1,92E-02	4,07
1	GO:0010466	negative regulation of peptidase activit,,,	2	1,94E-02	2,02
1	GO:0055072	**iron ion homeostasis**	7	1,96E-02	4,39
1	GO:0043170	macromolecule metabolic process	122	2,01E-02	8,04
1	GO:0006265	DNA topological change	2	2,26E-02	-3,47
1	GO:0090333	**regulation of stomatal closure**	6	2,34E-02	0,95

Table S5. ...continued.

1	GO:0019432	triglyceride biosynthetic process	3	2,36E-02	3,46
1	GO:0071483	**cellular response to blue light**	4	2,59E-02	5,10
1	GO:0009854	oxidative photosynthetic carbon pathway	2	2,61E-02	2,76
1	GO:0010152	pollen maturation	3	3,16E-02	4,34
1	GO:0050832	**defense response to fungus**	15	3,40E-02	2,53
1	GO:0033473	indoleacetic acid conjugate metabolic pr,,,	1	3,61E-02	-6,51
1	GO:0072489	methylammonium transmembrane transport	1	3,61E-02	-1,49
1	GO:0035444	nickel cation transmembrane transport	1	3,61E-02	2,22
1	GO:0006069	ethanol oxidation	1	3,61E-02	1,92
1	GO:0006784	heme a biosynthetic process	1	3,61E-02	3,64
1	GO:0062034	L-pipecolic acid biosynthetic process	1	3,61E-02	1,35
1	GO:0055068	cobalt ion homeostasis	1	3,61E-02	2,22
1	GO:0006824	cobalt ion transport	1	3,61E-02	2,22
1	GO:0019236	response to pheromone	1	3,61E-02	-1,03
1	GO:0071461	cellular response to redox state	1	3,61E-02	5,95
1	GO:2000604	negative regulation of secondary growth	1	3,61E-02	-5,20
1	GO:0006435	threonyl-tRNA aminoacylation	1	3,61E-02	5,47
1	GO:1903647	negative regulation of chlorophyll catab,,,	1	3,61E-02	-2,84
1	GO:0015996	chlorophyll catabolic process	3	3,74E-02	-8,03
1	GO:0055062	**phosphate ion homeostasis**	3	3,84E-02	-4,00
1	GO:0010030	positive regulation of seed germination	3	4,59E-02	3,95
1	GO:0010304	**PSII associated light-harvesting complex,,,**	2	4,62E-02	-2,26
1	GO:0006826	iron ion transport	5	4,99E-02	2,03
3	GO:0010193	**response to ozone**	7	1,50E-07	4,10
3	GO:0009695	**jasmonic acid biosynthetic process**	3	2,20E-03	-6,01

Table S5. ...continued.

3	GO:0033617	**mitochondrial respiratory chain complex „,,**	2	2,20E-03	0,42
3	GO:1901140	p-coumaryl alcohol transport	2	2,20E-03	8,64
3	GO:0055070	copper ion homeostasis	2	3,40E-03	0,42
3	GO:0009643	**photosynthetic acclimation**	2	3,70E-03	0,63
3	GO:0080051	cutin transport	2	4,10E-03	8,64
3	GO:0000379	tRNA-type intron splice site recognition„,,	1	4,40E-03	-3,19
3	GO:0015692	lead ion transport	2	4,50E-03	8,64
3	GO:0080086	stamen filament development	2	5,70E-03	-3,25
3	GO:0080168	abscisic acid transport	2	7,00E-03	8,64
3	GO:0051455	attachment of spindle microtubules to ki„,,	1	8,70E-03	2,64
3	GO:0034063	stress granule assembly	2	9,60E-03	6,38
3	GO:0010597	green leaf volatile biosynthetic process	2	1,01E-02	-3,25
3	GO:0009901	anther dehiscence	2	1,19E-02	-3,25
3	GO:0034605	**cellular response to heat**	3	1,25E-02	7,36
3	GO:2000685	positive regulation of cellular response„,,	1	1,30E-02	3,20
3	GO:0042797	tRNA transcription by RNA polymerase III	1	1,30E-02	-3,04
3	GO:1904975	response to bleomycin	1	1,30E-02	3,20
3	GO:0042908	xenobiotic transport	2	1,37E-02	8,64
3	GO:0006629	lipid metabolic process	8	1,48E-02	-2,33
3	GO:0051754	meiotic sister chromatid cohesion, centr„,,	1	1,73E-02	2,64
3	GO:0061387	regulation of extent of cell growth	1	1,73E-02	4,94
3	GO:1904526	regulation of microtubule binding	1	1,73E-02	2,31
3	GO:0009644	**response to high light intensity**	4	2,10E-02	-1,77
3	GO:0071555	cell wall organization	6	2,41E-02	1,26
3	GO:0010496	intercellular transport	2	2,56E-02	8,64
3	GO:0051174	regulation of phosphorus metabolic proce„,,	2	2,57E-02	-0,62

Table S5. ...continued.

3	GO:0015739	sialic acid transport	1	2,59E-02	5,38
3	GO:0015074	DNA integration	1	2,59E-02	3,20
3	GO:2001108	positive regulation of Rho guanyl-nucleo„,,	1	3,01E-02	3,70
3	GO:0090332	**stomatal closure**	3	3,03E-02	5,28
3	GO:0019605	butyrate metabolic process	1	3,43E-02	3,58
3	GO:0006432	phenylalanyl-tRNA aminoacylation	1	3,43E-02	-3,79
3	GO:0033198	response to ATP	1	3,85E-02	-2,94
3	GO:0034982	mitochondrial protein processing	1	3,85E-02	1,80
3	GO:1901141	regulation of lignin biosynthetic proces„,,	2	4,23E-02	8,64
3	GO:0071492	**cellular response to UV-A**	1	4,27E-02	3,73
3	GO:0006360	**transcription by RNA polymerase I**	1	4,27E-02	-3,04
3	GO:0055073	**cadmium ion homeostasis**	1	4,27E-02	-2,92
3	GO:0009611	**response to wounding**	6	4,34E-02	-4,98
3	GO:0042868	**antisense RNA metabolic process**	1	4,69E-02	-2,84
3	GO:0002679	**respiratory burst involved in defense re„,,**	1	4,69E-02	-2,94
3	GO:0042754	**negative regulation of circadian rhythm**	1	4,69E-02	2,79
3	GO:0009617	**response to bacterium**	6	4,69E-02	-0,75
4	GO:0016104	triterpenoid biosynthetic process	3	7,00E-04	6,10
4	GO:0006824	cobalt ion transport	2	7,80E-04	10,68
4	GO:0035444	nickel cation transmembrane transport	2	7,80E-04	10,68
4	GO:0055068	cobalt ion homeostasis	2	7,80E-04	10,68
4	GO:0050832	**defense response to fungus**	27	1,60E-03	7,18
4	GO:0015936	coenzyme A metabolic process	3	2,29E-03	0,93
4	GO:0060560	developmental growth involved in morphog„,,	20	2,34E-03	-4,00
4	GO:0019287	isopentenyl diphosphate biosynthetic pro„,,	4	3,92E-03	-0,60

Table S5. ...continued.

4	GO:0033512	L-lysine catabolic process to acetyl-CoA,,,	2	4,50E-03	-2,34
4	GO:0033214	iron assimilation by chelation and trans,,,	3	5,03E-03	5,90
4	GO:0050829	**defense response to Gram-negative bacter,,,**	5	6,68E-03	-3,40
4	GO:0015746	citrate transport	2	7,36E-03	5,27
4	GO:0010037	response to carbon dioxide	4	7,67E-03	-0,49
4	GO:0042372	phylloquinone biosynthetic process	3	9,25E-03	5,15
4	GO:0080156	mitochondrial mRNA modification	6	9,46E-03	-4,59
4	GO:0016106	sesquiterpenoid biosynthetic process	4	1,08E-02	1,03
4	GO:0019285	glycine betaine biosynthetic process fro,,,	2	1,08E-02	3,40
4	GO:0009617	**response to bacterium**	42	1,23E-02	9,10
4	GO:0044257	cellular protein catabolic process	18	1,49E-02	-3,62
4	GO:2000185	regulation of phosphate transmembrane tr,,,	2	1,49E-02	-5,33
4	GO:0010304	**PSII associated light-harvesting complex,,,**	3	1,51E-02	-1,52
4	GO:0006879	**cellular iron ion homeostasis**	9	1,68E-02	11,58
4	GO:0009768	**photosynthesis, light harvesting in phot,,,**	3	1,73E-02	2,51
4	GO:0018298	**protein-chromophore linkage**	4	1,75E-02	2,99
4	GO:0006083	acetate metabolic process	2	1,95E-02	-4,72
4	GO:0019605	butyrate metabolic process	2	1,95E-02	-4,72
4	GO:1901045	negative regulation of oviposition	2	1,95E-02	2,68
4	GO:0060776	simple leaf morphogenesis	2	1,95E-02	-4,71
4	GO:0106146	sideretin biosynthesis	2	1,95E-02	2,68
4	GO:0070534	protein K63-linked ubiquitination	3	1,98E-02	-0,86
4	GO:0010027	**thylakoid membrane organization**	6	2,44E-02	-2,24
4	GO:0006097	glyoxylate cycle	2	2,46E-02	-4,72

Table S5. ...continued.

4	GO:0051762	sesquiterpene biosynthetic process	2	2,46E-02	-1,94
4	GO:0071281	cellular response to iron ion	2	2,46E-02	2,68
4	GO:0042908	xenobiotic transport	4	2,70E-02	4,04
4	GO:0000454	**snoRNA guided rRNA pseudouridine synthes„,,**	1	2,79E-02	1,20
4	GO:0097549	**chromatin organization involved in negat„,,**	1	2,79E-02	-2,62
4	GO:0010421	hydrogen peroxide-mediated programmed ce„,,	1	2,79E-02	6,45
4	GO:0006182	cGMP biosynthetic process	1	2,79E-02	-1,87
4	GO:0033396	beta-alanine biosynthetic process via 3-„,,	1	2,79E-02	2,92
4	GO:0016049	cell growth	23	2,84E-02	-5,96
4	GO:2000122	**negative regulation of stomatal complex „,,**	2	3,02E-02	3,32
4	GO:1904821	chloroplast disassembly	2	3,02E-02	0,52
4	GO:0010106	**cellular response to iron ion starvation**	2	3,02E-02	10,68
4	GO:0009809	lignin biosynthetic process	12	3,07E-02	7,90
4	GO:0008285	negative regulation of cell proliferatio„,,	5	3,11E-02	-1,81
4	GO:0055078	**sodium ion homeostasis**	3	3,16E-02	-3,15
4	GO:1900367	**positive regulation of defense response „,,**	3	3,16E-02	3,55
4	GO:0010205	**photoinhibition**	3	3,50E-02	-1,52
4	GO:0010345	suberin biosynthetic process	4	3,64E-02	-1,84
4	GO:0048564	**photosystem I assembly**	3	3,86E-02	-1,52
4	GO:0010187	negative regulation of seed germination	4	4,17E-02	5,94
4	GO:0010777	meiotic mismatch repair involved in reci„,,	2	4,27E-02	4,70
4	GO:0009911	positive regulation of flower developmen„,,	6	4,39E-02	-2,38
5	GO:0098734	macromolecule depalmitoylation	1	1,60E-02	-5,96

Table S5. ...continued.

5	GO:0009871	**jasmonic acid and ethylene-dependent sys...**	1	2,92E-02	3,32
5	GO:0010930	**negative regulation of auxin mediated si...**	1	3,89E-02	0,52
5	GO:0009866	**induced systemic resistance, ethylene me...**	1	6,46E-02	10,68
5	GO:0071588	hydrogen peroxide mediated signaling pat...	1	6,46E-02	7,9
5	GO:0010597	green leaf volatile biosynthetic process	1	1,13E-01	-1,81
5	GO:0009862	**systemic acquired resistance, salicylic ...**	1	1,19E-01	-3,15
5	GO:0009410	**response to xenobiotic stimulus**	1	1,23E-01	3,55
5	GO:0010187	negative regulation of seed germination	1	1,51E-01	-1,52
5	GO:0030968	endoplasmic reticulum unfolded protein r...	1	1,65E-01	-1,84
5	GO:0050832	**defense response to fungus**	2	1,68E-01	-1,52
5	GO:0015706	nitrate transport	1	2,34E-01	5,94
5	GO:0042938	dipeptide transport	1	2,38E-01	4,7
5	GO:0009059	macromolecule biosynthetic process	2	2,74E-01	-2,38
5	GO:0042026	protein refolding	1	2,82E-01	-1,52
5	GO:0051085	chaperone cofactor-dependent protein ref...	1	2,88E-01	-2,38
5	GO:0030433	ubiquitin-dependent ERAD pathway	1	2,94E-01	-1,84
5	GO:0009627	**systemic acquired resistance**	2	3,35E-01	-1,52

Table S6. Genes related to trichome formations found to be differentially targeted and expressed in CG.

Ecotype pair	**environment**	**gene**	**protein ID**	**GO terms**	**GO IDs**

Table S6. ...continued.

1 / 4	CG / CG	HELPU_021926	enolase (2-phospho-D-glycerate hydroylase)	phosphopyruvate hydratase complex, nucleus, chloroplast stroma, magnesium ion binding, transcription coregulator activity, phosphopyruvate hydratase activity, protein binding, glycolytic process, regulation of transcription, DNA-templated, response to abscisic acid, trichome morphogenesis, regulation of vacuole fusion, non-autophagic	GO:0000015, GO:0005634, GO:0009570, GO:0000287, GO:0003712, GO:0004634, GO:0005515, GO:0006096, GO:0006355, GO:0009737, GO:0010090, GO:0032889
1 / 3 / 1	CG / CG / RT_dw	HELPU_017437	homeodomain GLABROUS 2	nucleus, transcription cis-regulatory region binding, DNA-binding transcription factor activity, protein binding, plant-type cell wall loosening, trichome branching, maintenance of floral organ identity, regulation of post-embryonic development	GO:0005634, GO:0000976, GO:0003700, GO:0005515, GO:0009828, GO:0010091, GO:0048497, GO:0048580
4	CG	HELPU_007108	AAA-type ATPase family protein	nucleus, multivesicular body, plasmodesma, microtubule cytoskeleton, protein binding,ATP binding, microtubule-severing ATPase activity, hydrolase activity,endosome organization, vacuole organization, multidimensional cell growth, plant-type cell wall biogenesis, trichome branching, endosomal transport, cortical microtubule organization,negative regulation of reciprocal meiotic recombination, microtubule severing, potassium ion homeostasis, sodium ion homeostasis	GO:0005634, GO:0005771, GO:0009506, GO:0015630, GO:0005515, GO:0005524, GO:0008568, GO:0016787, GO:0007032, GO:0007033, GO:0009825, GO:0009832, GO:0010091, GO:0016197, GO:0043622, GO:0045128, GO:0051013, GO:0055075, GO:0055078

Table S6. ...continued.

4	CG	HELPU_020641	filament-like protein (DUF869)	plasma membrane, cortical microtubule, microtubule binding, trichome morphogenesis, microtubule polymerization	GO:0005886, GO:0055028, GO:0008017, GO:0010090, GO:0046785
4 / 1	CG / RT_up	HELPU_017210	basic helix-loop-helix (bHLH) DNA-binding superfamily protein	nucleus,transcription cis-regulatory region binding,DNA-binding transcription factor activity,protein binding,regulation of transcription, DNA-templated,jasmonic acid mediated signaling pathway,epidermal cell fate specification,trichome branching,seed coat development,positive regulation of anthocyanin biosynthetic process,regulation of proanthocyanidin biosynthetic process	GO:0005634, GO:0000976, GO:0003700, GO:0005515, GO:0006355, GO:0009867, GO:0009957, GO:0010091, GO:0010214, GO:0031542, GO:2000029
1	RT_dw	HELPU_017457	Protein kinase family protein	nucleoplasm,peroxisome, cytosol, endomembrane system, cell periphery, nucleotide binding, protein serine/threonine kinase activity, GTPase binding, trichome branching, protein autophosphorylation, defense response to fungus, cellular response to ethylene stimulus	GO:0005654, GO:0005777, GO:0005829, GO:0012505, GO:0071944, GO:0000166, GO:0004674, GO:0051020, GO:0010091, GO:0046777, GO:0050832, GO:0071369

Table S6. ...continued.

3	RT_dw	HELPU_008597	phytochrome and flowering time regulatory protein (PFT1)	mediator complex,DNA binding,protein binding,red, far-red light phototransduction,jasmonic acid mediated signaling pathway,positive regulation of flower development,trichome branching,response to red light,response to far red light,positive regulation of defense response,positive regulation of transcription, DNA-templated,defense response to fungus,trichome papilla formation	GO:0016592, GO:0003677, GO:0005515, GO:0009585, GO:0009867, GO:0009911, GO:0010091, GO:0010114, GO:0010218, GO:0031349, GO:0045893, GO:0050832, GO:1905499
3	RT_dw	HELPU_022480	MYB transcription factor	response to karrikin, transcription cis-regulatory region binding, trichome morphogenesis, root hair cell differentiation, jasmonic acid mediated signaling pathway, response to ethylene, sucrose mediated signaling, response to auxin, nucleus, DNA-binding transcription factor activity, protein binding, response to oomycetes, positive regulation of transcription, DNA-templated, removal of superoxide radicals, mucilage biosynthetic process involved in seed coat development, cell fate commitment, positive regulation of anthocyanin biosynthetic process	GO:0080167, GO:0000976, GO:0010090, GO:0048765, GO:0009867, GO:0009723, GO:0009745, GO:0009733, GO:0005634, GO:0003700, GO:0005515, GO:0002239, GO:0045893, GO:0019430, GO:0048354, GO:0045165, GO:0031542

Table S7. Enriched GO terms in differentially targeted genes detected in RT and that are also differentially expressed in the same environment(Chapter 2 of this thesis).

Ecotype pair	**Growing site**	**GO ID**	**GO term**	**DTGs number**	**adjp-val**
1	dw	GO:0071555	cell wall organization	13	6,00E-04
1	dw	GO:0042343	indole glucosinolate metabolic process	4	1,70E-03
1	dw	GO:0009611	response to wounding	13	2,90E-03
1	dw	GO:0033198	response to ATP	2	3,40E-03
1	dw	GO:0009414	**response to water deprivation**	18	4,40E-03
1	dw	GO:0071577	zinc ion transmembrane transport	2	7,30E-03
1	dw	GO:0010037	response to carbon dioxide	3	9,60E-03
1	dw	GO:0009051	pentose-phosphate shunt, oxidative branc„,	2	9,70E-03
1	dw	GO:0006012	galactose metabolic process	2	9,70E-03
1	dw	GO:0042183	formate catabolic process	1	1,01E-02
1	dw	GO:0033617	mitochondrial respiratory chain complex „,	2	1,10E-02
1	dw	GO:0098542	**defense response to other organism**	30	1,13E-02
1	dw	GO:0072593	reactive oxygen species metabolic proces„,	6	1,15E-02
1	dw	GO:0009409	**response to cold**	15	1,21E-02
1	dw	GO:0009294	DNA mediated transformation	4	1,29E-02
1	dw	GO:0045493	xylan catabolic process	2	1,38E-02
1	dw	GO:1900366	**negative regulation of defense response „,**	2	1,38E-02
1	dw	GO:0009828	plant-type cell wall loosening	3	1,38E-02
1	dw	GO:0010193	**response to ozone**	4	1,44E-02
1	dw	GO:0055070	copper ion homeostasis	2	1,69E-02
1	dw	GO:0016441	**posttranscriptional gene silencing**	3	1,70E-02
1	dw	GO:0009408	**response to heat**	10	1,75E-02
1	dw	GO:0006226	dUMP biosynthetic process	1	2,00E-02
1	dw	GO:0046081	dUTP catabolic process	1	2,00E-02
1	dw	GO:0010335	response to non-ionic osmotic stress	1	2,00E-02
1	dw	GO:0080167	response to karrikin	8	2,13E-02
1	dw	GO:0097502	mannosylation	2	2,59E-02
1	dw	GO:0009617	**response to bacterium**	23	2,91E-02
1	dw	GO:0042742	**defense response to bacterium**	16	2,94E-02
1	dw	GO:0034355	NAD salvage	1	2,99E-02
1	dw	GO:0032366	intracellular sterol transport	1	2,99E-02
1	dw	GO:0015970	guanosine tetraphosphate biosynthetic pr„,	1	2,99E-02
1	dw	GO:0071275	cellular response to aluminum ion	1	2,99E-02

Table S7. ...continued.

1	dw	GO:0051973	**positive regulation of telomerase activi„,,**	1	2,99E-02
1	dw	GO:0009788	**negative regulation of abscisic acid-act„,,**	4	3,20E-02
1	dw	GO:0006970	**response to osmotic stress**	23	3,33E-02
1	dw	GO:0090333	**regulation of stomatal closure**	4	3,37E-02
1	dw	GO:0050832	**defense response to fungus**	11	3,40E-02
1	dw	GO:0009058	biosynthetic process	52	3,49E-02
1	dw	GO:0001666	response to hypoxia	5	3,52E-02
1	dw	GO:0034220	ion transmembrane transport	14	3,58E-02
1	dw	GO:0006730	one-carbon metabolic process	2	3,63E-02
1	dw	GO:0007231	osmosensory signaling pathway	2	3,63E-02
1	dw	GO:0060862	negative regulation of floral organ absc„,	1	3,96E-02
1	dw	GO:0019481	L-alanine catabolic process, by transami„,	1	3,96E-02
1	dw	GO:0006788	heme oxidation	1	3,96E-02
1	dw	GO:0050992	dimethylallyl diphosphate biosynthetic p„,	1	3,96E-02
1	dw	GO:0006384	**transcription initiation from RNA polyme„,**	1	3,96E-02
1	dw	GO:0008615	pyridoxine biosynthetic process	1	3,96E-02
1	dw	GO:0010124	phenylacetate catabolic process	1	3,96E-02
1	dw	GO:0010111	glyoxysome organization	1	3,96E-02
1	dw	GO:0015671	oxygen transport	1	3,96E-02
1	dw	GO:0009651	**response to salt stress**	16	4,05E-02
1	dw	GO:0031408	oxylipin biosynthetic process	2	4,09E-02
1	dw	GO:0070301	cellular response to hydrogen peroxide	2	4,09E-02
1	dw	GO:0010411	xyloglucan metabolic process	3	4,52E-02
1	dw	GO:0019432	triglyceride biosynthetic process	2	4,57E-02
1	dw	GO:0010027	thylakoid membrane organization	3	4,67E-02
1	dw	GO:0019632	shikimate metabolic process	1	4,93E-02
1	dw	GO:0098734	macromolecule depalmitoylation	1	4,93E-02
1	dw	GO:0006516	glycoprotein catabolic process	1	4,93E-02
1	up	GO:0009414	**response to water deprivation**	7	3,50E-03
1	up	GO:0009407	toxin catabolic process	2	5,20E-03
1	up	GO:1990573	potassium ion import across plasma membr„,	2	5,40E-03
1	up	GO:0010203	**response to very low fluence red light s„,**	1	7,00E-03

Table S7. ...continued.

1	up	GO:0009409	**response to cold**	6	7,20E-03
1	up	GO:0006384	transcription initiation from RNA polyme„,	1	9,30E-03
1	up	GO:0060862	negative regulation of floral organ absc„,	1	9,30E-03
1	up	GO:0019632	shikimate metabolic process	1	1,17E-02
1	up	GO:2000029	regulation of proanthocyanidin biosynthe„,	1	1,17E-02
1	up	GO:0006516	glycoprotein catabolic process	1	1,17E-02
1	up	GO:0055129	L-proline biosynthetic process	1	1,40E-02
1	up	GO:1990619	**histone H3-K9 deacetylation**	1	1,40E-02
1	up	GO:0010201	**response to continuous far red light sti„,**	1	1,40E-02
1	up	GO:0031542	**positive regulation of anthocyanin biosy„,**	1	1,63E-02
1	up	GO:1902000	homogentisate catabolic process	1	1,63E-02
1	up	GO:0071491	**cellular response to red light**	2	1,81E-02
1	up	GO:0009957	epidermal cell fate specification	1	1,86E-02
1	up	GO:0043693	monoterpene biosynthetic process	1	1,86E-02
1	up	GO:0032091	negative regulation of protein binding	1	1,86E-02
1	up	GO:1902459	positive regulation of stem cell populat„,	1	1,86E-02
1	up	GO:0071492	**cellular response to UV-A**	1	2,32E-02
1	up	GO:1901672	positive regulation of systemic acquired„,	1	2,32E-02
1	up	GO:0016139	glycoside catabolic process	1	2,55E-02
1	up	GO:0002230	**positive regulation of defense response „,**	1	2,55E-02
1	up	GO:0034052	**positive regulation of plant-type hypers„,**	1	2,78E-02
1	up	GO:0046256	2,4,6-trinitrotoluene catabolic process	1	2,78E-02
1	up	GO:1902290	**positive regulation of defense response „,**	1	2,78E-02
1	up	GO:0071483	**cellular response to blue light**	2	3,16E-02
1	up	GO:0090333	**regulation of stomatal closure**	2	3,26E-02
1	up	GO:0045892	**negative regulation of transcription, DN„,**	4	3,38E-02
1	up	GO:0071486	**cellular response to high light intensit„,**	1	3,46E-02
1	up	GO:0033617	mitochondrial respiratory chain complex „,	1	3,69E-02

Table S7. ...continued.

1	up	GO:0010262	somatic embryogenesis	1	3,91E-02
1	up	GO:0006656	phosphatidylcholine biosynthetic process	1	4,37E-02
1	up	GO:0055070	copper ion homeostasis	1	4,59E-02
1	up	GO:0043447	alkane biosynthetic process	1	4,59E-02
1	up	GO:1902458	**positive regulation of stomatal opening**	1	4,81E-02
3	dw	GO:0009809	lignin biosynthetic process	10	6,30E-05
3	dw	GO:0009611	**response to wounding**	15	7,80E-05
3	dw	GO:0072718	response to cisplatin	2	8,70E-05
3	dw	GO:0006145	purine nucleobase catabolic process	3	9,20E-05
3	dw	GO:0009753	**response to jasmonic acid**	12	7,10E-04
3	dw	GO:0010496	intercellular transport	4	1,77E-03
3	dw	GO:0010136	ureide catabolic process	2	1,78E-03
3	dw	GO:0010193	**response to ozone**	5	1,81E-03
3	dw	GO:0042631	**cellular response to water deprivation**	5	1,90E-03
3	dw	GO:0019605	butyrate metabolic process	2	2,36E-03
3	dw	GO:0080168	abscisic acid transport	3	2,47E-03
3	dw	GO:0010114	**response to red light**	6	2,79E-03
3	dw	GO:0010597	green leaf volatile biosynthetic process	3	4,25E-03
3	dw	GO:0042754	**negative regulation of circadian rhythm**	2	4,55E-03
3	dw	GO:0010321	regulation of vegetative phase change	2	6,37E-03
3	dw	GO:0010264	myo-inositol hexakisphosphate biosynthet„,	2	6,37E-03
3	dw	GO:1905177	tracheary element differentiation	3	7,10E-03
3	dw	GO:0071230	cellular response to amino acid stimulus	2	7,38E-03
3	dw	GO:0009759	indole glucosinolate biosynthetic proces„,	2	8,47E-03
3	dw	GO:0050832	**defense response to fungus**	11	9,02E-03
3	dw	GO:0016054	organic acid catabolic process	3	9,37E-03
3	dw	GO:0015727	lactate transport	1	9,38E-03
3	dw	GO:0097056	selenocysteinyl-tRNA(Sec) biosynthetic p„,	1	9,38E-03
3	dw	GO:0016480	**negative regulation of transcription by „,**	1	9,38E-03
3	dw	GO:0048700	**acquisition of desiccation tolerance in „,**	1	9,38E-03
3	dw	GO:1901140	p-coumaryl alcohol transport	2	9,62E-03
3	dw	GO:0048830	**adventitious root development**	2	9,62E-03
3	dw	GO:0040009	regulation of growth rate	2	1,08E-02
3	dw	GO:0042128	**nitrate assimilation**	3	1,09E-02

Table S7. ...continued.

3	dw	GO:0055085	**transmembrane transport**	26	1,25E-02
3	dw	GO:0060919	**auxin influx**	3	1,33E-02
3	dw	GO:0010183	pollen tube guidance	3	1,41E-02
3	dw	GO:0009723	**response to ethylene**	7	1,74E-02
3	dw	GO:0080051	cutin transport	2	1,79E-02
3	dw	GO:0009617	**response to bacterium**	20	1,86E-02
3	dw	GO:0050482	arachidonic acid secretion	1	1,87E-02
3	dw	GO:0042989	sequestering of actin monomers	1	1,87E-02
3	dw	GO:0044648	**histone H3-K4 dimethylation**	1	1,87E-02
3	dw	GO:0072702	**response to methyl methanesulfonate**	1	1,87E-02
3	dw	GO:0070158	**mitochondrial seryl-tRNA aminoacylation**	1	1,87E-02
3	dw	GO:0033194	response to hydroperoxide	1	1,87E-02
3	dw	GO:0051555	**flavonol biosynthetic process**	3	1,92E-02
3	dw	GO:0015692	lead ion transport	2	1,94E-02
3	dw	GO:0007064	mitotic sister chromatid cohesion	2	1,94E-02
3	dw	GO:0009408	**response to heat**	9	2,21E-02
3	dw	GO:0009734	**auxin-activated signaling pathway**	6	2,24E-02
3	dw	GO:0009684	indoleacetic acid biosynthetic process	2	2,28E-02
3	dw	GO:0098739	import across plasma membrane	5	2,55E-02
3	dw	GO:0048527	**lateral root development**	8	2,58E-02
3	dw	GO:0043982	**histone H4-K8 acetylation**	1	2,79E-02
3	dw	GO:0043983	**histone H4-K12 acetylation**	1	2,79E-02
3	dw	GO:0043987	**histone H3-S10 phosphorylation**	1	2,79E-02
3	dw	GO:0043988	**histone H3-S28 phosphorylation**	1	2,79E-02
3	dw	GO:0010422	regulation of brassinosteroid biosynthet,,,	1	2,79E-02
3	dw	GO:0046110	xanthine metabolic process	1	2,79E-02
3	dw	GO:0009964	**negative regulation of flavonoid biosynt,,,**	1	2,79E-02
3	dw	GO:0001666	**response to hypoxia**	4	3,00E-02
3	dw	GO:0030007	**cellular potassium ion homeostasis**	2	3,01E-02
3	dw	GO:0007568	aging	4	3,07E-02
3	dw	GO:0070301	cellular response to hydrogen peroxide	2	3,61E-02
3	dw	GO:0000256	allantoin catabolic process	1	3,70E-02
3	dw	GO:0030187	melatonin biosynthetic process	1	3,70E-02

Table S7. ...continued.

3	dw	GO:1901017	**negative regulation of potassium ion tra„,,**	1	3,70E-02
3	dw	GO:0043968	**histone H2A acetylation**	1	3,70E-02
3	dw	GO:0048354	mucilage biosynthetic process involved i„,,	2	3,82E-02
3	dw	GO:0032259	**methylation**	5	4,04E-02
3	dw	GO:0006850	mitochondrial pyruvate transmembrane tra„,,	1	4,60E-02
3	dw	GO:0042554	superoxide anion generation	1	4,60E-02
3	dw	GO:0046622	positive regulation of organ growth	1	4,60E-02
3	dw	GO:0060359	response to ammonium ion	1	4,60E-02
3	dw	GO:0046168	glycerol-3-phosphate catabolic process	1	4,60E-02
3	dw	GO:0010230	alternative respiration	1	4,60E-02
3	dw	GO:0009745	sucrose mediated signaling	1	4,60E-02
3	dw	GO:0052544	**defense response by callose deposition i„,,**	2	4,93E-02
3	up	GO:0006065	UDP-glucuronate biosynthetic process	1	8,30E-03
3	up	GO:0006024	glycosaminoglycan biosynthetic process	1	8,30E-03
3	up	GO:0033528	S-methylmethionine cycle	1	8,30E-03
3	up	GO:1905691	lipid droplet disassembly	1	8,30E-03
3	up	GO:0010951	negative regulation of endopeptidase act„,,	1	8,30E-03
3	up	GO:0035019	somatic stem cell population maintenance	1	1,24E-02
3	up	GO:0019285	glycine betaine biosynthetic process fro„,,	1	1,24E-02
3	up	GO:0015720	allantoin transport	1	1,45E-02
3	up	GO:0010589	leaf proximal/distal pattern formation	1	1,45E-02
3	up	GO:0018874	benzoate metabolic process	1	1,45E-02
3	up	GO:0043100	pyrimidine nucleobase salvage	1	1,65E-02
3	up	GO:0006432	phenylalanyl-tRNA aminoacylation	1	1,65E-02
3	up	GO:0071918	urea transmembrane transport	1	1,65E-02
3	up	GO:1904821	chloroplast disassembly	1	2,06E-02
3	up	GO:0071475	**cellular hyperosmotic salinity response**	1	2,26E-02
3	up	GO:1903791	uracil transmembrane transport	1	2,47E-02
3	up	GO:1990822	basic amino acid transmembrane transport	1	2,47E-02
3	up	GO:0033214	iron assimilation by chelation and trans„,,	1	2,67E-02
3	up	GO:0046482	para-aminobenzoic acid metabolic process	1	2,67E-02

Table S7. ...continued.

3	up	GO:0010264	myo-inositol hexakisphosphate biosynthet„,,	1	2,67E-02
3	up	GO:0080024	indolebutyric acid metabolic process	1	2,87E-02
3	up	GO:0048830	adventitious root development	1	3,27E-02
3	up	GO:0015809	arginine transport	1	3,27E-02
3	up	GO:0045814	**negative regulation of gene expression, „,,**	2	3,45E-02
3	up	GO:1902183	regulation of shoot apical meristem deve„,,	1	3,47E-02
3	up	GO:1900366	**negative regulation of defense response „,,**	1	3,68E-02
3	up	GO:0010077	maintenance of inflorescence meristem id„,,	1	3,68E-02
3	up	GO:0010586	miRNA metabolic process	1	3,88E-02
3	up	GO:0015808	L-alanine transport	1	3,88E-02
3	up	GO:0110126	phloem loading	1	4,08E-02
3	up	GO:0006614	SRP-dependent cotranslational protein ta„,,	1	4,28E-02
3	up	GO:0009616	**virus induced gene silencing**	1	4,47E-02
3	up	GO:0071219	**cellular response to molecule of bacteri„,,**	1	5,07E-02
3	up	GO:0098712	L-glutamate import across plasma membran„,,	1	5,07E-02
3	up	GO:0071323	cellular response to chitin	1	5,86E-02
3	up	GO:0010582	floral meristem determinacy	1	6,25E-02
3	up	GO:1900865	chloroplast RNA modification	1	6,25E-02
3	up	GO:0009086	methionine biosynthetic process	1	6,25E-02
3	up	GO:0070301	cellular response to hydrogen peroxide	1	6,44E-02
3	up	GO:0042343	indole glucosinolate metabolic process	1	7,80E-02
3	up	GO:1905177	tracheary element differentiation	1	8,37E-02
3	up	GO:0050829	**defense response to Gram-negative bacter„,,**	1	8,56E-02
3	up	GO:0002213	**defense response to insect**	2	8,69E-02
3	up	GO:0048658	anther wall tapetum development	1	8,76E-02
3	up	GO:0016226	iron-sulfur cluster assembly	1	8,95E-02
3	up	GO:0034614	cellular response to reactive oxygen spe„,,	2	9,24E-02
3	up	GO:0009934	regulation of meristem structural organi„,,	1	1,03E-01
3	up	GO:0010212	response to ionizing radiation	1	1,05E-01
3	up	GO:0010183	pollen tube guidance	1	1,06E-01
3	up	GO:0006995	**cellular response to nitrogen starvation**	1	1,06E-01

Table S7. ...continued.

3	up	GO:2000022	**regulation of jasmonic acid mediated sig„,,**	1	1,14E-01
3	up	GO:0009955	adaxial/abaxial pattern specification	1	1,21E-01
3	up	GO:0035195	**gene silencing by miRNA**	1	1,36E-01
3	up	GO:0010167	**response to nitrate**	1	1,38E-01
3	up	GO:0009696	**salicylic acid metabolic process**	1	1,47E-01
3	up	GO:0016246	**RNA interference**	1	1,48E-01
3	up	GO:0052546	cell wall pectin metabolic process	1	1,52E-01
3	up	GO:0080167	response to karrikin	2	1,56E-01
3	up	GO:0009933	meristem structural organization	2	1,58E-01
3	up	GO:0007131	reciprocal meiotic recombination	1	1,59E-01
3	up	GO:0016556	**mRNA modification**	1	1,68E-01
3	up	GO:0030433	ubiquitin-dependent ERAD pathway	1	1,75E-01
3	up	GO:0009911	positive regulation of flower developmen„,,	1	1,75E-01
3	up	GO:0010305	leaf vascular tissue pattern formation	1	1,76E-01
3	up	GO:0010154	fruit development	2	1,77E-01
3	up	GO:1900150	**regulation of defense response to fungus**	1	1,78E-01
3	up	GO:0042631	**cellular response to water deprivation**	1	1,78E-01
3	up	GO:0060560	developmental growth involved in morphog„,,	2	1,88E-01
3	up	GO:0000209	protein polyubiquitination	1	1,88E-01
3	up	GO:0006508	proteolysis	5	1,90E-01
3	up	GO:0009850	auxin metabolic process	2	1,98E-01
3	up	GO:0070918	**production of small RNA involved in gene„,,**	1	2,07E-01
3	up	GO:0048583	**regulation of response to stimulus**	3	2,08E-01
3	up	GO:0046283	**anthocyanin-containing compound metaboli„,,**	1	2,08E-01
3	up	GO:0009846	pollen germination	1	2,18E-01
3	up	GO:0010016	shoot system morphogenesis	2	2,20E-01
3	up	GO:0002758	**innate immune response-activating signal„,,**	1	2,25E-01
3	up	GO:0009626	**plant-type hypersensitive response**	1	2,52E-01
3	up	GO:0006302	double-strand break repair	1	2,58E-01
3	up	GO:0016036	**cellular response to phosphate starvatio„,,**	1	2,68E-01
3	up	GO:0071705	nitrogen compound transport	5	2,73E-01
3	up	GO:0009749	response to glucose	1	2,86E-01

Table S7. ...continued.

3	up	GO:0006511	ubiquitin-dependent protein catabolic pr,,,	2	3,00E-01
3	up	GO:0006417	regulation of translation	1	3,04E-01
3	up	GO:0009617	**response to bacterium**	4	3,07E-01
3	up	GO:0010218	**response to far red light**	1	3,12E-01
3	up	GO:0045893	**positive regulation of transcription, DN,,,**	2	3,22E-01
3	up	GO:0045087	**innate immune response**	3	3,52E-01
3	up	GO:0071555	cell wall organization	2	3,83E-01
3	up	GO:0009965	leaf morphogenesis	1	3,89E-01
3	up	GO:0009555	pollen development	2	4,11E-01
3	up	GO:0006457	protein folding	1	4,12E-01
3	up	GO:0006952	**defense response**	7	4,15E-01
3	up	GO:0009553	embryo sac development	1	4,47E-01
3	up	GO:0009737	**response to abscisic acid**	3	4,56E-01
3	up	GO:0007623	**circadian rhythm**	1	4,74E-01

Conclusions and outlook

The present work explored the molecular processes driving similar phenotypes during parallel adaptation to different ecological niches. We had two major aims in mind: (1) assessing repeatability in evolution, and (2) investigating the complex connection between short-term adjustments to environmental change and long-term adaptive outcomes. We examined these subjects in altitudinal ecotypes of the plant *Heliosperma pusillum*, contributing to confirm this species as a novel important plant system to investigate molecular mechanisms behind parallel evolution.

We started by quantifying repeatability of gene expression divergence, selection outliers, and functional networks related to the diverged loci detected, across four parallelly evolved ecotype pairs. To support our observations, we investigated the demographic history of the analyzed populations, as well as the patterns of genetic variation. Despite the great amount of studies on parallel evolution in both natural and laboratory systems, a clear expectation regarding the repeatability of the evolutionary process is lacking. One of the more significant findings to emerge from our work is that the independent evolution of similar phenotypes results from highly diverse patterns of molecular divergence. It follows that the polygenic nature of most adaptive traits likely reduces the constraints on the genetic mechanisms leading to adaptive changes. Organisms, and especially plants, are depicted as evolutionary flexible units that do not necessarily rely on one or few single genomic loci to adapt. Importantly, our study does not rule out the possibility that some, still undetected, genetic variation might have followed more parallel routes across the ecotype pairs analyzed. Nevertheless, I believe that the importance of our study lies in shifting the attention to the heterogeneity of evolutionary patterns, rather than focusing

on one shared putative driver of divergence. This is not a minor consideration, since decades of studies in evolutionary biology focused on parallel patterns, raising the implicit idea that non-parallel ones are not equally relevant to the evolutionary process. This shift of focus has major implications for our interpretations of how evolutionary processes, such as selection and local adaptation, shape divergence. Finally, studies on a broad range of organisms are clearly needed to obtain an overview of repeatability in evolution.

The second chapter was concerned with one fundamental process affecting real-time adjustments of populations to the environment, namely phenotypic plasticity. Via reciprocal transplantations at the natural growing sites we were able to dissect the relative contribution of plastic vs constitutive gene expression changes to ecotype divergence. Our findings revealed a pivotal role of expression plasticity in shaping differentiation. More specifically, enhanced levels of plasticity appeared to have evolved in the montane ecotype in both ecotype pairs analyzed. Higher plasticity likely represents a derived state in this system, and is beneficial in the highly stressful montane niche under cliffs. Thus, our second major finding was that in addition to being a key feature to survive in variable environments, differing degrees of plasticity can establish on the longer term and shape part of the ecological divergence observed. Further work needs to be done to establish whether plasticity differences in this system are truly adaptive, a difficult problem to tackle but highly relevant to fully understand the contribution of plasticity to adaptation.

The regulation of gene transcription and mRNA translation by small RNAs (smRNAs) is an important mechanism behind phenotypic plasticity and the epigenetic responses to environmental change. To achieve deeper insights into the mechanisms underlying gene expression divergence and plasticity, the third chapter provides one of the few assessments to date of the regulatory activity of smRNAs in differentially adapted natural populations. First, this investigation shows that smRNAs likely contribute to different degrees of expression plasticity in the ecotypes. This implies that how plasticity evolved in the ecotypes in response to the surrounding environment is at least partly associated with the evolution of smRNAs regulatory activity. Further, smRNAs evolution appears to proceed at different rates than genetic variation and gene expression, such that more

pronounced differences in smRNAs profiles are recovered among evolutionary replicates. These results add to the rapidly expanding field of smRNAs research, proposing that these regulatory elements driving (epi-)genetic modifications, are a fast evolving source of phenotypic variation that likely affects not only short-term individual adjustments, but also long-term evolutionary change.

Bibliography

Agrawal, A. A. (2017). Toward a predictive framework for convergent evolution: integrating natural history, genetic mechanisms, and consequences for the diversity of life. *American Naturalist*, *190*, S1–S12.

Alló, M., Buggiano, V., Fededa, J. P., Petrillo, E., Schor, I., de la Mata, M., ... Kornblihtt, A. R. (2009). Control of alternative splicing through siRNA-mediated transcriptional gene silencing. *Nature Structural and Molecular Biology*, *16*, 717–724.

Alves, J. M., Carneiro, M., Cheng, J. Y., Lemos de Matos, A., Rahman, M. M., Loog, L., ... Jiggins, F. M. (2019). Parallel adaptation of rabbit populations to myxoma virus. *Science*, *363*(6433), 1319–1326.

Arendt, J., & Reznick, D. (2008). Convergence and parallelism reconsidered: what have we learned about the genetics of adaptation? *Trends in Ecology and Evolution*, *23*(1), 26–32.

Arif, S., Murat, S., Almudi, I., Santos Nunes, M. D., Bortolamiol-Becet, D., Mcgregor, N., ... Mcgregor, A. (2013). Evolution of mir-92a underlies natural morphological variation in *Drosophila melanogaster*. *Current Biology*, *23*, 1–6.

Arnold, P. A., Kruuk, L. E. B., & Nicotra, A. B. (2019). How to analyse plant phenotypic plasticity in response to a changing climate. *New Phytologist*, *222*(3), 1235–1241.

Arnold, P. A., Nicotra, A. B., & Kruuk, L. E. B. (2019). Sparse evidence for selection on phenotypic plasticity in response to temperature. *Philosophical Transactions of the Royal Society B: Biological Sciences*, *374*(1768), 20180185.

Auld, J. R., & Relyea, R. A. (2011). Adaptive plasticity in predator-induced defenses in a common freshwater snail: altered selection and mode of predation due to prey phenotype. *Evolutionary Ecology*, *25*(1), 189–202.

Axtell, M. J. (2013). Classification and comparison of small RNAs from plants. *Annual Review of Plant Biology*, *64*(1), 137–159.

Balao, F., Trucchi, E., Wolfe, T., Hao, B.-H., Lorenzo, M. T., Baar, J., ... Paun, O. (2017). Adaptive sequence evolution is driven by biotic stress in a pair of orchid species (*Dactylorhiza*) with distinct ecological optima. *Molecular Ecology*, *26*(14), 3649–3662.

Barghi, N., Hermisson, J., & Schlötterer, C. (2020). Polygenic adaptation: a unifying framework to understand positive selection. *Nature Reviews Genetics*, *21*, 769–781.

Barghi, N., Tobler, R., Nolte, V., Jakšić, A. M., Mallard, F., Otte, K. A., … Schlötterer, C. (2019). Genetic redundancy fuels polygenic adaptation in *Drosophila*. *PLoS Biology*, *17*(2), 1–31.

Barley, J. M., Cheng, B. S., Sasaki, M., Gignoux-Wolfsohn, S., Hays, C. G., Putnam, A. B., … Kelly, M. (2021). Limited plasticity in thermally tolerant ectotherm populations: evidence for a trade-off. *Proceedings of the Royal Society B: Biological Sciences*, *288*(1958), 20210765.

Bartel, D. P. (2004). MicroRNAs: genomics, biogenesis, mechanism, and function. *Cell*, *116*(2), 281–297.

Bathia, G., Patterson, N., Sankararaman, S., & Price, A. (2013). Estimating and interpreting F_{st}: the impact of rare variants. *Genome Research*, *23*(9), 1514–1521.

Beltran, T., Shahrezaei, V., Katju, V., & Sarkies, P. (2020). Epimutations driven by small RNAs arise frequently but most have limited duration in *Caenorhabditis elegans*. *Nature Ecology & Evolution*, *4*, 1–10.

Bertel, C., Buchner, O., Schönswetter, P., Frajman, B., & Neuner, G. (2016). Environmentally induced and (epi-)genetically based physiological trait differentiation between *Heliosperma pusillum* and its polytopically evolved ecologically divergent descendent, *H. veselskyi* (Caryophyllaceae: Sileneae). *Botanical Journal of the Linnean Society*, *182*(3), 658–669.

Bertel, C., Hülber, K., Frajman, B., & Schönswetter, P. (2016). No evidence of intrinsic reproductive isolation between two reciprocally non-monophyletic, ecologically differentiated mountain plants at an early stage of speciation. *Evolutionary Ecology*, *30*(6), 1031–1042.

Bertel, C., Rešetnik, I., Frajman, B., Erschbamer, B., Hülber, K., & Schönswetter, P. (2018). Natural selection drives parallel divergence in the mountain plant *Heliosperma pusillum* s.l. *Oikos*, *127*, 1355–1367.

Bertel, C., Schönswetter, P., Frajman, B., Holzinger, A., & Neuner, G. (2017). Leaf anatomy of two reciprocally non-monophyletic mountain plants (*Heliosperma* spp.): does heritable adaptation to divergent growing sites accompany the onset of speciation? *Protoplasma*, *254*(3), 1411–1420.

Bohutínská, M., Vlček, J., Yair, S., Laenen, B., Konečná, V., Fracassetti, M., … Kolár, F. (2021). Genomic basis of parallel adaptation varies with divergence in *Arabidopsis* and its relatives. *Proceedings of the National Academy of Sciences of the United States of America*, *118*(21), 1–10.

Bolger, A. M., Lohse, M., & Usadel, B. (2014). Trimmomatic: a flexible trimmer for Illumina sequence data. *Bioinformatics*, *30*(15), 2114–2120.

Bolnick, D. I., Barrett, R. D. H., Oke, K. B., Rennison, D. J., & Stuart, Y. E. (2018). (Non-)Parallel evolution. *Annual Review of Ecology, Evolution, and Systematics*, *49*, 303–330.

Borges, F., & Martienssen, R. A. (2015). The expanding world of small RNAs in plants. *Nature Reviews Molecular Cell Biology*, *16*, 727–741.

Bourc'his, D., & Voinnet, O. (2010). A small-RNA perspective on gametogenesis, fertilization, and early zygotic development. *Science*, *330*, 617–22.

Bourret, V., Dionne, M., & Bernatchez, L. (2014). Detecting genotypic changes associated with selective mortality at sea in Atlantic salmon: Polygenic multilocus analysis surpasses genome scan. *Molecular Ecology*, *23*(18), 4444–4457.

Boyle, E. A., Yang, I. L., & Pritchard, J. K. (2017). An expanded view of complex traits: from polygenic to omnigenic. *Cell*, *169*(7), 1177–1186.

Bradley, D., Xu, P., Mohorianu, I.-I., Whibley, A., Field, D., Tavares, H., ... Coen, E. (2017). Evolution of flower color pattern through selection on regulatory small RNAs. *Science*, *358*(6365), 925–928.

Brennan, R. S., deMayo, J. A., Dam, H. G., Finiguerra, M., Baumann, H., & Pespeni, M. H. (2021). Loss and recovery of transcriptional plasticity after long-term adaptation to global change conditions in a marine copepod. *bioRxiv*.

Buckley, J., Widmer, A., Mescher, M. C., & De Moraes, C. M. (2019). Variation in growth and defence traits among plant populations at different elevations: implications for adaptation to climate change. *Journal of Ecology*, *107*(5), 2478–2492.

Bull, J. J., Badgett, M. R., Wichman, H. A., Huelsenbeck, J. P., Hillis, D. M., Gulati, A., ... Molineux, I. J. (1997). Exceptional convergent evolution in a virus. *Genetics*, *147*(4), 1497–1507.

Cabrera, J., Barcala, M., García, A., Rio-Machín, A., Medina, C., Jaubert-Possamai, S., ... Escobar, C. (2016). Differentially expressed small RNAs in *Arabidopsis* galls formed by *Meloidogyne javanica*: a functional role for mir390 and its tas3-derived tasiRNAs. *New Phytologist*, *209*(4), 1625–1640.

Cai, Z., Zhou, L., Ren, N. N., Xu, X., Liu, R., Huang, L., ... Ge, S. (2019). Parallel speciation of wild rice associated with habitat shifts. *Molecular Biology and Evolution*, *36*(5), 875–889.

Campbell, M. S., Holt, C., Moore, B., & Yandell, M. (2014). Genome annotation and curation using MAKER and MAKER-P. *Current Protocols in Bioinformatics*, *48*, 4.11.1–4.11.39.

Campos, C., Sundaram, A. Y. M., Valente, L. M. P., Conceição, L. E. C., Engrola, S., & Fernandes, J. M. O. (2014). Thermal plasticity of the miRNA transcriptome during senegalese sole development. *BMC genomics*, *15*, 525.

Cantu, D., Vanzetti, L. S., Sumner, A., Dubcovsky, M., Matvienko, M., Distelfeld, A., ... Dubcovsky, J. (2010). Small RNAs, DNA methylation and transposable elements in wheat. *BMC Genomics*, *11*.

Chan, Y. F., Marks, M. E., Jones, F. C., Villarreal, G., Shapiro, M. D., Brady, S. D., ... Kingsley, D. M. (2010). Adaptive evolution of pelvic reduction in sticklebacks by recurrent deletion of a pitxl enhancer. *Science*, *327*(5963), 302–305.

Chang, J., Yu, T., Yang, Q., Li, C., Xiong, C., Gao, S., ... Ye, Z. (2018). Hair, encoding a single C2H2 zinc-finger protein, regulates multicellular trichome formation in tomato. *Plant Journal*, *96*(1), 90–102.

Charlesworth, B., Lande, R., & Slatkin, M. (1982). A neo−darwinian commentary on macroevolution. *Evolution*, *36*.

Charlesworth, B., Morgan, M. T., & D, C. (1993). The effect of deleterious mutations on neutral molecular variation. *Genetics*, *134*(4), 1289–1303.

Chevin, L.-M., & Hoffmann, A. A. (2017). Evolution of phenotypic plasticity in extreme environments. *Philosophical Transactions of the Royal Society B: Biological Sciences*, *372*(1723), 20160138.

Chopra, D., Mapar, M., Stephan, L., Albani, M. C., Deneer, A., Coupland, G., ... Hülskamp, M. (2019). Genetic and molecular analysis of trichome development in *Arabis alpina*. *Proceedings of the National Academy of Sciences of the United States of America*, *116*(24), 12078–12083.

Cieślik, M., & Chinnaiyan, A. M. (2018). Cancer transcriptome profiling at the juncture of clinical translation. *Nature Reviews Genetics*, *19*(2), 93–109.

Clop, A., Marcq, F., Takeda, H., Pirottin, D., Tordoir, X., Bibe, B., ... Georges, M. (2006). A mutation creating a potential illegitimate microRNA target site in the myostatin gene affects muscularity in sheep. *Nature genetics*, *38*, 813–8.

Colosimo, P. F., Hosemann, K. E., Balabhadra, S., Jr, G. V., Dickson, M., Grimwood, J., ... Kingsley, D. M. (2005). Widespread parallel evolution in sticklebacks by repeated fixation of Ectodysplasin alleles. *Science*, *307*(5717), 1928–1933.

Cooper, T. F., Rozen, D. E., & Lenski, R. E. (2003). Parallel changes in gene expression after 20,000 generations of evolution in *Escherichia coli*. *Proceedings of the National Academy of Sciences of the United States of America*, *100*(3), 1072–1077.

Corl, A., Bi, K., Luke, C., Challa, A. S., Stern, A. J., Sinervo, B., & Nielsen, R. (2018). The genetic basis of adaptation following plastic changes in coloration in a novel environment. *Current Biology*, *28*(18), 2970–2977.e7.

Cota-Sánchez, J. H., Remarchuk, K., & Ubayasena, K. (2006). Ready-to-use DNA extracted with a CTAB method adapted for herbarium specimens and mucilaginous plant tissue. *Plant Molecular Biology Reporter*, *24*(2), 161–167.

Dalal, A., Attia, Z., & Moshelion, M. (2017). To produce or to survive: how plastic is your crop stress physiology? *Frontiers in Plant Science*, *8*.

Danecek, P., Auton, A., Abecasis, G., Albers, C. A., Banks, E., DePristo, M. A., ... 1000 Genomes Project Analysis Group (2011). The variant call format and VCFtools. *Bioinformatics*, *27*(15), 2156–2158.

Darwin, C. (1859). *On The Origin Of Species By Means Of Natural Selection, Or, The Preservation Of Favoured Races In The Struggle For Life*. London: John Murray.

Davis, P. H. (1951). Cliff vegetation in the eastern mediterranean. *Journal of Ecology*, *39*(1), 63–93.

Derome, N., Duchesne, P., & Bernatchez, L. (2006). Parallelism in gene transcription among sympatric lake whitefish (*Coregonus clupeaformis* Mitchill) ecotypes. *Molecular Ecology*, *15*(5), 1239–1249.

DeWitt, T. J., Sih, A., & Wilson, D. S. (1998). Costs and limits of phenotypic plasticity. *Trends in Ecology & Evolution*, *13*(2), 77–81.

Ding, M., Ye, W., Lin, L., He, S., Du, X., Chen, A., ... Rong, J. (2015). The hairless stem phenotype of cotton (*Gossypium barbadense*) is linked to a copia-like retrotransposon insertion in a homeodomain-leucine zipper gene (HD1). *Genetics*, *201*(1), 143–54.

Ding, Y., Fromm, M., & Avramova, Z. (2012). Multiple exposures to drought 'train' transcriptional responses in *Arabidopsis*. *Nature Communications*, *3*.

Dobin, A., Davis, C. A., Schlesinger, F., Drenkow, J., Zaleski, C., Jha, S., ... Gingeras, T. R. (2013). STAR: Ultrafast universal RNA-seq aligner. *Bioinformatics*, *29*(1), 15–21.

Dobler, S., Dalla, S., Wagschal, V., & Agrawal, A. A. (2012). Community-wide convergent evolution in insect adaptation to toxic cardenolides by substitutions in the Na,K-ATPase. *Proceedings of the National Academy of Sciences of the United States of America*, *109*(32), 13040–13045.

Dowen, R., Pelizzola, M., Schmitz, R., Lister, R., Dowen, J., Nery, J., ... Ecker, J. (2012). Widespread dynamic DNA methylation in response to biotic stress. *Proceedings of the National Academy of Sciences of the United States of America*, *109*(32), E2183–E2191.

Dudley, S. A., & Schmitt, J. (1996). Testing the adaptive plasticity hypothesis: density-dependent selection on manipulated stem length in *Impatiens capensis*. *The American Naturalist*, *147*(3), 445–465.

Dutcher, H. A., Raghavan, R., Storz, G., & Papenfort, K. (2018). Origin, evolution, and loss of bacterial small RNAs. *Microbiology Spectrum*, *6*(2).

Ehrenreich, I., & Pfennig, D. (2016). Genetic assimilation: a review of its potential proximate causes and evolutionary consequences. *Annals of Botany*, *117*, 769—779.

Elmer, K. R., Fan, S., Kusche, H., Luise Spreitzer, M., Kautt, A. F., Franchini, P., & Meyer, A. (2014). Parallel evolution of Nicaraguan crater lake cichlid fishes via non-parallel routes. *Nature Communications*, *5*, 5168.

Elmer, K. R., & Meyer, A. (2011). Adaptation in the age of ecological genomics: insights from parallelism and convergence. *Trends in Ecology and Evolution*, *26*(6), 298–306.

Eriksson, M. C., Szukala, A., Tian, B., & Paun, O. (2020). Current research frontiers in plant epigenetics: an introduction to a Virtual Issue. *New Phytologist*, *226*(2), 285–288.

Evanno, G., Regnaut, S., & Goudet, J. (2005). Detecting the number of clusters of individuals using the software STRUCTURE: A simulation study. *Molecular Ecology*, *14*(8), 2611–2620.

Excoffier, L., Dupanloup, I., Huerta-Sánchez, E., Sousa, V. C., & Foll, M. (2013). Robust demographic inference from genomic and SNP data. *PLoS Genetics*, *9*(10), e1003905.

Fang, B., Kemppainen, P., Momigliano, P., Feng, X., & Merilä, J. (2020). On the causes of geographically heterogeneous parallel evolution in sticklebacks. *Nature Ecology and Evolution*, *4*, 1105–1115.

Felsenstein, J. (1976). The theoretical population genetics of variable selection and migration. *Annual Review of Genetics*, *10*(1), 253–280. (PMID: 797310)

Feng, D., Yu, H., Liu, S., Kong, L., & Du, S. (2020). Integrated analysis of microRNA and mRNA expression profiles in *Crassostrea gigas* to reveal functional miRNA and miRNA-targets regulating shell pigmentation. *Scientific Reports*, *10*(1), 20238.

Feng, X., & Guang, S. (2013). Small RNAs, RNAi and the inheritance of gene silencing in *Caenorhabditis elegans*. *Journal of Genetics and Genomics*, *40*(4), 153–60.

Fischer, E. K., Song, Y., Hughes, K. A., Zhou, W., & Hoke, K. L. (2021). Non-parallel transcriptional divergence during parallel adaptation. *Molecular Ecology*, *30*(6), 1516–1530.

Flatscher, R., Frajman, B., Schönswetter, P., & Paun, O. (2012). Environmental heterogeneity and phenotypic divergence: can heritable epigenetic variation aid speciation? *Genetics Research International*, *698421*, 1–9.

Foll, M., Gaggiotti, O. E., Daub, J. T., Vatsiou, A., & Excoffier, L. (2014). Widespread signals of convergent adaptation to high altitude in Asia and America. *American Journal of Human Genetics*, *95*(4), 394–407.

Fong, S. S., Joyce, A. R., & Palsson, B. Ø. (2005). Parallel adaptive evolution cultures of *Escherichia coli* lead to convergent growth phenotypes with different gene expression states. *Genome Research*, *15*(10), 1365–1372.

Forester, B. R., Lasky, J. R., Wagner, H. H., & Urban, D. L. (2018). Comparing methods for detecting multilocus adaptation with multivariate genotype–environment associations. *Molecular Ecology*, *27*(9), 2215–2233.

Formey, D., Sallet, E., Lelandais-Brière, C., Ben, C., Bustos-Sanmamed, P., Niebel, A., ... Crespi, M. (2014). The small RNA diversity from *Medicago truncatula* roots under biotic interactions evidences the environmental plasticity of the miRNAome. *Genome Biology*, *15*, 457.

Fox, R. J., Donelson, J. M., Schunter, C., Ravasi, T., & Gaitán-Espitia, J. D. (2019). Beyond buying time: the role of plasticity in phenotypic adaptation to rapid environmental change. *Philosophical Transactions of the Royal Society B: Biological Sciences*, *374*(1768), 20180174.

Fraïsse, C., Belkhir, K., Welch, J. J., & Bierne, N. (2016). Local interspecies introgression is the main cause of extreme levels of intraspecific differentiation in mussels. *Molecular Ecology*, *25*(1), 269–286.

Fraïsse, C., Roux, C., Gagnaire, P.-A., Romiguier, J., Faivre, N., Welch, J. J., & Bierne, N. (2018). The divergence history of European blue mussel species reconstructed from Approximate Bayesian Computation: the effects of sequencing techniques and sampling strategies. *PeerJ*, *6*, e5198.

Frajman, B., Eggens, F., & Oxelman, B. (2009). Hybrid origins and homoploid reticulate evolution within *Heliosperma* (*Sileneae*, Caryophyllaceae) - A multigene phylogenetic approach with relative dating. *Systematic Biology*, *58*(3), 328–345.

Frajman, B., & Oxelman, B. (2007). Reticulate phylogenetics and phytogeographical structure of *Heliosperma* (*Sileneae*, Caryophyllaceae) inferred from chloroplast and nuclear DNA sequences. *Molecular Phylogenetics and Evolution*, *43*(1), 140–155.

Friedrich, T., Faivre, L., Bäurle, I., & Schubert, D. (2019). Chromatin-based mechanisms of temperature memory in plants. *Plant Cell and Environment*, *42*(3), 762–770.

García, D., & Zamora, R. (2003). Persistence, multiple demographic strategies and conservation in long-lived Mediterranean plants, journal = Journal of Vegetation Science. , *14*(6), 921–926.

Gelaw, T., & Sanan, N. (2021). Non-coding RNAs in response to drought stress. *International Journal of Molecular Sciences*, *22*, 12519.

Giesecke, T., Brewer, S., Finsinger, W., Leydet, M., & Bradshaw, R. H. (2017). Patterns and dynamics of European vegetation change over the last 15,000 years. *Journal of Biogeography*, *44*(7), 1441–1456.

Goldstein, D. B., & Holsinger, K. E. (1992). Maintenance of polygenic variation in spatially structured populations: roles for local mating and genetic redundancy. *Evolution*, *46*(2), 412–429.

Götz, S., García-Gómez, J. M., Terol, J., Williams, T. D., Nagaraj, S. H., Nueda, M. J., ... Conesa, A. (2008). High-throughput functional annotation and data mining with the Blast2GO suite. *Nucleic Acids Research*, *36*(10), 3420–3435.

Gramlich, S., Liu, X., Favre, A., Alex Buerkle, C., & Karrenberg, S. (2021). A polygenic architecture with conditionally neutral effects underlies ecological differentiation in *Silene*. *bioRxiv*, 2021.07.06.451304.

Griffith, M., Walker, J. R., Spies, N. C., Ainscough, B. J., & Griffith, O. L. (2015). Informatics for RNA sequencing: a web resource for analysis on the cloud. *PLOS Computational Biology*, *11*(8), 1–20.

Guleria, P., Mahajan, M., Bhardwaj, J., & Yadav, S. (2011). Plant small RNAs: biogenesis, mode of action and their roles in abiotic stresses. *Genomics, Proteomics & Bioinformatics*, *9*, 183–99.

Haas, B. J., Papanicolaou, A., Yassour, M., Grabherr, M., Philip, D., Bowden, J., ... Regev, A. (2013). *De novo* transcript sequence recostruction from RNA-Seq: reference generation and analysis with Trinity. *Nature Protocols*, *8*(8), 1494–1512.

Hämälä, T., Guiltinan, M. J., Marden, J. H., Maximova, S. N., DePamphilis, C. W., & Tiffin, P. (2020). Gene expression modularity reveals footprints of polygenic adaptation in *Theobroma cacao*. *Molecular Biology and Evolution*, *37*(1), 110–123.

Hancock, A. M., Alkorta-Aranburu, G., Witonsky, D. B., & Di Rienzo, A. (2010). Adaptations to new environments in humans: the role of subtle allele frequency shifts. *Philosophical Transactions of the Royal Society B: Biological Sciences*, *365*(1552), 2459–2468.

Heard, E., & Martienssen, R. (2014). Transgenerational epigenetic inheritance: myths and mechanisms. *Cell*, *157*, 95–109.

Hermisson, J., & Pennings, P. S. (2017). Soft sweeps and beyond: understanding the patterns and probabilities of selection footprints under rapid adaptation. *Methods in Ecology and Evolution*, *8*(6), 700–716.

Hewezi, T. (2020). Epigenetic mechanisms in nematode–plant interactions. *Annual Review of Phytopathology*, *58*(1), 119–138.

Hicks, S. C., Townes, F. W., Teng, M., & Irizarry, R. A. (2018). Missing data and technical variability in single-cell RNA-sequencing experiments. *Biostatistics*, *19*(4), 562–578.

Hilscher, J., Schlötterer, C., & Hauser, M. T. (2009). A single amino acid replacement in ETC2 shapes trichome patterning in natural *Arabidopsis* populations. *Current Biology*, *19*(20), 1747–1751.

Hoekstra, H. E., Hirschmann, R. J., Bundey, R. A., Insel, P. A., & Crossland, J. P. (2006). A single amino acid mutation contributes to adaptive beach mouse color pattern. *Science*, *313*(5783), 101–104.

Hoekstra, H. E., & Nachman, M. W. (2003). Different genes underlie adaptive melanism in different populations of rock pocket mice. *Molecular Ecology*, *12*(5), 1185–1194.

Hoff, K. J., Lange, S., Lomsadze, A., Borodovsky, M., & Stanke, M. (2016). BRAKER1: unsupervised RNA-Seq-based genome annotation with GeneMark-ET and AUGUSTUS. *Bioinformatics*, *32*(5), 767–769.

Hoffmann, F. G., McGuire, L. P., Counterman, B. A., & Ray, D. A. (2015). Transposable elements and small RNAs: Genomic fuel for species diversity. *Mobile Genetic Elements*, *5*(5), 63–66.

Holeski, L. M., Jander, G., & Agrawal, A. A. (2012). Transgenerational defense induction and epigenetic inheritance in plants. *Trends in Ecology and Evolution*, *27*(11), 618–626.

Höllinger, I., Pennings, P. S., & Hermisson, J. (2019). Polygenic adaptation: from sweeps to subtle frequency shifts. *PLoS Genetics*, *15*(3), 1–26.

Hollister, J. D., Smith, L. M., Guo, Y.-L., Ott, F., Weigel, D., & Gaut, B. S. (2011). Transposable elements and small RNAs contribute to gene expression divergence between *Arabidopsis thaliana* and *Arabidopsis lyrata*. *Proceedings of the National Academy of Sciences*, *108*(6), 2322–2327.

Huang, Y., & Agrawal, A. F. (2016). Experimental evolution of gene expression and plasticity in alternative selective regimes. *PLOS Genetics*, *12*(9), 1–23.

Hülskamp, M. (2004). Plant trichomes: a model for cell differentiation. *Nature Reviews Molecular Cell Biology*, *5*(6), 471–480.

Hülskamp, M., Miséra, S., & Jürgens, G. (1994). Genetic dissection of trichome cell development in *Arabidopsis*. *Cell*, *76*(3), 555–566.

Jablonka, E., & Raz, G. (2009). Transgenerational epigenetic inheritance: prevalence, mechanisms, and implications for the study of heredity and evolution. *The Quarterly Review of Biology*, *84*(2), 131–176.

James, M. E., Arenas-Castro, H., Groh, J. S., Allen, S. L., Engelstädter, J., & Ortiz-Barrientos, D. (2021). Highly Replicated Evolution of Parapatric Ecotypes. *Molecular Biology and Evolution*, *38*(11), 4805–4821.

James, M. E., Wilkinson, M. J., Bernal, D. M., Liu, H., North, H. L., Engelstädter, J., & Ortiz-Barrientos, D. (2021). Phenotypic and genotypic parallel evolution in parapatric ecotypes of *Senecio*. *Evolution*, *75*(12), 3115–3131.

Jones, F. C., Grabherr, M. G., Chan, Y. F., Russell, P., Mauceli, E., Johnson, J., ... Kingsley, D. M. (2012). The genomic basis of adaptive evolution in threespine sticklebacks. *Nature*, *484*(7392), 55–61.

Kawecki, T. J., & Ebert, D. (2004). Conceptual issues in local adaptation. *Ecology Letters*, *7*(12), 1225–1241.

Kelemen, O., Convertini, P., Zhang, Z., Wen, Y., Shen, M., Falaleeva, M., & Stamm, S. (2013). Function of alternative splicing. *Gene*, *514*(1), 1–30.

Kelly, M. W., Pankey, M. S., DeBiasse, M. B., & Plachetzki, D. C. (2017). Adaptation to heat stress reduces phenotypic and transcriptional plasticity in a marine copepod. *Functional Ecology*, *31*(2), 398–406.

Khosla, A., Paper, J. M., Boehler, A. P., Bradley, A. M., Neumann, T. R., & Schrick, K. (2014). HD-Zip proteins GL2 and HDG11 have redundant functions in *Arabidopsis* trichomes, and GL2 activates a positive feedback loop via MYB23. *Plant Cell*, *26*(5), 2184–2200.

Kimura, M. (1968). Evolutionary rate at the molecular level. *Nature*, *217*, 624–626.

Kimura, M. (1983). *The Neutral Theory Of Molecular Evolution*. Cambridge University Press.

Kitano, J., Yoshida, K., & Suzuki, Y. (2013). RNA sequencing reveals small RNAs differentially expressed between incipient japanese threespine sticklebacks. *BMC genomics*, *14*, 214.

Knotek, A., Konečná, V., Wos, G., Požárová, D., Šrámková, G., Bohutínská, M., ... Kolář, F. (2020). Parallel alpine differentiation in *Arabidopsis arenosa*. *Frontiers in Plant Science*, *11*, 561526.

Konečná, V., Nowak, M. D., & Kolář, F. (2019). Parallel colonization of subalpine habitats in the central European mountains by *Primula elatior*. *Scientific Reports*, *9*(1), 1–12.

Korneliussen, T. S., Albrechtsen, A., & Nielsen, R. (2014). ANGSD: analysis of Next Generation Sequencing data. *BMC Bioinformatics*, *15*(365).

Lande, R. (2009). Adaptation to an extraordinary environment by evolution of phenotypic plasticity and genetic assimilation. *Journal of Evolutionary Biology*, *22*(7), 1435–1446.

Láruson, Á. J., Yeaman, S., & Lotterhos, K. E. (2020). The importance of genetic redundancy in evolution. *Trends in Ecology and Evolution*, *35*(9), 809–822.

Lee, K. M., & Coop, G. (2019). Population genomics perspectives on convergent adaptation. *Philosophical Transactions of the Royal Society B: Biological Sciences*, *374*(1777), 20180236.

Leinonen, T., McCairns, S., O'Hara, B., & Merilä, J. (2013). QST-FST comparisons: evolutionary and ecological insights from genomic heterogeneity. *Nature Reviews Genetics*, *14*, 179–190.

Levis, N. A., Isdaner, A. J., & Pfennig, D. W. (2018). Morphological novelty emerges from pre-existing phenotypic plasticity. *Nature ecology & evolution*, *2*(8), 1289–1297.

Levis, N. A., & Pfennig, D. W. (2016). Evaluating 'plasticity-first' evolution in nature: key criteria and empirical approaches. *Trends in Ecology Evolution*, *31*(7), 563–574.

Li, H., Handsaker, B., Wysoker, A., Fennell, T., Ruan, J., Homer, N., ... Abecasis, G. (2009). The sequence alignment/map format and samtools. *Bioinformatics*, *25*, 2078–2079.

Liao, Y., Smyth, G. K., & Shi, W. (2014). FeatureCounts: an efficient general purpose program for assigning sequence reads to genomic features. *Bioinformatics*, *30*(7), 923–930.

Lim, M. C., Witt, C. C., Graham, C. H., & Dávalos, L. M. (2019). Parallel molecular evolution in pathways, genes, and sites in high-elevation hummingbirds revealed by comparative transcriptomics. *Genome Biology and Evolution*, *11*(6), 1552–1572.

Liu, H., Able, A., & Able, J. (2021). Small RNAs and their targets are associated with the transgenerational effects of water-deficit stress in durum wheat. *Scientific Reports*, *11*, 3613.

Lomsadze, A., Burns, P. D., & Borodovsky, M. (2014). Integration of mapped RNA-Seq reads into automatic training of eukaryotic gene finding algorithm. *Nucleic Acids Research*, *42*(15), e119.

Losos, J. B. (2011). Convergence, adaptation, and constraint. *Evolution*, *65*(7), 1827–1840.

Louis, M., Galimberti, M., Archer, F., Berrow, S., Brownlow, A., Fallon, R., ... Gaggiotti, O. E. (2021). Selection on ancestral genetic variation fuels repeated ecotype formation in bottlenose dolphins. *Science Advances*, *7*(44), eabg1245.

Lowry, D. B. (2012). Ecotypes and the controversy over stages in the formation of new species. *Biological Journal of the Linnean Society*, *106*(2), 241–257.

Luo, Y., Widmer, A., & Karrenberg, S. (2014). The roles of genetic drift and natural selection in quantitative trait divergence along an altitudinal gradient in *Arabidopsis thaliana*. *Heredity*, *114*(2), 220–8.

Lynch, M., Ackerman, M. S., Gout, J. F., Long, H., Sung, W., Thomas, W. K., & Foster, P. L. (2016). Genetic drift, selection and the evolution of the mutation rate. *Nature Reviews Genetics*, *17*(11), 704–714.

Ma, X. F., Hall, D., St. Onge, K. R., Jansson, S., & Ingvarsson, P. K. (2010). Genetic differentiation, clinal variation and phenotypic associations with growth cessation across the *Populus tremula* photoperiodic pathway. *Genetics*, *186*(3), 1033–1044.

Ma, Y., Dias, M. C., & Freitas, H. (2020). Drought and salinity stress responses and microbe-induced tolerance in plants. *Frontiers in Plant Science*, *11*, 591911.

Machado, A., Wu, Y., Yang, Y., Llewellyn, D. J., & Dennis, E. S. (2009). The MYB transcription factor GhMYB25 regulates early fibre and trichome development. *The Plant Journal*, *59*(1), 52–62.

MacPherson, A., & Nuismer, S. L. (2017). The probability of parallel genetic evolution from standing genetic variation. *Journal of Evolutionary Biology*, *30*(2), 326–337.

Mallard, F., Nolte, V., & Schlötterer, C. (2020). The evolution of phenotypic plasticity in response to temperature stress. *Genome Biology and Evolution*, *12*(12), 2429–2440.

Manceau, M., Domingues, V. S., Linnen, C. R., Rosenblum, E. B., & Hoekstra, H. E. (2010). Convergence in pigmentation at multiple levels: mutations, genes and function. *Philosophical Transactions of the Royal Society B: Biological Sciences*, *365*(1552), 2439–2450.

Mandic, M., Ramon, M. L., Gerstein, A. C., Gracey, A. Y., & Richards, J. G. (2018). Variable gene transcription underlies phenotypic convergence of hypoxia tolerance in sculpins. *BMC Evolutionary Biology*, *18*(163).

Manolio, T., Collins, F., Cox, N., Goldstein, D., Hindorff, L., Hunter, D., ... Visscher, P. (2009). Finding the missing heritability of complex diseases. *Nature*, *461*, 747–53.

Marina, P., & Martin, H. (2009). One, two, three... models for trichome patterning in *Arabidopsis? Current Opinion in Plant Biology*, *12*(5), 587–592.

McCairns, R. J. S., & Bernatchez, L. (2010). Adaptive divergence between freshwater and marine sticklebacks: insights into the role of phenotypic plasticity from an integrated ananlysis of candidate gene expression. *Evolution*, *64*(4), 1029–1047.

Meirmans, P. G. (2019). Subsampling reveals that unbalanced sampling affects Structure results in a multi-species dataset. *Heredity*, *122*(3), 276–287.

Meisner, J., & Albrechtsen, A. (2018). Inferring population structure and admixture proportions in low-depth NGS data. *Genetics*, *210*(2), 719–731.

Minuto, L., Guerrina, M., Roccotiello, E., & Casazza, G. (2012). Demographic structure and reproductive success of *Primula allionii*, a plant endemic to maritime alps. *Bollettino dei musei e degli istituti biologici dell'università di Genova*, *74*, 38-54.

Monroe, J. G., Srikant, T., Carbonell-bejerano, P., Becker, C., Lensink, M., Exposito-alonso, M., ... Weigel, D. (2022). Mutation bias reflects natural selection in *Arabidopsis thaliana*. *Nature*, *602*(7895), 101–105.

Moss, E. (2001). RNA interference: it's a small RNA world. *Current Biology*, *11*(19), R772–5.

Nair, S., Wang, N., Turuspekov, Y., Pourkheirandish, M., Sinsuwongwat, S., Chen, G., ... Komatsuda, T. (2010). Cleistogamous flowering in barley arises from the suppression of microRNA-guided hvap2 mRNA cleavage. *Proceedings of the National Academy of Sciences of the United States of America*, *107*(1), 490–5.

Narum, S., & Campbell, N. (2015). Transcriptomic response to heat stress among ecologically divergent populations of redband trout. *BMC Genomics*, *16*, 1–12.

Nguyen Ba, A. N., Cvijović, I., Rojas Echenique, J. I., Lawrence, K. R., Rego-Costa, A., Liu, X., ... Desai, M. M. (2019). High-resolution lineage tracking reveals travelling wave of adaptation in laboratory yeast. *Nature*, *575*(7783), 494–499.

Nicotra, A. B., Segal, D. L., Hoyle, G. L., Schrey, A. W., Verhoeven, K. J. F., & Richards, C. L. (2015). Adaptive plasticity and epigenetic variation in response to warming in an alpine plant. *Ecology and Evolution*, *5*(3), 634–647.

Nordborg, M., Charlesworth, B., & Charlesworth, D. (1996). The effect of recombination on background selection. *Genetical Research*, *67*(2), 159–174.

Nosil, P., Feder, J. L., Flaxman, S. M., & Gompert, Z. (2017). Tipping points in the dynamics of speciation. *Nature Ecology and Evolution*, *1*, 0001.

Nosil, P., Harmon, L. J., & Seehausen, O. (2009). Ecological explanations for (incomplete) speciation. *Trends in Ecology and Evolution*, *24*(3), 145–156.

Nowak, M. A., Boerlijst, M. C., Cooke, J., & Smith, J. M. (1997). Evolution of genetic redundancy. *Nature*, *388*, 167–171.

Obenchain, V., Lawrence, M., Carey, V., Gogarten, S., Shannon, P., & Morgan, M. (2014). VariantAnnotation: a Bioconductor package for exploration and annotation of genetic variants. *Bioinformatics*, *30*(14), 2076–2078.

Oke, K. B., Rolshausen, G., LeBlond, C., & Hendry, A. P. (2017). How parallel is parallel evolution? A comparative analysis in fishes. *American Naturalist*, *190*(1), 1–16.

Oksanen, J., Blanchet, F. G., Friendly, M., Kindt, R., Legendre, P., McGlinn, D., ... Wagner, H. H. (2019). vegan: community ecology package. R package version 2.5-6. , *[online]*. Retrieved from `https://CRAN.R-project.org/package=vegan`

Ozsolak, F., & Milos, P. M. (2011). RNA sequencing: advances, challenges and opportunities. *Nature Reviews Genetics*, *12*(2), 87–98.

Pál, C., & Miklós, I. (1999). Epigenetic inheritance, genetic assimilation and speciation. *Journal of theoretical biology*, *200*, 19–37.

Pan, Y., Bo, K., Cheng, Z., & Weng, Y. (2015). The loss-of-function GLABROUS 3 mutation in cucumber is due to LTR-retrotransposon insertion in a class IV HD-ZIP transcription factor gene CsGL3 that is epistatic over CsGL1. *BMC Plant Biology*, *15*, 302.

Passow, C. N., Henpita, C., Shaw, J. H., Quackenbush, C. R., Warren, W. C., Schartl, M., ... Tobler, M. (2017). The roles of plasticity and evolutionary change in shaping gene expression variation in natural populations of extremophile fish. *Molecular Ecology*, *26*(22), 6384–6399.

Paun, O., Bateman, R. M., Fay, M. F., Hedrén, M., Civeyrel, L., & Chase, M. W. (2010). Stable epigenetic effects impact adaptation in allopolyploid orchids (*Dactylorhiza*: Orchidaceae). *Molecular Biology and Evolution*, *27*(11), 2465–2473.

Paun, O., Schönswetter, P., Winkler, M., & Tribsch, A. (2008). Evolutionary history of the *Ranunculus alpestris* group (Ranunculaceae) in the European Alps and the Carpathians. *Molecular ecology*, *17*, 4263–75.

Perbal, L. (2015). The case of the gene. *EMBO reports*, *16*(7), 777–781.

Popovic, I., Bierne, N., Gaiti, F., Tanurdžić, M., & Riginos, C. (2021). Pre-introduction introgression contributes to parallel differentiation and contrasting hybridization outcomes between invasive and native marine mussels. *Journal of Evolutionary Biology*, *34*(1), 175–192.

Priest, H. D., Fox, S. E., Rowley, E. R., Murray, J. R., Michael, T. P., & Mockler, T. C. (2014). Analysis of global gene expression in *Brachypodium distachyon* reveals extensive network plasticity in response to abiotic stress. *PLOS ONE*, *9*(1), 1–15.

Pritchard, J. K., Pickrell, J. K., & Coop, G. (2010). The genetics of human adaptation: hard sweeps, soft sweeps, and polygenic adaptation. *Current Biology*, *20*(4), R208–R215.

Projecto-Garcia, J., Natarajan, C., Moriyama, H., Weber, R. E., Fago, A., Cheviron, Z. A., ... Storz, J. F. (2013). Repeated elevational transitions in hemoglobin function during the evolution of Andean hummingbirds. *Proceedings of the National Academy of Sciences of the United States of America*, *110*(51), 20669–20674.

Puechmaille, S. J. (2016). The program structure does not reliably recover the correct population structure when sampling is uneven: subsampling and new estimators alleviate the problem. *Molecular Ecology Resources*, *16*(3), 608–627.

Purcell, S. M., Moran, J. L., Fromer, M., Ruderfer, D., Solovieff, N., Roussos, P., ... Sklar, P. (2014). A polygenic burden of rare disruptive mutations in schizophrenia. *Nature*, *506*(7487), 185–190.

Quinlan, A. R., & Hall, I. M. (2010). BEDTools: a flexible suite of utilities for comparing genomic features. *Bioinformatics*, *26*(6), 841–842.

Quint, M., Delker, C., Franklin, K. A., Wigge, P. A., Halliday, K. J., & Van Zanten, M. (2016). Molecular and genetic control of plant thermomorphogenesis. *Nature Plants*, *2*, 15190.

Ramìrez, F., Ryan, D. P., Grüning, B., Bhardwaj, V., Kilpert, F., Richter, A. S., ... Manke, T. (2016). deepTools2: a next generation web server for deep-sequencing data analysis. *Nucleic Acids Research*, *44*(W1), W160–W165.

Ravinet, M., Westram, A., Johannesson, K., Butlin, R., André, C., & Panova, M. (2016). Shared and nonshared genomic divergence in parallel ecotypes of *Littorina saxatilis* at a local scale. *Molecular Ecology*, *25*(1), 287–305.

Reichholf, B., Herzog, V., Fasching, N., Manzenreither, R., Sowemimo, I., & Ameres, S. (2019). Time-resolved small RNA sequencing unravels the molecular principles of microRNA homeostasis. *Molecular Cell*, *75*(4), 756–768.e7.

Rellstab, C., Zoller, S., Sailer, C., Tedder, A., Gugerli, F., Shimizu, K. K., ... Fischer, M. C. (2020). Genomic signatures of convergent adaptation to Alpine environments in three Brassicaceae species. *Molecular Ecology*, *29*(22), 4350–4365.

Ritland, K., Newton, C., & Marshall, H. D. (2001). Inheritance and population structure of the white-phased "Kermode" black bear. *Current Biology*, *11*(18), 1468–1472.

Robinson, M. D., McCarthy, D. J., & Smyth, G. K. (2010). edgeR: a Bioconductor package for differential expression analysis of digital gene expression data. *Bioinformatics*, *26*(1), 139-140.

Roda, F., Ambrose, L., Walter, G. M., Liu, H. L., Schaul, A., Lowe, A., ... Ortiz-Barrientos, D. (2013). Genomic evidence for the parallel evolution of coastal forms in the *Senecio lautus* complex. *Molecular Ecology*, *22*(11), 2941–2952.

Rosenblum, E. B., Hoekstra, H. E., & Nachman, M. W. (2004). Adaptive reptile color variation and the evolution of the *MC1R* gene. *Evolution*, *58*(8), 1794–1808.

Rosenblum, E. B., Römpler, H., Schöneberg, T., & Hoekstra, H. E. (2010). Molecular and functional basis of phenotypic convergence in white lizards at White Sands. *Proceedings of the National Academy of Sciences of the United States of America*, *107*(5), 2113–2117.

Rougeux, C., Gagnaire, P. A., Praebel, K., Seehausen, O., & Bernatchez, L. (2019). Polygenic selection drives the evolution of convergent transcriptomic landscapes across continents within a Nearctic sister species complex. *Molecular Ecology*, *28*(19), 4388–4403.

Sasaki, M. C., & Dam, H. G. (2021). Negative relationship between thermal tolerance and plasticity in tolerance emerges during experimental evolution in a widespread marine invertebrate. *Evolutionary Applications*, *14*(8), 2114–2123.

Savolainen, O., Lascoux, M., & Merilä, J. (2013). Ecological genomics of local adaptation. *Nature Reviews Genetics*, *14*(11), 807–820.

Schlichting, C., & Pigliucci, M. (1998). *Phenotypic Evolution: A Reaction Norm Perspective*. Sinauer Associates Inc, Sunderland, Massachusetts.

Schluter, D., & Nagel, L. (1995). Parallel speciation by natural selection. *The American Naturalist*, *146*, 292–301.

Schönswetter, P., & Tribsch, A. (2005). Vicariance and dispersal in the alpine perennial *Bupleurum stellatum* L. (Apiaceae). *Taxon*, *54*(3), 725–732.

Schwander, T., & Leimar, O. (2011). Genes as leaders and followers in evolution. *Trends in Ecology Evolution*, *26*, 143–151.

Scoville, A. G., Barnett, L. L., Bodbyl-Roels, S., Kelly, J. K., & Hileman, L. C. (2011). Differential regulation of a MYB transcription factor is correlated with transgenerational epigenetic inheritance of trichome density in *Mimulus guttatus*. *New Phytologist*, *191*(1), 251–263.

Scoville, A. G., & Pfrender, M. E. (2010). Phenotypic plasticity facilitates recurrent rapid adaptation to introduced predators. *Proceedings of the National Academy of Sciences of the United States of America*, *107*(9), 4260–4263.

Serna, L., & Martin, C. (2006). Trichomes: different regulatory networks lead to convergent structures. *Trends in Plant Science*, *11*(6), 274–280.

Shao, H.-B., Guo, Q.-J., Chu, L.-Y., Zhao, X.-N., Su, Z.-L., Hu, Y.-C., & Cheng, J.-F. (2007). Understanding molecular mechanism of higher plant plasticity under abiotic stress. *Colloids and Surfaces B: Biointerfaces*, *54*(1), 37–45.

Shi, P., Fu, X., Shen, Q., Liu, M., Pan, Q., Tang, Y., ... Tang, K. (2018). The roles of AaMIXTA1 in regulating the initiation of glandular trichomes and cuticle biosynthesis in *Artemisia annua*. *New Phytologist*, *217*(1), 261–276.

Sikkink, K. L., Reynolds, R. M., Ituarte, C. M., Cresko, W. A., & Phillips, P. C. (2019). Environmental and evolutionary drivers of the modular gene regulatory network underlying phenotypic plasticity for stress resistance in the nematode *Caenorhabditis remanei*. *G3 Genes|Genomes|Genetics*, *9*(3), 969–982.

Silva, W., Otto, S., & Immler, S. (2021). Evolution of plasticity in production and transgenerational inheritance of small RNAs under dynamic environmental conditions. *PLOS Genetics*, *17*, e1009581.

Simão, F. A., Waterhouse, R. M., Ioannidis, P., Kriventseva, E. V., & Zdobnov, E. M. (2015). BUSCO: assessing genome assembly and annotation completeness with single-copy orthologs. *Bioinformatics*, *31*(19), 3210–3212.

Simon, A., Arbiol, C., Nielsen, E. E., Couteau, J., Sussarellu, R., Burgeot, T., ... Bierne, N. (2020). Replicated anthropogenic hybridisations reveal parallel patterns of admixture in marine mussels. *Evolutionary Applications*, *13*(3), 575–599.

Skotte, L., Korneliussen, T. S., & Albrechtsen, A. (2013). Estimating individual admixture proportions from Next Generation Sequencing data. *Genetics*, *195*(3), 693–702.

Sloan, D. B., Keller, S. R., Berardi, A. E., Sanderson, B. J., Karpovich, J. F., & Taylor, D. R. (2012). De novo transcriptome assembly and polymorphism detection in the flowering plant *Silene vulgaris* (Caryophyllaceae). *Molecular Ecology Resources*, *12*(2), 333–343.

Smith, J. M., & Haigh, J. (1974). The hitch-hiking effect of a favourable gene. *Genetical Research*, *23*(1), 23–35.

Solé Medina, A., Robledo-Arnuncio, J., & Ramírez-Valiente, J. (2022). Multi-trait genetic variation in resource-use strategies and phenotypic plasticity correlates with local climate across the range of a mediterranean oak (*Quercus faginea*). *New Phytologist in press*.

Sommer, R. J. (2020). Phenotypic plasticity: from theory and genetics to current and future challenges. *Genetics*, *215*(1), 1–13.

Soria-Carrasco, V., Gompert, Z., Comeault, A. A., Farkas, T. E., Parchman, T. L., Johnston, J. S., ... Nosil, P. (2014). Stick insect genomes reveal natural selection's role in parallel speciation. *Science*, *344*(6185), 738–742.

Stanke, M., Keller, O., Gunduz, I., Hayes, A., Waack, S., & Morgenstern, B. (2006). AUGUSTUS: *ab initio* prediction of alternative transcripts. *Nucleic Acids Research*, *34*(2), W435–W439.

Stearns, S. C. (1989). The evolutionary significance of phenotypic plasticity: phenotypic sources of variation among organisms can be described by developmental switches and reaction norms. *BioScience*, *39*(7), 436–445.

Steiner, C. C., Römpler, H., Boettger, L. M., Schöneberg, T., & Hoekstra, H. E. (2009). The genetic basis of phenotypic convergence in beach mice: similar pigment patterns but different genes. *Molecular Biology and Evolution*, *26*(1), 35–45.

Stern, D. L. (2013). The genetic causes of convergent evolution. *Nature Reviews Genetics*, *14*(11), 751–764.

Stotz, G., Salgado-Luarte, C., Escobedo, V., Valladares, F., & Gianoli, E. (2021). Global trends in phenotypic plasticity of plants. *Ecology Letters*, *24*, 2267–2281.

Strader, L. C., Culler, A. H., Cohen, J. D., & Bartel, B. (2010). Conversion of endogenous indole-3-Butyric acid to indole-3-Acetic acid drives cell expansion in *Arabidopsis* seedlings. *Plant Physiology*, *153*(4), 1577–1586.

Stuart, Y. E., Veen, T., Weber, J. N., Hanson, D., Ravinet, M., Lohman, B. K., ... Bolnick, D. I. (2017). Contrasting effects of environment and genetics generate a continuum of parallel evolution. *Nature Ecology and Evolution*, *1*, 158.

Su, H., Fan, J., Ma, D., & Zhu, H. (2021). Identification and characterization of osmoregulation related micrornas in gills of hybrid tilapia under three types of osmotic stress. *Frontiers in Genetics*, *12*.

Sun, Y. B., Fu, T. T., Jin, J. Q., Murphy, R. W., Hillis, D. M., Zhang, Y. P., & Che, J. (2018). Species groups distributed across elevational gradients reveal convergent and continuous genetic adaptation to high elevations. *Proceedings of the National Academy of Sciences of the United States of America*, *115*(45), E10634–E10641.

Sun, Z., Wang, Y., Mou, F., Tian, Y., Chen, L., Zhang, S., ... Li, X. (2016). Genome-wide small RNA analysis of soybean reveals auxin-responsive microRNAs that are differentially expressed in response to salt stress in root apex. *Frontiers in Plant Science*, *6*.

Szukala, A., Lovegrove-Walsh, J., Luqman, H., Fior, S., Wolfe, T., Frajman, B., ... Paun, O. (2022). Polygenic routes lead to parallel altitudinal adaptation in *Heliosperma pusillum* (caryophyllaceae). *Molecular Ecology in press*.

Tal, O., Kisdi, E., & Jablonka, E. (2010). Epigenetic contribution to covariance between relatives. *Genetics*, *184*(4), 1037–1050.

Tan, Y., Barnbrook, M., Wilson, Y., Molna, A., Bukys, A., & Hudson, A. (2020). Shared mutations in a novel glutaredoxin repressor of multicellular trichome fate underlie parallel evolution of *Antirrhinum* species. *Current Biology*, *30*(8), 1357–1366.

Temsch, E. M., Temsch, W., Ehrendorfer-Schratt, L., & Greilhuber, J. (2010). Heavy Metal Pollution, Selection, and Genome Size: The Species of the Žerjav Study Revisited with Flow Cytometry. *Journal of Botany*, *2010*, 596542.

Therkildsen, N. O., Wilder, A. P., Conover, D. O., Munch, S. B., Baumann, H., & Palumbi, S. R. (2019). Contrasting genomic shifts underlie parallel phenotypic evolution in response to fishing. *Science*, *365*(6452), 487–490.

Theron, E., Hawkins, K., Bermingham, E., Ricklefs, R. E., & Mundy, N. I. (2001). The molecular basis of an avian plumage polymorphism in the wild. *Current Biology*, *11*(8), 550–557.

Thiel-Egenter, C., Alvarez, N., Holderegger, R., Tribsch, A., Englisch, T., Wohlgemuth, T., ... Gugerli, F. (2011). Break zones in the distributions of alleles and species in alpine plants. *Journal of Biogeography*, *38*(4), 772–782.

Thompson, K. A., Osmond, M. M., & Schluter, D. (2019). Parallel genetic evolution and speciation from standing variation. *Evolution Letters*, *3*(2), 129–141.

Tominaga-Wada, R., Ishida, T., & Wada, T. (2011). New insights into the mechanism of development of *Arabidopsis* root hairs and trichomes. *International Review of Cell and Molecular Biology*, *286*, 67–106.

Trucchi, E., Frajman, B., Haverkamp, T. H., Schönswetter, P., & Paun, O. (2017). Genomic analyses suggest parallel ecological divergence in *Heliosperma pusillum* (Caryophyllaceae). *New Phytologist*, *216*(1), 267–278.

Trucchi, E., Mazzarella, A. B., Gilfillan, G. D., Lorenzo, M. T., Schönswetter, P., & Paun, O. (2016). BsRADseq: Screening DNA methylation in natural populations of non-model species. *Molecular Ecology*, *25*(8), 1697–1713.

Tsai, C.-H., Liao, R., Chou, B., Palumbo, M., & Contreras, L. (2014). Genome-wide analyses in bacteria show small-RNA enrichment for long and conserved intergenic regions. *Journal of Bacteriology*, *197*(1).

Turesson, G. (2010). The species and the variety as ecological units. *Hereditas*, *3*, 100-113.

Turner, T. L., Bourne, E. C., Von Wettberg, E. J., Hu, T. T., & Nuzhdin, S. V. (2010). Population resequencing reveals local adaptation of *Arabidopsis lyrata* to serpentine soils. *Nature Genetics*, *42*(3), 260–263.

Van Belleghem, S. M., Vangestel, C., De Wolf, K., De Corte, Z., Möst, M., Rastas, P., ... Hendrickx, F. (2018). Evolution at two time frames: polymorphisms from an ancient singular divergence event fuel contemporary parallel evolution. *PLoS Genetics*, *14*(11), e1007796.

Van der Auwera, G. A., & O'Connor, B. D. (2020). *Genomics in the Cloud: Using Docker, GATK, and WDL in Terra*. Sebastopol, CA: O'Reilly Media, Inc.

Van Kleunen, M., & Fischer, M. (2005). Constraints on the evolution of adaptive phenotypic plasticity in plants. *New Phytologist*, *166*(1), 49–60.

Velasquez, S. M., Barbez, E., Kleine-Vehn, J., & Estevez, J. M. (2016). Auxin and cellular elongation. *Plant Physiology*, *170*(3), 1206–1215.

Voskarides, K. (2017). Plasticity vs mutation. the role of microRNAs in human adaptation. *Mechanisms of ageing and development*, *163*, 36–39.

Waddington, C. H. (1942). Canalization of development and the inheritance of acquired characters. *Nature*, *150*, 563–565.

Wang, M., Zhao, Y., & Zhang, B. (2015). Efficient Test and Visualization of Multi-Set Intersections. *Scientific Reports*, *5*(1), 16923.

Wang, Q., Nian, L., Yang, X., Tu, L., & Zhang, X. (2016). Small RNA-mediated responses to low- and high-temperature stresses in cotton. *Scientific Reports*, *6*, 35558.

Wendel, J., Jackson, S., Meyers, B., & Wing, R. (2016). Evolution of plant genome architecture. *Genome Biology*, *17*, 37.

Wichman, H. A., Badgett, M. R., Scott, L. A., Boulianne, C. M., & Bull, J. J. (1999). Different trajectories of parallel evolution during viral adaptation. *Science*, *285*(5426), 422–424.

Wilkens, H., & Strecker, U. (2003). Convergent evolution of the cavefish *Astyanax* (Characidae, Teleostei): Genetic evidence from reduced eye-size and pigmentation. *Biological Journal of the Linnean Society*, *80*(4), 545–554.

Witt, K. E., & Huerta-Sánchez, E. (2019). Convergent evolution in human and domesticate adaptation to high-altitude environments. *Philosophical Transactions of the Royal Society B: Biological Sciences*, *374*(1777), 20180235.

Wolfe, T. M., Balao, F., Trucchi, E., Bachmann, G., Gu, W., Baar, J., ... Paun, O. (2021). Recurrent allopolyploidization events diversify eco-physiological traits in marsh orchids. *bioRxiv*, 2021.08.28.458039.

Wood, D. P., Holmberg, J. A., Osborne, O. G., Helmstetter, A. J., Dunning, L. T., Ellison, A. R., ... Papadopulos, A. S. (2021). Genetic assimilation of ancestral plasticity during parallel adaptation. *bioRxiv*, 2021.11.30.470425.

Wrigth, S. (1931). Evolution in mendelian populations. *Genetics*, *202*(2), 97–159.

Wund, M. A. (2012). Assessing the impacts of phenotypic plasticity on evolution. *Integrative and Comparative Biology*, *52*(1), 5–15.

Xu, F., Guang, S., & Feng, X. (2018). Distinct nuclear and cytoplasmic machineries cooperatively promote the inheritance of RNAi in *C. elegans*. *Biology of the Cell*, *110*(10), 217–224.

Yeaman, S. (2015). Local adaptation by alleles of small effect. *American Naturalist*, *186*, S74–S89.

Yeaman, S., Gerstein, A. C., Hodgins, K. A., & Whitlock, M. C. (2018). Quantifying how constraints limit the diversity of viable routes to adaptation. *PLoS Genetics*, *14*(10), e1007717.

Yeaman, S., Hodgins, K. A., Lotterhos, K. E., Suren, H., Nadeau, S., Degner, J. C., ... Aitken, S. N. (2016). Convergent local adaptation to climate in distantly related conifers. *Science*, *353*(6306), 1431–1433.

Zhao, X., Yu, H., Kong, L., & Liu, S. (2016). High throughput sequencing of small RNAs transcriptomes in two *Crassostrea* oysters identifies microRNAs involved in osmotic stress response. *Scientific Reports*, *6*, 22687.

Zhen, Y., Aardema, M. L., Medina, E. M., Schumer, M., & Andolfatto, P. (2012). Parallel molecular evolution in an herbivore community. *Science*, *337*(6102), 1634–1637.

Zheng, J., Zeng, E., Du, Y., He, C., Hu, Y., Jiao, Z., ... Liu, S. (2019). Temporal small RNA expression profiling under drought reveals a potential regulatory role of small nucleolar RNAs in the drought responses of maize. *The Plant Genome*, *12*(1), 180058.

Zimin, A. V., Marçais, G., Puiu, D., Roberts, M., Salzberg, S. L., & Yorke, J. A. (2013). The MaSuRCA genome assembler. *Bioinformatics*, *29*(21), 2669–2677.

Zuo, Z.-F., He, W., Li, J., Mo, B., & Liu, L. (2021). Small RNAs: the essential regulators in plant thermotolerance. *Frontiers in Plant Science*, *12*, 726762.

A. Appendix - Current research frontiers in plant epigenetics: an introduction to a Virtual Issue

Authors: Eriksson M, **Szukala A**, Tian B & Paun O.

Reference: Eriksson M, **Szukala A**, Tian B & Paun O. 2020. Current research frontiers in plant epigenetics: an introduction to a Virtual Issue. *New Phytologist*, **226**:285288.

New Phytologist

Forum

Check for updates

Commentary

Current research frontiers in plant epigenetics: an introduction to a Virtual Issue

Without directly altering the underlying DNA sequence, epigenetic signals such as histone modifications, DNA methylation and RNA interference (RNAi) can be specific to particular internal or external conditions and they can have phenotypic implications (e.g. Alonso *et al.*, 2019b; Ding *et al.*, 2019; Gehring, 2019; Li *et al.*, 2019; Zhao *et al.*, 2019). Epigenetics was first addressed in *New Phytologist* in 2003 in the context of genomic changes after whole genome doubling (Soltis *et al.*, 2003). A dedicated review on plant evolutionary epigenetics followed in 2005 (Rapp & Wendel, 2005). Since then, *New Phytologist* has published over 80 articles that mention epigenetics, mirroring the steady increase of literature that discusses the biological implications of epigenetic variation (Fig. 1). Following the successful 40th New Phytologist Symposium on 'Plant epigenetics: from mechanisms to ecological relevance' (see Heer *et al.*, 2018), this Virtual Issue on the topic is now being released. In this introductory Commentary we highlight several of the included papers that cover four main research frontiers.

Epigenetic regulation of plant responses to abiotic conditions

Epigenetic diversity in natural populations is generally found to be structured and related to environmental variation (Richards *et al.*, 2017), as for example in a large-scale survey of DNA methylation across populations of *Plantago lanceolata* included in this Virtual Issue (Gáspár *et al.*, 2019). Although a considerable portion of epigenetic variation correlates with trans-acting genetic variants (Dubin *et al.*, 2016; Kawakatsu *et al.*, 2016), its nonrandom spatial distribution often exceeds the genetic structuring of natural populations. In addition, transcriptional rewiring through various epigenetic signals has been observed in plants upon multigenerational exposure to abiotic stresses (Lämke & Bäurle, 2017), such as extreme temperatures (Ding *et al*, 2019; Friedrich *et al.*, 2019), drought (Huang *et al.*, 2019) and salinity (Yang & Guo, 2018). However, a dynamic interplay between specific genetic and epigenetic variants is commonly unravelled by studies of plant stress responses. For example, a loss-of-function genetic mutation at JMJ17 histone demethylation in *Arabidopsis thaliana* has been reported to cause a genome-wide increase in histone 3 lysine 4 trimethylation (H3K4me3) that, in turn, activates multiple dehydration stress-responsive genes (Huang *et al.*, 2019).

Plants that are convergently adapted to extreme abiotic conditions can be particularly useful in understanding the molecular mechanisms that shape these adaptations. Several clades of mangroves, for example, evolved extreme ultraviolet (UV) light-, salinity- and hypoxia-resistance when independently adapting to the specific intertidal environments. However, such stressful conditions can activate transposable elements (TEs; Lyu *et al.*, 2017). Recently, Wang *et al.* (2018) were able to show that stress-induced reactivations of TEs become epigenetically controlled by siRNAs-mediated CHH methylation in the mangrove *Rhizophora apiculata*, but the short active windows of TEs can trigger genetic variation, possibly facilitating adaptation to new conditions.

'Epigenetic diversity in natural populations is generally found to be structured and related to environmental variation . . .'

It is of interest whether epigenetic responses to abiotic stress are localized in the genome, or if they are rather diffuse and multilayered. In a survey across three Brassicaceae species with different levels of resistance to drought, Marín-de la Rosa *et al.* (2019) observed an overall signal of upregulation of epigenetic reprogramming transcripts in the most drought-adapted species. They conclude that response to drought is a complex phenotype resulting from an interplay of different traits, and therefore complex underlying regulatory patterns should be expected. Multilayered pathways to modulate gene expression have been indeed reported by Ding *et al.* (2019), this time for plants under cold stress, including regulation by post-translational histone modifications and DNA methylation, but also by miRNAs and cold-responsive long noncoding RNAs. A study focused on histone modifications in *Brachypodium distachyon* (Huan *et al.*, 2018) reported vernalization-induced, dose-dependent epigenetic changes for multiple genes that coordinate various biological processes to prepare for floral transition. Importantly, the study also reports a quantitative, but rather short-term epigenetic memory, allowing for a faster response to seasonal temperature changes in the descendant generation.

Biotic interactions and plant epigenetics

Although highly context-dependent, plant biotic-responses seem to reflect to a certain degree common pathways and epigenetic alterations to those induced by abiotic stress, with or without involving mediating signalling molecules such as jasmonic acid, salicylic acid and reactive oxygen species (Balao *et al.*, 2018; Alonso *et al.*, 2019b; Ding *et al.*, 2019). In this Virtual Issue, Alonso *et al.* (2019b) review the latest knowledge on the epigenetic relevance of

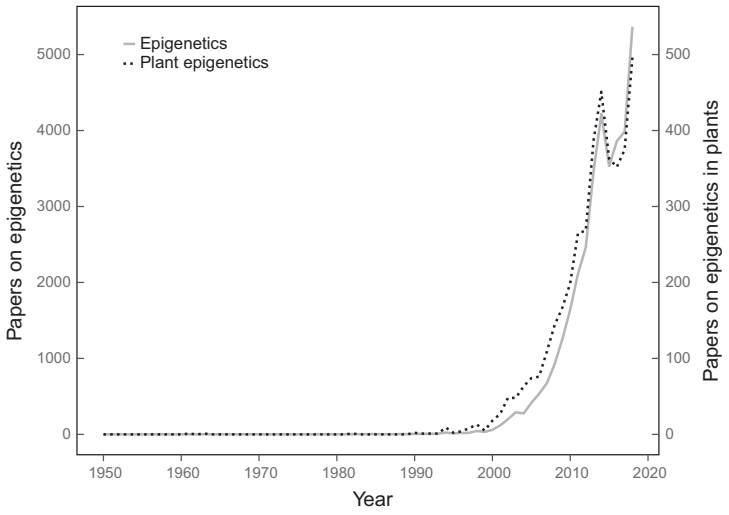

Fig. 1 Number of published studies mentioning 'epigenetics' (filled line, left scale), and 'plant' and 'epigenetics' (dotted line, right scale) by publication year during the period 1950–2018 as output by searches in all Web of Science databases (at 15 July 2019).

biotic interactions, but point out that relevant primary studies are still sparse to allow generalizations. Moreover, most available studies address only the epigenetic consequences of biotic responses, rather than directly approaching the role of epigenetic configurations in determining those responses.

Much of the currently available studies aim to understand plant–pathogen interactions, in particular studying noncoding RNAs. For example, biotrophic fungi infection of *Aegilops tauschii* is reported to trigger a significant downregulation of ARGONAUTE4a that in turn reduces the level of 24-nt siRNAs and CHH methylation especially for genes near TEs, some with stress response relevant functions (Geng *et al.*, 2019). This is, in fact, a more general pattern: epigenetic alterations following biotic stress are frequently observed around genomic regions containing defence-related genes and their transcriptional activation upon stress is often mediated via neighbouring TEs (Alonso *et al.*, 2019b). In another study (Wang *et al.*, 2017), chromatin states driven by both repressive and active histone marks, and facilitated by the presence/absence of a TE upstream of a CCT domain-containing gene (*ZmCCT*), can lead to resistance to *Gibberella* stalk rot in maize. Additional relevant case studies of plant–animal, plant–microbe and plant–plant interactions are critically discussed in Alonso *et al.* (2019b).

Recent papers (for example Alonso *et al.*, 2019b; Ding *et al.*, 2019; Gáspár *et al.*, 2019; Geng *et al.*, 2019) suggest that a better understanding of the epigenetic responses to environmental (i.e. both abiotic and biotic) stress is key to understanding rapid plant adaptation, plant immunity and for developing sustainable strategies for crops' improvement in the face of global warming. Indeed, the spontaneous and fluctuating nature of epimutations was suggested to enhance the adaptation potential to varying abiotic stimuli (e.g. Becker *et al.*, 2011; Johannes & Schmitz, 2019). Particularly relevant to this, Johannes & Schmitz (2019) review the biological implications of stochastic epimutations, also addressing cases where these lead to trans-generational changes in gene expression. Nonetheless, epigenetic responses to abiotic stresses that are independent of genetic variation tend, in general, to be transitory after removing the stressor (Gutzat & Mittelsten Scheid, 2012), whereas for biotic stress some true transgenerational effects (i.e. those that are heritable for at least two generations, Lämke & Bäurle, 2017) are visible, but more studies are required to allow for generalizations.

Epigenetic relevance of hybridization and whole genome doubling

Hybridization and whole genome doubling, individually or in combination (i.e. allopolyploidization), are prevalent in plants and, as genomic stressors, can trigger systemic alterations across the epigenetic landscape. The epigenetic remodelling triggered helps to re-establish the functional and structural balance of the affected genomes (e.g. Song & Chen, 2015; Alonso *et al.*, 2016), but it can have ecological implications (e.g. Paun *et al.*, 2010). Given their prevalence, disentangling the effects of hybridization and polyploidy from one another promises to improve our knowledge about plant genome evolution. Li *et al.* (2019) report a large-scale methylome stability across several rice accessions, including diploid parents, diploid F_1 hybrids and allotetraploids. However, they observed in the allopolyploids considerable but regional re-patterning in the DNA methylation landscape that was missing in the diploid hybrid genomes, indicating that in this system hybridity can exacerbate, only in combination with polyploidy, a rewiring of epigenetic and gene expression landscape. The instability in the DNA methylation landscape is even greater in the case of interploidal hybrids as shown in a study of several natural and artificial cytotypes of *Solanum* (Cara *et al.*, 2019).

The remodelling of the epigenetic landscape can be seen as a consequence of a phenomenon long depicted as 'genomic shock'

New Phytologist

Commentary Forum 287

(McClintock, 1984). The strength and effect of this 'stress state' is determined by the divergence in TE load between the parental species (Mhiri *et al.*, 2018). These 'selfish' and often deleterious elements can be seen as genomic magnets for epigenetic silencing. Building on these ideas, it has been proposed that the subgenome with a higher TE load will have more genes in proximity to TEs, therefore at greater silencing risk, causing an expression bias towards the genome with less TE load (Woodhouse *et al.*, 2014; Gaebelein *et al.*, 2019). Similarly, it has been shown that the dominant genome can be targeted by less silencing in comparison to the parental level, while the recessive genome retains the parental level of silencing (reviewed in Bird *et al.*, 2018). The 'TE model' of subgenome-specific bias and its influence on *cis–trans* interactions and homoeologue expression are discussed in a recent paper by Hu & Wendel (2019). In addition to the 'TE model', a transcription factor model is also highlighted as a strong candidate in shaping the fate of the divergent subgenomes (Hu & Wendel, 2019).

Epigenetics and plant development

Epigenetic mechanisms are also major players during plant development, and have a role in shaping phenotypic plasticity (Gallusci *et al.*, 2017). The latest advances in understanding the epigenetic dynamics associated with reproductive development in angiosperms are reviewed by Gehring (2019). Gehring stresses that epigenetic reprogramming during plant reproductive development does not entail a genome-wide erasure of epigenetic signals, in stark contrast for example to mammals. A particular dynamism during reproductive development has been observed in DNA methylation in the CHH context (Gehring, 2019), but their relevance is still unclear and a topic for forthcoming studies.

Histone modifications also appear involved in fine-tuning different phases of plant development. They can, for example, influence flowering time (Crevillen *et al.*, 2019) and the switch from the heterotrophic to the photosynthetic stages during early seedling development in *Arabidopsis* (Benoit *et al.*, 2019). Through the use of mutants and crossing experiments a further study by Zhao *et al.* (2019) uncovers interactive roles of the HUB2 and SDG8 histone-modifying enzymes in controlling expression of specific genes, regulating proper plant growth and development. The dynamics of chromosomal states during development is linked to the activity of a histone chaperone, chromatin assembly factor 1 (CAF-1; Cheloufi *et al.*, 2015). Starting from the observation that selfing CAF-1 mutants over generations progressively aggravates the specific phenotype, Mozgova *et al.* (2018) show that this is linked to an increasing upregulation of plant defence-related genes that has an epigenetic nature. Through crossings of different generations of selfed mutants they also document a preferred maternal transgenerational transmission of the phenotype.

Finally, epigenetic mechanisms involving small RNAs, in particular siRNAs, are relevant during plant reproduction, for example during a phase of global reactivation of TEs in gametes. During this stage an intercellular movement of siRNAs between companion cells and male gametic cells has been observed, and recent studies have elucidated the function of sperm-delivered siRNAs during early seed development (reviewed by Wu & Zheng, 2019).

'Our understanding of the control and function of structural modifications to DNA has, in recent years, been complemented by developmental and ecological perspectives of epigenetics.'

Conclusions

Our understanding of the control and function of structural modifications to DNA (e.g. Law & Jacobsen, 2010) has, in recent years, been complemented by developmental and ecological perspectives of epigenetics (Richards *et al.*, 2017; Alonso *et al.*, 2019a; Gáspár *et al.*, 2019). Important examples are described in detail in the present Virtual Issue. Several review articles, including Tansley insight papers in this issue define current research topics and set the foundation for forthcoming themes in plant epigenetics. Given the recent conceptual advances (e.g. Douma *et al.*, 2017; Alonso *et al.*, 2019b; Johannes & Schmitz, 2019), the relevant methodological developments (e.g. Paun *et al.*, 2019), and the rapid increase of available genomic resources for a broad array of organisms, there is no doubt that plant epigenetics will continue to thrive and deliver important scientific insights, building on the foundation set by previous research.

Acknowledgements

The authors would like to acknowledge the organizers and attendees of the 40th New Phytologist Symposium for seeding the present Virtual Issue. This article was supported by Austrian Science Fund (FWF) projects Y661-B16 to OP and DK W1225-B20, and by grant 201807855003 from China Scholarship Council to BT.

ORCID

Ovidiu Paun https://orcid.org/0000-0002-8295-4937

Mimmi C. Eriksson[1,2], Aglaia Szukala[1,2], Bin Tian[1,3] and Ovidiu Paun[1]*

[1]Botany and Biodiversity Research, University of Vienna, Rennweg 14, A-1030 Vienna, Austria;
[2]Vienna Graduate School of Population Genetics, Veterinärplatz 1, A-1210 Vienna, Austria;
[3]Southwest Forestry University, Kunming 650224, China
(*Author for correspondence: tel +43 1 4277 540 57; email ovidiu.paun@univie.ac.at)

References

Alonso C, Balao F, Bazaga P, Perez R. 2016. Epigenetic contribution to successful polyploidizations: variation in global cytosine methylation along an extensive ploidy series in *Dianthus broteri* (Caryophyllaceae). *New Phytologist* **212**: 571–576.

Alonso C, Medrano M, Perez R, Canto A, Parra-Tabla V, Herrera CM. 2019a. Interspecific variation across Angiosperms in global DNA methylation: phylogeny, ecology and plant features in Tropical and Mediterranean communities. *New Phytologist* **224**: 949–960.

Alonso C, Ramos-Cruz D, Becker C. 2019b. The role of plant epigenetics in biotic interactions. *New Phytologist* **221**: 731–737.

Balao F, Paun O, Alonso C. 2018. Uncovering the contribution of epigenetics to plant phenotypic variation in Mediterranean ecosystems. *Plant Biology* **20**: 38–49.

Becker C, Hagmann J, Müller J, Koenig D, Stegle O, Borgwardt K, Weigel D. 2011. Spontaneous epigenetic variation in the *Arabidopsis thaliana* methylome. *Nature* **480**: 245–249.

Benoit M, Simon L, Desset S, Duc C, Cotterell S, Poulet A, Le Goff S, Tatout C, Probst AV. 2019. Replication-coupled histone H3.1 deposition determines nucleosome composition and heterochromatin dynamics during *Arabidopsis* seedling development. *New Phytologist* **221**: 385–398.

Bird KA, VanBuren R, Puzey JR, Edger PP. 2018. The causes and consequences of subgenome dominance in hybrids and recent polyploids. *New Phytologist* **220**: 87–93.

Cara N, Ferrer MS, Masuelli RW, Camadro EL, Marfil CF. 2019. Epigenetic consequences of interploidal hybridisation in synthetic and natural interspecific potato hybrids. *New Phytologist* **222**: 1981–1993.

Cheloufi S, Elling U, Hopfgartner B, Jung YL, Murn J, Ninova M, Hubmann M, Badeaux AI, Euong Ang C, Tenen D *et al.* 2015. The histone chaperone CAF-1 safeguards somatic cell identity. *Nature* **528**: 218–224.

Crevillen P, Gomez-Zambrano Á, Lopez JA, Vazquez J, Pineiro M, Jarillo JA. 2019. *Arabidopsis* YAF9 histone readers modulate flowering time through NuA4-complex-dependent H4 and H2A.Z histone acetylation at FLC chromatin. *New Phytologist* **222**: 1893–1908.

Ding Y, Shi Y, Yang S. 2019. Advances and challenges in uncovering cold tolerance regulatory mechanisms in plants. *New Phytologist* **222**: 1690–1704.

Douma JC, Vermeulen PJ, Poelman EH, Dicke M, Anten NPR. 2017. When does it pay off to prime for defense? A modeling analysis. *New Phytologist* **216**: 782–797.

Friedrich T, Faivre L, Bäurle I, Schubert D. 2019. Chromatin-based mechanisms of temperature memory in plants. *Plant, Cell & Environment* **42**: 762–770.

Gaebelein R, Schiessl SV, Samans B, Batley J, Mason AS. 2019. Inherited allelic variants and novel karyotype changes influence fertility and genome stability in *Brassica* allohexaploids. *New Phytologist* **223**: 965–978.

Gallusci P, Dai Z, Génard M, Gauffretau A, Leblanc-Fournier N, Richard-Molard C, Vile D, Brunel-Muguet S. 2017. Epigenetics for plant improvement: current knowledge and modeling avenues. *Trends in Plant Science* **22**: 610–623.

Gáspár B, Bossdorf O, Durka W. 2019. Structure, stability and ecological significance of natural epigenetic variation: a large-scale survey in *Plantago lanceolata*. *New Phytologist* **221**: 1585–1596.

Gehring M. 2019. Epigenetic dynamics during flowering plant reproduction: evidence for reprogramming? *New Phytologist* **224**: 91–96.

Gutzat R, Mittelsten Scheid O. 2012. Epigenetic responses to stress: triple defense? *Current Opinion in Plant Biology* **15**: 568–573.

Heer K, Mounger J, Boquete MT, Richards CL, Opgenoorth L. 2018. The diversifying field of plant epigenetics. *New Phytologist* **217**: 988–992.

Hu G, Wendel JF. 2019. Cis–trans controls and regulatory novelty accompanying allopolyploidization. *New Phytologist* **221**: 1691–1700.

Huan Q, Mao Z, Chong K, Zhang J. 2018. Global analysis of H3K4me3/H3K27me3 in *Brachypodium distachyon* reveals VRN 3 as critical epigenetic regulation point in vernalization and provides insights into epigenetic memory. *New Phytologist* **219**: 1373–1387.

Huang S, Zhang A, Jin JB, Zhao B, Wang TJ, Wu Y, Wang S, Liu Y, Wang J, Guo P *et al.* 2019. *Arabidopsis* histone H3K4 demethylase JMJ 17 functions in dehydration stress response. *New Phytologist* **223**: 1372–1387.

Johannes F, Schmitz RJ. 2019. Spontaneous epimutations in plants. *New Phytologist* **221**: 1253–1259.

Lämke J, Bäurle I. 2017. Epigenetic and chromatin-based mechanisms in environmental stress adaptation and stress memory in plants. *Genome Biology* **18**: 124.

Law JA, Jacobsen SE. 2010. Establishing, maintaining and modifying DNA methylation patterns in plants and animals. *Nature Reviews Genetics* **11**: 204–220.

Li N, Xu C, Zhang A, Lv R, Meng X, Lin X, Gong L, Wendel JF, Liu B. 2019. DNA methylation repatterning accompanying hybridization, whole genome doubling and homoeolog exchange in nascent segmental rice allotetraploids. *New Phytologist* **223**: 979–992.

Lyu H, He Z, Wu CI, Shi S. 2017. Convergent adaptive evolution in marginal environments: unloading transposable elements as a common strategy among mangrove genomes. *New Phytologist* **217**: 428–438.

Marín-de la Rosa N, Lin CW, Kang YJ, Dhondt S, Gonzalez N, Inzé D, Falter-Braun P. 2019. Drought resistance is mediated by divergent strategies in closely related Brassicaceae. *New Phytologist* **223**: 783–797.

McClintock B. 1984. The significance of responses of the genome to challenge. *Science* **226**: 792–801.

Mhiri C, Parisod C, Daniel J, Petit M, Lim KY, Dorlhac de Borne F, Kovarik A, Leitch AR, Grandbastien M. 2018. Parental transposable element loads influence their dynamics in young *Nicotiana* hybrids and allotetraploids. *New Phytologist* **221**: 1619–1633.

Mozgova I, Wildhaber T, Trejo-Arellano MS, Fajkus J, Roszak P, Kohler C, Hennig L. 2018. Transgenerational phenotype aggravation in CAF-1 mutants reveals parent-of-origin specific epigenetic inheritance. *New Phytologist* **220**: 908–921.

Paun O, Bateman RM, Fay MF, Hedrén M, Civeyrel L, Chase MW. 2010. Stable epigenetic effects and adaptation in allopolyploid orchids (*Dactylorhiza*: Orchidaceae). *Molecular Biology and Evolution* **27**: 2465–2473.

Paun O, Verhoeven KJF, Richards CL. 2019. Opportunities and limitations of reduced representation bisulfite sequencing in plant ecological epigenomics. *New Phytologist* **221**: 738–742.

Rapp RA, Wendel JF. 2005. Epigenetics and plant evolution. *New Phytologist* **168**: 81–91.

Richards CL, Alonso C, Becker C, Bossdorf O, Bucher E, Colome-Tatche M, Durka W, Engelhardt J, Gáspár B, Gogol-Doring A *et al.* 2017. Ecological plant epigenetics: evidence from model and non-model species, and the way forward. *Ecology Letters* **20**: 1576–1590.

Soltis DE, Soltis PS, Tate JA. 2003. Advances in the study of polyploidy since *Plant speciation*. *New Phytologist* **161**: 173–191.

Song Q, Chen ZJ. 2015. Epigenetic and developmental regulation in plant polyploids. *Current Opinion in Plant Biology* **24**: 101–109.

Wang C, Yang Q, Wang W, Li Y, Guo Y, Zhang D, Ma X, Song W, Zhao J, Xu M. 2017. A transposon-directed epigenetic change in ZmCCT underlies quantitative resistance to *Gibberella* stalk rot in maize. *New Phytologist* **215**: 1503–1515.

Wang Y, Liang W, Tang T. 2018. Constant conflict between Gypsy LTR retrotransposons and CHH methylation within a stress-adapted mangrove genome. *New Phytologist* **220**: 922–935.

Woodhouse MR, Cheng F, Pires JC, Lisch D, Freeling M, Wang X. 2014. Origin, inheritance, and gene regulatory consequences of genome dominance in polyploids. *Proceedings of the National Academy of Sciences, USA* **111**: 5283–5288.

Wu W, Zheng B. 2019. Intercellular delivery of small RNAs in plant gametes. *New Phytologist* **224**: 86–90.

Yang Y, Guo Y. 2018. Elucidating the molecular mechanisms mediating plant salt-stress responses. *New Phytologist* **217**: 523–539.

Zhao W, Neyt P, Van Lijsebettens M, Shen WH, Berr A. 2019. Interactive and noninteractive roles of histone H2B monoubiquitination and H3K36 methylation in the regulation of active gene transcription and control of plant growth and development. *New Phytologist* **221**: 1101–1116.

Key words: abiotic stress, biotic interactions, DNA methylation, histone modifications, hybridization, plant development, whole genome doubling.

B. Appendix - Testing the effects of methylation inhibition on ecotype growth

Epigenetics of adaptation to different altitudes: the effects of methylation inhibition on ecotype growth.

Authors: **Aglaia Szukala**, Daniel Schubert, and Ovidiu Paun.

Outline of the project

This appendix describes a laboratory project that was designed to test if differences in genome methylation are involved in shaping ecotype divergence in the plant species *Heliosperma pusillum*. I carried out this work during a three-months research stay in the lab of Daniel Schubert at Free University, Berlin, Germany. In the second and third chapters of this thesis we showed that (1) the montane ecotype bears higher potential for plastic expression changes and (2) a high amount of small RNAs, including 23-24 nt long ones, differentially targets the ecotypes, including putative genes underlying phenotypic divergence. Thus we aimed to test if the two ecotypes show different responses to whole-genome demethylation. A difference in the ability to reestablish methylation patterns in the two ecotypes might suggest that methylation is a driving mechanism behind plastic responses to stress.

Material and methods

Plant material and *in vitro* cultivation. Seeds were collected from wild populations in July 2019 and August 2020 in Lienzer Dolomiten, Kärnten (Austria) (alpine site: 46.762 N 12.877 E, 2,055 m, montane site: 46.774 N 12.901 E, 790 m) and in Dolomiti di Braies, Trentino-Alto Adige (Italy) (alpine site: 46.644 N 12.205 E, 2190 m, montane site: 46.645 N 12.233 E, 1420 m). Seeds were exposed to a period of vernalization of 20 days at -4 °C before the experiment was started. Sterilization of seeds was carried out using the following procedure: 1) shortly rinse in tap water, 2) rinse in 10% Ethanol (5 min), 3) lay in 12% NaOCl + few drops of Tween 20 (20 min), 4) 3 x rinse in sterile water (5 min) and 1 x rinse in sterile water (10 min). Following sterilization, seeds were laid on a ½ MS 0,8% Agar + Sucrose plate (pH 5,7) and plates were placed in a long day climate chamber (16 h, 20 °C day /18 °C night). Seeds took 6-8 days to germinate. Two weeks after the seeds were sown on plates (i.e. ca. one week after germination) 25 and 10 seedlings were transferred to a new plate with 10uM (Fig.1) and 50uM Zebularine (691400-10MG, Millipore Sigma), respectively. We grew a total of 25 control plants + 25 plants treated with 10uM Zebularine (Fig. 1) + 10 plants treated with 50uM Zebularine for each ecotype for two additional weeks before transferring the plants to soil and performing phenotyping. Plants treated with 50 uM Zebularine were not transferred to soil, instead leaf material was placed in

liquid nitrogen and stored at -80 °C for subsequent RNA extraction and qPCR. The experiment was run twice with seeds collected in Dolomiti di Braies (2 experimental replicates) and one time with seeds collected in Lienzer Dolomiten. These three pseudo replicates of the same experiments are hereafter referred to as "experimental runs". This experimental design was dictated by the amount of seeds available, since the montane populations at the natural sites are small (< 100 individuals).

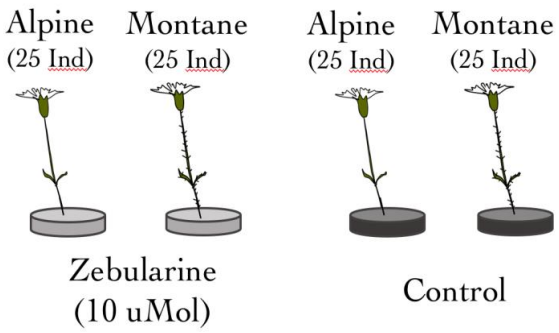

Figure 1. Synthetic representation of the experimental design. Plants from both ecotypes were grown on substrate containing zebularine (10uMol) and without (control).

Plants phenotyping. Phenotyping of treated (10uM Zebularine) and control plants was carried out, in order to see if the treatment would differentially affect the two ecotypes in terms of phenotype and development. First, plant growth was monitored, conducting repeated measurements (i.e. 30, 36 and 42 days after germination) of the length of the second leaves pair, the size of the main stem axis and total number of leaves produced. We carried out multiple measurements to test if the ecotypes would recover from the treatment over time and if the recovery would happen at a different pace between the ecotypes.

The retrieved data was analyzed applying a generalized linear model of the type trait ~ treatment*day*ecotype. Statistical significance of the effect of the explanatory variables on the ecotype growth was assessed using ANOVA.

Results and Discussion

Phenotyping of plants grown on 10uMol zebularine and controls showed that the de-methylation treatment always had a significant effect on the ecotype growth in both ecotypes (Fig. 2, Anova, $p < 0.00001$). Plants from both ecotypes growing on zebularine showed reduced growth affecting the measured traits similarly in all three experimental runs (Fig. 2). Interestingly, while the first measurement revealed similar effects on both ecotypes ($p < 0.01$ in both ecotypes and all three

experimental runs), over time the observed effect became less significant in the montane ecotype,

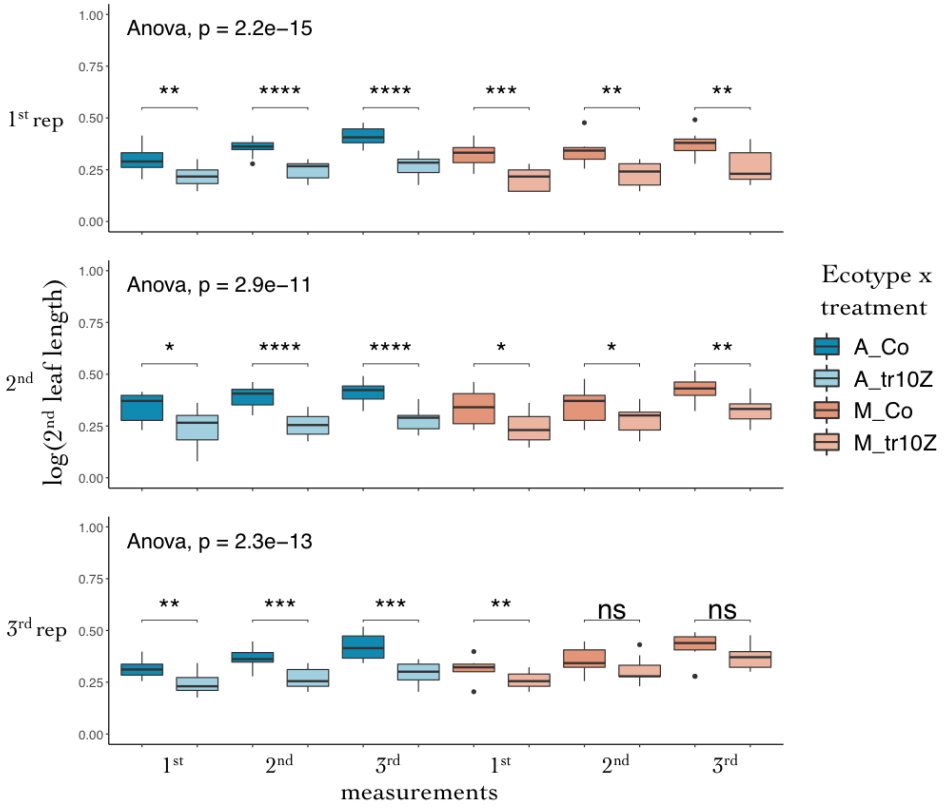

Figure 2. Effect of zebularine treatment on both ecotypes, exemplified by measurements of the 2nd leaf length. First, second, and third experimental runs are shown on the first, second, and third row, respectively. The X-axis displays the time points at which measurements were taken, i.e., 30, 36 and 42 days after germination. Blue, alpine ecotype; orange, montane ecotype. Darker color shades, controls; lighter shades, treated plants. The Significance codes of p-values: (***) 0.0001, (**) 0.001, (*) 0.01.

while it increased in the alpine (Fig. 2). This result suggests that the montane ecotype recovers more easily from the de-methylation shock and is likely faster at re-establishing overall genome methylation and pathways. This result seems consistent with the known enhanced plasticity of the montane ecotype, which might allow faster recovery from multiple stressors, including de-methylation stress.

C. Appendix - Conference contributions

48TH Annual Meeting of the Ecological Society of Germany, Austria and Switzerland

September 2018, Vienna, Austria

Oral presentation

Authors: **Szukala A**, Frajman B, Schoenswetter P, Baar J, Lovegroove-Walsh J, Ferrè Ortega C & Paun O.

Title: **Convergent and adaptive processes driving parallel adaptation to warmer and drier habitats in the alpine plant species *Heliosperma pusillum*.**

Abstract

To which extent can species adapt to an increasingly changing environment? Species distributed along the altitudinal gradient are ideal models to study the mechanisms underlying local adaptation in sensitive and dynamic habitats. We investigate the contribution of neutral and adaptive processes in shaping early stages of divergence during adaptation to drier and warmer habitats. The study system are morphologically differentiated ecotypes (alpine glabrous vs. montane pubescent) of the species *Heliosperma pusillum* (Caryophyllaceae). The ecological divergence features not only temperature differences, but also moisture (dry montane vs. wet alpine habitats), availability of light (shaded montane vs. open alpine) and biotic divergence in the phyllosphere of the plants. RADseq analyses support a scenario of multiple parallel origins of the montane ecotype from the alpine across population pairs at different localities in the south-eastern Alps. With RNAseq we performed comparative transcriptomics on 24 representative individuals (i.e. 3 individuals $\times$ 4 populations pairs) grown in a common garden. We test for divergent patterns between the two ecotypes in each independent origin and search for overlapping patterns across origins. Our data show that drift and locally-relevant selection shape a major portion of expressed patterns. By contrast, enriched gene expression shared by independent divergence events show that natural selection shapes the expression patterns of a few ecologically relevant genes. The dry and shaded montane ecotype adapted to its new environment by up-regulating genes involved in epicuticular wax biosynthesis, responses to desiccation and biotic stress, while down-regulating other cellular responses to high light intensity and UV. Our study sheds light on the evolutionary processes allowing alpine populations to adapt to warmer and drier habitats. Given the recurrence of the divergence events, this appears to be relatively easy achieved in *H.pusillum*.

Evolution

June 2019, Providence, USA

Oral presentation

Authors: **Szukala A**, Fani A, Schoenswetter P, Frajman B & Paun O.

Title: **An integrative perspective of adaptation to different altitudes in an alpine plant.**

Abstract

Independent instances of divergence with similar phenotypic outcome (convergent evolution) provide natural evolutionary replicates to investigate the relative contribution of drift and selection during adaptation to new ecological niches. The alpine plant *Heliosperma pusillum* comprises two ecotypes (low vs. high elevation) that maintain different phenotypes (trichomy vs. glabrous) when grown under the same conditions for several generations. Consistent with a strong difference in distribution (patchy, small populations vs. widespread intermixed) different amount of gene flow and drift have been estimated among populations and ecotypes. Noteworthy, genome-wide SNPs previously showed that the mountain ecotype diverged multiple times independently in at least five different geographic areas from the alpine populations. We seek to confirm this evolutionary scenario and understand the genetic changes that lead to patterns of divergence across origins. Differential expression analysis was performed on plants cultivated in a common garden and reciprocal transplantations. This double approach is thought to pinpoint the genes that play a role in the adaptation to the differing ecological conditions. Reciprocal transplantations confirm local adaptation as a home site fitness advantage of each of the two ecotypes. We find that the hairy low-elevation ecotype adapted to poor light conditions by upregulating genes involved in trichome formation, pigmentation and DNA repair in response to light damage, while several genes involved in light harvesting and processing are downregulated. The analysis of more than one million SNPs from RNA-seq confirms that at least three instances of divergence are independent but also finds patterns of shared ancestry that had not been detected using RAD-seq. Our current analyses of posttranscriptional regulation by small RNAs and of DNA methylation variation, as well as within-ecotype crosses designed to clarify the genetic control of the divergent traits, will further clarify the evolutionary scenario and genetic mechanisms underlying divergence in this exciting system.

ESEB

August, 2019, Turku, Finland

Oral presentation

Authors: **Szukala A**, Fani A, Schoenswetter P, Frajman B & Paun O.

Title: **An integrative perspective of adaptation to different altitudes in an alpine plant.**

Abstract

Independent instances of divergence with similar phenotypic outcome (convergent evolution) provide natural evolutionary replicates to investigate the relative contribution of drift and selection during adaptation to new ecological niches. The alpine plant *Heliosperma pusillum* comprises two ecotypes (low vs. high elevation) that maintain different phenotypes (trichomy vs. glabrous) when grown under the same conditions for several generations. Consistent with a strong difference in distribution (patchy, small populations vs. widespread intermixed) different amount of gene flow and drift have been estimated among populations and ecotypes. Noteworthy, genome-wide SNPs previously showed that the mountain ecotype diverged multiple times independently in at least five different geographic areas from the alpine populations. We seek to confirm this evolutionary scenario and understand the genetic changes that lead to patterns of divergence across origins. Differential expression analysis was performed on plants cultivated in a common garden and reciprocal transplantations. This double approach is thought to pinpoint the genes that play a role in the adaptation to the differing ecological conditions. Reciprocal transplantations confirm local adaptation as a home site fitness advantage of each of the two ecotypes. We find that the hairy low-elevation ecotype adapted to poor light conditions by upregulating genes involved in trichome formation, pigmentation and DNA repair in response to light damage, while several genes involved in light harvesting and processing are downregulated. The analysis of more than one million SNPs from RNA-seq confirms that at least three instances of divergence are independent but also finds patterns of shared ancestry that had not been detected using RAD-seq. Our current analyses of posttranscriptional regulation by small RNAs and of DNA methylation variation, as well as within-ecotype crosses designed to clarify the genetic control of the divergent traits, will further clarify the evolutionary scenario and genetic mechanisms underlying divergence in this exciting system.

Institute of Science and Technology (IST): EvoLunch

April, 2020, IST Vienna, Austria

Invited talk

Authors: **Szukala A** & Paun O.

Title: **Parallel and adaptive processes during ecotype formation.**

Abstract

Independent instances of divergence with similar phenotypic outcome (parallel evolution) provide natural evolutionary replicates to investigate the adaptation to new ecological niches. The alpine plant *Heliosperma pusillum* comprises two ecotypes (low vs. high elevation) that maintain different phenotypes (trichomy vs. glabrous) when grown under the same conditions for several generations and show a home-site advantage in reciprocal transplantations. Noteworthy, genome-wide SNPs from RAD-seq previously suggested that the low-elevation ecotype diverged from the high-elevation ecotype multiple times independently in five different geographic areas. We seek to confirm this evolutionary scenario and understand the genetic changes that lead to divergence across origins. We compare alternative demographic scenarios using the site frequency spectrum as summary statistic and perform differential expression analyses of plants grown in a common garden. Our results confirm the independent instances of divergence but also find complex patterns of shared variation that were previously undetected. We find that the hairy low-elevation ecotype adapted to poor light and dry conditions by upregulating genes involved in trichomes formation and response to water deprivation, while several genes involved in light harvesting and photosynthesis are downregulated. Despite the parallelism found at the functional level, we detect very low overlap of genes differentially expressed between ecotypes across origins and treatments, indicating that changes in different genes and pathway components led to similar outcomes independently. Polygenic traits appear key to parallel evolution, by providing the substrate to reproducible outcomes in independent divergence events.

Botany

July, 2020, USA virtual

Oral presentation

Authors: **Szukala A**, Frajman B, Schoenswetter P & Paun O.

Title: **An integrative perspective of adaptation to different altitudes in the Alps.**

Abstract

Independent instances of divergence with similar phenotypic outcome (parallel evolution) provide natural evolutionary replicates to investigate the adaptation to new ecological niches. The alpine plant *Heliosperma pusillum* Waldst. & Kit. comprises two ecotypes (low vs. high elevation) that maintain different phenotypes (trichomy vs. glabrous) when grown under the same conditions for several generations. We show that the low-elevation ecotype diverged from the high-elevation ecotype multiple times independently by comparing alternative demographic scenarios using the site frequency spectrum as summary statistic. To understand the genetic basis of adaptation to different altitudes, we performed differential expression analyses of plants grown in a common garden and reciprocal transplantations. Our results show that the hairy low-elevation ecotype adapted to poor light and dry conditions by upregulating genes involved in trichomes formation and response to water deprivation, while several genes involved in light harvesting and photosynthesis are downregulated. Despite the parallelism found at the functional level, we detect very low overlap of genes differentially expressed between ecotypes across origins and treatments, indicating that changes in different genes and pathway components led to similar outcomes independently. Reciprocal transplantations show a clear home-site advantage and that the low-elevation ecotype bears higher plasticity of gene expression. Polygenic traits appear key to parallel evolution, by providing the substrate to reproducible outcomes in independent divergence events. Finally, higher phenotypic plasticity might facilitate the adaptation to drier and warmer environments in this plant system.

Biodiversity Genomics

October, 2020, UK virtual

Oral presentation

Authors: **Szukala A**, Frajman B, Schoenswetter P & Paun O.

Title: **A transcriptomic perspective of adaptation to different altitudes in the Alps.**

Abstract

Independent instances of divergence with similar phenotypic outcome (parallel evolution) provide natural evolutionary replicates to investigate the adaptation to new ecological niches. The alpine plant *Heliosperma pusillum* Waldst. & Kit. comprises two ecotypes (low vs. high elevation) that maintain different phenotypes (pubescent vs. glabrous) when grown under the same conditions for several generations. We show that the low-elevation ecotype diverged from the high-elevation ecotype multiple times independently by comparing alternative demographic scenarios using the site frequency spectrum as summary statistic. To understand the genetic basis of adaptation to different altitudes, we performed differential expression analyses of plants grown in a common garden and reciprocal transplantations. Our results show that the hairy low-elevation ecotype adapted to poor light and dry conditions by upregulating genes involved in trichomes formation and response to water deprivation, while several genes involved in light harvesting and photosynthesis are downregulated. Despite the parallelism found at the functional level, we detect very low overlap of genes differentially expressed between ecotypes across origins and treatments, suggesting that changes in different genes and pathway components led to similar outcomes independently. Reciprocal transplantations show a clear home-site advantage and that the low-elevation ecotype bears higher plasticity of gene expression. Polygenic traits appear key to parallel evolution, by providing the substrate to reproducible outcomes in independent divergence events. Finally, higher phenotypic plasticity might facilitate the adaptation to drier and warmer environments in this plant system.

SMBE

July, 2021, virtual

Oral presentation

Authors: **Szukala A**, Frajman B, Schoenswetter P, Schubert D & Paun O.

Title: **The role of gene expression plasticity during recurrent altitudinal divergence.**

Abstract

Independent instances of divergence with similar phenotypic outcome (parallel evolution) provide natural evolutionary replicates to investigate the adaptation to different ecological niches. The alpine plant *Heliosperma pusillum* Waldst. & Kit. comprises two elevational ecotypes (i.e. montane and alpine) that diverged multiple times independently in at least five geographic regions. The montane and alpine growing sites significantly differ in terms of temperature, and light and water availability (i.e. warmer/drier/shaded montane vs colder/humid/exposed alpine). To understand the genetic basis of adaptation to different altitudes and respective ecology, we performed transcriptomic analyses of plants grown in reciprocal transplantations at the natural growing sites. Our results show that the adaptation to the different altitudes involves a minor proportion of constitutive changes in gene expression. Interestingly, we observe that the montane ecotype bears significantly higher plasticity of gene expression then the alpine. Genes that change expression plastically are involved in response to high light, flavonoid biosynthesis, oxidation-reduction processes and methylation. We further tested if the two ecotypes are differentially affected by global inhibition of methylation using zebularine. We show that the montane ecotype recovers faster from the de-methylation shock, possibly thank to higher plastic potential of methylation-related genes. We conclude that higher phenotypic plasticity, possibly mediated by dynamic methylation rewiring, likely evolved in response to drier and warmer environments in this plant system.